CHARGE TRANSPORT IN LIQUID HYDROCARBONS FOR MICRODOSIMETRY

Mamdouh Chaar

A Thesis Submitted for the Degree of PhD
at the
University of St Andrews

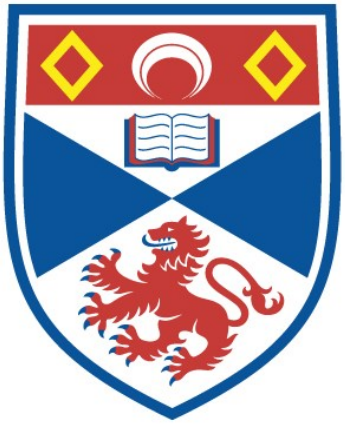

1998

Full metadata for this item is available in
St Andrews Research Repository
at:
http://research-repository.st-andrews.ac.uk/

Please use this identifier to cite or link to this item:
http://hdl.handle.net/10023/13367

This item is protected by original copyright

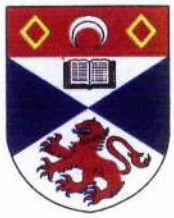

Charge transport in liquid hydrocarbons for microdosimetry

Ph.D. thesis submitted

by

Mamdouh Chaar

School of Physics and Astronomy
University of St. Andrews

January 1998

ProQuest Number: 10170650

All rights reserved

INFORMATION TO ALL USERS
The quality of this reproduction is dependent upon the quality of the copy submitted.

In the unlikely event that the author did not send a complete manuscript
and there are missing pages, these will be noted. Also, if material had to be removed,
a note will indicate the deletion.

ProQuest 10170650

Published by ProQuest LLC (2017). Copyright of the Dissertation is held by the Author.

All rights reserved.
This work is protected against unauthorized copying under Title 17, United States Code
Microform Edition © ProQuest LLC.

ProQuest LLC.
789 East Eisenhower Parkway
P.O. Box 1346
Ann Arbor, MI 48106 – 1346

Content of the thesis

Declaration i

Certification ii

Dedications iii

Acknowledgements iv

Abstract v

Table of contents viii

List of figures xiii

List of tables xviii

Charge transport in liquid hydrocarbons for microdosimetry . . 1

Appendix 166

References of appendix B 188

References of the thesis 196

Declaration

I, Mamdouh Chaar, hereby certify that this thesis is approximately 31,000 words in length, has been written by me, that is the record of work carried out by me and that it has not been submitted in any previous application for a higher degree.

This research has been carried out in the Department of Physics and Astronomy in the University of St. Andrews under the supervision of Dr. D.E. Watt.

Date.....

Signature of candidate

.....

Mamdouh Chaar

Certification

I hereby certify that the candidate Mamdouh Chaar, has fulfilled the conditions of the resolution and regulations for the degree of Doctor of Philosophy in the University of St. Andrews and that the candidate is qualified to submit this thesis in application for that degree.

Date.....

Signature of supervisor

.....

Dr. D.E. Watt

Research Supervisor

Dedications

To my **wife** Chaza Afandi

My **daughter** Raghad Chaar

My **son** Mohamed Tariq Chaar

I dedicate this thesis

Mamdouh Chaar

Acknowledgments

I wish to express my sincere and great thanks to my supervisor, Dr. D.E. Watt, for his supervision and guidance throughout the present work and providing the relevant and up-to-date information during the study. I should extend my gratitude to Dr. D. Foster from chemistry department in this university for consultancy and guidance concerning the chemical purification of the TMS liquid used in the present work; to the persons contributed directly or indirectly to the project from the mechanical and electronic workshop (especially Mr. J. Clark, Mr F. Akerboom, Mr. G. Radley, Mr. J. Park, and Mr. Ian McLaren) in the physics department; to all my colleagues, especially those in the radiation biophysics group.

I would like to thank the government of Syria for awarding me a scholarship.

My thank should go to every person who helped in whatever ways to make this study possible and complete.

Thank you very much.

Abstract

During the last two decades there has been growing interest in the application of organic di-electric liquids for dosimetry of ionizing radiations. The main problem associated with the liquid application in radiation detectors has been the difficulty in securing saturation charge collection and controlled charge multiplication to permit operation in the ionization chamber and proportional counter modes. In an attempt to understand better the fundamental mechanisms involved in the limitation to charge collection an extensive review has been made of the published theoretical and experimental research.

The theoretical work attributes the unattainability of saturation charge collection to losses caused by different types of recombination depending on the initial separation of ions liberated and on the magnitude of the applied electric field. None of the presented theories is found to be fully consistent with the reported experimental results obtained for a range of different di-electric liquids, especially in high field regions.

Liquid hydrocarbons, especially those characterised by high charge mobility and high yield of ions, have been widely investigated experimentally to explore the mechanisms responsible. The experimental measurements are found to be strongly dependent on: the purity of the liquids, their chemical structure, the type of materials used for the electrodes in contact with the liquid and on the temperature. These conclusions reflect inadequacies both in the theoretical knowledge of charge transport in liquids and in the practical difficulties of measurement which indicate the need for more detailed experimental investigation.

The origin of the natural intrinsic dark current in liquids is found to be due to the

presence of impurities; the effect of cosmic-ray interactions; and the presence of radioactivity in the construction materials of the detector. Upon application of high electric fields other factors such as electron emission, molecular dissociation and field ionization become significant.

The extensive range of results reported on transport properties (mobility, free ion-yield, conduction band energy, di-electric strength, and theoretical W-values) of charge carriers in liquid hydrocarbons and liquified rare-gases, and their dependence on the electric field and temperature have been compiled into tabulated form in appendix B to provide a ready reference.

New experimental work, aimed at assessing the role and the key factors involved, was conducted with two separate ionization chambers filled with liquid tetramethylsilane (TMS). Information was obtained on the dependence of the current-field characteristic, for the dark and ionization currents, on various parameters such as purity, electrode separation, surface asperities, electrode construction material, and the charge collection area. For the ionization current, the dependence on the radiation intensity, produced with a 4 mCi source of ^{57}Co of γ-rays, was also measured. Liquid purity was confirmed to be very important. Chemical and electrical purification, could lead to orders of magnitude reduction in the background dark current.

Tests, made to assess the efficiency of ion collection in liquid TMS, indicated the need for much larger, and more uniform, electric fields. These were achieved by fitting electrodes made from tissue-equivalent plastic. The improved surface smoothness of the latter was found to improve the current-to-noise ratio by a factor of 2-3 orders of magnitude. From the results of the present investigation at fields $\leq$ 500 kV/cm it was concluded that true saturation collection of charge was attainable.

Limitation to achieving saturation is discussed in terms of charge multiplication produced inside localised gas bubbles on the electrode surfaces. Field induced polarization of liquid molecules could be a contributing factor at high fields.

There appears to be realistic prospects of achieving saturation collection of charge, and possibly proportional multiplication, by appropriate design using advanced technology to ensure ultra-smooth surfaces and uniform electric fields.

Table of contents

Chapter 1

General introduction

1.1 Objectives 1

1.2 Dosimetry 2

Chapter 2

Charge transport in liquid

2.1 Ionization and charge transport in gases 6

2.2 General remarks on ionization and charge carriers in liquid . 9

2.3 Radiation and excess electrons in liquids 12

2.4 Review of theory for electron-ion recombination in liquids . 13

2.4.1 Jaffe theory 14

2.4.2 Lea theory 15

2.4.3 Onsager theory 16

2.4.3.1 Mozumder modification 17

2.4.3.2 A few comments on Onsager theory 20

2.4.4 Tachiya theory 23

2.4.5 Schiller theory 27

2.5 Models of electron transport in liquid 30

2.5.1 Introduction 30

2.5.2 Quasi-free electron model 31

2.5.3 Electron trap model 32

2.5.4 Self trapping electron model 34

2.5.5 Extension of the electron trapping model 35

2.6 Electron transport in liquefied rare-gases 36

2.6.1 Electron mobility and drift velocity 37

2.6.1.1 Field dependence 37

2.6.1.2 Dependence on molecular solute 40

2.6.1.3 Temperature dependence 41

Chapter 3

Electrical conductivity and transport properties of liquid hydrocarbons

3.1 Hydrocarbon liquids 43

3.2 Physicochemical properties of liquid hydrocarbons . . 43

3.2.1 Dipole moment 43

3.2.2 Polarity of bonds 44

3.2.3 Molecular polarizability 45

3.2.4 Intermolecular forces 47

3.3 Electron transport in liquid hydrocarbons 48

3.3.1 Electron mobility 49

3.3.1.1 Electric field dependence 50

3.3.1.2 Temperature dependence 54

3.3.1.3 Structure effect 57

3.2.2 Free-ion yields 60

3.3.2.1 Structure, temperature, and field dependence . . . 61

3.3.2.2 Methods of measurement of the free-ion yield . . . 64

3.3.3 Conduction-band energy 66

3.4 Electron transport in hydrocarbon mixtures 68

Chapter 4

Intrinsic conduction in liquid hydrocarbons

4.1 Introduction 72

4.2 Low field conductivity 73

4.3 High field conductivity 75

4.3.1 Electron emission 75

4.3.2 Dissociation and ionization induced by the applied electric field . 78

4.3.3 Ionization by collision 80

Chapter 5

Experimental studies with liquid ionization chamber

5.1 Introduction 83

5.2 Liquid ionization chamber (SS type) 84

5.3 Liquid ionization chamber (glass type) 88

5.4 Associated equipments 91

5.5 The choice of dielectric liquid 92

5.6 Purification of TMS 94

5.6.1 Chemical purification 94

5.6.1.1 Drying of TMS 95

5.6.1.2 Degassing of TMS 98

5.6.2 Cleaning and preparation of the liquid chambers . . . 98

5.6.3 Electrical purification 99

Chapter 6

Results and discussion

6.1 SS-parallel-plate ionization chamber 102

6.1.1 prestressing of the liquid 102

6.1.2 Time variation of the dark charge 105

6.1.3 Dark current 106

6.1.3.1 The high dark current 110

6.1.3.2 Effect of impurity 113

6.1.3.3 Stability of the current 115

6.1.3.4 Steps of applying the voltage 117

6.1.3.5 Dependence of the dark current on electrode area . . 118

6.1.4 Ionization current 120

6.1.4.1 Dependence of ionization current on liquid purity . . 124

6.1.4.2 Dependence of ionization current on electrode material . . 127

6.1.4.3 Dependence of ionization current on radiation intensity . . 130

6.1.4.4 Dependence of ionization current on electrode area . . 133

6.1.4.5 The current-noise ratio 135

6.1.4.6 Dependence of ionization current on liquid volume . . 135

6.1.4.7 The geometrical factor 141

6.1.4.8 'Apparent W-values' in liquid TMS 142

6.2 Glass-ionization chamber 149

6.2.1 Liquid pre-stressing 149

6.2.2 Dark current-field characteristic 151

6.2.3 Hysteresis effect 154

6.2.4 Ionization current 156

6.2.5 Estimation of the apparent W-value 158

6.2.6 Gas chromatography 161

6.3 Conclusion 163

6.4 Future work 164

List of figures

Figure (2-1): General current-field characteristic in di-electric liquid. 11

Figure (2-2): An electron, produced in ionization, diffuses away from its parent positive ion under the influence of their mutual attraction and the externally applied electric field. 11

Figure (2-3): Electron escape probability in liquid TMS as a function of the applied electric field. 19

Figure (2-4): Electron escape probability in liquid TMS as a function of ion separation. 19

Figure (2-5): The escape probability as a function of the initial separation for a variety of values of the mean free time. 25

Figure (2-6): The effect of applied electric field on the escape probability for a variety of values of the mean free time. $r/r_c = 0.2$. 25

Figure (2-7): The effect of applied electric field on the escape probability for a variety of values of the mean free time. $r/r_c = 0.4$. 26

Figure (2-8): The effect of applied electric field on the escape probability for a variety of values of the mean free time. $r/r_c = 1.0$. 26

Figure (3-1): The dependence of the drift velocity on the applied electric field in variety of liquid hydrocarbons with different mobility. 53

Figure (3-2): The dependence of the electron mobility on temperature in a number of liquid alkane different in their electron mobility. 58

Figure (3-3): The mobility dependence of liquid and solid methane on temperature near the critical point and the triple point. 58

Figure (3-4): Three dimensional representations of large hydrocarbon molecules with decreasing sphericity. 59

Figure (5-1): Liquid ionization chamber (Stainless-steel type). 85

Figure (5-2): The stainless steel ionization chamber and its auxiliary parts. 87

Figure (5-3): Liquid ionization chamber (Glass type). 90

Figure (5-4): The glass ionization chamber and its associated equipment. 93

Figure (5-5): Purification system for drying and degassing liquid TMS. 96

Figure (6-1): Dependence of dark current on time for liquid TMS using SS and TE electrodes. 104

Figure (6-2): Dependence of dark charge on time for liquid TMS using SS and TE electrodes. 107

Figure (6-3): Dependence of dark current on applied voltage for SS and TE electrodes. 109

Figure (6-4): Dependence of dark current on applied field for SS and TE electrodes. 111

Figure (6-5): Dependence of dark current per electrode spacing on applied field for SS and TE electrodes. 112

Figure (6-6): Variation of ln of dark current with the square-root of the field for two electrodes of different materials at high values of the electric field E. 115

Figure (6-7): Dependence of dark current on applied field for high and low purity samples of TMS. 116

Figure (6-8): Dependence of dark current-field characteristic on area of collector. 119

Figure (6-9): Net ionization current versus applied electric field for different electrode spacings, using SS electrodes. 122

Figure (6-10): Net ionization current versus applied electric field for different electrode spacings, using TE electrodes. 123

Figure (6-11): Dependence of ionization current-field characteristic on liquid purity for different electrode spacings. 126

Figure (6-12): Variation of net ionization current with electric field for electrodes of different materials, and electrode spacing of 2 mm. 128

Figure (6-13): Variation of net ionization current with electric field for electrodes of different materials, and electrode spacing of 5 mm. 129

Figure (6-14): Dependence of ionization current on applied field for different of radiation intensity, using SS electrodes of 2 mm separation. 131

Figure (6-15): Variation of net ionization current with distance from source for electrode separation, d=2 mm at different values of E. 132

Figure (6-16): Dependence of ionization current-field characteristic on area of the anode. 134

Figure (6-17): Variation of the ratio I^2_{ion}/I_d with applied electric field for two values of electrode spacing and two electrodes materials. 136

Figure (6-18): Net ionization current versus applied electric field for different electrode spacings, using SS electrodes. 138

Figure (6-19): Net ionization current versus applied electric field for

different electrode spacings, using TE electrodes. 139

Figure (6-20): Variation of net ionization current with sensitive volume for two electrode materials. 140

Figure (6-21): Variation of ionization current per Gxd with electric field for SS electrodes and different spacings. 143

Figure (6-22): Variation of ionization current per Gxd with electric field for TE electrodes and different spacings. 144

Figure (6-23): Variation of the `apparent W-value` with applied electric field for two values of electrode spacings and two electrode materials. 145

Figure (6-24): Dependence of the `apparent W-value` on electrode separation at a fixed electric field and two electrode materials. 148

Figure (6-25): Variation of the dark current with time for the glass chamber at two values of the electric field. 150

Figure (6-26): Dependence of the dark current on applied electric field for the glass chamber at two different values of electrode spacing. 152

Figure (6-27): Dependence of the dark current on applied electric field for the glass chamber at some values of electrode spacing. 153

Figure (6-28): Dependence of the dark current on the direction of application of the electric field. 155

Figure (6-29): Variation of the net ionization current with applied field for some values of electrode spacing. 157

Figure (6-30): Variation of the `apparent W-value` with electric field for the glass chamber at different values of the electrode spacing. 160

Figure (6-31): Gas chromatography analysis of liquid sample of TMS after the processes of prestressing of the sample. 162

List of tables

Table (2-1): Electron mobility and free ion yield in liquid hydrocarbons of linear chain molecules 21

Table (2-2): Electron mobility and free ion yield in liquid hydrocarbons of sphere-like molecules 22

Table (2-3): The mobility of electron and positive ion in rare-gas liquids. 38

Table (2-4): Some properties of rare-gas liquids. 39

Table (3-1): The effective range of electron-molecule interaction and the polarizability of sphere-like liquid hydrocarbons. 46

Table (3-2): The effective range of electron-molecule interaction for chain-like liquid hydrocarbons. 58

Table (6-1): Energy transmission factor for different electrode materials. 125

Table (6-2): Geometrical factor for two different electrode materials at various electrode spacings. 141

Table (6-3): Apparent W-values for two values of electrode spacings and different values of the electric field for the SS chamber fitted with the SS and TE electrodes. 146

Table (6-4): Apparent W-values for various values of electrode spacings at certain values of the electric field for the SS chamber fitted with the SS and TE electrodes. 146

Table (6-5): Apparent W-values for the TMS contained in the glass chamber at some values of the electric field. 158

Chapter 1

General introduction

1.1 Objectives

Since the classic experiments on charge transport in liquids by Townsend in the early 1930's there have been many attempts to devise practical ionization chambers for dosimetry applications in radiation protection and radiotherapy. Only very limited success has been achieved in non-noble liquids. It has not been possible to demonstrate, unambiguously, the saturation collection of ionization in parallel plate ion chambers or the controlled multiplication of charge when operated in the proportional counter mode. Varied mechanisms responsible for charge production have been proposed.

In the present study, a fundamental re-assessment is made of charge transport in organic liquids when used as di-electric in parallel plate ionization chambers with the intention of identifying better the mechanisms responsible for charge production in liquids subjected to applied electric fields with, and without, the presence of ionizing radiation. The ultimate objective of the study is to determine, using logical arguments based on theory and experiment, the reasons for the limitations to total charge collection and to make decisions on the potential for designing liquid filled radiation detectors for application in dosimetry.

1.2 Dosimetry

Historically, radiation dosimeters were first designed to have an instrumental response to ionizing radiation which simulated that of unit mass of soft tissue in the human body. In the 1970's, advances in radiobiology proved that the radiosensitive sites existed in the microscopic nucleus of the mammalian cell. Consequently, new dosimeters of micron dimensions were designed to simulate the response of the mammalian cell nuclei. This is the subject of microdosimetry. However, in the 1980's it became clear that the radiosensitive sites were of nanometre dimensions and were probably segments of the double-stranded DNA in the intra-cellular chromosomes. There is now a need for dosimeters with sensitive volumes of nanometre size (Watt et al, 1986, Watt 1997). Here, the use of liquid filled ionization detectors, with their large density advantage over gases, should facilitate the desired miniaturisation.

For dosimetry, the materials of the detector should be tissue-equivalent and arranged to ensure charged particle equilibrium in the sensitive volume. Organic liquids are typically sufficiently close to the atomic composition of soft tissue to be approximated as tissue-equivalent (e.g. Adamczewski 1965). There is a wide range of tissue substitutes available in solid, liquid and gaseous forms (ICRU Report 44, 1989).

Other attractions for employing a small detecting medium, by using a liquid chamber instead of a gas chamber, is the facilitation of the process of reaching the condition of equilibrium and the low polarity effects which are more favourable in liquid detectors than in gas detectors (Wickman and Nystrom 1992). This is in addition to the great reduction in the perturbation effects which are largely encountered in gas detectors (Adamczewski 1964).

Amongst other applications of liquid ionization chambers in dosimetry, these detectors have been used in mixed radiation fields since they have demonstrated different sensitivities for different qualities of radiation (Ladu and Pelliccioni 1966, Blance et al. 964). This LET (Linear Energy Transfer) dependent response of the liquid chamber may provide information on the individual type of radiation in a mixed radiation field. If the radiation field is a mixture of gamma and neutron fields, this dependence is limited by the proportion of the neutron component in that field since a liquid ionization chamber is more sensitive to gamma radiation than to neutrons (Chu et al. 1980).

In the field of radiation dosimetry, hydrocarbon liquids in particular have attracted special attention since they have some important properties viz:

i- High ion yield for unit absorbed energy.

ii- Some of these liquids exhibit a high electron mobility.

iii- Very low permanent dipole moment approaching to zero.

iv- High density close to 1 $g.cm^{-3}$.

However, the employment of liquid in dosimeter is accompanied by several problems. This is in addition to our lack of knowledge of the exact mechanisms of the charge transport in these substances. The most important problem of using liquid lies in the inability to attain total charge collection despite the high field application with the consequence of electrical breakdown. Another common problem is the difficulty of obtaining a very pure liquid and maintaining its purity over a long time since the conductivity of liquid is highly sensitive to impurities. In addition, extra high purity is known to result in a remarkable improvement to the physical transport of charge in liquids. In fact, the problem of impurity can be considered at least partially solved as

the conductivity approaches the order of 10^{-17}-10^{-19} $\Omega^{-1}.cm^{-1}$ which could be obtained if a special care is tendered in the processes of purification.

Due to the fact that liquids have a density almost three orders of magnitude higher than that of gases at normal pressure, the distances between the ions formed in the track of an ionizing particle are much shorter than in the gas. This means that recombination of ions in liquid is more probable than in gas. An additional problem of using liquid in a dosimeter is the possibility of losing liquid by evaporation. This is more likely to be the case for warmed liquids which have a boiling point near that of room temperature. This fact can influence the measurement of charge by tending to change the hydrostatic pressure inside the liquid chamber. Evaporation is expected to be much more intensive in the immediate vicinity of the sharp points which are spread throughout the surface of the high field electrode.

Although hydrocarbon liquids have very low dipole moments, the eventual limitation to transport is attributed to the existence of dipole moments induced by the strong action of the high electric field. Such a dipole may also play an essential part in charge transport at high electric fields.

The present work is concerned with the study of the mechanism of charge transport and collection in di-electric liquid. The investigation is aimed mainly towards identifying and finding a solution to the fundamental problems associated with the difficulty of attaining saturation charge collection in liquid. Scientific justification for the conclusions is made on the basis of the experimental results.

Plateaux of saturation charge collection in ionization chambers have been observed for some liquified inert gases but not for liquid hydrocarbons. For experimental studies, the use of liquids at room temperatures are clearly more practical than those which are

liquid at cryogenic temperatures. Despite the lack of a defined plateau in these liquids, multiplication is attainable at large field strengths (Haidara and Denat 1990).

The approach used to identify and investigate the fundamental problem involved the use of two liquid ionization chambers. The di-electric liquid selected in the present investigation was high purity tetramethylsilane (TMS). This liquid was selected for several reasons: it is almost tissue equivalent for photons; the fast agitational velocity, ~ 3.10^5 cm/s; its high di-electric strength 1.84 F/m; the relatively high free ion yield of about 0.60 ion pair/100eV, and long electron life-time ~ μ sec but dependent on purity. There are well-known limitations to the collection of charge, attributable to recombination in the liquid and to loss of electrons in impurity traps.

The recombination problem can be overcome in gases by application of a sufficiently high electric field which is required for attaining saturation. The upper limit to the field is dependent on the condition of the electrode surface. In other words, the exact yields attained at high electric fields are masked by the extra charges produced through the processes of charge multiplication. The latter phenomena is thought to take place inside vapour bubbles formed in the immediate vicinity of the sharp points covering the surface of the high field electrode. This, in fact, imposes some limitations on the interpretation of the experimental results since the actual values of the measurements are subject to some ambiguity.

In accordance with the present investigation and the results obtained, it is deduced that the latter model is likely to be the most important limiting factor to attainment of total saturation charge collection.

Chapter 2

Charge transport in liquids

2.1 Ionization and charge transport in gases

For a better understanding of charge transport in liquids it is convenient to consider first of all the behaviour of charge carriers in gases. This is because of the perceived similarity of these processes in the gaseous and liquid state. Moreover, gas is a less complicated matter than liquid because of the almost negligible level of intermolecular forces.

The early observation of charge carriers through gases exposed to high energy X-rays was reported by Thomson and Rutherford in (1896). Later a theoretical treatment of electrical conduction in ionized gas was published (Thomson 1899).

A gas in its normal state is regarded as a good insulator. However, under the action of a sufficiently high electric field and as a result of ionizing radiation, gas can become a conductor. The transition from the insulating medium to an almost completely conducting state, is called electric breakdown.

Interaction between the ionizing radiation and atoms of a gas appears in the form of two processes, ionization and excitation. These processes result in liberation of positive and negative ions which are randomly distributed in the medium. For heavy ionizing particles the majority of ions are distributed inhomogeneously. They may undergo preferential recombination in which the negative electrons recombine with

their parent ions (Bragg et al. 1906). The release of charge carriers produces no signal provided the gas, confined between two conducting plates, is not subject to an electric field. At this stage the electrons and positive ions are in random motion with an average kinetic energy equal to the mean thermal translational energy of the gas molecules ($3k_BT/2$). In general charge carriers in the gas collide with each other as they diffuse away from regions of high density. In this way charge transfer, attachment, neutralisation, and recombination may take place. At low electric field, the random motion of the charge carriers will be disturbed resulting in a small general drift in a direction parallel to the electric field. At the same time their agitation energy, especially for electrons, is increased above the mean thermal value of $3k_BT/2$. When the electric field is increased, the effects of recombination and space charge are reduced due to the high drift velocity, ϑ_d, acquired by both the positive and negative charge carriers. Because of the big difference in the mass between individual electron and positive ions and a larger interaction cross section in the case of the positive ion, the drift velocity of electrons is much higher than that of positive ions. As a result, electrons are collected at the anode before the positive ions have made any significant move towards the negative electrode. At a sufficiently high electric field, recombination is overcome and the total collection of the charge carriers in a gas may be established. The value of this saturation current is calculated by knowing the density of charges, i.e.

$$I_s = n_0.e_0.A.d \qquad (2\text{-}1)$$

where A is the collector area, e_0 is the electronic charge, n_0 is the initial number of

charges released per second by the ionizing agent in unit volume, and d is the inter-electrode spacing. The average drift velocity in gas ϑ_d varies with the applied electric field and the gas pressure. It is given in the form

$$\vartheta_d = \mu E/P \qquad (2\text{-}2)$$

where μ is the mobility of the charge carriers, P is the pressure and E is the electric field strength. A typical value of the mobility for the positive ion in gas is of the order of 1 cm^2/Vs. at 760 torr. Thus at P=1 torr and E=1 kV/cm the electron drift velocity is $\vartheta_d=10^3$ cm/s. Therefore the ion transit time across 1 cm gap is approximately 1 ms. However, with respect to an electron of much lower mass and thus higher mobility this time is of the order of microseconds. These values depend on the applied electric field, the nature of the gas and its pressure. If the applied field is higher than the value at which saturation collection of charge occurs electrons released in the primary ionization might gain enough energy between collisions to produce secondary electrons. These electrons are indistinguishable from the original electrons produced by the primary track of ionizing particles in the gas. The persistency of these processes at sufficiently high fields may lead to gas multiplication. The typical value of the applied field required for gas multiplication at 760 torr is in the region of 10^5 V/cm.

In low pressure gases the interaction mean free paths of electrons and positive ions moving in the gas medium is large with respect to the gap between the electrodes. Thus, saturation is readily achievable. On the other hand gases under high pressure have proved to be much more complex than originally anticipated. In such cases, and

due to the high density, various types of recombination, such as preferential, columnar, and volume recombination, are involved. This means achieving saturation collection of charge is a more difficult task. For example, a gradual increase in the pressure of argon or xenon gas results in a continuous reduction in the width of the plateau of saturation (Pisarev et al. 1973). When the pressure approaches the value 7.6×10^4 torr, the plateau disappeared.

2.2 General remarks on ionization and charge carriers in liquid.

The first observation of charge carriers, made in irradiated liquid vaseline, was first reported by Thomson around the turn of the 20th century (Thomson 1897). He remarked that the increase of electrical conductance of the liquid was the result of high energy irradiation. Later a similar effect, using radium rays, was observed by Curie in 1902.

As charged particles slows down in a liquid medium, some ions are created in clusters. For a highly energetic particles the overall picture is a significant inhomogeneous distribution of ions. In each ionic group, due to the strong coulomb force, a large fraction of the ions undergo initial or geminate recombination. This recombination occurs in a relatively short time period, of the order of several picoseconds, immediately after ionization (Giveranud et al. 1992). In the absence of an electric field, the ions recombine, neutralise, or otherwise lose energy in elastic and inelastic collisions until they eventually thermalise. The fraction of electrons that escape the initial recombination can be collected at the anode. Under the influence of the electric field more ions are freed from clusters and a homogenous distribution is

gradually attained. At this stage volume recombination, general recombination, has commenced. The general recombination in liquid tetramethysilane (TMS) was found not to exceed 2% in a pulsed radiation field and at dose rates up to 7 Gy/min (Wickman and Nystrom 1992).

The number of free ion yields in liquid is a property of the medium. It depends on the initial formation and distribution of the ions (Schmidt and Allen 1968, Schmidt and Allen 1970). Furthermore it is affected by the temperature (Onsager 1938), di-electric constant, impurities, and the external electric field strength (Mozumder 1974b, Bartczak and Hummel 1986). It is not influenced by the dose rate (Wickman and Nystrom 1992). The temperature dependence in liquids was found to be as small as 0.2% $^{\circ}C^{-1}$ (Wickman and Nystrom 1992).

In a high density liquid, the apparent unattainability of the saturation current was explained on the basis of columnar recombination in which electrons and positive ions are formed in a cylindrical distribution along the track of ionizing particles (Jaffe 1913). This type of recombination is reduced by an appreciable increase in the electric field. If the electric field is strong enough, a homogeneous distribution of the ions in the medium is attained. The general behaviour of the ionization current in the liquid with respect to the electric field is shown in the figure (2-1). It has been claimed that the ionization current in liquids depends on the radiation intensity, the energy of the incident radiation (Pao 1943), the sensitive volume of the liquid, and the electrode area. It is independent of the electrode material (Januszajtis 1963).

The oversimple view might lead to the conclusion that saturation collection in liquid depends purely on the application of a high electric field. However, studies carried out in liquids, up to very high field strengths, have not revealed charge saturation

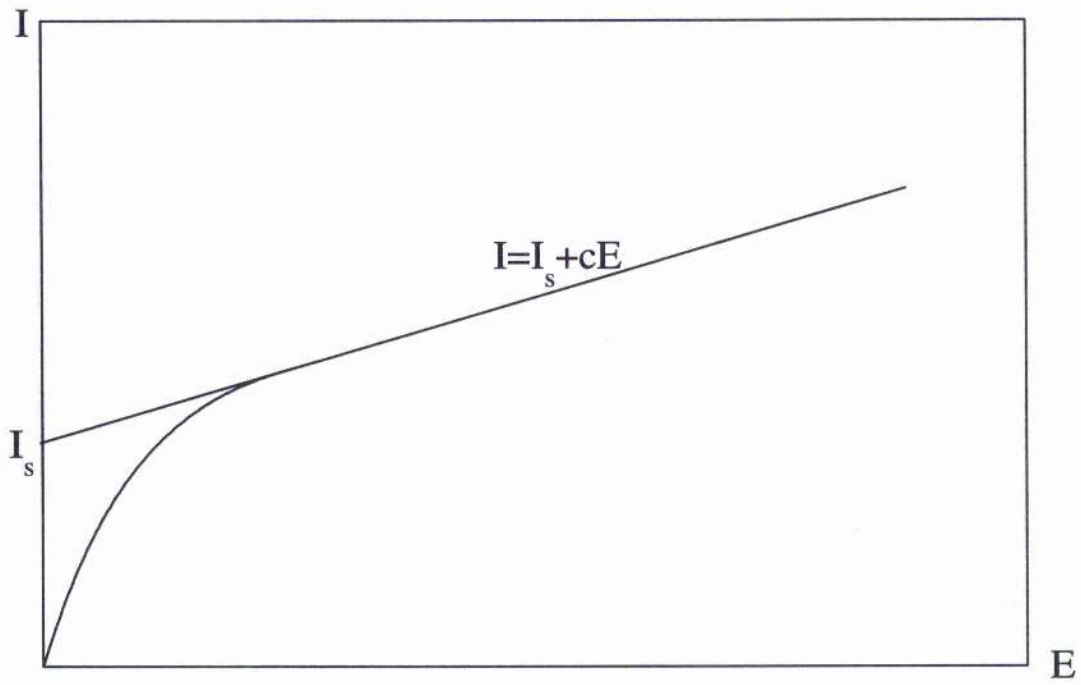

Fig(2-1): General Current-Field characteristic in dielectric liquid

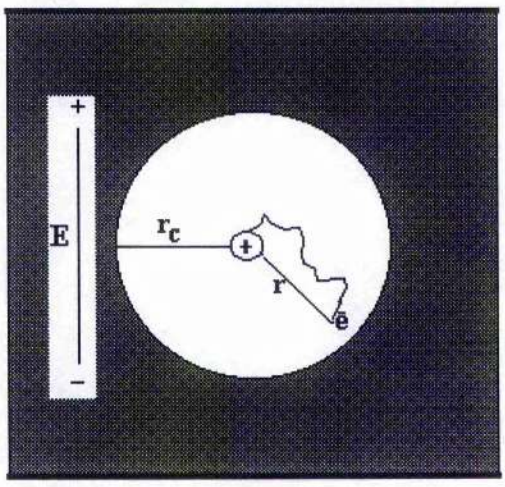

Fig(2-2): An electron produced in ionization diffuses away from its parent positive ion under the influence of their mutual attraction and the externally applied electric field.

characteristics.

2.3 Radiation and excess electrons in liquids

Radiation sources, X-ray generators, and accelerators have been used in the study of electron transport and radiation-induced conductivity in liquids. The liberation of excess electrons in liquids has been accomplished using a variety of techniques including field emission, photoionization, radiolysis, and ionization. Thermionic emission at ordinary temperatures for cathodes in contact with di-electric liquids has also been observed (Baker and Boltz 1937, Le Page and Du Bridge 1940). The principle of field emission is that, if a voltage is applied on a sharp point made of an appropriate material, the intense electric field formed at the point causes electrons to be stripped away from the atoms there and emitted from the tip. The magnitude of the required voltage for electron emission is directly proportional to the tip radius. This phenomenon is attributed to the quantum tunnelling effect. Recently silicon microtips, only a few micrometres in height with a tip radius of about ten nanometres have been fabricated (Prewett 1997). With such a radius the required voltage for emission is as small as 50-60 V. Photoemission produced by a short pulse of UV radiation has been used by many workers as a method of injecting electrons into the liquid. In this method, electrons are ejected from the surface of a metal cathode of sufficiently low work function. Minday used this method to measure the mobility of electrons in liquid argon (Minday 1971a). The electrons were produced by illuminating a thin film of barium, deposited on a quartz window, by means of ultraviolet radiation from an 85 W mercury discharge lamp. The deposition of barium was performed by resistively

heating, under a vacuum, an iron-clad barium wire. The measured photocurrents were typically (10^{-11}-10^{-8}) A. Later the same technique was adopted (Eibl et al. 1990, Lamp et al. 1990) employing a gold-sputtered quartz plate and a pulse of ultraviolet light emitted from a Xe-flash lamp. With a pulse duration of 1 μs, and a repetition rate of (0 to 10) Hz, the number of excess electrons injected into the liquid, at an electric field of 4 V/cm, was 4×10^3. At a field of 50 V/cm the number of excess electrons was 5×10^4. For special studies X-ray generators (Holroyd and Sham 1985, Shinsaka et al. 1988) and radioactive sources have been used (Munoz et al. 1986, Benetti et al. 1993, Aprile et al. 1993, Carugno et al. 1991). In the latter case, emitters are either located outside or deposited inside one electrode. Radiation sources can also be dissolved in liquid in order to reduce interaction with the wall materials.

In using one of the aforementioned techniques, electrons can be created in the di-electric medium between two electrode plates of the measuring cell. The resulting current flows through the external circuit.

2.4 Review of theory for electron-ion recombination in liquids

Shortly after the observation of charge carriers in an irradiated liquid, the difficulty in obtaining a saturation current was reported (Curie 1902). Since then, and in an attempt to explain the electron-ion collection processes in liquids, a number of theories have been developed. However, theoretical investigations have focused on the analysis of recombination processes and their field dependence.

2.4.1 Jaffe theory

In Jaffe's classical treatment, the ionization current was assumed to be represented by the sum of two current components (Jaffe 1908). Both components are functions of the applied field with a stronger dependence for the low field one. For sufficiently high electric fields the latter component should give rise to saturation. This assumption was replaced five years later by a new theoretical description of the ionization phenomenon in liquid (Jaffe 1913). In this theory the difficulty in securing saturation was attributed to the columnar recombination of ion pairs distributed in a cylindrical configuration along the track of a heavy ionizing particle. Jaffe, in his physical treatment, assumed that both types of charge carriers have the same mobility and diffusion constant. The mathematical difficulties involved in solving the differential equation required Jaffe to introduce further approximations by first considering only diffusion, and later only recombination. This treatment led to the following equation:

$$1/I = (1/I_s)[1+cf(x)] \qquad (2\text{-}3)$$

where I is the ionization current, I_s is the saturation current, and c is a constant that takes into account parameters such as diffusion, recombination, and the initial number of ions created. f(x) is a function of 1/E at high field strengths. If 1/I is plotted as a function of 1/E a straight line should be obtained in the region of high electric field starting from a certain value. Furthermore, the value of $1/I_s$ is represented by the interception point with the 1/I axis. Although this theory was formulated for heavy charged particles in gases, it has also been tried in liquid applications (Mathieu 1967,

Giova et al. 1967, Schmidt 1970, Duhm et al. 1989).

In 1952, Kramer criticised the application of Jaffe theory to liquids on the basis that charge recombination in liquid plays a more significant role than in gas. However, Kramer's theory, developed for liquids, differs significantly from Jaffe's only at low field strengths.

2.4.2 Lea theory.

In 1934, Lea proposed a similar treatment to that of Jaffe but with the difference that the cylindrical distribution of the ions was replaced by a spherical distribution. According to this model ions are created, initially, in groups as a result of secondary electrons, δ-rays, produced at very short distances from the primary tracks. In each group preferential recombination in which the electron returns to its parent positive ion occurs. As a result of diffusion, ions from different clusters start to interact forming columns which progressively expand into a uniform distribution. Lea investigated, using γ-rays, the ion collection in gases at different pressures. He concluded that in liquid almost 30% of the ions, that have been created by secondary electrons, are extractable by the field. However, a much higher collection efficiency of ions was found, in the same year, by Mohler and Taylor in liquid carbon disulphide irradiated by X-rays (Mohler and Taylor 1934). This result was later confirmed for liquid hexane irradiated by low energy X-rays (Adamczewski 1939). From the trend of the ion collection ratio observed at intermediate field regions in his experiment, he predicted that a field strength of the order of 100 MV/m would be required for total collection of the initial charges in liquid.

2.4.3 Onsager theory

Four years after the presentation of Lea's theory, Onsager treated the problem of geminate recombination in high pressure gases ionized by low LET radiation (Onsager 1938). In this theory he adopted Lea's basic model with the assumption that ions and electrons are generated in isolated pairs. He estimated the probability of escape of an ion pair diffusing under the influence of their mutual Coulombic attraction in an externally applied electric field, figure (2-2). In the absence of the electric field the escape probability is given by:

$$P(r)=\exp(-r_c/r) \qquad (2\text{-}4)$$

where r is the "initial separation" or the average distance between the ion pair after thermalization, and r_c is "Onsager distance" which represents the critical distance at which the coulomb attraction force between the ion pair equals the thermal energy of the electron k_BT. For an electronic charge, e, in a medium of di-electric constant ε, it is given in the form

$$r_c=e^2_0/\varepsilon k_BT \qquad (2\text{-}5)$$

The approximate value of the Onsager distance in liquid hydrocarbons at about 300 K is 3.5 nm (Dodelet et al. 1972).

In the presence of an electric field the ionic escape probability is represented by a series in r and E which is given by

$$P(r,\theta,E) = \exp\left[-\frac{r_c}{r} - ry\right] \sum_{m,n=0}^{\infty} y^{m+n} \frac{r_c^{\,m} r^{\,n}}{m!\,(m+n)!} \qquad (2\text{-}6)$$

with

$$y(\theta,E) = \frac{e_0 E}{2k_B T}(1+\cos\theta) \qquad (2\text{-}7)$$

where E is the electric field strength, θ is the angle between the direction of the field and the shortest distance between the electron and the positive ion, y is a function of reciprocal length, and T is the absolute temperature.

2.4.3.1 Mozumder modification

Later, the Onsager formula was rearranged by Mozumder for easy numerical evaluation of ion escape probability (Mozumder 1974). The new general expression is given in the following form:

$$P(r,E) = 1 - (2\zeta)^{-1} \sum_{s=0}^{\infty} A_s(\eta) A_s(2\zeta) \qquad (2\text{-}8)$$

where $\zeta = e_0 Er/2k_B T$, $\eta = r_c/r$, and the coefficient A_s is given by,

$$A_{s+1}(\eta) = A_s(\eta) - \exp\left(-\frac{\eta}{(s+1)!}\right) \qquad (2\text{-}9)$$

$$A_0(\eta) = 1\text{-}\exp(-\eta) \qquad (2\text{-}10)$$

Equations (2-8) to (2-10) may be easily solved by computer to yield the P(r,E). Results were calculated in the present work for liquid tetramethylsilane (TMS). The initial separation, r = 21 nm, and the Onsager distance, r_c = 31.3 nm, for liquid TMS, were taken from literature (Schmidt and Allen 1968, Duhm et al. 1989). The variation of electron escape probability with electric field strength, in liquid TMS at room temperature and up to 1 MV/cm is shown in the fig (2-3). From this figure, it is clear that almost 92% of the electrons escape recombination when the applied electric field approaches 200 kV/cm. These results appears to be consistent with the present work, see chapter 6. For total charge collection, fields of several orders of magnitude higher are required.

The dependence of the escape probability on the initial separation of the ions in liquid TMS, at room temperature and with an applied field of 100 kV/cm is shown in figure (2-4). The relationship shown in the figure (2-4) suggests that the molecular structure of liquid may play a controlling role. This is because of the dependence of the structure on the ion separation distance.

Structural studies of fast-electron tracks in a cloud chamber revealed that the majority of clusters contain only one ion pair and only 1% contain more than five ion pairs (Chu et al. 1980). This result seems to be consistent with the Onsager theory. In fact, in clusters of multiple ion pairs, ions may undergo cross recombination in addition to geminate recombination

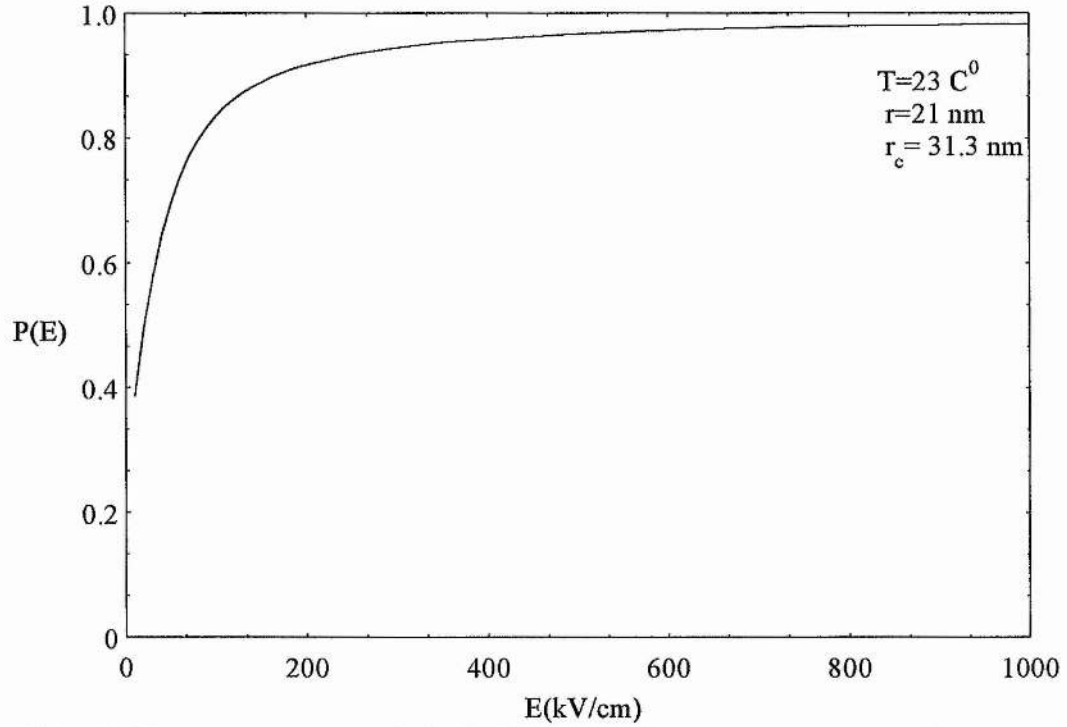

Fig(2-3): Electron escape probability P(E) in liquid TMS as a function of applied electric field.

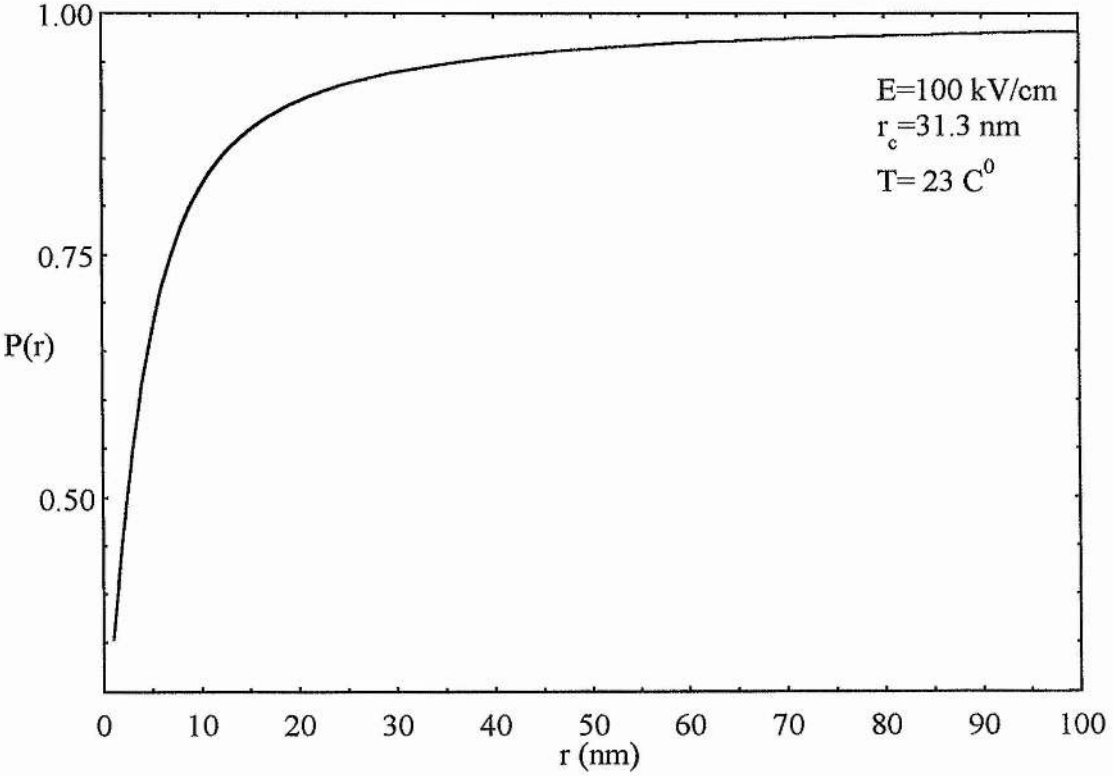

Fig(2-4): Electron escape probability P(r) in liquid TMS as a function of ion separation.

2.4.3.2 A few comments on Onsager theory

In a study of a liquid ionization chamber applied to neutron dosimetry, the theoretical models developed by Jaffe and Onsager were compared (Chu et al. 1980). Under the same experimental conditions Onsager theory seemed to be more appropriate for use in liquid applications. However, the use of the Onsager theory in the high mobility liquids, or liquids in which the electron transport mean free path is relatively large, such as liquid argon (Scalettar et al. 1982), methane (Nakamura et al. 1983), neopentane, and tetramethylsilane (Choi et al. 1982) appears to be questionable. In conclusion the Onsager theory is applicable only in liquids which feature an electron transport mean free path which is short compared with the Onsager distance. The Onsager distance is found, experimentally, to increase with decreasing temperature and di-electric constant (Dodelet et al. 1972). High mobility liquids seem to sustain larger free ion yields as shown in tables (2-1) and (2-2) for liquid hydrocarbons.

The break down of the Onsager theory in these liquids may be related to the existence of more than one ion pair in the majority of ion clusters the fact which is not consistent with the main assumption of Onsager theory. Values of the free ion yields of liquid hydrocarbons are shown in appendix B along with some other properties.

When the transport mean free path of electrons slowing down in liquid is small, thermalization processes can occur within the Onsager region of radius r_c. This fast thermalization is believed to be the cause of high recombination rates in the low mobility liquids.

Among liquid hydrocarbons, tetramethylsilane (TMS) is known to have a high electron mobility. However, many workers have been unable to detect saturation in this liquid.

Table (2-1): Electron mobility and free ion yield in liquid hydrocarbons of linear chain molecules.

Compound	Formula	μ_e (cm^2/Vs)	T(K)	Ref**.	G_{fi} ($/10^2$ eV)	T (K)	Radiation*	ε (F/m)	Ref**
Methane	CH_4	$4.20x10^{+2}$	123	121	$9.40x10^{-1}$	298	HE X-Rays	1.44	40
Ethane	C_2H_6	$3.70x10^{+1}$	298	37	$1.30x10^{-1}$	183	HE X-Rays	1.80	104
Propane	C_3H_8	$2.63x10^{+0}$	297	36	$4.30x10^{-1}$	297	HE X-Rays	1.90	40
n-Butane	C_4H_{10}	$4.00x10^{-1}$	296	114	$1.90x10^{-1}$	296	HE X-Rays	1.76	113
n-Pentane	C_5H_{12}	$1.60x10^{-1}$	296	114	$1.45x10^{-1}$	296	HE X-Rays	1.84	113
n-Hexane	C_6H_{14}	$8.00x10^{-2}$	296	3	$1.30x10^{-1}$	296	HE X-Rays	1.89	113
n-Heptane	C_7H_{16}	$4.60x10^{-2}$	296	98	$1.30x10^{-1}$	296	HE X-Rays	1.92	110
n-Octane	C_8H_{18}	$4.00x10^{-2}$	296	98	$1.20x10^{-1}$	296	HE X-Rays	1.94	113
n-Nonane	C_9H_{20}	$2.80x10^{-2}$	294	40	$1.20x10^{-1}$	296	HE X-Rays	1.97	113
n-Decane	$C_{10}H_{22}$	$2.50x10^{-2}$	296	29	$1.20x10^{-1}$	296	HE X-Rays	1.99	113
n-Undecane	$C_{11}H_{22}$	$2.40x10^{-2}$	296	40	$1.30x10^{-1}$	296	HE X-Rays	2.00	40
n-Dodecane	$C_{12}H_{24}$	$2.00x10^{-2}$	295	39	$1.20x10^{-1}$	295	HE X-Rays	2.01	40
** Numbers of references refer to those of appendix B,					* HE: high energy				

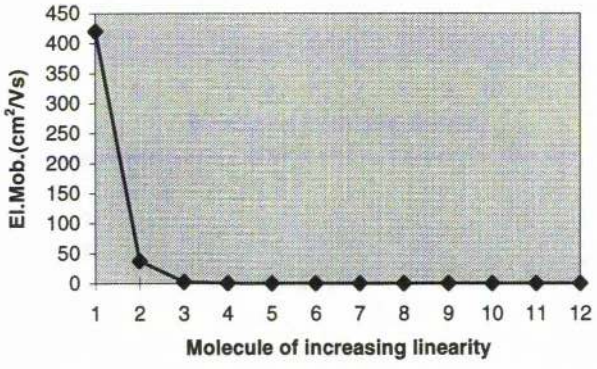

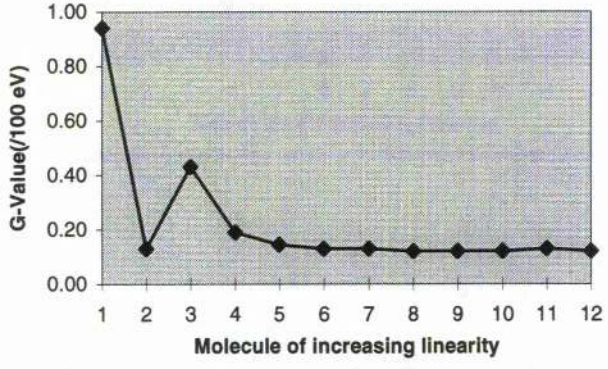

Table (2-2): Electron mobility and free ion yield in liquid hydrocarbons of sphere-like molecules.

Compound	Formula	$\mu_e(cm^2/Vs)$	T(K)	Ref**.	${}^0G_{fi}(/10^2eV)$	Radiation*	ε (F/m)	Ref**.
Methane	CH_4	420	123	121	$9.40x10^{-1}$	HE X-Rays	1.440	40
Tetramethylsilane	$SiMe_4$	100	297	118	$7.40x10^{-1}$	HE X-Rays	1.840	113
Neopentane	CMe_4	60	294	14	$9.00x10^{-1}$	HE X-Rays	1.777	135
2,2,3,3 Tetramethylbutane	Me_3CCMe_3				$8.00x10^{-1}$	HE X-Rays	1.840	28
2,2,4,4 Tetramethylpentane	$Me_3CCH_2CMe_3$	24	295	28	$8.30x10^{-1}$	HE X-Rays	1.980	28
2,2,5,5 Tetramethylhexane	$Me_3C[CH_2]_2CMe_3$	12	293	28	$6.70x10^{-1}$	HE X-Rays	1.970	28
2,2,6,6 Tetramethylheptane	$Me_3C[CH_2]_3CMe_3$				$4.70x10^{-1}$	HE X-Rays	1.970	28
2,2,7,7 Tetramethyloctane	$Me_3C[CH_2]_4CMe_3$				$3.40x10^{-1}$	HE X-Rays	2.130	28
2,2,3,3 Tetramethylpentane	$Me_3CCMe_2CH_2CH_3$	5.20	295	28	$4.20x10^{-1}$	HE X-Rays	2.050	28
Cyclohexane	$Me_3CCH{=}CH_2$	0.45	294	28	$1.50x10^{-1}$	HE X-Rays	2.022	113
** Numbers of references refer to those of appendix B, * HE: high energy.								

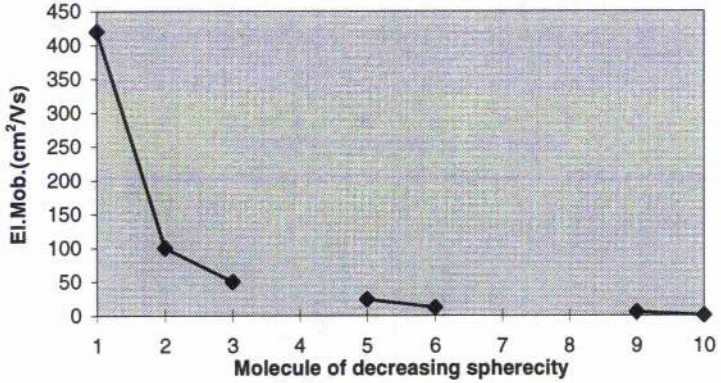

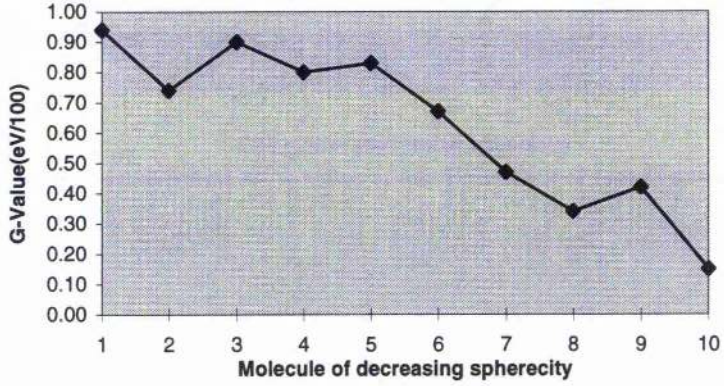

On the other hand, saturation was attained in rare gas liquids such as liquid argon which is characterized by a mobility of several orders of magnitude higher than that of liquid TMS (Miller et al. 1968, Yoshino et al. 1976). The lack of saturation in liquid TMS was attributed to the high rate of recombination caused by the large concentration of thermalized ions. The rapid thermalization in liquid TMS was ascribed to the excitation of abundant low energy levels of the TMS molecules (Duhm et al. 1989). This low energy excitation mode is expected to be negligible in liquid argon which results in a quasifree movement of electrons. As thermalization increases a space charge of thermalized ions in the close proximity of the track particle is formed. This phenomenon would partially suppress the effect of an externally applied electric field resulting in more events of recombination.

2.4.4 Tachiya theory

In 1988, Tachiya succeeded in extending the Onsager theory to the case where the electron interaction mean free path is comparable to, or larger than, the Onsager distance, r_c (Tachiya 1988b). In his paper he studied the problem of geminate electron-ion recombination by performing Monte Carlo calculations of the electron escape probability as a function of both the electron interaction mean free path and the initial separation of the ion pair. In his numerical computation the electron interaction mean free path was considered to represent the strength of the electron scattering by the liquid atoms. Assuming a constant velocity of the electron and for the ease of computer calculation, the mean free path was replaced by the mean interaction time of the electron with the liquid atoms. The results of the numerical calculations were

found to be comparable with those obtained by Onsager's method only in the case where the electron interaction mean free path (or mean interaction time) is negligibly short when compared with the Onsager distance r_c. In the limit of long mean free path the Tachiya escape probability was much higher than the Onsager one. In the absence of the electric field and for a variety of values of mean interaction time τ, the electron escape probability, P, was found to be sub-linearly proportional to the initial separation of ions r. These data together with the Onsager predicted result are presented in fig (2-5). The effect of an applied electric field on the escape probability for a variety of values of the mean interaction time τ, and a constant initial separation was also investigated. The result of this study, for three values of the initial separation, is shown in figures (2-6, 7, 8). In all these figures the escape probability increases with increasing electric field. Furthermore, the escape probability for a constant initial separation and a fixed value of the applied electric field also increases with the mean free time. For liquid TMS the initial separation, r, was assumed to be equal to r = 12.2 nm ($r/r_c = 0.4$). Tachiya followed his numerical investigation by a theoretical treatment of geminate electron-ion recombination (Tachiya et al. 1989). Later, he derived an analytical expression for the escape probability in the limit of a large mean free path (mean interaction time) by using the concept of diffusion in energy space rather than the initial separation of ion pairs. His consideration was based on the following: in the limit of a small mean free path the electron energy is not significant since it is rapidly lost to the medium due to the frequent scattering by the liquid molecules. In the case of large mean free paths the electron is allowed to revolve repeatedly in its orbit around the positive ion, presumably due to the coulomb force, before it is scattered by the liquid molecules. Thus due to the infrequent scattering events in the latter case

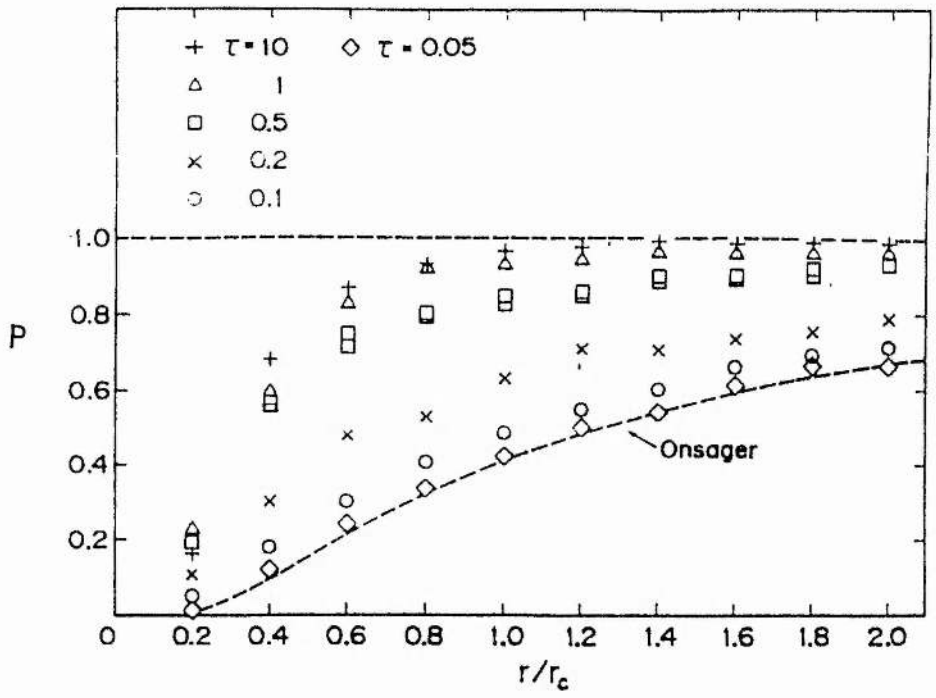

Figure(2-5): The escape probability P as a function of the initial separation r for a variety of values of the mean free time τ, r_c is the Onsager distance. (Tachiya 1988)

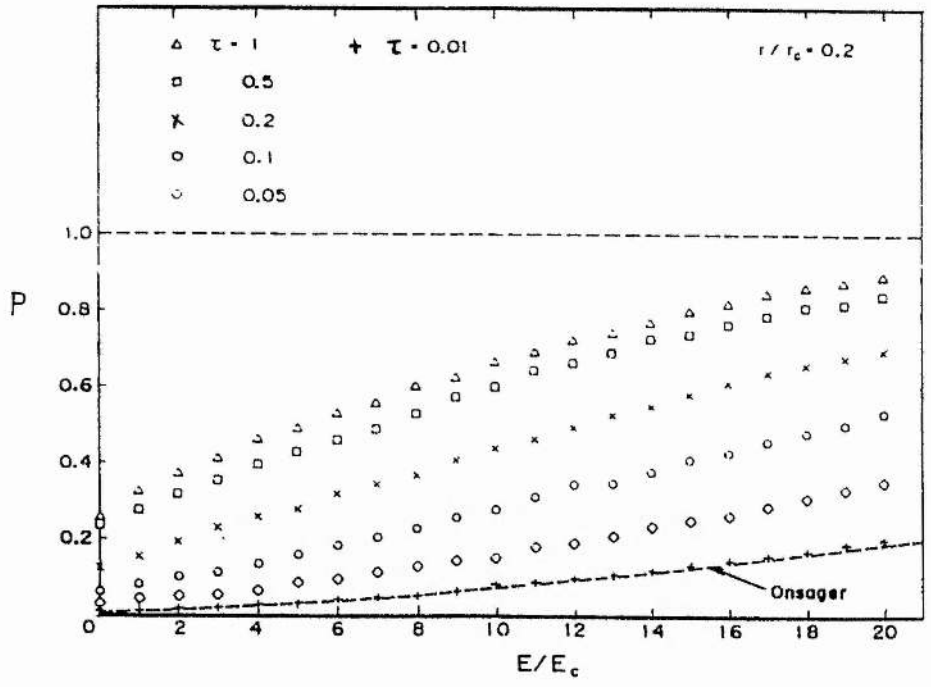

Figure (2-6): The effect of the applied electric field E on the escape probability P for a variety of values of the mean free time τ. $E_c=e_0/\varepsilon r_c^2$. The initial separation is $r/r_c=0.2$. (Tachiya 1988)

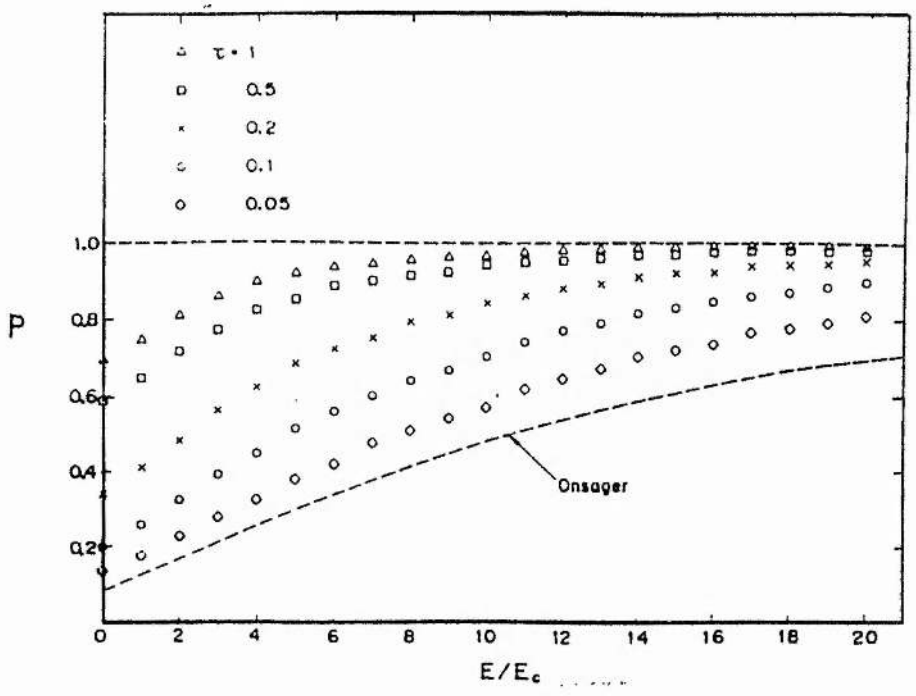

Figure (2-7): The effect of the applied electric field E on the escape probability P for a variety of values of the mean free time τ. $E_c=e_0/\varepsilon r_c^2$. The initial separation is $r/r_c=0.4$. (Tachiya 1988)

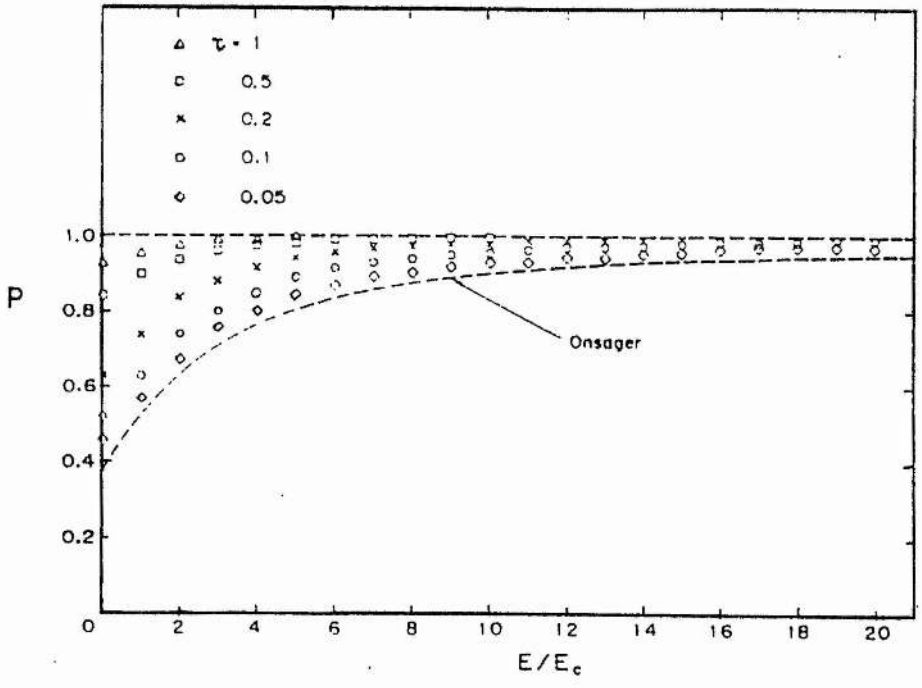

Figure (2-8): The effect of the applied electric field E on the escape probability P for a variety of values of the mean free time τ. $E_c=e_0/\varepsilon r_c^2$. The initial separation is $r/r_c=1.0$. (Tachiya 1988)

the energy relaxes slowly and becomes an important factor. The Tachiya theoretical formula for the escape probability is given in the following form.

$$P(E_0/k_\beta T) = \frac{\int_{-\infty}^{E_0\beta} \exp(-x)^{3/2} dx}{\int_{-\infty}^{0} \exp(-x)^{3/2} dx} \qquad (2\text{-}11)$$

where E_0, is the initial electron energy and $\beta = 1/k_BT$. Tachiya acknowledged that his theoretical treatment does not allow for the angular momentum which, in hindsight, could be of considerable importance.

2.4.5 Schiller theory

In 1992, Schiller proposed a new theoretical description for geminate ion-electron recombination in nonpolar liquids (Schiller 1992). The solitary ion-electron pair, with an electron energy below about 1 eV, is regarded as a high Rydberg state of an H-like atom embedded in a relaxing and fluctuating di-electric continuum. This simple model was adopted in his previous theoretical investigation of condensed polar media with the difference being that the electron-ion pair is considered as the ground state of the H-like atom (Schiller 1990). The low energy electron is said to be moderated when its energy, as a result of slowing down in liquid, approaches the thermal energies in the di-electric medium. Thermalized electrons are recombined with the negative ions and neutralized; or otherwise are associated with the molecules of the liquid. The latter process is called electron solvation where the solvated electrons result in polarisation

of the di-electric medium. This di-electric polarisation is encountered in condensed polar media and is described in the form of a deep polarization potential well. The electron escape probability is a function of the depth of the polarization potential well in the medium. It is also influenced by the energy fluctuation in the di-electric medium. In the derivation of the escape probability in condensed polar media, the electron was considered to be energetically capable of leaving the parent positive ion only when its energy is elevated by the energy fluctuation in the medium to a value which exceeds the potential energy in the bound state (Schiller 1990). In fact this condition may not be enough since electrons can escape this fate as they may be influenced by the polarization potential resulting from similar localized solvated electrons. This form of trapping is called self trapping which will be encountered later. The electron escape probability in condensed polar media is then given by

$$P=\frac{1}{2}erfc(\frac{-2E_1}{\sigma}) \qquad (2\text{-}12)$$

with

$$\sigma^2=k_B C_v T^2 \qquad (2\text{-}13)$$

where "erfc" means the complementary error function and C_v is the heat capacity at constant volume of the electron's environment (J/K). E_1 is the electron energy in the ground state of the possible states given by the general formula:

$$E_n = \frac{-me^4}{2\pi\hbar^2\epsilon_s^2 n^2} \tag{2-14}$$

where m and e are electron mass and charge, respectively, $2\pi\hbar$ is the Planck's constant, and ϵ_s is the statistical relative permittivity of the di-electric medium. In the case of nonpolar liquids the polarization well is not deep, a fact which abolishes the importance of the di-electric relaxation found in condensed polar media. This new consideration requires some alteration to the basic model and in the method followed for calculating the escape probability. The ion-pair in this case was assumed to be in a high Rydberg state of an H-like atom embedded in a di-electric continuum. Ion pairs in such high states may lose energy by spontaneous de-excitation and may also exchange energy with the nearby atoms as a result of energy fluctuation in the neighbouring portions of the medium. The energy lost by the ion pair is dissipated to the di-electric medium in the form of heat. In this model the detailed calculation revealed that practically all the H-like atoms are populated in the n=4 state where the three lowest states are strongly influenced by the energy fluctuation in the medium (Schiller 1992, Schiller 1993). As a result, electrons are considered to be set free when they are promoted by the assistance of the energy fluctuations in the medium from the stationary Rydberg state (n = 4) to the bottom of the conduction band (V_0) in the di-electric medium. The electron escape probability in a nonpolar liquid is given by

$$P(x) = \frac{1}{2}\left[1 - sgn(x)\, erfc(x)\right] \tag{2-15}$$

with

$$x = \frac{(-2E_4 + V_0)}{\sigma} \qquad (2\text{-}16)$$

where sgn (x) is the sign function. Eq.(2-15) shows the dependence of the electron escape probability on the energy of the quasifree electron at the bottom of the conduction band. In fact V_0, in the equation (2-16), is the only liquid property factor involved which explains the difference in the yields of free ions obtained in different liquid hydrocarbons, tables (2-1) and (2-2). Despite all the efforts that have been made to produce one theory which can explain the mechanism of charge transport in liquids, as yet no single theory has been widely accepted. It seems that the theories most adopted in liquid applications are still those of Jaffe and Onsager which were formulated in the first half of this century. However, the frequent philosophical and theoretical developments, combined with continuous progressive technological advances, along with developments in the field of radiation detection and dosimetry, seem to be promising in finding a solution to this problem.

2.5 Models of electron transport in liquids

2.5.1 Introduction

For many years electron transport and electrical conductivity in liquids, especially nonpolar liquids, have received a considerable attention in fields such as radiation measurements and dosimetry. One of the most important objectives in the examination

of charge transport in liquids has been the identification of the actual charge carriers (Reif and Meyer 1960). Early measurements of mobility revealed low values which indicated that the charge carriers were negative ions (Oliver and Leblance 1959). The negative ions are formed in liquids as a result of either the attachment of injected electrons to a neutral molecule or by electron capture by impurities such as oxygen molecules. Later, by ensuring a higher degree of purification, free electrons were observed by different independent laboratories (Tewari et al. 1968, Minday et al. 1969, Schmidt and Allen 1969, Conrad and Silverman 1969). Excess electrons are highly reactive towards some impurities and therefore their mobility can be measured accurately only in very pure liquids. Consequently, careful purification has been demonstrated to be an essential first step in a meaningful study of electrical conduction in liquids. A large number of laboratories have investigated the state of electrons in liquid hydrocarbons and different models have been proposed (Freeman and Fayadh 1965, Schmidt and Allen 1970, Kestner and Jortner 1973).

2.5.2 Quasi-free electron model

Several models have been proposed for a better understanding of the mechanism of electron transport in liquids. The simplest model is the quasi-free model which has been widely proposed to explain the behaviour of electrons in liquids of high zero-field electron mobility, $\mu_0 > 10$ cm^2/V.s (Cohen and Lekner 1967, Bakale and Schmidt 1973). In this model the electron is assumed to be in an extended, delocalized state and it travels progressively through the liquid whilst undergoing multiple elastic scattering with the molecules. The quasi-free electron in this model is regarded as a

plane wave moving in the liquid. A later extension of this model took into account the effect of incoherent inelastic scattering which restricted the degrees of freedom of the electron (Davis et al. 1971). This extension was applied to the high mobility polyatomic liquids.

2.5.3 Electron Trap model

Another widely accepted model is the electron trap model which has been applied mainly to liquids of low zero-field electron mobility (Oliver and Leblance 1959, Khrapak et al. 1990), $\mu_0 < 0.1$ $cm^2/V.s$, and to polar media. Here the electron is assumed to be temporarily trapped in a localized state until it is released and progresses to an extended state. Although the trap model has been referred to by many authors, various different reasons have been suggested for localization and on the mechanism for release of electrons from trapping. Furthermore the energy at which electrons can be localized are disputable. For example, Freeman proposed that trapping of a secondary electron could occur when the energy of the electron fell below the vibrational energy, ~ 0.2 eV, of the liquid molecules (Freeman and Fayadh 1965) whereas Mozumder assumed that trapping occurred at the thermalization stage, ~ 0.03 eV (Mozumder and Magee 1967).

In general, trapping is believed to be caused by natural traps owing to the skeletal structure of the molecule; due to impurities present in the liquid, and/or polarization arising from the localization of the solvated electrons. Moreover, the frequency of inelastic collision of electrons in the liquid results in a stage of temporary trapping of electrons. This latter type of trapping leads to the formation of a short lived transient

anion, (lifetime ~ 10^{-15}-10^{-3}) s. This type of trapping is called resonant trapping which occurs at very low electron energy (Christophorou 1994). The temporary trapping sites in Schmidt's opinion are the result of "fortuitous coincidence" of local rotational fluctuations (Schmidt and Allen 1970a). Later the importance of the local fluctuations was emphasized and expected to present low local energy centers in which electrons are readily trapped (Schiller 1972).

The liquid volume may be considered to be full of cavities of various sizes, distributed among the liquid molecules and formed by the electrostatic attractive and repulsive forces (Freeman and Fayadh 1965). Hence a low energy electron, in a time period of about 10^{-15} s, either can become attached to an ion or molecule or alternatively find itself in a cavity. The thermal activation energy can later advance the electron to another trap. The previous model is similar to that adopted by Kestner in which the liquid medium is composed of two opposite regions, transparent and almost opaque to electron transmission (Kestner and Jortner 1973). One year later, Schmidt studied the transport of excess electrons in liquid ethane (Schmidt et al. 1974). In that work, the electron transport in liquid is considered as an activated process that takes place through successive migrations over barriers, each of an average height of E_a separated by an average distance λ. In the absence of the electric field, and at constant temperature and pressure, the jump frequency of the electron is constant. If an electric field is applied, the electron jump frequency is enhanced. In this case the net jump frequency of the electron is given by

$$f = 2\delta \sinh (\lambda eE/2k_BT) \qquad (2\text{-}17)$$

where δ is the exchange frequency, E the applied electric field and T is the absolute temperature.

Minday attributed electron trapping in liquid hydrocarbons to be caused by a suitable configuration of a group of molecules at a particular site in the liquid structure (Minday et al. 1969). Every such region is assumed to represent a deep potential energy well for the electron. The electron motion through these regions proceeds by a series of successive hops from one trap to another.

Impurities are known to be an essential cause of trapping. Prominent impurities in liquids are water, oxygen and other substances, and submicroscopic particles. Impurities such as CO_2 are characterized by a reversible mode of trapping. In this kind of trapping the electron is captured by an ion and released back into the liquid after a very short time (Holroyd and Anderson 1985). This form of trapping is observed in liquid TMS (Holroyd et al. 1975).

2.5.4 Self trapping electron model

Electron localization has also been thought to be caused as a result of self-produced polarization charges (Schiller 1992). This type of trapping is called self-trapping since the electron is trapped by its own trapping centers formed by solvated electrons. Thus a new travelling electron, before getting solvated, is trapped in one of these centers. The solvation processes are believed to be the cause of polarization in the di-electric medium. In this case the fluctuation of the local medium density, either inherent or temperature induced, will tend to scatter the electron away from the trap.

In the study of electron transport in liquid neon, Schmidt proposed another mode of

self trapping (Schmidt et al. 1993). In this mode electrons are trapped inside bubbles which are regarded as localisation states. The bubble model is quantitatively described elsewhere (Borghesani and Santini 1994). In this model the localization states are formed as a result of two processes. In the first stage the quasi-free electrons rapidly lose energy to the liquid medium through multiple elastic collisions and, under the influence of the atomic fluctuations, are temporarily localized in virtual or resonant states. In the second stage the occupied resonant state moves slowly under the electron pressure and the expansion of the void. These processes result eventually in the formation of bubbles. Inside a bubble a free, delocalized, electron can transfer its excess kinetic energy to the walls of the bubble and become localized.

2.5.5 Extension of the electron trapping model

A new theoretical concept for electron transport in liquid hydrocarbon was discussed by Jamal and Watt in 1981. In this model two states of trapping are considered to be present in liquid alkanes: A deep trap through the interaction with C-C bonds, and a shallow trap through the interaction with the methyl (CH_3) groups. On the basis of the molecular structure these traps are assumed to be present in all alkanes. The difference in the electron mobility in different alkanes is ascribed to the difference in the frequency of electron trapping in each state and not to the difference in the states. The probability of scattering by each type of trap is given by the following expression

$$P_{CC}=\frac{n_{CC}}{(n_{CC}+n_{CH_3})} \qquad (2\text{-}18)$$

(2-19)

$$P_{CH_3} = \frac{n_{CH_3}}{(n_{CC}+n_{CH_3})}$$

where n_{CC} represents the number of C-C bonds in the molecule and n_{CH3} is the number of methyl groups. In fact this type of trapping is directly linked to the structure of the liquid molecule which will be discussed later in this work.

The probability of trapping in polar liquids is known to be higher than that in nonpolar liquids due to the existence of dipole moment. However, if the dipole moment is the essential cause of trapping, then a considerable part of this problem could be solved by employing nonpolar liquids. This is because the need for a high electric field, even in nonpolar liquids, to overcome recombination would result in induced dipole moments. A pulsed electric field with a certain time duration, less than that needed for the dipole to initiate, may reduce this effect.

2.6 Electron transport in liquefied rare-gases.

Rare-gas liquids have a relatively simple structure (Schnyders et al. 1966). They are either mono or diatomic and are simple disordered materials. However the investigation of the mechanism of electron transport in these media forms an important step toward the study of more complicated media such as liquid hydrocarbons. Among the rare-gas liquids Ar, Kr, and Xe are characterized by their remarkably high electron mobility, a property which makes them desirable in experimental applications such as radiation detection. While electrons in the noble liquid are regarded as quasi-free electrons, in extended states, those in liquid helium are considered to be in the

localised state. However, the motion of the electrons in liquid neon proceeds in both, localised and extended states (Khrapak et al. 1990, Sakai et al. 1992, Sakai et al. 1992). The motion of electrons in liquid Ar, Kr, and Xe is assumed to be governed by elastic scattering at moderate and low energies and by inelastic scattering at high energies. On the other hand electrons in liquid helium (Meyer et al. 1962)and neon (Khrapak et al. 1990, Schmidt et al. 1993) have been reported to reside in microscopic bubbles which constitute the trapping mechanism.

2.6.1 Electron mobility and drift velocity.

As will have become apparent from the earlier discussion, an important characteristic of electron motion is the electron mobility. It is defined as the electron drift velocity, ϑ_d, per unit applied electric field strength, E: $\mu_e = \vartheta_d/E$. Values of the electron mobility and other properties of electrons in rare-gas liquids are shown in tables (2-3) and (2-4) respectively. In the following is discussed the various factors affecting the mobility of charge in liquified rare-gas media.

2.6.1.1 Field dependence

The effect of electric field on the electron motion in rare-gas liquids has been studied by many authors. Miller investigated experimentally the electron drift velocity in liquid Ar, Kr, and Xe under an externally applied electric field strength ranging from 10 V/cm to 100 kV/cm (Miller et al. 1968). Inspection of the experimental data reveals that there is a sub-linear increase in the drift velocity, ϑ_d, which starts

Table (2-3): The electron and positive ion mobility in rare-gas liquids (cm^2/Vs).

Compound	μ_e (cm^2/Vs)	μ_+ (cm^2/Vs)	Temp.(K)	Ref*.
Ar	$1.70x10^{+3}$		147	80
	$1.58x10^{+3}$		144	125
	$2.85x10^{+2}$		111.5	103,123
	$4.90x10^{+2}$		87	80,125
	$4.75x10^{+2}$		85	86,121
		$2.61x10^{-3}$	145	26
		$1.22x10^{-3}$	111.5	26
		$6.61x10^{-4}$	90	26
		$1.00x10^{-3}$	85	121
Kr	$3.57x10^{+2}$		200	62
	$1.31x10^{+3}$		120.4	121
	$1.20x10^{+3}$		120	121,146
	$1.80x10^{+3}$		117	82,86
		$1.10x10^{-3}$	184.3	26
		$6.69x10^{-4}$	141	26
Xe	$1.10x10^{+3}$		167	76
	$2.00x10^{+3}$		165	121,146
	$2.20x10^{+3}$		163	82,86
	$2.00x10^{+3}$		161	107
		$3.29x10^{-4}$	192.1	26
		$2.85x10^{-4}$	184.2	26
		$4.00x10^{-3}$	168	97
4He	$2.16x10^{-2}$		4.2	25
		$5.30x10^{-2}$	4.2	97
3He	$3.70x10^{-2}$		3	97
Ne	$1.00x10^{-3}$		27	14
N_2		$2.00x10^{-3}$	77	53
H		$8.30x10^{-3}$	21	174
O2		$8.00x10^{-3}$	77	53
* Numberes of references refer to those of appendix B.				

Table(2-4): Some properties of rare-gas liquids.

Compound	W_g(eV)	W_l(eV)	I_{ion}(eV)	T(K)	V_0(eV)	Radiation	Ref*.
Ar		25.7+3		87		LE X-rays	137
		22.5+3		87		HE X-rays	77
		26.00		87		^{238}Pu-α	131
		19.5+2		rt		Heavy ion	54
		27.5+2.8		rt		α-Particle	54
		25.1+2.5		rt		1MeV El.	54
		23.60		rt			124
	26.2+0.2			87		HE X-rays	51
	26.3+0.1			87		^{238}Pu-α	51
	26.40			rt			34
				84	-0.20		119
Kr			11.56	121	-0.40		120
				116	-0.40		119
Xe		14.7+1.5				Heavy ion	54
		19.6+2.0				α-Particle	54
		16.3+0.3				α-Particle	90
		23.7+2.4				1MeV El.	54
			9.2	161	-0.67		119,120
He				4	1.05		119
N2	36.30						34
Ne				25	0.67		119
O_2	32.10						34
Co_2	34.10						34
Carbon disulfide	26.00			rt		LE X-Rays	136
		24		rt		LE X-Rays	90
* Numberes of references refer to those of appendix B.							
W_g and W_l are W-values for gas and liquid respectively, I_{ion} is the ionization potential, V_0 is the energy of the bottom of conduction band. HE and LE refer to high and low energy respectively.							

immediately after a linear increase at lower fields. The transition to the sub-linear region occurs when ϑ_d approaches the velocity of sound u_m in the medium. In the high electric field region a saturated curve of the drift velocity was attained. These features were congruent in all the liquids studied but extends over a longer range in the case of Ar. Lekner described theoretically the dependence of the electron drift velocity on the electric field strength in liquid Ar up to 10^4 V/cm (Lekner 1967). At high electric fields, his mathematical calculation predicted a maximum in the drift velocity, followed by a decrease rather than saturation. However, the agreement between the calculated and the experimental observations in the other regions of the electric field is satisfactory. Lekner ascribed the failure of his theory at high electric fields to insufficient accuracy in the calculated electron scattering cross section. On the other hand the deviation of the drift velocity from linearity at intermediate electric fields is believed to be caused by an increase of the electron mean free energy (Miller et al. 1968). This increase results from collisions with the liquid molecules during which the electron acquires more energy. This effect is called heating up. In the case of the low mobility rare-gas liquids such as liquid helium the field dependence of the drift velocity is much weaker than that of the high mobility liquids (Meyer and Reif 1958, Schmidt et al. 1993). This is an expected result since the state of electrons in these liquids are known to be localised whereas those in the high mobility liquids are extended states.

2.6.1.2 Dependence on molecular solute

The saturation region (the high field region) of the drift velocity observed in liquid Ar

was shifted up when a low concentration of either liquid nitrogen, hydrogen, or one of the liquid hydrocarbons was added (Yoshino et al. 1976). Moreover, for high concentrations of liquid hydrocarbons in liquid Ar this effect, i.e. shifting up, was extended to the intermediate region. In the low field region, and with high solute concentrations, the drift velocity of electrons in the diluted liquid seemed to be lower than that of the pure liquid. The latter behaviour was also observed at low fields in the mixtures of liquids N_2/Ar, where a gradual increase in the fraction of N_2 resulted in a gradual decrease in the observed drift velocity (Sakai et al. 1993). It is concluded that the addition of a diatomic molecular solute to a monatomic liquid produces new scattering centers at which the released electrons are scattered inelastically. This means that an electron travelling in one of these liquid mixtures will suffer a larger rate of energy loss than it would in the pure liquid. However, In the low field region, the energy lost in the effective scattering processes does not totally balance the energy gained from the electric field. Thus, the drift velocity drops below that of the pure liquid. In the high field region and due to the higher rate of energy loss, the influence of the electric field on the electron is greater than that in the pure liquid. Hence the drift velocity in the diluted liquid is higher than that in the pure liquid. Sakai predicted a change in liquid Ar would take place when a higher concentration of liquid N_2 is added (Sakai et al. 1993). Moreover, he expected the hopping electron transport model to be a possible mechanism to describe the electron motion in the diluted rare-gas liquid.

2.6.1.3 The temperature dependence

The effect of temperature on the electron mobility in rare-gas liquids is of interest,

especially near the triple temperature point. Eible studied the mobility of excess electrons in liquid Ar in the temperature range T_c-45≤T≤T_c (where T_c=150.9 K) and at applied electric fields up to 10^3 V/cm (Eibl et al 1990). The mobility was reported to be higher at lower field strengths and the maximum shifts towards lower temperatures. The mobility maximum, $\mu_m \approx 1550$ $cm^2/V.s.$, was obtained at the lowest field, E=12 V/cm, and was centred at $T(\mu_m) = T_c - 4.8$ K. An even higher value of the electron mobility in liquid Ar was reported at a lower value of the electric field (Lamp et al. 1990). While the mobility exhibits a small temperature dependence below the mobility maximum $T(\mu_m)$ a sharp drop in the electron mobility appeared at temperatures approaching the critical temperature T_c. The strong dependence of the electron mobility in the close proximity of T_c was ascribed to the change in density of the medium. This effect results in a decrease of the electron mobility owing to an increase in the electron scattering (Lamp et al. 1990). Very similar result was also published by Shinsaka who presented an interesting effect of the phase change on the electron mobility (Shinsaka et al. 1988). In his work he reported an electron mobility, in solid Ar, which was about 3.4 times higher than that in the liquid phase near the triple point (T_p= 83.8 K) and at an electric field strength of 100 V/cm.

Chapter 3

Electrical conductivity and transport properties of liquid hydrocarbons

3.1 Hydrocarbon liquids

Liquid hydrocarbons belong to a class of organic compounds that contain only two elements, hydrogen and carbon. They fall into three categories: aliphatic, alicyclic, and aromatic hydrocarbons. While the first group is characterized by open carbon chains, the others have ring carbon arrangements. Alkanes (C_nH_{2n+2}) form an essential family in the group of aliphatic hydrocarbons. They are saturated with hydrogen atoms. Due to this fact an alkane molecule is either non-polar or very weakly polar. In addition, the intermolecular forces (Van der Waals), between two small alkane molecules are tiny and thus can be easily overcome by the thermal energy. This fact explains the very low boiling point in the first four members in the chain of liquid alkanes. The intermolecular forces become increasingly significant in more complex molecules.

3.2 Physicochemical properties of liquid hydrocarbons

3.2.1 Dipole moment

The tendency of an atom to attract electrons is expressed by a quantity called

electronegativity. Low electronegativity may be associated with the effective screening on the nucleus of the atom caused by the inner electrons or to the large distance of the outer electrons from the nucleus. Different atoms generally exhibit different electronegativity. Thus molecules that are formed with unlike atoms will have an asymmetrical distribution of charges. Consequently such molecules have a permanent dipole moment. However if the atoms forming the molecule are identical, as in H_2 or O_2, no permanent dipole can exist. Furthermore, the dipole moment is thought to be negligibly small when the liquid molecule is nearly spherical. Hydrocarbon compounds are known to have very small dipole moments, in the region of 0.1 debye (1 D = 3.336×10^{-29} C.m) for liquid alkanes. This feature is desirable in their use in the study of electrical conduction . Additionally, it should be noted that when a molecule is placed in a high electric field, a dipole moment may be induced regardless of whether the molecule has a permanent dipole moment or not.

3.2.2 Polarity of bonds

In most cases atoms joined by a covalent bond do not share the mutual electron cloud equally. In other words, the electron cloud is denser about one atom than the other. Hence one end of the bond appears in the form of a negative pole while the other end displays a positive pole. Such a bond is said to be a polar bond.

It has been suggested that electrons travelling in liquid alkanes can be trapped by the chemical bonds such as C-C and C-H bonds (Jamal and Watt 1981). The C-C bond is considered to form a deep trap and the C-H bond a shallow trap for the electron. Furthermore the probability of trapping by C-C bonds is found to increase with the

number of C-C bonds in the liquid alkane molecule.

3.2.3 Molecular polarizability

The ability of a molecule to acquire an electric dipole moment under the action of an electric field is called the polarizability (α). Then the induced dipole moment, P_{ind}, is given by

$$P_{ind} = \alpha.E \qquad (3\text{-}1)$$

The unit of the polarizability is in C^2m^2/J.

In a spherically symmetrical molecule the induced dipole moment, and therefore the polarizability α, is a scalar quantity which coincides with the direction of the applied electric field. In non-spherical molecules, the induced moment will have different magnitudes and directions. Then the polarizability is represented by a tensor of nine components. The mean polarizability α_m and the anisotropy α_a of a rigid molecule are given by:

$$\alpha_m = \frac{1}{3}(\alpha_1+\alpha_2+\alpha_3) \qquad (3\text{-}2)$$

$$(\alpha_a)^2 = \frac{1}{2}[(\alpha_1-\alpha_2)^2+(\alpha_2-\alpha_3)^2+(\alpha_3-\alpha_1)^2] \qquad (3\text{-}3)$$

where α_1, α_2, and α_3 are the real quantities representing the principle values of the tensor α. Mean values of the polarizability and the anisotropy of polarizability have

been calculated for the C_5-C_{12} alkanes of sphere-like molecule (Dodelet and Freeman 1972). The results are shown in the table (3-1) along with values of the secondary electron range, b, and the liquid density, d, in these media. This result indicates that the efficiency of the energy loss processes in liquid hydrocarbons, represented by the magnitude of b.d, is a function of the degree of anisotropy of polarizability of the molecules. In the group of isotropically polarizable molecules (α_a= 0), increasing the complexity of the molecule results in a decrease in the value of b.d. Different results were reported when the degree of anisotropy was higher. This behaviour was ascribed to an additional component of anisotropy which resulted from antisymmetric vibrations in the molecule, and to the short range of the electron-induced dipole interaction.

Table (3-1): The effective range of electron-molecule interaction and the polarizability of sphere-like liquid hydrocarbons.

Compound	Formula	b(nm)	b.d(g/cm^{2}x10^8)	T(K)	Ref*.	α (nm)^3	α_a	Ref*.
Methane	CH_4	50	210	298	104	0.0026	0.00	28
Tetramethylsilane	$SiMe_4$	15.9		295	113			
Neopentane	CMe_4	21.5	127	294	28	0.0098	0.00	28
2,2,3,3 TM. butane	Me_3CCMe_3	13	85.0	397	28	0.0152	0.70	28
2,2,4,4 TM. pentane	$Me_3CCH_2CMe_3$	15.8	114	295	28	0.017	0.00	28
2,2,5,5 TM. hexane	$Me_3C[CH_2]_2CMe_3$	13.8	99.0	293	28	0.0188	0.70	28
2,2,6,6 TM. heptane	$Me_3C[CH_2]_3CMe_3$	11.3	81.0	293	28			
2,2,7,7 TM. octane	$Me_3C[CH_2]_4CMe_3$	8.3	66.0	316	28			
2,2,3,3 TM. pentane	$Me_3CCMe_2CH_2CH_3$	10.2	77.0	295	28			
Cyclohexane	$Me_3CCH{=}CH_2$	6.70	52.0	296	28	0.0112	2.10	28
* Numbers of references refer to those of appendix B.								

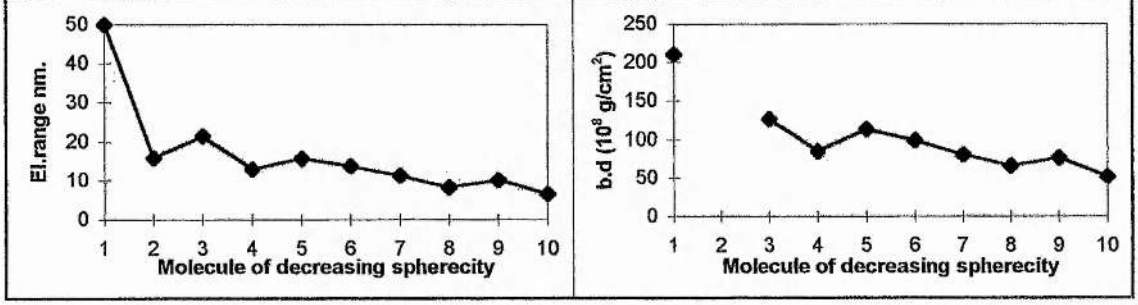

α is the mean value of the polarizability, and α_a is the anisotropy of polarizability.

Equation (3-1) reflects the linear dependence of the induced polarities on the applied electric field. In fact the induced polarizability takes a sub-linear form at high electric fields (Sutton 1946). This state is called hyperpolarizability.

3.2.4 Intermolecular forces

Intermolecular forces are those that act between atoms and molecules and thus govern their behaviour in the molecular medium. They are relatively long-range forces and their strength determines the properties and the states of the molecules. As far as the force acting between molecules is concerned, interaction between different types of dipole form an important group of interactions. Dipole-dipole interactions occur between two adjacent molecules. The different orientations of the dipole moments, due to the random motion of molecules, cause the polar molecules to attract and repel each other. However, in liquids the attractive orientations are energetically more favourable and thus the attractive forces slightly dominate over the repulsive forces. If the thermal energy of the medium is relatively weak, both dipoles of the nearby molecules can rotate freely and hence the stronger dipole may align the other in its direction or otherwise to form a favourable arrangement. The general formula for the interaction energy, U, for two dipoles of moments D_1 and D_2 separated by a distance r is given by

$$U=\frac{-D_1 \cdot D_2}{4\pi\epsilon_0\epsilon r^3}\left[2\cos\theta_1\cos\theta_2-\sin\theta_1\sin\theta_2\cos\Phi\right] \qquad (3-4)$$

where θ_1 and θ_2 are the orientation angles of the dipoles D_1 and D_2 respectively, with

respect to the line joining them, and Φ is the azimuthal angle. From this equation it is apparent that when both dipoles are lying in line ($\theta_1 = \theta_2 = 0^0$), the attraction is maximum whereas if they are in parallel ($\theta_1 = \theta_2 = 90^0$), the interaction energy is only half that of the maximum.

A polar molecule can induce, due to the effect of its local field, a dipole moment in a neighbouring molecule. However in non-polar liquids only the external electric field can induce such a dipole. If the permanent dipole, or the electrically induced dipole in the non-polar liquids, alters its direction the other induced dipole will follow the same direction instantaneously. In this way dipole-induced dipole and induced dipole-induced dipole interaction can take place. In both types of interactions the maximum interaction also occurs when both dipoles are aligned.

3.3 Electron transport in liquid hydrocarbons

Although many rare-gas liquids have the advantages of easy purification, high electron mobility, and free dipole moments, there has been a high tendency to replace them with liquid hydrocarbons in the study of electron transport. This is due to the practical advantage that most are liquid at room-temperature and consequently less restrictions are required for handling them experimentally. This trend has been growing through the years since the first indication of the existence of free electrons in them (Tewari and Freeman 1968, Minday et al. 1969, Schmidt and Allen 1969, Conrad and Silverman 1969). The considerable attention payed to these liquids was manifest in intensive theoretical (Hutton 1972, Schiller et al. 1982, Belevtsev 1990) and experimental investigations of the motion of electrons in them (Rao et al. 1977, Faidas

et al. 1990). While there seems to be a general understanding of the mechanism of electron transport in rare-gas liquids, the situation is less clear in the case of liquid hydrocarbons. Furthermore, the saturation collection of charge in liquid hydrocarbons has yet to be demonstrated and is still raises important problems to be explained. It is the intention in this section to review the status of the basic properties of electron transport in liquid hydrocarbons and to attempt to understand the basic mechanisms involved.

3.3.1 Electron mobility

In order to define the states of electron, and to gain a better insight into the interaction mechanism of electrons in liquid hydrocarbons, many experimental techniques have been devised, particularly for determination of their mobilities. These experiments led to the proposal that two restricted states for electron transport could exist: The localized state and extended state. Measurements of electron mobility, μ_e, in liquid hydrocarbons were accomplished using a variety of techniques (Gzowski and Terlecki 1959, Schmidt and Allen 1970, Minday et al. 1971). The oldest and the most commonly adopted technique is `time of flight`. In this method the time required for a group of electrons, produced by a variety of methods, such as low energy X-ray irradiation, to cross the gap between two parallel electrodes is measured. This time, t, together with the inter-electrode distance d, and the applied voltage V, gives a measure of the electron mobility according to the following equation:

$$\mu_e = d^2/t.V \qquad (3\text{-}5)$$

where the drift time of electrons from one electrode to the other can be measured from the trace of the current vs. time on the oscilloscope.

Different liquid hydrocarbons, with similar physical and chemical properties, have been found to differ in their electron mobilities by factors as large as three orders of magnitude (Schmidt and Allen 1970). Sometimes, the values of electron mobility reported by different laboratories for one particular liquid differ by almost on order of magnitude, (see appendix B). The latter discrepancy is presumably due to different concentrations of impurities in the respective liquid samples and not to differences in the adopted measurement technique. The electron mobilities in liquid hydrocarbons differ by almost four order of magnitudes, 10^{-2}-10^{+2} $cm^2/V.s.$, see tables (2-1) and (2-2). This is even one order of magnitude higher in the case of rare-gas liquids. However, it was suspected that low values of electron mobility in some of the liquid hydrocarbons may rest in the existence, and also the interactions, of small dipoles in the close proximity of the C-H bonds which form scattering centers for the free electrons (Schmidt and Allen 1970a, Davis et al. 1971).

It is known that the mechanism of electron transport in liquid hydrocarbons is a function of various parameters such as the electric field, temperature, ...etc.

3.3.1.1 Electric field dependence

The investigation of the effect of the electric field strength on the electron mobility, $\mu_e=\vartheta_d/E$, in liquid hydrocarbons shows a different behaviour depending on the states of electrons in the liquid and on the strength of the applied fields. It seems that at high electric fields, electrons in liquids of low zero-field electron mobility acquire more

energy than do those in liquids having high values of the zero-field electron mobility. The study of the electric field dependence of the electron mobility is divided into three categories relative to the electron mobility. The result, in terms of the drift velocity, for liquids with various values of the electron mobility is shown in figure (3-1).

i- In liquid hydrocarbons characterized by high zero-field electron mobility, μ_0>10 $cm^2/V.s$, the electron mobility is independent of the electric field up to a fairly high value, E_c. In other word, the drift velocity, ϑ_d, increases with increasing the electric field. At high values of the electric field, starting from the critical value E_c, a sub-linear increase in the electron drift velocity of the form $\vartheta_d \sim E^{1/2}$ occurs. However, the departure from linearity, in this group of liquid hydrocarbons, shifts towards lower values of the electric field for liquids of higher values of μ_0 (Schmidt 1977, Schmidt 1993). Branched liquid hydrocarbons, and liquid tetramethylsilane (TMS), which belong to the same category of the electron mobility, exhibit similar sort of behaviour (Faidas et al. 1990).

In comparison with rare-gas liquids the trend is analogous with the difference that the onset of non-linearity for the rare-gas liquids in the high field region occurs at much lower values of the electric field (Schmidt 1993).

The sub-linear dependence of the drift velocity perceived at high fields was attributed to an increase in the mean kinetic energy of the electrons, through subsequent collisions with the molecules of the liquid, to a value higher than that of the thermal energy of the liquid medium (Schmidt 1977, Rao et al. 1977). At this stage the influence of the electric field is presumably less and thus the electron mobility is lower.

ii- In liquid hydrocarbons having low zero-field electron mobility, μ_0< 1 $cm^2/V.s$, an

opposite trend of the drift velocity to that detected in liquid hydrocarbons of high zero-field electron mobility was reported. In other words, with respect to the electric field, the drift velocity, and therefore the electron mobility, exhibits a super-linear increase at higher fields after a fairly long linear growth in the lower field region. As the zero-field electron mobility, μ_0, approaches the value 1 $cm^2/V.s$. the super-linearity disappears and a pure linear behaviour is attained at μ_0=1 $cm^2/V.s$. This type of behaviour has been interpreted on the basis of the hopping transport mechanism (Schmidt 1977). According to this mechanism, the attempt escape frequency of the electron increases with increasing electric field until it reaches a value at which the electron acquires sufficient energy to jump from its trap into another trap resulting in a super-linear increase in the electron mobility.

iii- An interesting type of field dependence was reported by Schmidt in liquid hydrocarbons of intermediate values of the zero-field electron mobility, $1<\mu_0<10$ $cm^2/V.s$ (Schmidt 1977). In these media, the linear increase of the drift velocity which was attained in the low field region and followed by the super-linear increase in the higher field region, was regained with further increase of the electric field. It seems that at such a value of the electric field the electron mobility becomes comparable to those of high zero-field electron mobility liquids and thus a parallel behaviour of the electron mobility to that of these media should follow. Bearing in mind the sub-linear increase of the electron drift velocity in the high zero-field electron mobility liquids at high fields and the super-linear increase of the electron mobility in the low zero-field electron mobility liquids, the net result is a linear behaviour. This may also explain the gradual disappearance of the super-linearity behaviour of the drift velocity in liquids of high zero-field electron mobility when approaching the value, 1 $cm^2/V.s$.

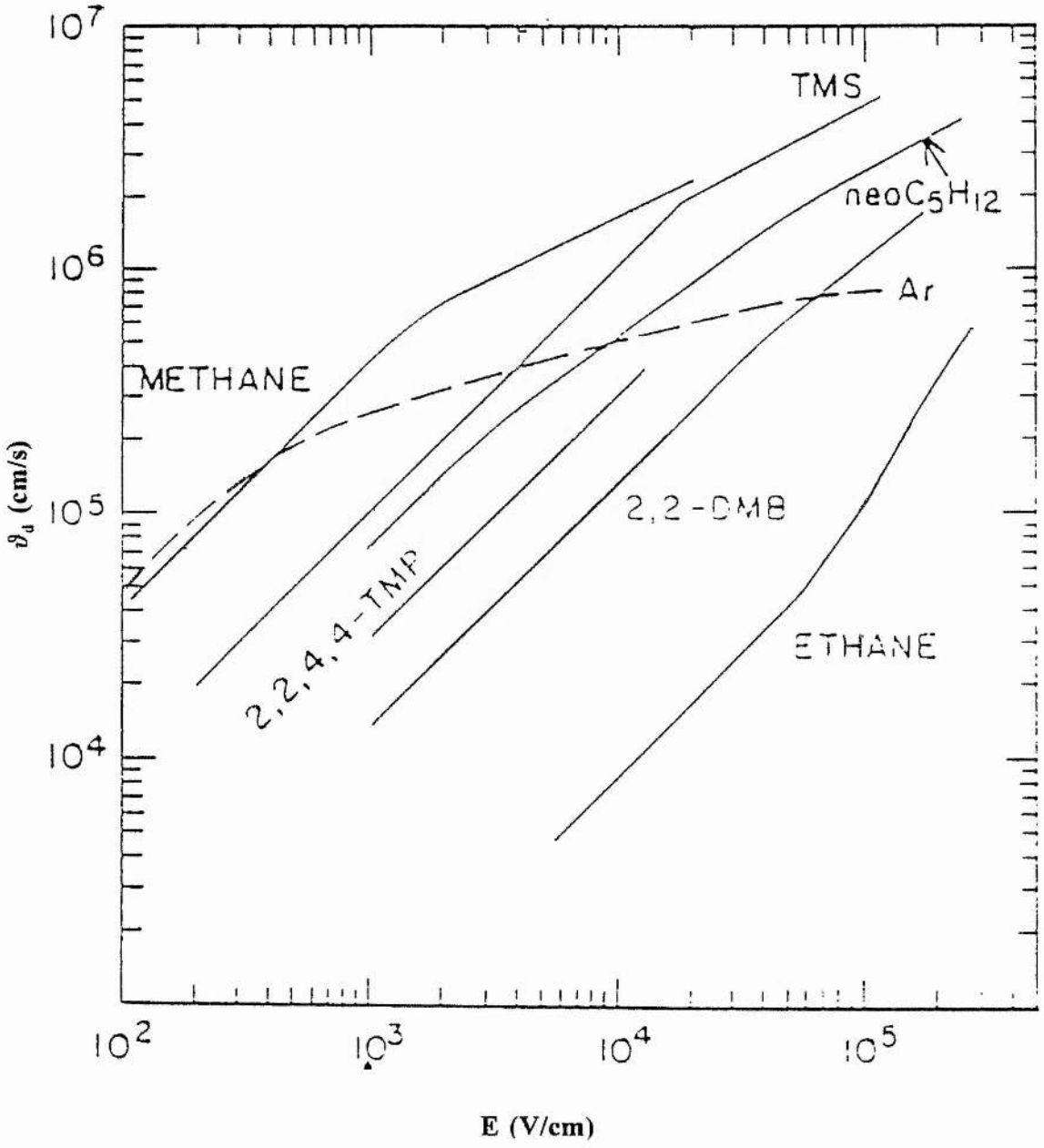

Figure(3-1): The dependence of the drift velocity, ϑ_d, on the applied electric field, E, in variety of liquid hydrocarbons with different mobilities. (Holroyd 1985).

3.3.1.2 Temperature dependence

Studies of the temperature dependence of the electron mobility in liquid hydrocarbons revealed an increase in the electron mobility with raising temperature (Gee et al. 1988), with the exception of some liquids, such as methane (Robinson and Freeman 1974, Nakamura et al. 1983), neopentane (Namba et al. 1979), and 2,2,4,4 tetramethylpentane (TMP) (Cipollini and Allen 1977, Ryan and Freeman 1978), in which an opposite trend was detected in the low temperature region. In other words, the electron mobility in the latter media exhibits a negative rather than a positive temperature coefficient.

A third perceived behaviour is that for liquid tetramethylsilane (TMS) in which the electron mobility shows no dependence on the temperature in the temperature range of (223-296) K, (Shinsaka et al. 1993).

In general, the increase rate, k_μ, of the regular increase of the electron mobility with temperature, witnessed in most liquid hydrocarbons, is of an Arrhenius form

$$k_\mu = A \exp(-E_a/k_B T) \qquad (3\text{-}6)$$

Here A is a constant that is a function of the structure of the liquid. E_a is the activation energy which seems to have lower values in the branched hydrocarbon liquids of high electron mobilities (Schmidt 1977). Furthermore, the correlation of the electron mobility with temperature in the high mobility liquids tends to be weaker than those of the low mobility values. This result is represented in figure (3-2) which shows the temperature dependence of electron mobility in many liquid alkanes.

Ryan studied the dependence of the electron mobility on temperature in a number of branched liquid hydrocarbons (Ryan and Freeman 1978). In that work attention was paid to the behaviour of the electron mobility near the critical temperature (T_c). In these liquids a maximum was attained close to the critical temperature. These maxima became more pronounced in liquids that have higher values of the electron mobility at room temperature. The maximum was most pronounced in the case of liquid 2,2,4,4 TMP which then fell abruptly to a relatively low value at $T=T_c$. The latter behaviour is analogous to that reported for liquid methane as shown in figure (3-3) (Nakamura et al. 1983).

The general increase of the electron mobility with temperature in liquid hydrocarbons was concluded to be due to the presence of a relatively high concentration of the scattering centres in liquids represented by points of transient fluctuations (Schmidt and Allen 1970a). These centres have a relatively short life time at high temperatures which serves to enhance the electron mobility. However, in the case of high mobility liquids, such as liquid methane, and in the low temperature region, these centres are of negligible importance due to the increased orderliness. Thus no significant influence of the temperature on the electron mobility is expected.

The study of the temperature dependence of the electron mobility in liquid hydrocarbons was extended to include the effect of liquid-solid phase change on the electron mobility (Namba et al. 1979, Nakamura et al. 1983). These investigations revealed a sharp rise in the electron mobility as the phase altered from liquid to solid figure (3-3). For example, in the case of liquid TMS the reported mobility in the solid phase was from three to four times higher than that in the liquid phase (Nakamura et al. 1980). This fact supports the assumption of trapping by the transient fluctuation

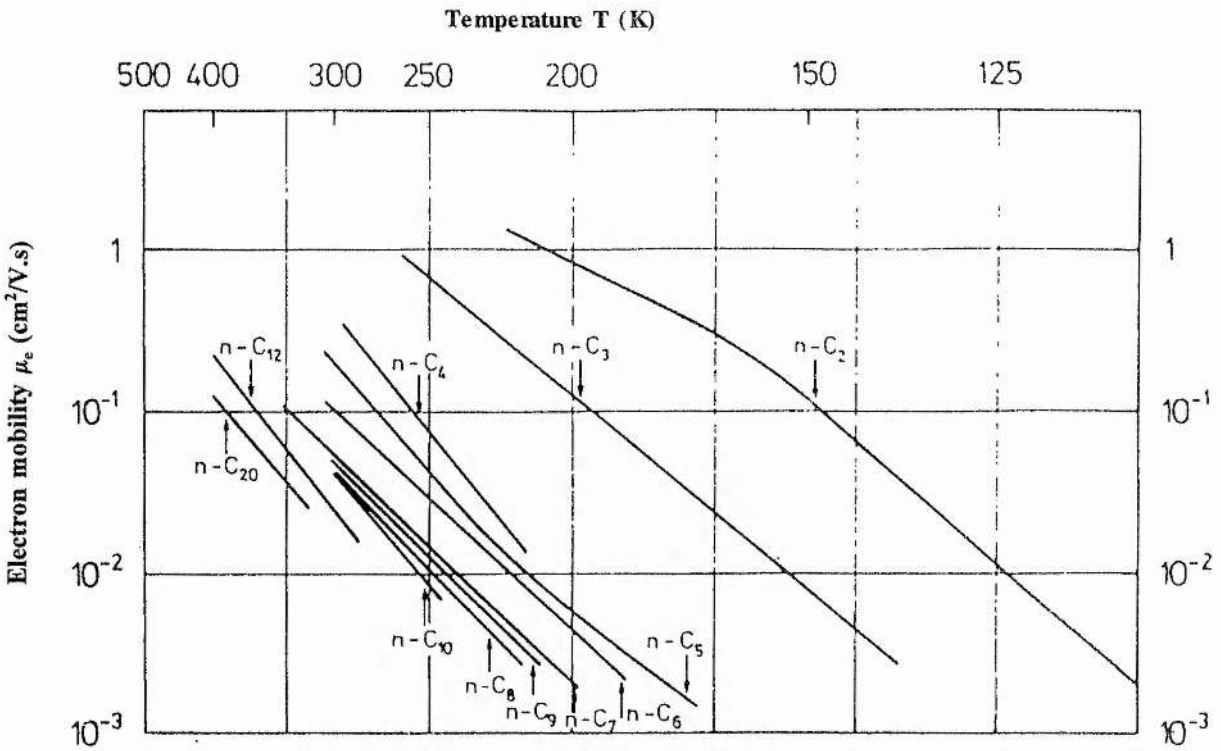

Figure (3-2): The dependence of the electron mobility, μ_e, on temperature, T, in a number of liquid alkane different in their electron mobility. (Schmidit 1977).

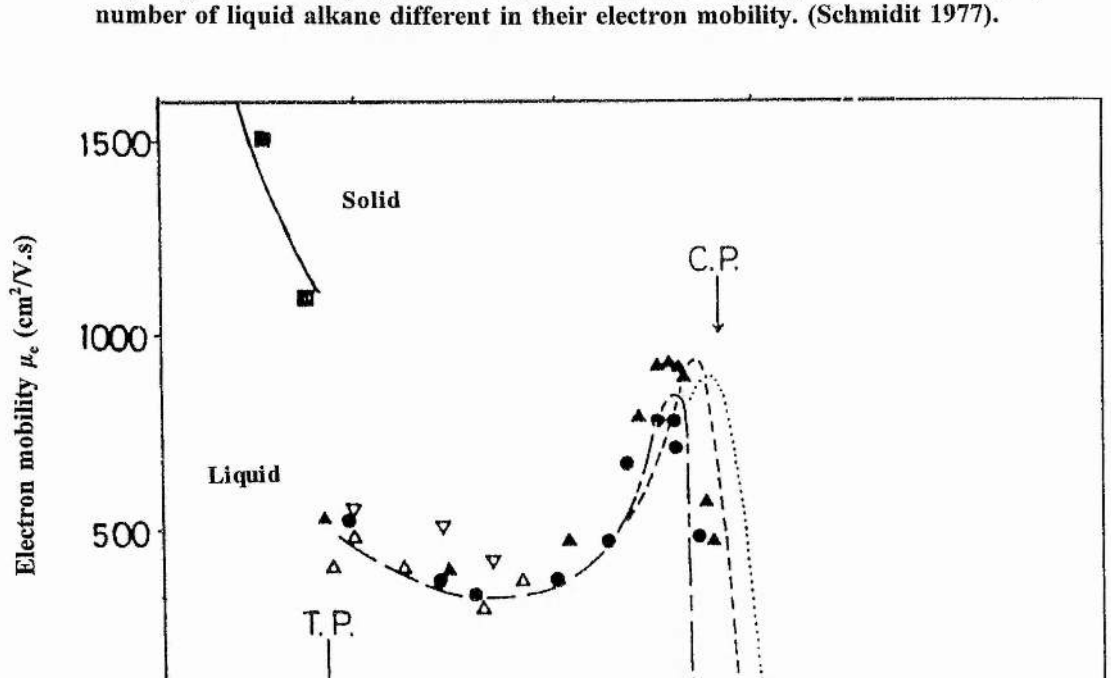

Figure(3-3): The mobility dependence of liquid and solid methane on temperature near the critical point (C.P) and the triple point (T.P) (Nakamura 1983)

centres, presumably in the molecular vibrational and rotational states which would be absent in the solid phase.

3.3.1.3 Structure effect

A clear correlation between the electron mobilities in liquid hydrocarbons and the molecular structure has been demonstrated by many authors (Tewari and Freeman 1968, Gee et al. 1988). Generally, liquid alkanes exhibit a slow monotonical decrease in the electron mobility as the length of the C-C chain progressively increases. However, a striking increase of the electron mobility occurs in going from chain-like molecules to sphere-like molecules. This effect is also perceived when the methyl groups, of semi-spherical structure, on the molecule are enhanced (Dodelet and Freeman 1972). The electron mobility in such molecules achieve their highest values when the methyl substitution forms a spherical molecules as, for example, in neopentane and tetramethylsilane (TMS).

Figure (3-4) shows the structure of some liquid hydrocarbons with different values of electron mobility. Although the structure dependence of the electron mobility in liquid hydrocarbons is generally acknowledged, there is no clear evidence on the exact cause of this correlation. Investigations of the structure dependence of the electron mobility proposed that the mobility may be influenced by a dipole field formed in the immediate vicinity of each C-H bonds (Schmidt and Allen 1970a) whereas other studies ascribed the effect to the scattering of the free electron caused by both C-H and C-C bonds, with the later bond being more effective (Davis et al. 1971). However, the difference in the high values of the electron mobility observed in the sphere-like

molecules was attributed to a correlation between the degree of sphericity and the value of anisotropy of polarizability of the molecule (Dodelet and Freeman 1972). With respect to the structure configuration, the polarizability of the C-H bonds is isotropic, whereas the inner C-C bonds are of anisotropic polarizability. It has been found that the penetration rang of the secondary electron, b, and thus the product b.d, with d representing the density of the liquid, increases as the anisotropy of polarizability of the molecules decreases. Table (3-2) shows a parallel behaviour for each of the electron range, b, and the product b.d, with the electron mobility for chain-like liquids. On the other hand, the data in table (3-1) reflects the significance of the effect of the anisotropy on the latter parameters, b and b.d, in the sphere-like liquids.

Table (3-2): The effective range of electron-molecule interaction for chain-like liquid hydrocarbons.

Compound	Formula	b (nm)	b.d ($g/cm^2 x10^8$)	Ref*.	$\mu_e(cm^2/Vs)$	Ref*
Methane	CH_4	50	210	104	$4.20x10^{+2}$	121
Ethane	C_2H_6	12.9	81	104	$3.70x10^{+1}$	37
Propane	C_3H_8	9.7	69	104	$2.63x10^{+0}$	36
n-Butane	C_4H_{10}	8.29	47.7	113	$4.00x10^{-1}$	114
n-Pentane	C_5H_{12}	7.15	44.6	113	$1.60x10^{-1}$	114
n-Hexane	C_6H_{14}	6.74	44.2	113	$8.00x10^{-2}$	3
n-Heptane	C_7H_{16}	6.6	45	113	$4.60x10^{-2}$	98
n-Octane	C_8H_{18}	6.42	44.9	113	$4.00x10^{-2}$	98
n-Nonane	C_9H_{20}	6.22	44.5	113	$2.80x10^{-2}$	40
n-Decane	$C_{10}H_{22}$	6.16	44.8	113	$2.50x10^{-2}$	29
n-Undecane	$C_{11}H_{22}$	6.07	46.2	113	$2.40x10^{-2}$	40
* Numbers of references refer to those of appendix B.						

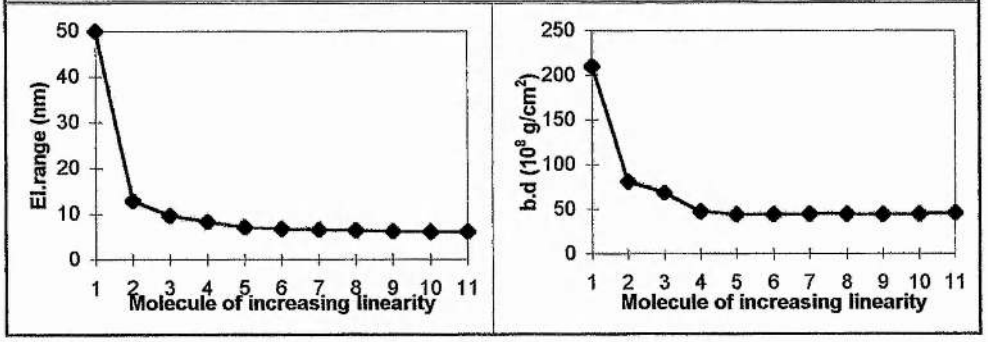

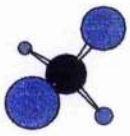

Methane

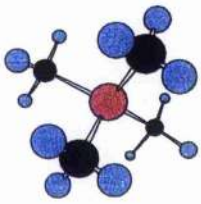

Tetramethylsilane

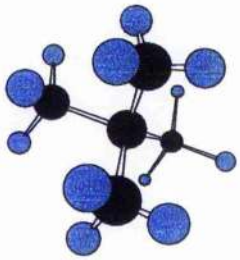

Neopentane

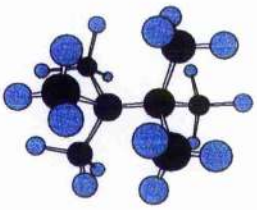

2,2,3,3-TMB

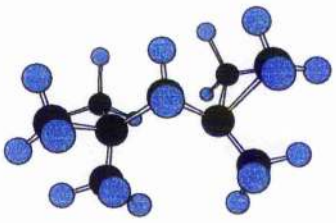

2,2,4,4-TMP

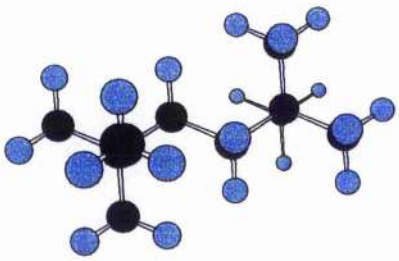

2,2,5,5-TMH

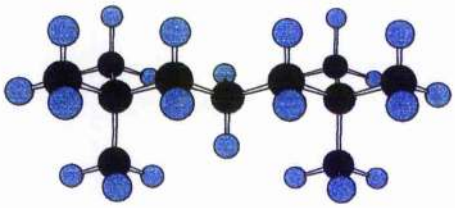

2,2,6,6-TMH$_p$

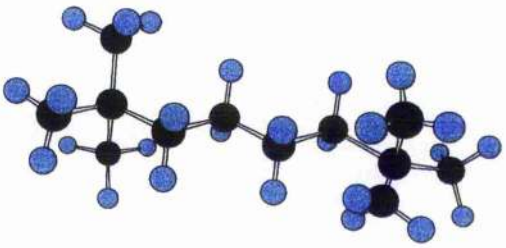

2,2,7,7-TMO

Carbon
Hydrogen
Silicon

Fig (3-4): Three dimensional representations of large hydrocarbon molecules with decreasing sphericity

The gradual decrease of the electron mobility, in liquid hydrocarbons of chain-like molecules, with stretching the length of the chain is expected to be the result of the incoherent interactions of the free electrons with the increasing number of the C-C bond. However, in liquids composed of sphere-like molecules, such as neopentane and TMS, the C-C bonds are screened by the clouds of C-H bonds which are the components of the methyl groups, CH_3, and thus in practice the free electrons are scattered only by the C-H bonds (Jamal and Watt 1981). Since the C-H bonds are relatively transparent to the free electrons, the electron mobility in these liquids is relatively high.

3.3.2 Free-ion yields

When an ionizing radiation passes into a liquid medium it produces ion pairs. Each ion pair is typically composed of an electron and positive ion. If the Columbic attraction force acting between an individual ion pair is significant with respect to the thermal energy of the medium, the ion pair may recombine. Alternatively, the electron can escape from the potential of its parent positive ion with excess kinetic energy. The electron then in a short time loses its energy to the medium and eventually thermalises at some distance, r, from the positive parent ion. However, before reaching thermalization energies, the electron may become trapped or attach itself to another positive ion to form a neutral molecule.

The free-ion yield, G_{fi},, is defined as the number of those ions which escape the primary recombination per 100 eV of absorbed energy. G_{fi} is an important factor in the study of the behaviour and the distribution of electrons in liquid media.

Measurement of the ion yield must be carried out in a highly purified sample of liquid to minimize the effect of impurities on the movement of charge carriers. A common method of quantifying the induced charge is through the electrical conductivity of the liquid di-electric. A rough estimate of the electrical induced conductivity, k, in liquids confined between two parallel plates separated by a distance L, can be achieved using the equation:

$$k=\frac{I.d}{V.A} \qquad (3\text{-}9)$$

where I is the low field induced current, V is the applied voltage, d is the inter-electrode spacing, and A is the area of the collecting electrode. A low value of k, typically $\leq 10^{-16}\ \Omega^{-1}.m^{-1}$, is considered to be an indication of a good level of purity.

3.3.2.1 Structure, temperature, and field dependence

Experimental values reported for the free-ion yield in liquid hydrocarbons are compiled in tables (2-1), and (2-2). These values indicate a clear dependence of the G_{fi} on the molecular structure of the liquid, where higher values of G_{fi} are obtained for liquids composed of highly spherical molecules (Tewari and Freeman 1968, Robinson et al. 1971). This behaviour is comparable to that observed for the electron mobility. The monotonical increase of G_{fi} with increasing sphericity of the hydrocarbon molecule may be associated with the longer ion separation distance resulting from the greater homogeneity of the ion distribution (Freeman and Fayadh 1965) rather than the longer distance traversed by the electron of the ion pair

(Mozumder and Magee 1967).

The effect of the electric field on G_{fi} has been intensively investigated (Munoz et al 1986, Mozamder 1974b). In general, the G_{fi} shows a sub-linear increase with raising field after a short linear increase in the low field region. The result can be extrapolated to zero field to get G_{fi}^0, known as zero field free-ion yield. The linear field dependence of the ion yield is extended over a longer field range in liquids exhibiting low values of the zero field free-ion yields. However, the field dependence of G_{fi} is stronger in liquids of higher G_{fi}^0 liquids such as methane and TMS (Shinsaka and Hatano 1988, Shinsaka et al. 1993). Raising the temperature of the liquid also tends to enhance the dependence of the G_{fi} on the electric field (Dodelet et al. 1971, Robinson and Freeman 1974).

Various attempts have been made to explain the effect of the electric field on the free-ion yield (Dodelet and Freeman 1971, Dodelet and Freeman 1972). Historically Jaffe and later Onsager discussed the influence of the electric field on the escape probability of an electron from the parent positive ion (Jaffe 1913, Onsager 1938). These theories are still of interest even in recent years. Schmidt extended the Onsager treatment to account for the free-ion yield (Schmidt and Allen 1968). He took a preliminary step by assuming that the distribution of thermalisation distances, between positive and negative ions is well represented by the three dimensional Gaussian distribution:

$$F(r) = \frac{4r^2}{\sqrt{\pi} b^3} \exp\left(-\frac{r^2}{b^2}\right) \qquad (3\text{-}10)$$

Then the free-ion yield is expressed by multiplying that function by the Onsager

escape probability, represented by equation (2-4), and averaging over all values of the thermalization distance, r. i.e.

$$G_{fi}=G_{tot}\int_0^{\infty} F(r)\,P(r,E)\,dr \qquad (3\text{-}11)$$

where F(r) is the initial separation distance distribution function, and P(r,E) is the probability of escape. Combining the Onsager escape probability and the Gaussian distribution gives

$$P=\frac{G_{fi}}{G_{tot}}=\frac{4}{\sqrt{\pi}}\int_0^{\infty}\left[\frac{r^2}{b^3}\exp\left(-\frac{r^2}{b^2}-\frac{e_0^2}{\epsilon r k_B T}\right)\right]dx \qquad (3\text{-}12)$$

where b is the electron range, ε is the di-electric constant of the medium, and G_{tot} represents the total number of ion pairs formed by 100 eV absorbed energy. By taking the G_{tot} as the ion yield in the vapour phase as an approximation, which was shown to be the case for some liquids at high electric field (Schmidt and Allen 1970), and measuring the G_{fi}, one can obtain the electron range b. Values of b in different liquid hydrocarbons at different temperatures is presented in tables (3-1) and (3-2). In fact, the Gaussian distribution was developed mainly for high energy X-ray radiations for which the rate of energy loss, dE/dx, is low. However, for liquids exposed to low energy X-ray radiations the dE/dx of the electron spectrum generated, and therefore the free-ion yield, is much higher (Poffenberger et al. 1993, Astbury et al. 1993). In this case, the Gaussian distribution is no longer valid and should be replaced by a

cylinder or track distribution (Jaffe 1913).

The free-ion yield in liquid hydrocarbons is almost a linear function of temperature (Schmidt and Allen 1970). The linear increase is less pronounced at high electric fields. This is presumably caused by the greater influence of the electric field compared to that of the temperature. An example is liquid iso-octane in which the temperature dependence of G_{fi} is as small as 0.18 % per ^{0}C (Wickman and Nystrom 1992).

The validity of the Gaussian distribution in liquid hydrocarbons was examined by studying the behaviour of the product of b.d with temperature since this is expected to show no dependence if the Gaussian distribution is a proper description (Schmidt and Allen 1970b). This is because G_{fi} is a function of temperature and the electron range b, according to equation (3-12), which in turn should vary inversely with the density d. The result of the study revealed that the Gaussian distribution compares better with the experimental results in many cases. However, this was not the case for liquid hydrocarbons of higher G_{fi} values such as neopentane and methane (Robinson et al. 1971). In these liquids the product bd decreases with raising temperature. This indicates that the Gaussian distribution is broader than the real distribution function. In other words, in liquids of higher G_{fi}^0 most of the electrons have a longer thermalization distance than those in the low G_{fi}^0 liquids.

3.3.2.2 Methods of measurement of the free-ion yield

Values of G_{fi} have been obtained in liquid hydrocarbons using a variety of techniques. The first adopted method is the low field conductivity method. In this the current

produced in a liquid, confined between two parallel plates, as a result of a constant intensity of ionizing radiation and a small applied electric field is measured. The G_{fi} is then given by (Freeman and Fayadh 1965, Hummel and Allen 1966).

$$G_{fi}=10^2\frac{k^2}{e^2D_R}\frac{\alpha}{(\mu_+-\mu_-)^2} \tag{3-13}$$

Here, μ_+ and μ_- are the mobility of positive and negative ions respectively, D_R is the dose rate (eV/cm^3 s), k is the conductivity which is given in equation (3-9), and α is the volume recombination coefficient (cm^3/s) which can be measured experimentally. A less complicated and more reliable way of measuring G_{fi} is the clearing field method. In this method, a sufficiently high electric field is triggered immediately after the termination of a short pulse of ionizing radiation. The immediate action of the high electric field should not allow for any appreciable amount of general recombination to take place and thus the free ions produced are most likely to be collected (Schmidt and Allen 1968). The fraction of the ions reaching the electrodes from the initial number of the produced ions, n_0, is

$$E_f=\frac{\ln(1+U)}{U} \tag{3-14}$$

with

$$U=\frac{eLn_0}{\epsilon_0\epsilon_r E} \tag{3-15}$$

If the collected charge is measured as a function of the absorbed dose and the slope of the curve, S(C/mrad), is determined then the value of the G_{fi} is given by

$$G_{fi} = 10^2 \text{ (S / nA)} \qquad (3\text{-}16)$$

where A is the sensitive volume, n is the density of the medium. In order to minimize the loss of ions by volume recombination during the pulse it is recommended to reduce the total dose per pulse and increase the pulse rate.

3.3.3 Conduction-band energy

The energy of the conduction band in the liquid, designated by V_0, is defined as the potential energy of the electron in the bottom of the conduction band of the liquid with respect to that in vacuum. It is also known as the energy of the quasifree electron state in a liquid relative to the vacuum level. In practice the value of V_0 can be determined, employing the photoelectric effect, by measuring the difference in the work function of a metal electrode immersed in the liquid, $\phi_{liq}' = \phi_{liq} - \phi_{met}$ and that for the electrode in vacuum $\phi'_{vac} = \phi_{vac} - \phi_{met}$, i.e.

$$V_0 = \phi'_{liq} - \phi'_{vac} = \phi_{liq} - \phi_{vac} \qquad (3\text{-}17)$$

This method has been adopted by many authors for liquid hydrocarbons (Holroyd and Allen 1971, Schiller 1972). Later the dependence of the electron mobility on the conduction-band energy, V_0, was also investigated theoretically (Kestner and Jortner 1973). Both theoretical and experimental investigations revealed a correlation between the electron mobility, μ_e, and V_0. In other words the values of V_0 in liquid

hydrocarbons tends to increase monotonically as the electron mobility decreases (Holroyd and Allen 1971, Wada et al. 1977). This suggests, considering equation (3-17), that the work function of a metal in contact with a liquid of high mobility, such as tetramethylsilane, will be lowered by a factor which depends on the value of V_0. This means that the electron emission from the metal will take place at a lower value of the electric field than for that in vacuum (Baker and Boltz 1937).

The dependence of electron mobility on the conduction-band energy, V_0, in liquid hydrocarbons may be represented empirically by (Wada et al 1977).

$$\mu_e = \frac{125}{1+360\exp(15V_0)} \qquad (3\text{-}18)$$

This equation is also applicable to liquid TMS, (see section 3.4, equation 3-23) .

The correlation between μ and V_0 was interpreted relative to the trapping model with reference to the depth of the trap caused by coincidence local-rotational phases (Holroyd and Allen 1971). However, the depth of the trap is considered to be less when the height of the conduction level is reduced. An alternative explanation, based on electron localisation inside vapour bubbles formed by the local energy fluctuation of the medium, was suggested by Schiller (Schiller 1972). Later, a semi-quantitative theoretical treatment of the electron transport in liquid hydrocarbons was developed. In this theory the electron is considered to be transported through two microscopic regions, one transparent and the other almost opaque, distributed randomly in the liquid medium (Kestner and Jortner 1973). The electron transport regions are expected to have been formed by the local rotational fluctuations in the liquid medium. Values of V_0 for some liquid hydrocarbons are listed in appendix B.

3.4 Electron transport in hydrocarbon mixtures

Some attention has been paid to the study of the electron transport in liquid mixtures. The motivation is the investigation of the change of the electron transport properties when the mixture is composed of two liquids which are significantly different in their electron transport state. In this regard, mixtures of high and low mobility liquids, such as neopentane ($\mu_e \approx 60$ cm^2/Vs) and n-hexane ($\mu_e \approx 0.08$ cm^2/Vs), have attracted special attention (Minday et al. 1972, Nyikos and Schiller 1975, Wada et al. 1977). Such studies postulate a dependence of the electron mobility on the composition of the mixture. In other words, a monotonical decrease in the electron mobility of the mixture is attained when the ratio of the low mobility liquid in the mixture is gradually increased. This fact indicates that a desired mobility, lying between the respective mobilities of the two components forming the mixture, can be obtained by suitably adjusting a certain ratio of one component to the other.

The composition dependence of the electron mobility in liquid mixtures of neopentane and n-hexane is well represented by the following equation (Minday et al. 1972, Wada et al. 1977).

$$\mu_{e\,mix} = \mu_{np}^{x_{np}} \cdot \mu_h^{x_h} \qquad (3\text{-}19)$$

where μ_{np} and x_{np} are the electron mobility and the mole fraction for liquid neopentane respectively, whereas μ_h and x_h are those for liquid n-hexane. This result is in agreement with that reported in mixtures containing liquid ethane, representing the low mobility liquid ($\mu_e \sim 10^{-3}$ cm^2/Vs), and liquid methane at T=111 K (Bakale et al. 1975).

The temperature dependence of the electron mobility in liquid mixtures is congruous to that observed in most of the pure liquids, which is of an Arrhenius type of the form (Minday et al. 1971, Minday et al. 1972, Holroyd and Tauchert 1974).

$$\mu_{e\,mix} = \mu_q \exp\,(-E_{a\,mix}/k_B T) \qquad (3\text{-}20)$$

where μ_q denotes the electron mobility in the quasifree state, and $E_{a\ mix}$ is the activation energy of the liquid mixture. The latter factor in neopentane-n-hexane mixtures exhibits a linear dependence on the mole fraction of hexane which is represented in the form

$$E_{a\,mix} = E_{a\,np}\, x_{np} + E_{a\,h}\, x_h \qquad (3\text{-}21)$$

Here $E_{a\,np}$ and $E_{a\,h}$ are the activation energy of neopentane and n-hexane respectively. For the same mixture, a linear relationship between the energy of the conduction band, V_0, and the mole fraction is also observed (Wada et al. 1977). Thus

$$V_{0\,mix} = V_{0\,np}\, x_{np} + V_{0\,h}\, x_h \qquad (3\text{-}22)$$

Fitting experimental values of μ_{np}, μ_h, $V_{0\,np}$, $V_{o\,h}$, $E_{a\,np}$, and $E_{a\,h}$ in the last three equations and solving for $\mu_{e\,mix}$, and $V_{0\,mix}$, the following empirical formulae are obtained

$$\mu_{e\,mix} = 0.35 \exp(-15\ V_{0\,mix}) \qquad (3\text{-}23)$$

$$V_{0\,mix} = -0.42 + 2.6\, E_{a\,mix} \qquad (3\text{-}24)$$

In order to account for the many liquid hydrocarbons, and TMS at room temperature, equation (3-23) was modified to take the form of equation (3-18).

The free ion yield of the mixtures of neopentane and n-hexane in the presence of the electric field can be calculated through equation (3-11), with F(r) represented by the three dimensional Gaussian distribution function (Wada et al. 1977). In this case the parameter b in the Gaussian distribution represents the most probable value of the thermalization distance, r, in the liquid mixture.

For low concentrations of the low mobility liquid, the mechanism of the electron transport of the mixture is almost similar to that of the high mobility liquid, i.e. the electron transport proceeds via extended states as a result of frequent scattering by the molecules. However, for high concentrations of the low mobility liquid, the state of the electron is localized and thus the trapping model is a more appropriate description. While the trapping process in liquid hydrocarbons generally is ascribed to individual effects such as vibration, dipole moment etc, the fact that the electron mobility, and therefore the activation energy, of liquid mixtures is a function of the fraction of the low mobility liquid indicates that this process in liquid mixtures is a collective property (Januszajtis 1963).

In fact the observed temperature dependence of the electron mobility in liquid mixtures suggest that the thermal activation energy is the spontaneous mechanism responsable for electron liberation from the trap. On the other hand, the application of an electric field enhances the efficiency of the electron transport by increasing the

jump frequency (Bakale et al. 1975). An alternative way for the electron to proceed through liquid mixtures is by tunnelling, rather than hopping (Minday et al. 1972). Another approach to elucidate the composition effect on the electron mobility in liquid mixtures is to apply percolation theory (Kestner and Jortner 1973). According to this theory, the liquid mixture is assumed to be composed of two regions with respect to the electron mobility where the volume fraction of each region relies on the mole fraction of each component in the mixture. Then the electron mobility in the liquid mixture, $\mu_{e\,mix}$, is determined by the following equation (Schiller et al. 1982)

$$\frac{\mu_{mix}}{\mu_h} = -\left(1-\frac{\mu_l}{\mu_{hi}}\right)\ln\left(1-\eta C^2\right)+\frac{\mu_l}{\mu_{hi}} \qquad (3\text{-}25)$$

where μ_{hi} and μ_l are the high and the low mobility liquids respectively, h is a constant related to the high mobility region, and C is the volume fraction of the high mobility liquid.

Chapter 4

Intrinsic conduction in liquid hydrocarbons

4.1 Introduction

When an electric field of a few kV/cm is applied to an ionization chamber filled with a carefully purified sample of liquid, a small current flows through the measuring circuit. However, if the range of the electric field values is extended the current can be demonstrated to have two main components, similar to those shown in figure (2-1). Moreover, at a certain value of the electric field, depending on the type of liquid used, a super-linear rise in the electric current is observed. The excess current is believed to be due to electron emission from the high field electrode (Kao and Calderwood 1965). The observed current is called the dark current, or residual current, due to its ambiguous origin. In fact a low value of the dark current is vital to the success of the processes of radiation detection since this value determines the lower limit of radiation intensity that can be clearly detected. If the dark current in a liquid filled ionization chamber is measured, then the electrical conductivity can be predicted using equation (3-9).

Although ionization and induced conductivity in liquid hydrocarbons have been discussed in previous chapters, in this chapter is considered the natural intrinsic conductivity of liquid hydrocarbons at low and high electric fields and the possible mechanisms involved.

4.2 Low field conductivity

Highly purified liquid hydrocarbons are among the best insulators known. Despite this fact, even in the presence of low electric field strengths a small conductivity is detected. The origin of such small currents has attracted a considerable amount of attention and stimulated theoretical and experimental studies into their cause. To date, there is no satisfactory explanation for the observed phenomena which has been generally adopted. However, the small electric conductivity present at low electric field strength is thought to be associated with the existence of charge carriers which are normally present in the liquid as a result of "virtually unavoidable" impurities; secondary radiations produced by cosmic-ray interactions; ions normally generated by the high voltage supply on both electrodes; and naturally ionizing particles, most probably alpha particles, which originate in the materials composing the chamber. Furthermore, it has been maintained that the natural conductivity observed at low electric fields is caused by a vanishingly small concentration of ions which result from the spontaneous dissociation of liquid molecules (Plumley 1941). At higher electric fields, it is claimed that molecules on the verge of dissociation, and with a wide range of dissociation energy levels, are provoked into dissociation by the assistance of the electric field. Similarly molecules which have been excited, presumably by the effect of natural environmental radioactivity, are expected at small electric fields to produce ions by collisions (Rice and Choi 1962). Investigation of the possible cosmic ray contribution to the low field intrinsic conductivity is the most controversial issue. This investigation is also a difficult task since it requires a liquid extremely high in purity, with natural conductivity of the order of 10^{-19}-10^{-20} $\Omega^{-1}.cm^{-1}$. A high level of purity

must be maintained throughout the whole experiment. Rogozinski measured the dark current produced in an ionization chamber filled with liquid n-hexane and having an electrical conductivity of the order of $10^{-19}\,\Omega^{-1}\,cm^{-1}$ (Rogozinski 1941). It was placed in an environment especially constructed for such a purpose. The result of this investigation revealed that at least 15% of the total measured current could be attributed to the effect of cosmic radiations. However, for the same liquid with an electrical conductivity one order of magnitude lower, this ratio rose to about 30% (Nikuradse 1932). Pao has described the results of various authors who support the effect of cosmic ray-induced electrical conductivity in liquids (Pao 1943). However, the results of the experimental work he conducted, using liquid isooctane of comparable conductivity, did not indicate a similar conclusion. He suggested that the difference was due to the much smaller volume, and thus the higher electric field employed, which produced an undetectable current density estimated to be of the order of 10^{-16} amp./cm^3.

In conclusion it seems that the most reasonable explanation for the low field natural conductivity of liquid hydrocarbons is the result of various collective processes. In other words, assuming the liquid used is very pure, ions produced in the liquid are only partially related to the effect of cosmic rays. A higher proportion of the current is assigned to the natural decay of radiation in the interior of the chamber materials. Other significant contributions come from impurities present in the interior structure of the chamber material and the opposite charge carriers produced on the electrode surface as a consequence of the initial operation of the high voltage supply. Then under the action of the electric field, ions created by the sum of the mentioned effects acquire sufficient energy to produce more ionizations by other means.

4.3 High field conductivity

The study of intrinsic conduction in the region of high electric field is complex as it involves many phenomena. Various attempts have been made to account for these phenomena and different theories have been proposed. These theories have, in general, not gained any widespread acceptance. Nevertheless, some of these theories, which are reviewed below, do provide reasonable explanations for the observed phenomena.

4.3.1 Electron emission

Electron emission from the cathode renders the most logical explanation for the intrinsic current. Electrons are presumed to be released from the electrodes into the liquid sample of an ionization chamber by two mechanisms, thermionic emission and field emission. In the former mechanism electrons are assumed to be ejected thermionically from a metal cathode into the liquid under the action of high electric field. The process is described by the Schottky equation:

$$I = I_0 \exp\left(\frac{e^{3/2} E^{1/2}}{\epsilon^{1/2} k_B T}\right) \qquad (4\text{-}1)$$

where I_0 is the thermionic current density at an absolute temperature T (Baker and Boltz 1937). However, if the thermionic emission theory is a proper description of the high field conductivity, the plotting log (I) as a function of $E^{1/2}$ should yield a straight line, known as the Schottky line, for the data in the high field region (Pao 1934, House 1957). Then I_0 is determined by extrapolating the straight line to zero

field. In the case of field emission, also known as cold emission, the surface electrons gain enough energy from the applied electric field to pass over, or tunnel through, the potential barrier of the metal-liquid interface into the liquid (Dornte 1940). The latter mechanism is represented by the Fowler-Nordheim equation :

$$I=6.2x10^{-6}\frac{F^{1/2}AE^{2}}{(F+\varphi)\,\varphi^{1/2}}\exp\left(\frac{-6.8x10^{7}\varphi^{3/2}}{E}\right) \quad (4-2)$$

where φ is the work function of the metal (eV), F is the Fermi level of electrons in the metal, which is approximately equal to 5 eV, A is the total emitting area of the cathode (cm^2), and E is the electric field strength (V/cm) (Watson and Sharbaugh 1960).

It is possible to explain the high field conductivity with the electron emission if we consider the combination of two facts. Firstly, It is well known that the work function of the electrode surface in the presence of liquid, with respect to that in vacuum, is much reduced. This phenomena may be ascribed to the extra force exerted by the liquid molecules on the metal surface (Baker and Boltz 1937, Pao 1943). Secondly, the actual strength of the electric field in the immediate vicinity of the metallic surface of the electrode is not uniform and consequently the effective microscopic work function may change. The actual cause of such a phenomena rests in the fact that the real nature of the electrode surface is, even for those which are highly polished, microscopically covered with sharp points. Over this surface, the magnitude of the electric field can deviate from the mean surface value by very large amounts (Baker and Boltz 1937).

At a sufficiently high electric field, the energy input at the asperities on the surface

may become high enough to cause local evaporation of the liquid thereby forming tiny vapour bubbles (Watson and Sharbaugh 1960). Formation of the consequent low density region, relative to the surrounding medium, may also be brought about by collapse of the space charge layer formed in the high field region adjacent to one electrode (Krasucki 1963, Charalambus 1967), or as a result of inadequate purification of the liquid which may leave small quantities of absorbed air or other gaseous products in the liquid sample. At low electric field the existence of bubbles in the sensitive volume of the liquid may cause fluctuations in the current which is a possible cause of the poor reproducibility of the results (Kao and Calderwood 1965). However, if a bubble, or train of bubbles, completely bridges the gap between the electrodes, and the electric field is sufficiently high, then electric breakdown in the weakly conducting region may be initiated. The observed fluctuations of current in liquid n-hexane was greatly reduced when the measurement was performed at high hydrostatic pressure, an observation which is consistent with the hypothesis of bubble formation (Haidara and Denat 1990, Yamashita et al. 1990).

Examinations of the electrical pre-breakdown in di-electric liquid have been performed using pure liquid doped with fluorescent additives such as anthracene or inorganic phosphors (House 1957, Darveniza and Topper 1961). Such materials have the characteristic of light emission under the influence of high electric fields. In this region of the field the free electrons initially present in the doped liquid, can gain enough energy to undergo excitation collisions with the liquid and additive molecules. However, in the collisions with the fluorescent molecules higher energy levels are excited some of which decay with associated light emission.

Information on the electron emission effect can be obtained by measuring the current

field characteristics at several different separations of the electrodes and for different electrode materials. In this regard, some of the measurements have revealed results which tend to support the electron emission mechanism as a proper description of the electrical conductivity in liquid (House 1957). However, other similar investigations have failed to reach the same conclusion (Pao 1943, Forster 1962). For example, Le Page and DuBridge have argued that thermionic emission alone cannot account for the observed high field conductivity in liquids (LePage and DuBridge 1940). Instead a combination of thermionic and field emission seems to be more appropriate. This conclusion is reached because their experimental data does not comply with the expected constant slope of the Schottky equation (4-1) as produced in the case of thermionic emission. In fact the effect of electron emission can be minimized by screening the high field electrodes by mesh held at an appropriate polarity so that electrons emitted from the high voltage electrode are suppresed from the sensitive volume.

4.3.2 Dissociation and ionization induced by the electric field

Ionization and dissociation of liquid molecules is believed to be achievable by the action of a high applied electric field. The required energy for dissociation, supplied by the applied electric field, may be significantly reduced if the molecules have been pre-excited to a higher energy state presumably by the effect of cosmic radiation or other naturally energetic radiation (Adamczewski 1937). Another possible cause of ion production in the liquid may be traces of polar impurities which are readily ionizable due to the favourable orientation of their ionic bonds with respect to that of the

electric field (Reiss 1937).

Plumley has applied dissociation theory successfully to his experimental data (Plumley 1941). He obtained the following expression for the electric current:

$$I=C_0\exp\left(\frac{2e^{3/2}E^{1/2}}{\sqrt{300\epsilon}k_BT}\right) \qquad (4\text{-}3)$$

where C_0 is a constant associated with the number of dissociated molecules at zero electric field, and ε is the di-electric constant of the liquid (F/m).

It has been proposed that at high electric field the action of the applied field is strong enough to weaken the energy of the C-H bonds of the liquid molecules (Plumley 1941). This effect leads to the formation of a hydrogen layer, regarded as a positive layer, on the cathode surface. A hydrogen layer may also be adsorbed on the electrode surface if that electrode is outgassed by heating in hydrogen. However, this layer can be replaced by an oxygen layer if the heating is performed in oxygen. The adsorbed layer of hydrogen on the surface of the cathode may reduce the work function of the cathode, resulting in higher current. This effect is attributed to the high electronegativity of hydrogen atoms towards electrons at the cathode surface (Baker and Boltz 1937, Green 1956). On the other hand, if the hydrogen layer is replaced by an oxygen layer the work function of that electrode is increased and thus the current is decreased. For a platinum electrode, heating by nitrogen seems to be more appropriate since the adsorption of this material on the electrode is very low and consequently it has a negligible effect on the work function.

In fact the presence of hydrogen, or other atoms on the electrode surface, may form

image charges in the metal producing dipole moments which may interfere with the investigation of the possible mechanisms of the high field conductivity (Baker and Boltz 1937). If the present theory describes a possible mechanism for the high field conductivity, the electrical current should depend on the volume of the liquid. Simpler evidence for confirming the effect can be obtained by changing the polarity of the applied voltage which should have no significant effect on the electric current. This was concluded in the measurement performed in liquid hexane (Terleki 1966). Experimental work aimed at such an investigation gave results which were consistent with the theory.

4.3.3 Ionization by collision.

It is assumed that, at high electric field, the small number of ions initially present in a liquid, as indicated by the low field conductivity, acquire sufficient energy to carry out multiplication by collision with the neutral molecules of the liquid, resulting in more ions. Then, if the applied voltage is increased there should be an exponential increase in the induced current. Collisional ionization may also take place inside a gas bubble, formed in the liquid by one of the mechanisms mentioned earlier, leading to charge multiplication which may be sufficient to initiate electrical breakdown (Fuhr and Schmidt 1986).

In fact at high electric field the process of charge multiplication by collision, which is greatly enhanced in the small volume of the liquid close to the high field electrode, interferes with the processes of electron emission from the high field electrode so that the exact contribution of each effect to the observed current is distorted. Furthermore,

at such values of the electric field at which electrical pre-breakdown of the liquid is expected, tiny tenacious spots of an insoluble wax-like substance is likely to be produced and spattered on the anode (Lepage and DuBridge 1940, Watson and Sharbaugh 1960). This was taken as evidence that electrons are emitted only from small pointed areas of non-uniformity on the metal cathode rather than from the whole area. This phenomena was ascribed to chemical action caused by electron bombardment nearby the cathode surface.

From the forgoing discussion it seems that there are two mechanisms responsible for the electrical conductivity at high electric field. One is associated with ions produced initially in the liquid. The other is due to the electron emission mechanism caused mainly by the high force of the electric field. Thus, a method aimed towards obtaining a better estimation of the total collection of ions in liquid hydrocarbons is likely to require two main actions. First, extreme minimization of the electrical conductivity by using highly pure liquids. It appears more appropriate to conduct the purification procedure, if possible, inside the ionization chamber as this will reduce any possible contamination introduced during transference of the liquid into the ionization chamber. Furthermore, such a process can be easily repeatable and keeps the interior of the chamber fresh and ensures that there will be no influence of dust particles. In fact a liquid having natural conductivity in the range of 10^{-17}-10^{-19} Ω^{-1} cm^{-1} seems to bear no significant effect on the measured ionization current up to moderate values of the electric field but the high electric field required for overcoming ion recombination enhances the role of impurities against obtaining a pure ionization signal.

The second important requirement for a better investigation of ion collection is the optimization of the applied electric field so that collision ionization, and more

importantly, electron emission can be neglected. Thus, if such requirements are met along with the employment of sufficiently strong ionizing radiation, the interference, or distortion, of the dark current with the processes of collection is minimized to its lowest values and thus an accurate measurement and a much better estimate of the actual mechanism of the ion collection in liquids could be attained.

Chapter 5

Experimental studies with liquid ionization chambers

5.1 Introduction

Special attention has been given to the study of electrical conduction in room temperature di-electric liquids. In order to investigate the fundamental mechanism and determine the factors limiting the processes of charge transport in these media, extensive experiments have been conducted. In these experiments different ionization chambers and various types of radiation sources were used.

For the preliminary investigations, a stainless-steel ionization chamber was developed. Later, having gained experience in its performance and capabilities a new chamber of different materials was constructed to enable better control of some factors involved, and for ease of cleaning. An important feature of the chambers is the possibility of varying the inter-electrode spacing. The materials used were selected to minimise possible production of organic impurities by chemical reaction with the contained liquid. Such impurities interfere with the free movement of charges produced in the liquid medium, thus limiting the process of charge collection (Carugno et al 1991, Wickman and Nystrom 1992).

The ionization chambers employed in this work are described in this section. Reasons are given for the choice of liquid di-electric selected. This liquid was subjected to further purification by adopting a specially devised purification procedure. A detailed

description of the chemical purification method applied to this liquid is presented along with details of the electrical purification method which is the final stage of purification. It is carried out inside the chamber after it was carefully cleaned.

5.2 Liquid ionization chamber (stainless-steel model)

A cross section of the stainless-steel (SS) ionization chamber is illustrated schematically in figure (5-1). The motivation for constructing this chamber was to conduct a preliminary investigation of the dependence of the current-field characteristic on factors such as liquid purity, electrode separation, and electrode material.

Although the material used for building the body and the electrodes of the chamber was stainless-steel, these electrodes were exchangeable and could be made in other materials. The insulators for the electrodes were made from teflon (PTFE), known for its excellent electrical insulation. However, there has been a critical report which claims that PTFE is not compatible with liquid TMS due to the presence of the fluorine which is an electronegative element (Aubert et al. 1992). This result appears to be anomalous as it was not confirmed in the present work. It may be that the type of teflon they used was of poor quality.

Initially stainless-steel electrodes were used. The circular collecting electrode was 1 cm in diameter surrounded by a guard ring of 3 cm external diameter. This guard protects the collector from stray current and assures uniformity of the applied electric field in the sensitive region. The high voltage electrode of negative polarity had a diameter of 4 cm. It was sandwiched between two teflon rings to insulate it from the

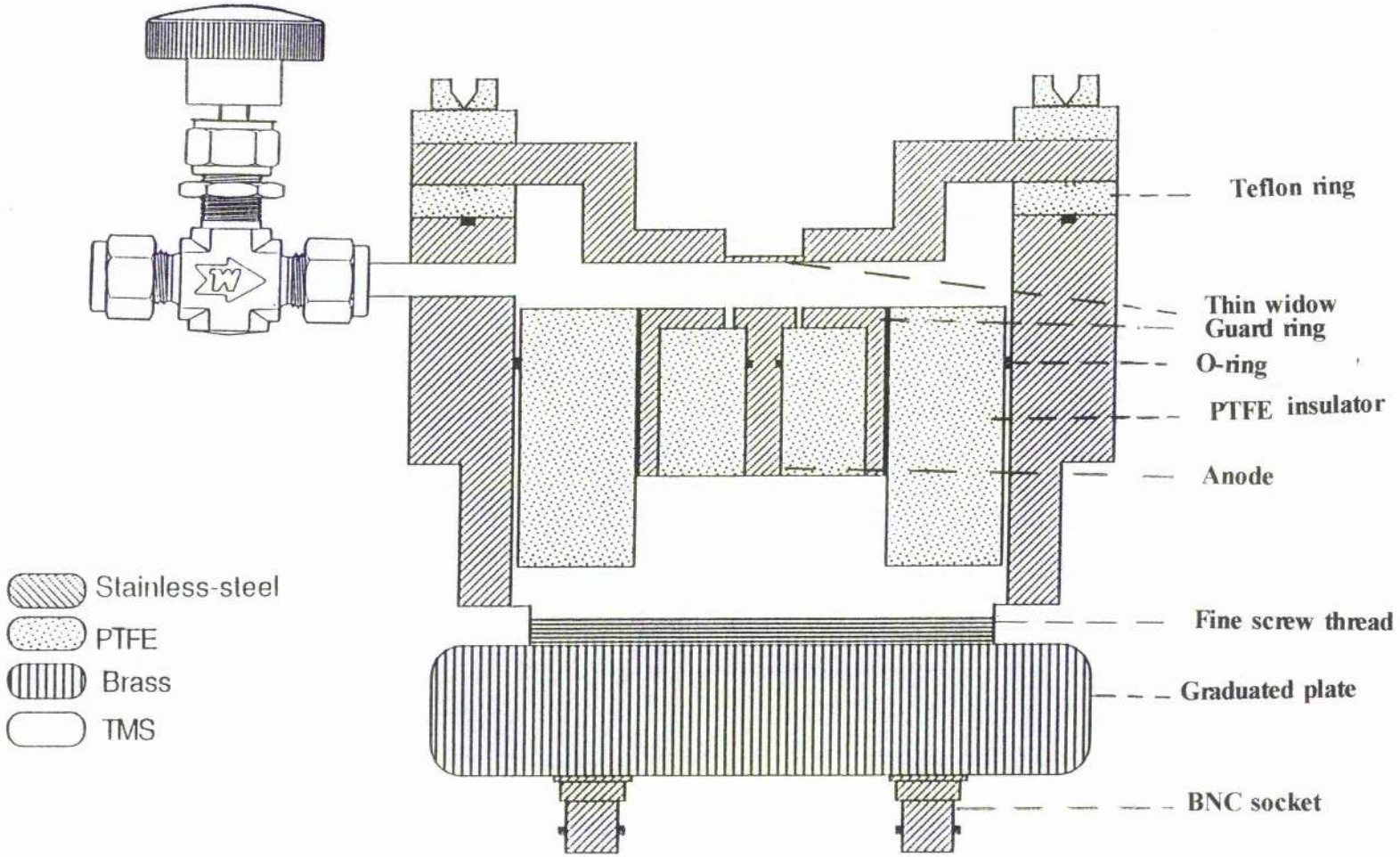

Fig (5-1): Liquid ionization chamber (stainless-steel type)

body of the chamber. The central spot of this electrode, serves as the window. It is 0.2 mm thick and has a diameter of 1 cm. It was placed exactly on top of the anode so that any deposition of radiation outside the sensitive volume is reduced.

A photograph of the SS chamber with its associated auxiliary parts is shown in figure (5-2). These parts are:

i- Aluminium electrodes of the same specification as those used for stainless-steel and mentioned above with the difference that the thickness of the circular window is 0.3 mm.

ii- Electrodes made from conducting plastic A-150 tissue-equivalent, with a window of thickness 1 mm. Windows of this material with thinner thicknesses were found to be impracticable as they were fragile and porous.

iii- Stainless-steel point anode with tip diameter 0.2 mm.

Graphite material was also tried for the construction of the chamber electrodes but found to be very fragile and porous so that no adequate vacuum could be maintained inside the chamber.

In the design of the chamber care was taken so that the collecting electrode could not 'see' the insulator in contact with the high voltage electrode. This is an essential requirement, since otherwise the collecting electrode would pick up stray charges tracking across the insulator. The lower part of the chamber was a graduated brass plate screwed to the body of the chamber and connected directly to the teflon cylinder housing the anode and its guard. This part allows for variation of the gap between electrodes within the limits 0-8 mm. The gap was considered to be closed when the electrodes just made contact. Commissioning of the chamber's parts was accomplished using rings of silicon rubber, since other materials might influence the vacuum

Figure (5-2): The stainless steel ionization chamber and its auxiliary parts

tightness of the chamber. For this purpose a pure indium gasket was favoured by some other worker (Carugno et al. 1991). This material was not used in the present work because of the proneness to leakage. In fact, the rubber rings used were firmly embedded in the body of the chamber and were not in direct contact with the liquid in the sensitive volume. This means that any possible contamination of the liquid caused by the use of this material should be insignificant.

5.3 Liquid ionization chamber (glass model).

The motivation for constructing this chamber was to remedy the few disadvantages found with the previous chamber. These are summarized as follows:

i- The need to refill the chamber with a new sample every time the gap between the electrodes was set. This demanded a repeat of part of the cleaning process including evacuation of the chamber which could alter the level of purity of the liquid.

ii- Possible contamination of the liquid sample contained in the chamber due to any impurities present in the microscopic cavities which presumably form on the surface of the teflon cylinder housing the anode. Such impurities, which are difficult to remove, are possibly introduced through machining and handling of this material.

iii- In some measurements taken with the SS chamber it was found that, after stressing the liquid for a few days, the anode of the chamber slipped back inside the teflon insulator. This was most probably due to the mechanical stress caused by high pressure developed by liquid vapour in the chamber.

With the present design, the parallel alignment of the electrodes was improved by fitting adjusting screws.

A schematic drawing of the glass ionization chamber is shown in figure (5-3). It is a parallel plate chamber with variable electrode spacing. It was designed so that both electrodes could be easily replaced by new electrodes as desired. The radius of the collecting electrode is 0.6 cm, and that of the cathode is 0.8 cm. The material of the electrodes is brass with extra electrodes of tissue equivalent plastic material, type A 150, of similar dimensions. The upper part of the chamber consisted of a brass cylinder holding a stainless-steel micrometer head of precision 0.001 mm. This permits the gap between the two electrodes to be varied from zero, when the electrodes just make contact, to 15 mm. The contact point was confirmed by a simple electric conductivity test. The lower part of the chamber is formed of a glass vessel and two metallic circular electrodes. This is another advantage over the previous chamber since the liquid is contained in an easy cleaned material. The lower electrode, representing the high voltage electrode, was screwed inside a teflon push-fit base in order to insulate it from the earthed metallic cylinder. The purpose of this cylinder, having a mesh widow allowing for radiation and observation, is to screen both electrodes from any interference caused by the electrostatic charges formed on the inner-surface of the glass envelope. Each electrode was insulated and guarded by a stainless-steel tube connected to a suitable potential. On the side of the chamber two teflon stoppers were fitted to maintain the required low pressure. Two 250 ml glass reservoirs were attached to the glass envelope through glass-metal seal tubes in order to facilitate filling and flushing of the chamber. The point of contact is very brittle so that care had to be taken whenever attachment or separation of the reservoirs is required. The upper electrode, representing the collector, is attached to a bellows-metal sliding feed-through which is controlled by the direct movement of a micrometer head. The

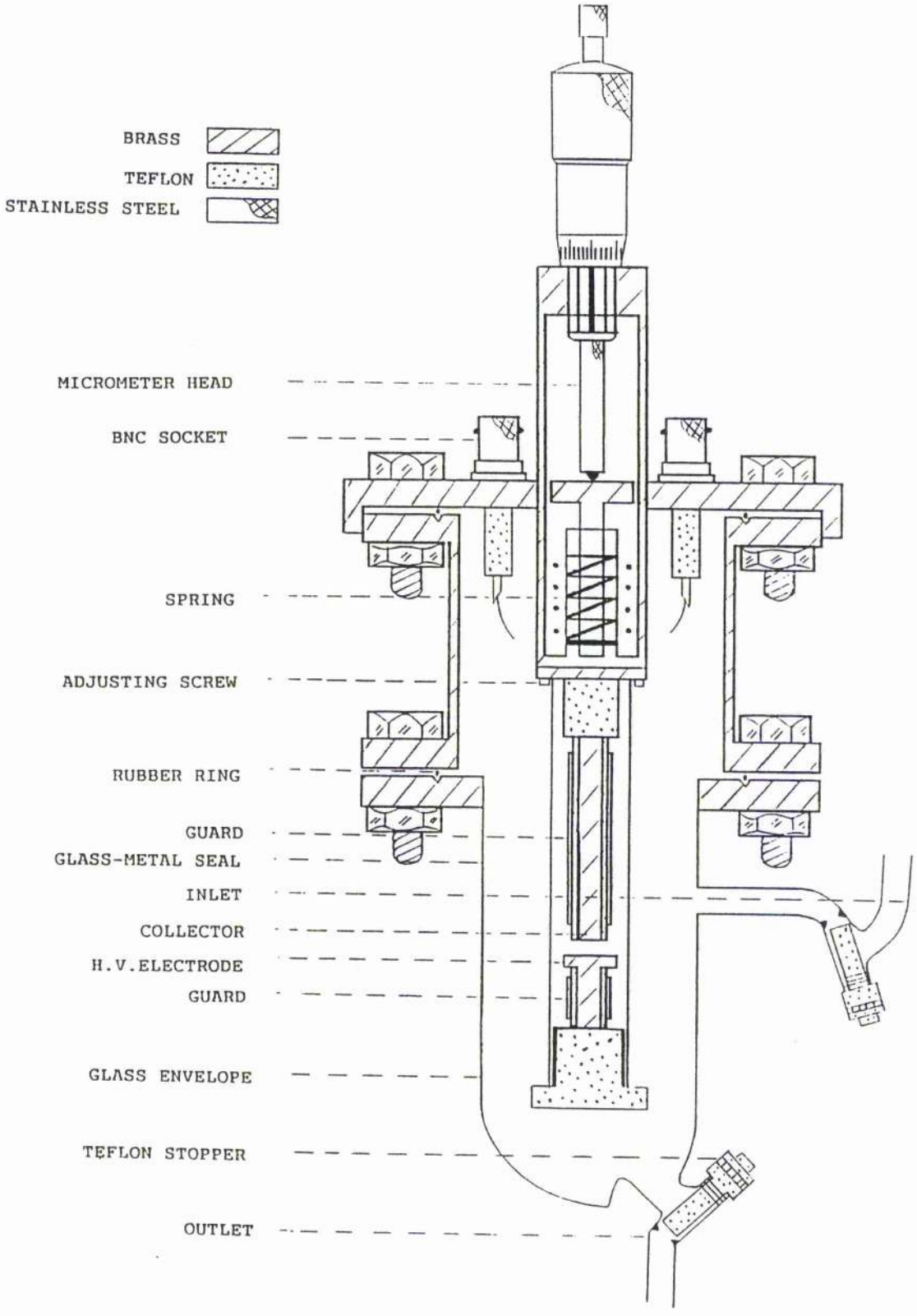

Fig (5-3): Liquid ionization chamber (glass type)

electrodes were mechanically polished. First using Brasso (metal polish) to remove the deeper scratches present on the surfaces. It was then further polished using Goddards (long term silver polish) to smooth down any observable fine scratches.

5.4 Associated equipments

Irradiation of the chambers was performed using a well screened ^{57}Co radiation source of initial activity of 4 mCi. In the case of the S.S chamber, the γ-radiation was fired through the thin window, parallel to the direction of the electric field. The intensity of the radiation was changed by placing the source at a variable distance from the window using teflon spacers of different thicknesses. However, for the glass-type chamber the radiation was fired through the glass wall in a direction perpendicular to the electric field. This will probably increase efficiency of charge separation thereby enhancing the charge collection.

In order to assure a good vacuum in the chamber; and for the purpose of high field applications, special BNC sockets, radiall type R-316 603 were used. Electrical connection was made using plugs of type, radiall R-316 007, attached to well screened low-noise coaxial cables specially designed for low level current measurements.

The power supply used in this experiment is a 5 kV high-voltage stabilized unit. Measurement of the electric current was performed using a Keithely model 602 electrometer. It is a solid-state battery-operated instrument which measures a wide range of current from 10^{-14} ampere full scale to 0.3 ampere.

The measuring set-up was placed inside a Faraday screened cage comprising a wooden frame covered with copper screening connected to the ground of the electrometer

circuit to reduce any unwanted generated currents which may affect the measurement accuracy. In the case of the glass chamber only the measuring circuit was screened, figure (5-4).

5.5 The choice of di-electric liquid

When selecting a non-polar liquid as di-electric for the study of free-electron charge transport, it is advantageous to consider factors that may make an important contribution to the investigation. In such a study, extremely high purity is essential. Other important quantities characterising the state of free moving charge carries are the high electron mobility; the negative value of electron affinity; and the high free ion-yield which contributes directly to the charge output signal. Such features are available in some rare-gas liquids but due to certain limitations involved in handling them, room temperature liquids with similar properties have been more preferred. Of these, branched non-polar liquids of symmetric molecular distribution, such as those listed in the table (2-5), have been widely used. A careful consideration of the data in appendix B shows that a high value of electron mobility corresponds, in many cases, with a high negative value of electron affinity, V_0.

Liquid TMS was selected for the experimental work performed here. This is because this liquid possesses the required features for a study of electrical conduction as mentioned above. In addition, liquid TMS has a few interesting properties, having a boiling point of 27 ^{0}C and low toxicity, which makes it more suitable for the present purpose.

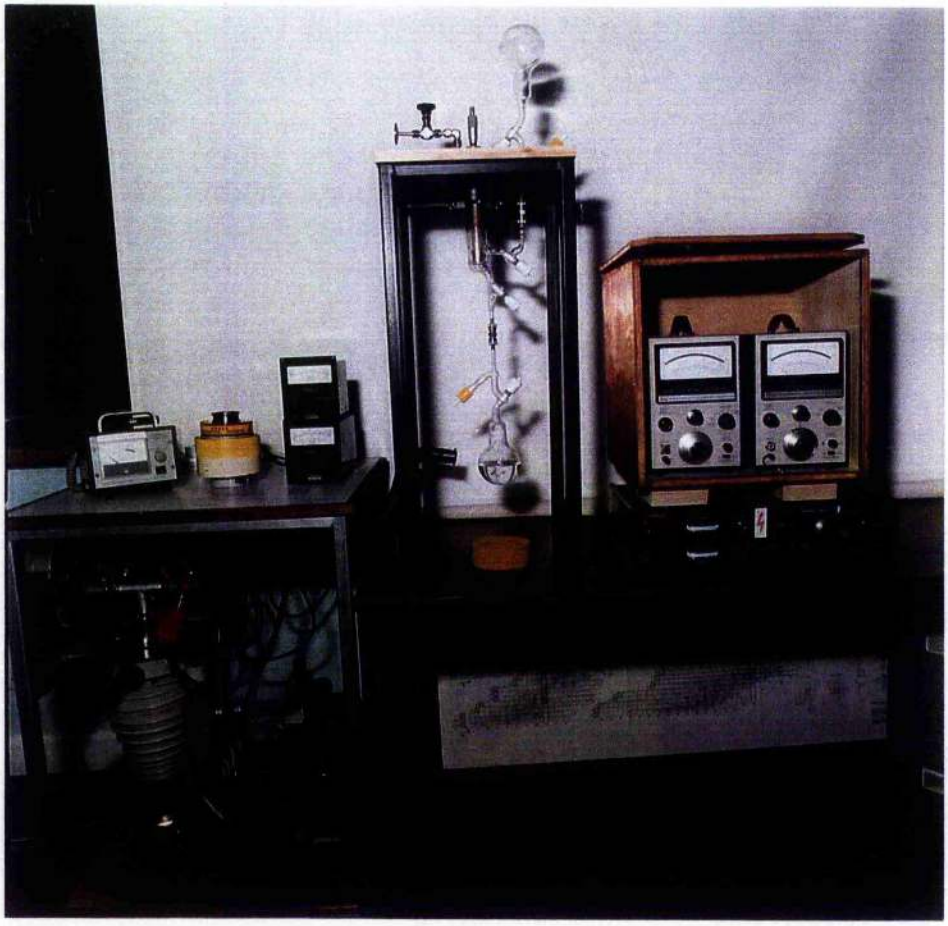

Figure (5-4): The glass ionization chamber and associated equipment.

5.6 Purification of TMS

As discussed earlier, an appropriately purified liquid is vital to the success of the study of electrical conductivity and breakdown in liquid hydrocarbons. This is because the charged carriers transported in the liquid are highly sensitive to any impurities present. In fact liquid of insufficient purity quite often leads to ambiguity and poor reproducibility of the results. However, it may in some cases alter some of the characteristic properties of the liquid. Di-electric liquids employed in some applications must have a high level of purity but for those used for particular investigations such as the study of electron transport, exceptionally high purity is required. The desired level of purity can be attained by carefully planning an appropriate purification technique.

The liquid used in the present work was bought from the Sigma-Aldrich Company Ltd. It was claimed to have a purity of only 99.9 %. As this liquid was necessarily exposed to air during the process of transfer from the original bottle to the flask attached to the test cell it was thought necessary to subject the liquid to further purification prior to the filling of the ionization chamber.

5.6.1 Chemical purification

In most cases the various techniques employed in the chemical purification of the liquid are simply concerned with drying and degassing. For rigorous drying of the liquid, appropriate agents should be used in order to avoid undesired reactions which in most cases are dangerous. For liquid hydrocarbons and TMS, efficient drying agents

are alumina (Al_2O_3), calcium hydride (CaH_2), and sodium wires (Na). If necessary, rigorous drying of the liquid is proceeded by a preliminary drying. In this case the liquid is allowed to pass through a column of activated molecular sieves (sodium and calcium aluminosilicates) of small pore size, approximately 3-4 ^{0}A. If the drying process of the liquid is completed the next task is to remove the drying agent. This can be done by fractionally distillating the dry liquid.

The process of chemical purification adopted here consists of two stages. In the first stage the TMS liquid was carefully dried from the traces of water using calcium hydride/sodium wire since even the slightest trace of water may markedly increase the intrinsic conduction of the liquid. In the second stage the liquid sample was degassed by using a freeze/pump/thaw technique.

5.6.1.1 Drying of TMS

The assembly used for the purification system in this experiment is shown in figure (5-5). It was designed to purify quantities of 250 ml of liquid. All parts that came in contact with the liquid or the vapour are made of teflon and glass to reduce possible contamination of the sample to a minimum. The teflon rods and taps were treated first in distilled water; acetone; dried then steeped in TMS liquid for an hour prior to use. With taps B and D open and tap C closed, the whole system was evacuated to 10^{-2} Torr through tap A. During pumping the glassware was thoroughly dried by heating its outer surface with a bunsen burner until no more condensation occurred on the glassware. Pumping was continued whilst the equipment was cooled to ambient temperature, before filling the system to atmospheric pressure with purified argon.

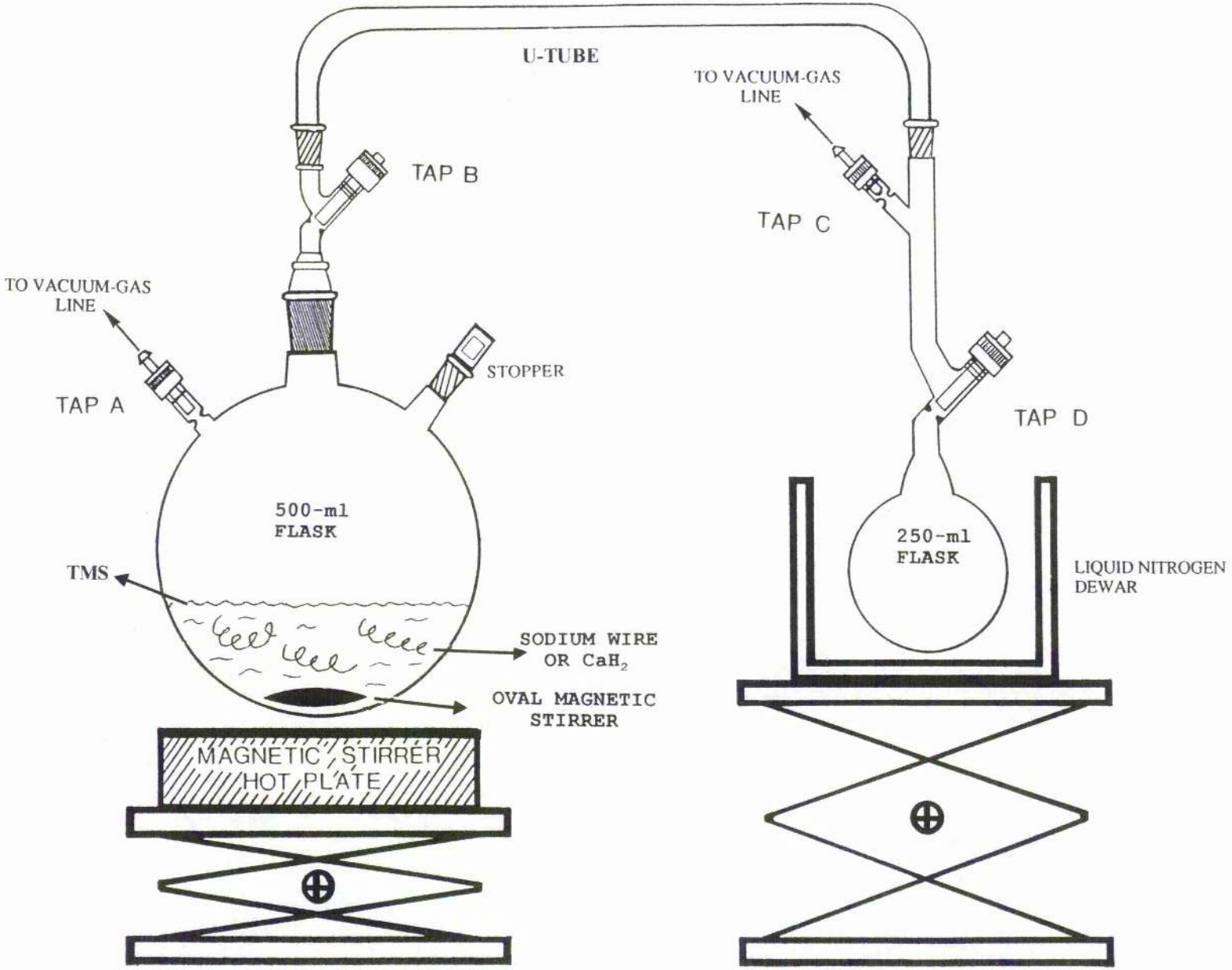

Figure (5-5): purification system for drying and degassing liquid TMS.

With tap B closed, the flask was purged with argon through tap A while the stopper was removed and 100 ml of TMS was added quickly to the flask together with either 10 g of freshly pressed sodium wire or 10 g of CaH_2. These are the preferred reagents for rigorous drying, then preliminary drying of the liquid is not essential. Then the stopper was replaced and tap A left open to a mercury manometer so that any hydrogen, formed from the reaction (5-1) of dissolved water with the sodium wire/CaH_2, could be safely vented.

$$\mathbf{CaH_2 + H_2O \text{ -------}\rightarrow CaO + 2H_2^{\uparrow}} \qquad (5\text{-}1)$$

The contents of the flask were stirred overnight to make sure that the TMS was thoroughly dried. Tap A was closed and a liquid nitrogen dewar was placed around the 500 ml flask whose contents were cooled using an acetone/dry-ice (solid carbon dioxide) mixture (-78 ^{0}C). A vacuum line was connected carefully through tap A which was re-opened to allow the gas to be removed from the flask without undue loss of the highly volatile TMS. When complete, tap A was again closed and the dewar removed to allow the TMS to warm up to ambient temperature.

With tap B kept closed and tap D open, tap C was used to evacuate the 250 ml storage bulb and interconnecting U-tube. Tap C was re-closed and the 250 ml storage bulb cooled to -198 ^{0}C by filling the dewar with liquid nitrogen. While the contents of the 500-ml flask were stirred, tap B was slowly opened so that the TMS was distilled under vacuum away from the sodium wire/CaH_2 and through the interconnecting tube into the 250 ml storage bulb. When complete, tap D was re-closed before filling the U-tube with air through tap C and disconnecting the 250 ml

storage bulb from the base of the U-tube. The neck of this storage bulb was then closed with a glass stopper and teflon sleeve. The water-free TMS stored in the storage bulb at this stage remained to be degassed.

5.6.1.2 Degassing of TMS.

The TMS in the 250 ml storage bulb was frozen employing a dewar filled with liquid nitrogen. A vacuum line was applied through tap C. Tap D was opened to pump away any gas above the frozen liquid sample. After pumping (10^{-2} torr) on the contents of the bulb for 2 minutes tap D was re-closed. The TMS was thawed using a hot-air gun and shaken for 1 minute before again being refrozen using liquid nitrogen. Tap D was again opened to pump on the contents of the flask for 2 minutes at 10^{-2} torr. This freeze/pump/thaw method, is a highly efficient degassing technique for liquids. It was repeated several times. Thus, extremely dry and highly degassed TMS was stored under vacuum in the storage bulb ready for transfer to the ionization chamber.

5.6.2 Cleaning and preparation of the liquid chambers

Thorough cleaning of the liquid chamber is regarded as a part of the process of purification. It is essential for maximum signal yield; better detection sensitivity of the electric current; and maintaining the level of purification achieved in the purification system.

Prior to the assembly of the ionization chambers all components, especially those

which come in direct contact with the liquid, were individually cleaned by treating them initially with liquid acetone; draining; and then rinsing copiously with distilled water. The last stage of the wet cleaning is to treat them with ethanol to remove any trace of oxygen. This was followed by a dry cleaning using a hot-air gun until no more moisture could be seen anywhere on the surfaces of the parts. Each chamber was then assembled on a clean bench and closed immediately afterwards. After assembly each conductance cell was evacuated down to 10^{-6} torr, and heated using a flexible electric heating tape connected to a temperature controller (Thermolyne 45500). After a few days of pumping, the heating was disconnected and the chamber was allowed to cool down slowly to the ambient temperature. Thereafter the storage bulb containing the highly purified liquid was connected to the chamber. Before introducing the liquid to the chamber, the whole system including the long neck of the storage bulb was evacuated down to 10^{-6} torr while the liquid is kept inside the bulb. The TMS sample was discarded and a new sample was introduced into the chamber after repeating the processes of filling. This was repeated a few times in order to obtain a very clean sample of liquid.

5.6.3 Electrical Purification

The so-called 'electrical purification' is simply achieved by subjecting the sample of liquid to a high electric field for a prolonged period of time. As this type of purification is carried out inside the ionization chamber it does not involve any particular difficulties. This method is considered to be a purification procedure since the outcome is a significant decrease in the electrical conduction with time, by as

much as several orders of magnitude. It was assumed that good purification was achieved when the current tended towards a low stable value. This value of the current is only altered if impurities are re-introduced to the liquid. This was found to be the case when the tissue equivalent electrodes (TE) were used. In that case the current exhibited a slow rise after passing through a minimum value. The slow contamination of the liquid sample, which eventually predominated over the electrical purification, was, presumably, caused by chemical reaction with the material of the electrodes.

The systematic decrease of the dark current with time is generally believed to be due to the removal of various type of impurities, such as gas and vapour bubbles, from the interior surfaces of the chamber and from the sensitive region of the liquid sample by the action of the high electric field (House 1957, Duhm et al. 1989). These impurities are eventually deposited on the electrodes surfaces. However, in order to keep the measuring electrodes clean, extra electrodes, placed far from the measuring electrodes, can be introduced to the test cell. Thus, if a high electric field is applied between these electrodes the impurities move from the liquid medium and are deposited on the purification electrodes leaving the measuring electrodes clean (Charalambus 1967). Adamczewski suggested that the systematic decrease of the electric current is the result of two processes (Adamczewski 1969). The first is the removal of traces of electrolytic impurities and the initiation of bubbles in the chamber. This stage occurs over a time period between 15-30 minutes and results in a rapid exponential decrease of the electric current of the form:

$$I_d = I_0 \exp(-\lambda t) \qquad (5\text{-}1)$$

where I_0 is the initial current which depends on the electrode spacing, and λ is a constant. In the second stage, subtle changes in the liquid structure occur. This is thought to be caused by the rearrangement of certain regions of the quasi-crystalline molecular lattice. It takes place over a relatively long time and results in a slow but systematic decrease in the electric current. Blance has also studied the background current in liquid and obtained the following relation:

$$I = I_0/(1+bt) \qquad (5\text{-}2)$$

where b is a constant (Blance et al. 1961).

The decrease in current with time was also explained as being due to the stripping of lightly adsorbed layers from the electrode surface (House 1957); decrease of concentration and drift velocity of charge carriers as a result of the inevitable present layer of oxide on the electrode surfaces (Kao and Calderwood 1965); and out-gassing of the materials used in constructing the chamber (Forster 1962). The latter mechanism is unlikely to be the reason, at least in the present case, since the chamber was degassed under heat and vacuum for one week before filling with liquid. In liquid hexane no influence of the purity was found when the conductivity was in the range of 10^{-16}-10^{-19} (Terlecki 1966). Within the framework of our purification procedure the conductivity obtained for the final samples of liquid was, for the SS-chamber, of the order of 10^{-16} and for the glass chamber, in the range of (10^{-17}-10^{-18}) which seems to be acceptable.

Chapter 6

Results and discussion

6-1 SS-Parallel-plate ionization chamber

6-1-1 Prestressing of the liquid

When the ionization chamber was filled with a fresh liquid sample of TMS, a high electric field was applied between the two electrodes for a time period of 24-40 hours. This procedure was repeated whenever a new sample of liquid was introduced. During this time a significant decrease of the dark current was observed. The dramatic part of the decrease took place in the first few minutes. Thereafter the current exhibited a slow, systematic decrease until a stable value was attained.

This phenomenon has been observed by most of those who carried out such an investigation and various explanations have been suggested, see (5.6.3).

The time variation of the dark current can be explained by assuming that the rate of charge carriers initially present in the liquid is systematically reduced as a result of a gradual increase of the hydrostatic pressure inside the chamber. The latter effect can be ascribed to the slow evaporation of the liquid sample at the microscopic sharp points, which are known to cover the surface of the high field electrode. At these extremities the intensity of the electric field, being inversely proportional to the radius of the tips, is significantly high. Over a relatively long time, the liquid vaporises

locally to form microscopic gas bubbles. Consequently, as a result of the slow increase of pressure in the chamber, the bubbles formed are reduced in size and diffuse from the region of the intense field to settle eventually on the interior surfaces of the chamber. The phenomenon is macroscopically similar to the formation of air bubbles on the surface of a glass containing water when the water is left in contact with air for a few days. As the pressure in the chamber approaches a maximum value, the effect is reduced to a minimum and the current thus reaches a low and stable value. The increase of pressure was evident in this work during the first few operations of the liquid chamber. In these runs the anode-guard assembly, which was initially inserted in the teflon insulating cylinder to form a flush surface, was found to become displaced as a result of subjecting the liquid for two days to a high electric field. In order to avoid such an effect small pins were fitted to fix the position of the electrode assembly securely.

The time variation of the dark current for certain values of the electric field was investigated in the parallel-plate ionization chamber. The highest electric field applied between the two electrodes was limited by the HV power supply and the smallest achievable gap.

Figure (6-1) shows the results obtained for an inter-electrode spacing of 4 mm using electrodes of different materials. Curve A corresponds to a sample of liquid taken directly from the supplied bottle and prestressed using stainless-steel electrodes (SS). Curve B, however, represents the behaviour of current with time for a special purified sample of liquid using the same pair of electrodes. This sample was additionally purified by the technique described earlier. Furthermore, it was introduced to the chamber under vacuum. In this case the stable current achieved was two to three

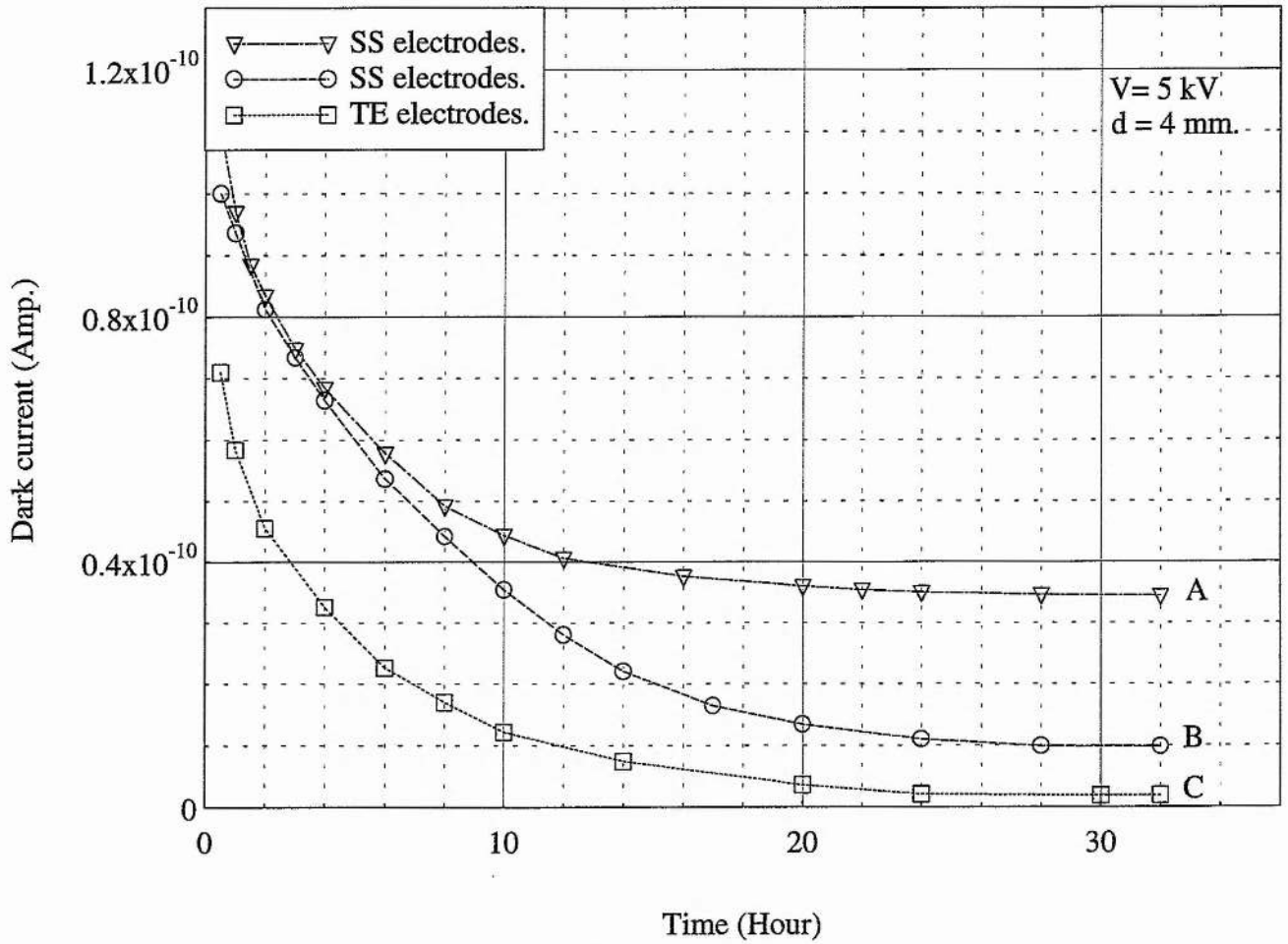

Fig (6-1): Dependence of dark current on time for liquid TMS using SS and TE electrodes.

orders of magnitude lower than that of the first sample. The significant difference of the dark current observed for the two samples of liquid provides evidence that an appreciable number of the charge carriers produced in the low purity sample of liquid originated from impurities. The impurities were probably introduced to the first sample, regarded as the low purity sample, during the process of transfer from the bottle to the chamber. These are in addition to other impurities which are inevitably present in the liquid due to a chemical reaction of the liquid with the interior surface of the constituent materials of the chamber.

An interesting observation is the behaviour of the dark current with time when a new high purity sample, obtained from the same bottle of that used with the SS electrodes, was pre-stressed using tissue-equivalent electrodes (TE) of conducting plastic A-150, curve C. In this case the dark current approached a value one order of magnitude lower than that of the stainless-steel electrodes. This can be attributed to the lower degree of asperity of the surface of the TE cathode. The difference in the surface condition can be ascribed to the higher influence of the heat generated during the mechanical construction of the surface of the TE electrode which tends to smooth down any sharp points that may be present. This effect is much smaller in the case of a metal electrode since with aluminum electrodes (AL) a similar result to that obtained with the SS electrodes was obtained.

6.1.2 Time variation of the dark charge.

Following the discussion of the behaviour of dark current with time for the TMS samples, it would be of particular interest to explain the variation of the dark charge

with time. This would be expected to be constant since the liquid in the chamber forms a static system operated under steady conditions. In fact, the time variation of the dark charge, plotted using the data of figure (6-1), indicates that this is not the case as shown in figure (6-2). For the low purity sample, curve A, the dark charge exhibits a rapid increase with time. However, for the high purity sample, curves B and C, the dark charge shows a relatively constant level after an initial increase at short times. From figure (6-2), it can be inferred that the time increase and the efficiency of the dark charge variation with time are sensitive to the purity and the nature of electrode surface, and therefore to the intensity of the electric field.

Had the general increase of the dark charge been due to charge leakage through the insulator, it would have shown a regular behaviour with time. We may therefore conclude that the difference in the behaviour is associated with the presence of impurities of electronegativity nature such as oxygen molecules. Hence, for the low purity sample the anode surface of the chamber is probably covered with a molecular layer of oxygen. Consequently, the oxygen molecules at the anode can extract electrons from the electrode surface forming slowly moving negative ions which accumulate at the anode. This process would proceed for a long time for the low purity sample due to the high concentration of such impurity molecules. However, for the high purity sample the effect is limited by the extremely low concentration of impurities and, thus, only a small increase of the dark charge occurs.

6.1.3 Dark current.

The dependence of the dark current on the applied voltage was recorded for the

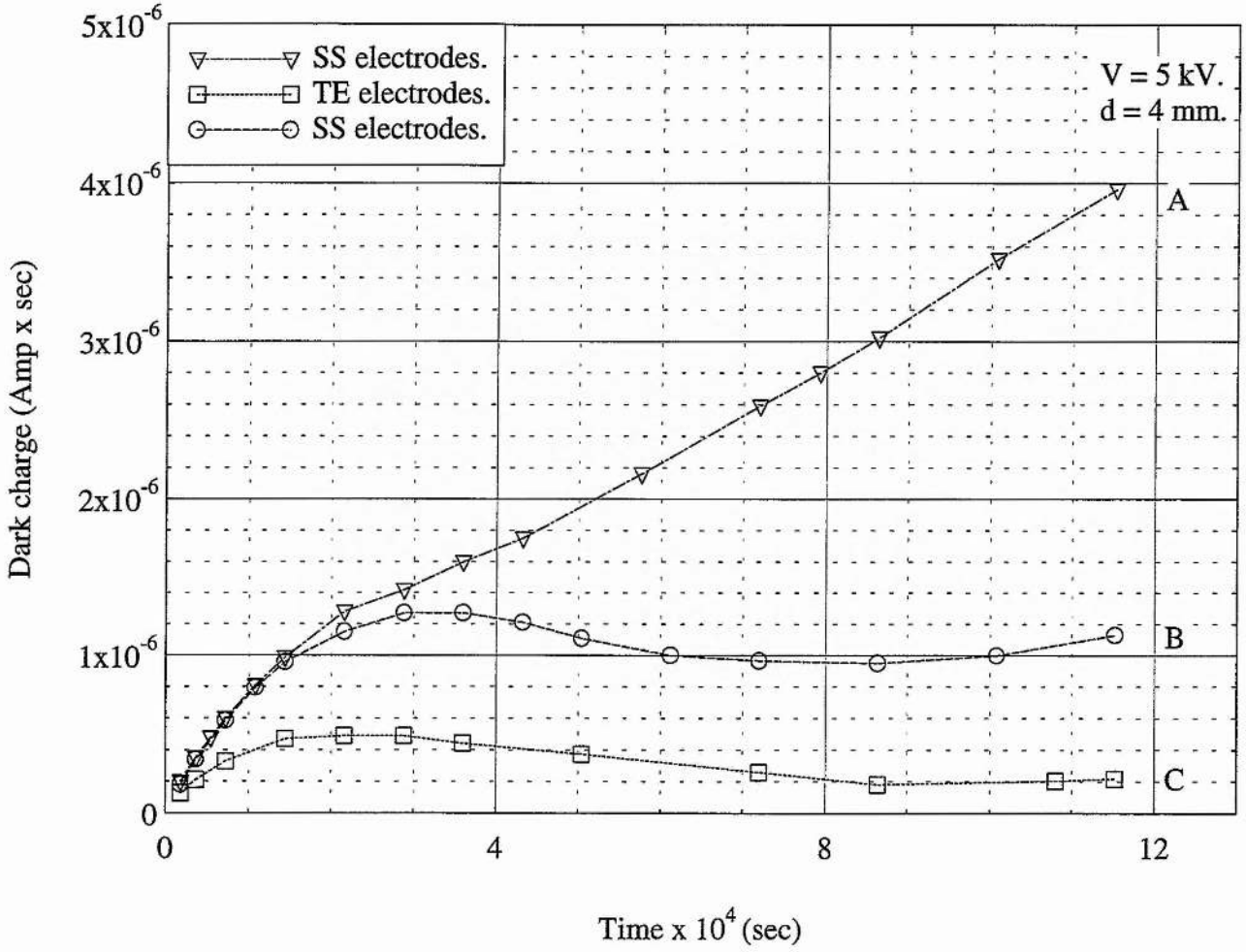

Fig (6-2): Dependence of dark charge on time for liquid TMS using SS and TE electrodes.

parallel-plate ionization chamber fitted with stainless-steel electrodes. Figure (6-3) shows the current-voltage characteristic for a set of measurements with a high purity sample at different inter-electrode spacing.

In general the dark current rises with increasing applied voltage, V. The rise of current is, however, greater for smaller electrode separation, d. The general increase of the current takes different forms depending on the region of the applied electric field, which is given for the parallel-plate arrangement by E=V/d. In the low field region the current rises linearly in accordance with Ohm's law. This can be associated with a general increase of the drift velocity, ϑ_d, of charge carriers in the liquid medium. For a further increase of the field the current displays a sub-linear rise of the form:

$$I_d = I_0 + cE \qquad (6\text{-}1)$$

where I_0 represents the interception point of the current with the axis of I_d. The value of the constant, c, depends on the kind of liquid, inter-electrode spacing, and the degree of purity. It is quite possible that in this region of the electric field a gradual increase of the hydrostatic pressure in the chamber takes place. This is believed to be caused by a slow evaporation of the liquid in close proximity to the cathode surface asperities. Consequently, the current exhibits a sub-linear rise.

In the region of high electric field the current shows a significant deviation from linearity where a sharp increase of the dark current is apparent. The critical value of the electric field at the onset of the sharp rise is about 18 kV/cm.

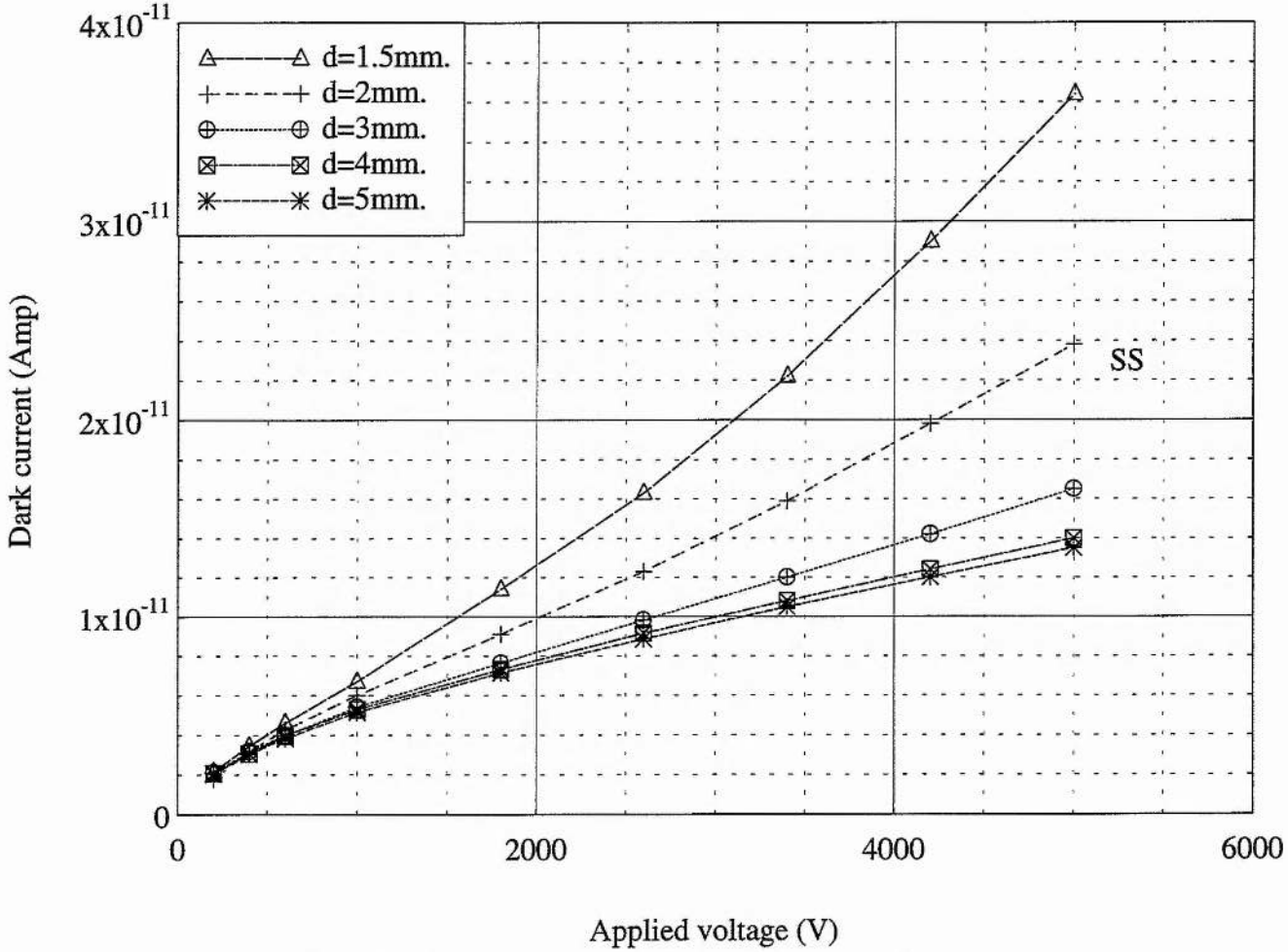

Fig (6-3): Dependence of dark current on applied voltage for SS electrodes.

6.1.3.1 The high dark current

If the origin of the sharp rise of the dark current is to be associated with electron emission from the cathode, then variation of the dark current with electric field should be dependent on the electrode material. Two sets of the current-field characteristic were plotted in figure (6-4) for two different electrode materials, stainless steel (SS) and plastic-tissue-equivalent (TE). For the sake of avoiding complexity, the current-field characteristic curves for electrodes of aluminum material, AL, was avoided as these curves were similar, in the shape and value, to those of the SS electrodes. The figure shows a distinct dependence of the dark current on the material of the electrode. Accordingly, the dark current would be expected to be entirely independent of the electrode separation for equal applied fields. This was investigated in figure (6-5), where the variation of the dark current per electrode spacing with the electric field was plotted for different electrode separations. The figure shows a clear dependence of the dark current on electrode separations for the SS electrodes. This finding, therefore, gives no support for electron emission. However, for the TE electrodes the dependence was not significant and may even be within the limits of reproducibility of the results.

The mechanisms of thermionic emission and dissociation can be examined using equations, (4-1) and (4-3) respectively. If these theories are of plausible application then plotting ln (I_d) as a function of $E^{1/2}$ should yield a straight lines of slopes of, $e^{3/2}/(\varepsilon^{1/2}\, k_B T)$ and $2e^{3/2}/[(300\varepsilon)^{1/2}\, k_B T]$ respectively. Accordingly, the theoretical values of the slopes are 3.933×10^{-3} m/V and 4.32×10^{-4} m/V respectively. In this calculation T= 293 ^{0}K and ε_r was taken as 1.84 F/m, see appendix (B). In order to obtain the

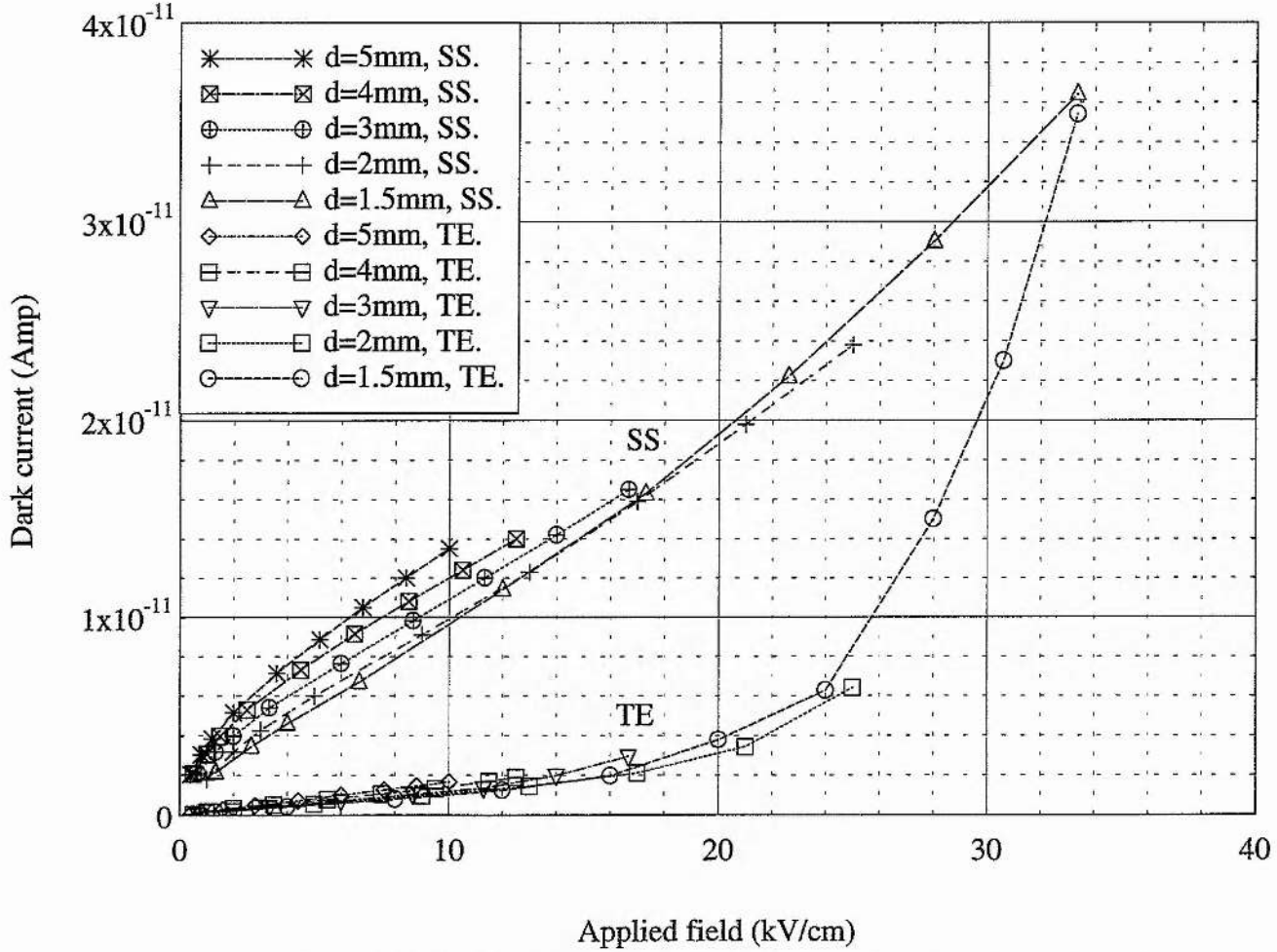

Fig (6-4): Dependence of dark current on applied field for SS and TE electrodes.

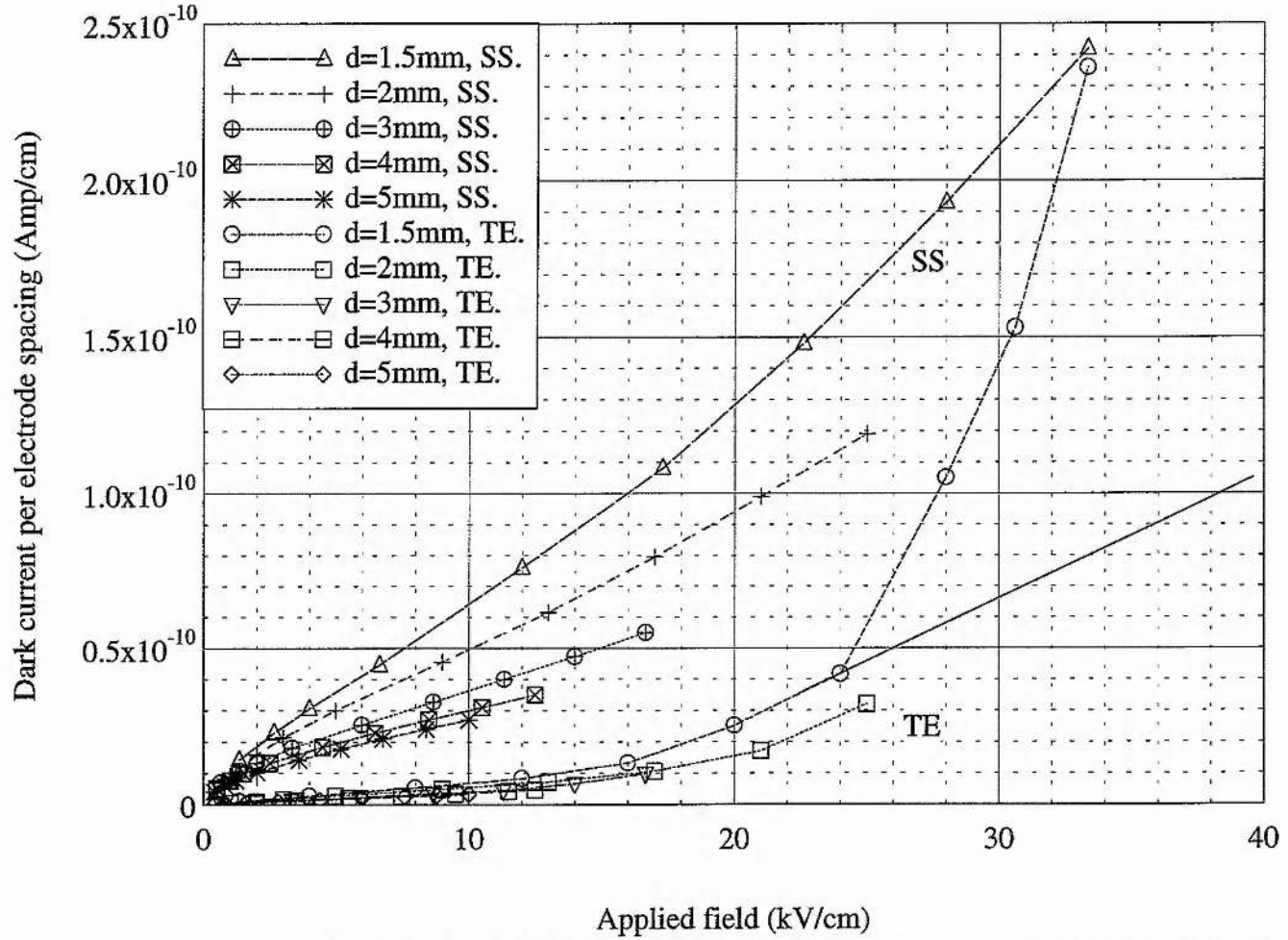

Fig (6-5): Dependence of dark current per electrode spacing on applied field for SS and TE electrodes.

related experimental values, the variation of ln (I_d) with $E^{1/2}$ was re-plotted from figure (6-4), only for values of the electric fields ≥ the critical value. This is illustrated in figure (6-6) for the two electrodes of different materials. For the SS pair of electrodes a straight line was obtained with a value of the slope equal to 5.15×10^{-3} m/V. This indicates that thermionic emission is likely to be the predominant mechanism. On the other hand, no clear straight line was detected for the TE electrodes and therefore the theories may not be applicable to the experimental data. This may be associated with a greater surface density of sharper points for the SS electrodes relative to that of the TE electrodes. This is because the values of the electric field required for electron emission is inversely proportional to the radius of the sharp point.

In fact the rapid increase of the dark current with the applied electric field is more likely to be a function of the surface irregularities of the cathode rather than being associated with its material. This is of particular importance at high values of the electric field where micro-bubble formation can take place. As the density of the bubbles grows channels of low density regions are formed across the electrodes. Along these filaments the charge carriers would have a relatively higher mobility. The existence of high mobility carriers would reduce the effect of space charge near the electrode surface thereby facilitating electron emission from the metal surface of the cathode.

6.1.3.2 Effect of impurity

Although, in general, values of the dark current were much lower for the TE electrodes than that of SS electrodes, the sharp rise of the dark current in the former

case was much more pronounced at high electric field, figure (6-5). This is ascribed to a significant contamination of the liquid. The cause of contamination is thought to be due to chemical reaction of the liquid with the electrode material. However, it also seems that the real increase of the dark current in the high field region should have been in accordance with the attached continuous line, as indicated in figure (6-5). This means that the difference between the continuous line and the dashed line is the net effect of impurity.

The effect of impurity was demonstrated in figure (6-7) which displays the current-field characteristic for two samples of TMS of different purity level in the chamber fitted with the SS electrodes. In this figure, apart from the generally similar trend of the current; and in addition to the higher value of the current obtained with the low purity sample, the current-field characteristic for the low purity sample (upper data set) is distorted and the curves are less smooth. This indicates that the reproducibility of the results for the high purity sample is much better than that of the low purity sample which was found to be the case in the present experiment. The poor reproducibility of the results for the low purity sample can be attributed to a change of the mobility of the charge carriers in the liquid medium. In other words, the charge carriers in the liquid are transported through media of different densities. These media show also a different distribution with time depending on the strength and shape of the electric field.

6.1.3.3 Stability of the current

In using electrodes of different materials, a difference in the stability of the

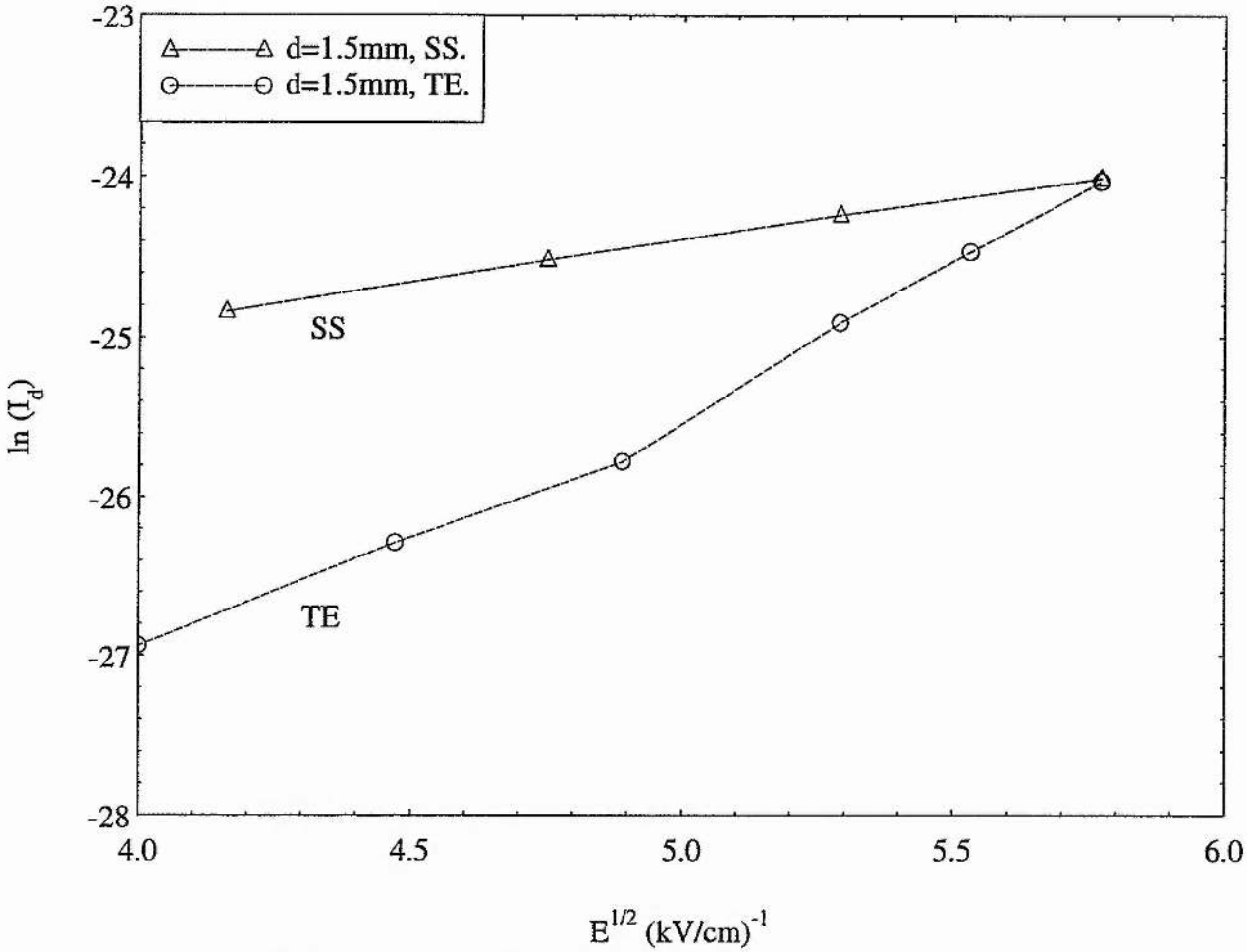

Fig (6-6): Variation of ln of dark current with the square-root of the field for two electrodes of different materials at high values of the electric field.

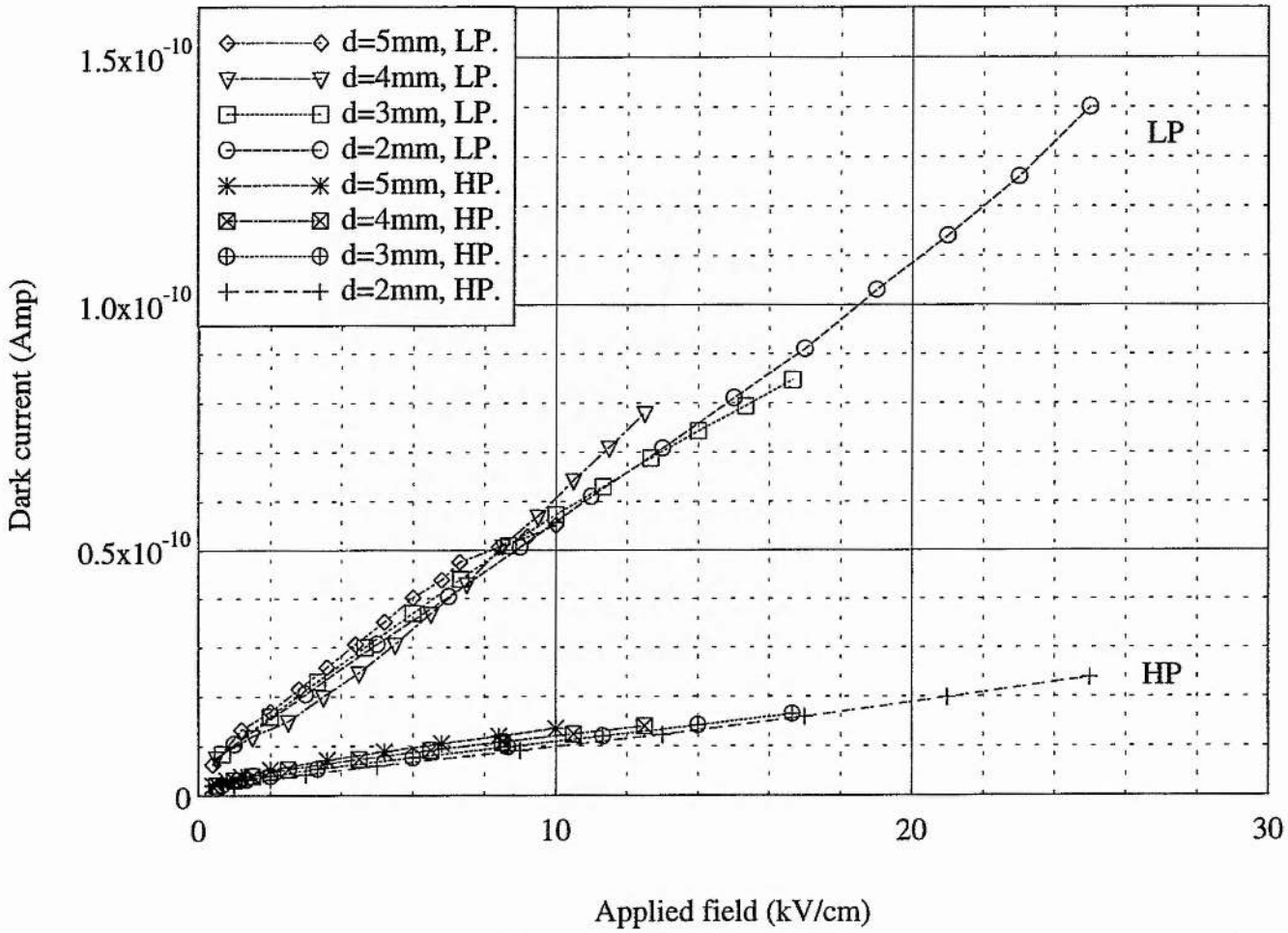

Fig (6-7): Dependence of dark current on applied field for high and low purity samples of TMS.

.

measurement was observed. In particular, for the stainless steel electrodes the instability was more accentuated. However, the instability was more apparent in the intermediate region of the electric field.

On the basis of the bubble formation model, at the cathode asperities, adopted in this work the effect can be explained satisfactorily. Accordingly, fluctuations are ascribed to the formation of tiny bubbles present in the sensitive volume of the liquid.

At low values of the electric field the intensity of the field at the asperities is low and, therefore, no bubbles are expected to form. This, therefore, has no effect on the stability of the current. A tolerable instability of the current is also observed in the region of high electric field. This is because the pressure developed in the chamber, as a result of liquid evaporation, reduces the efficiency of bubbles formation and their size to a minimum value.

In fact, the instability of the measurement is most apparent in the region of intermediate field where bubble formation starts to take place. During this time, bubbles formed at the close proximity of the cathode asperities diffuse away from the intense region of the field and occasionally cross the gap between electrodes. These bubbles form low density regions through which the charge carriers present in the liquid are transported with higher mobility. This clearly imbalances the process of charge collection leading to poorer stability of the current measurement.

6.1.3.4 Steps of applying the voltage.

Of further interest is the behaviour of the dark current beyond the critical value of the electric field where the current for the smaller electrode separation intersects with that

of the larger separation, figure (6-4). This is most probably caused by the fact that the variation of the values of the electric field was performed by decreasing the applied voltage in steps. Thus, the effects induced in the liquid sample at the high initial value of the electric field, which are also a function of the time of application, are stronger than that at the lower initial value, which is the case with larger electrode separation. This hysteresis effect is likely to be extended to lower values of the electric field. In order to test this, the experiment was repeated for the corresponding curves, first by increasing the electric field in steps. No interference was observed, which support the previous explanation. The reason for starting the measurement from a high value of the electric field is to commence the measurement directly at the final stage of electric purification and to reduce as much as possible any effects of fluctuation.

6.1.3.5 Dependence of the dark current on electrode area

In order to study the dependence of the dark current on the area of the anode the current-field characteristic was investigated for plane-point electrodes with an anode tip of radius 0.1 mm. This is shown in figure (6-8) for different electrode separations compared with these obtained with the stainless steel parallel-plate electrodes. Values of the electric field for the plane-point electrodes was calculated using the following formula (Denat et a. 1987)

$$E_p = \frac{2V_0}{r_p \ln(4d/r_p)} \qquad (6\text{-}2)$$

where V_0 is the applied electric field, r_p is the radius of the point electrode, and d is

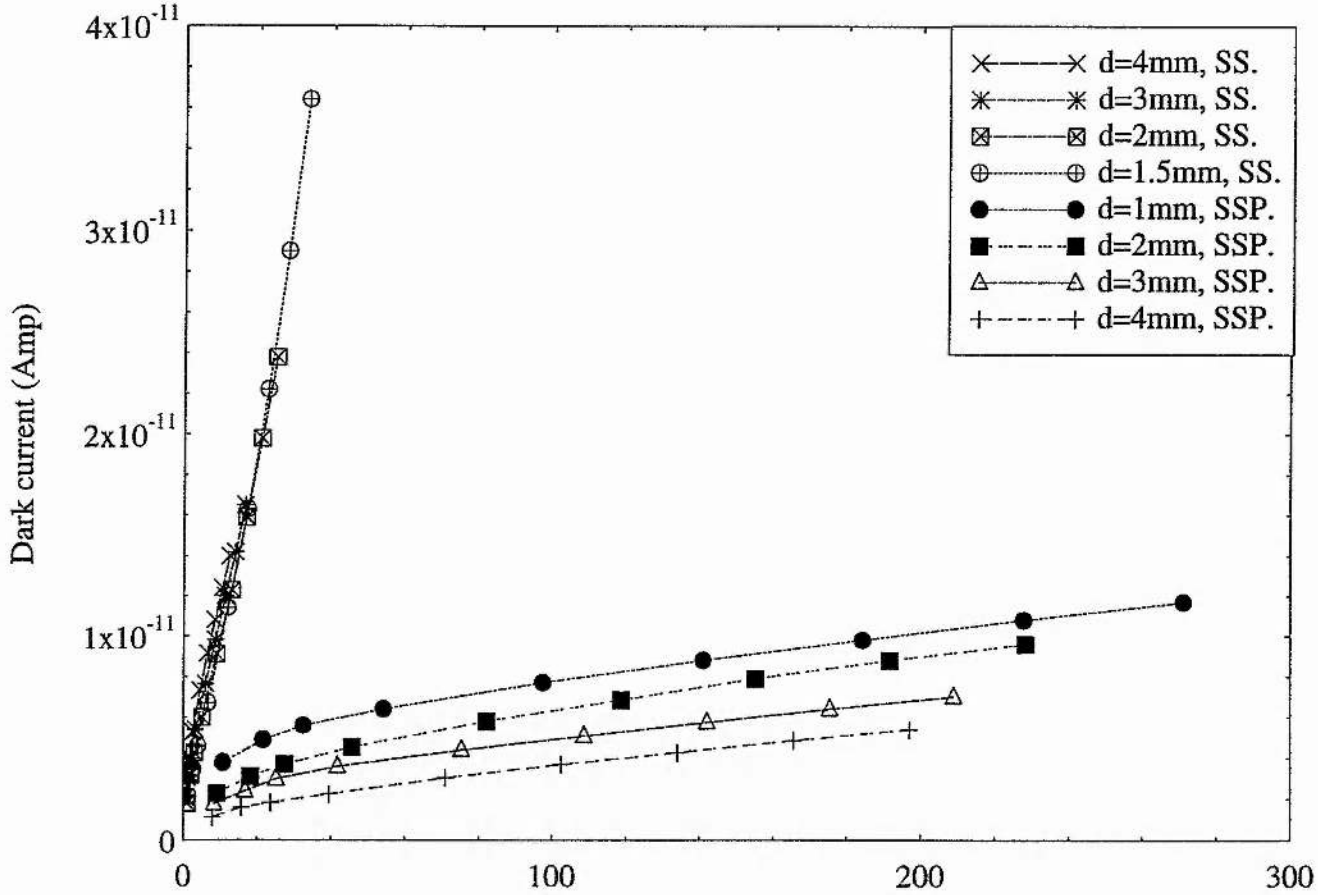

Figure (6-8): Dependence of dark current-field characteristic on area of collector. SSP and SS denote, point-plane and parallel-plate electrodes respectively.

the electrode separation.

Figure (6-8) shows that there is a clear dependence of the dark current-field characteristic on the area of the anode. In other words, decreasing the area of the anode lowers the sharpness of the current increase with electric field. The smaller value of the dark current obtained with the point-plan electrode relative to that of the parallel-plane electrodes is clearly due to the smaller area of the collector and also to the smaller sensitive volume, defined by the lines of force of the electric field.

The large difference of the current for the parallel plate electrodes as compared to point plane electrodes can be attributed to the higher influence of the electric field. In other words, the ratio of the area of the cathode to that of the anode is much bigger for the point-plane electrodes relative to that of the parallel-plate electrodes. Consequently, the influence of the electric field is higher; the pressure caused by the local evaporation is higher; the size of bubbles is smaller; and therefore multiplication is less condensed. This is believed to be also the reason for the flatter increase of the dark current for the point-plane electrode configuration.

6.1.4 Ionization current

The ionization current is known to consist of two main components expressed by

$$1/I = 1/ I_s (1+ C/E) \qquad (6\text{-}1)$$

where I_s is the saturation current, E is the electric field, and C is a constant which determines the fraction of ions that escape initial recombination (Johansson and

Wickman 1997). I is a function of electrode spacing and is dependent of the quality of the radiation field (Ladu and Pelliccioni 1967, Ladu et al. 1967). The value of the constant, C, is determined by the interception point of the extrapolated linear-part of the ionization curve with the axis of the applied field. The interception point of the extrapolated line with the I axis is assumed to define the value of the saturation current.

The current induced in purified liquid by a constant gamma radiation field of initial activity A= 4 mCi, emitted from a source of ^{57}Co was investigated. The γ–radiation was fired through a thin window in a direction parallel to the electric field.

The net ionization current, taken after subtracting the dark current, for the chamber fitted with the SS electrodes, was plotted as a function of the applied electric field for various electrode spacings, figure (6-9). The ionization current rises with increasing applied electric field indicating that the saturation current must occur at higher electric fields.

When the fitted SS electrodes were replaced with TE electrodes, the dependence of the ionization current on electric field was less accentuated and the magnitude of the ionization current was less, figure (6-10).

The behaviour of the observed ionization current is similar in trend to that of the dark current obtained earlier with the important difference that the ionization current shows no sharp rise in the high field region. This implies that the dark current is unlikely to be mainly due to the effect of background cosmic radiation such as γ-rays, since then the ionization current would have shown a closer behaviour to that of the dark current.

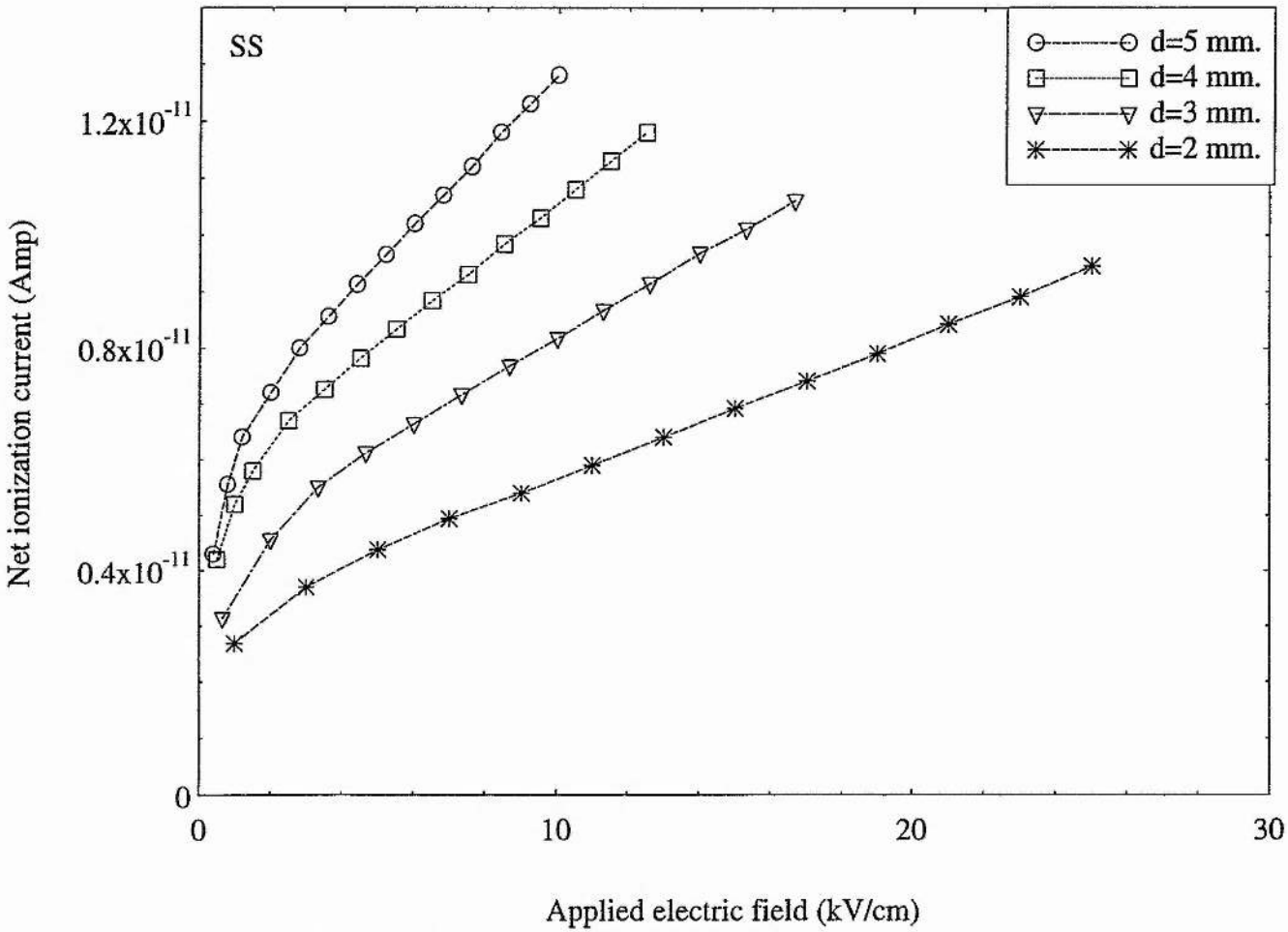

Figure (6-9): Net ionization current versus applied electric field for different electrode spacings, using SS electrodes.

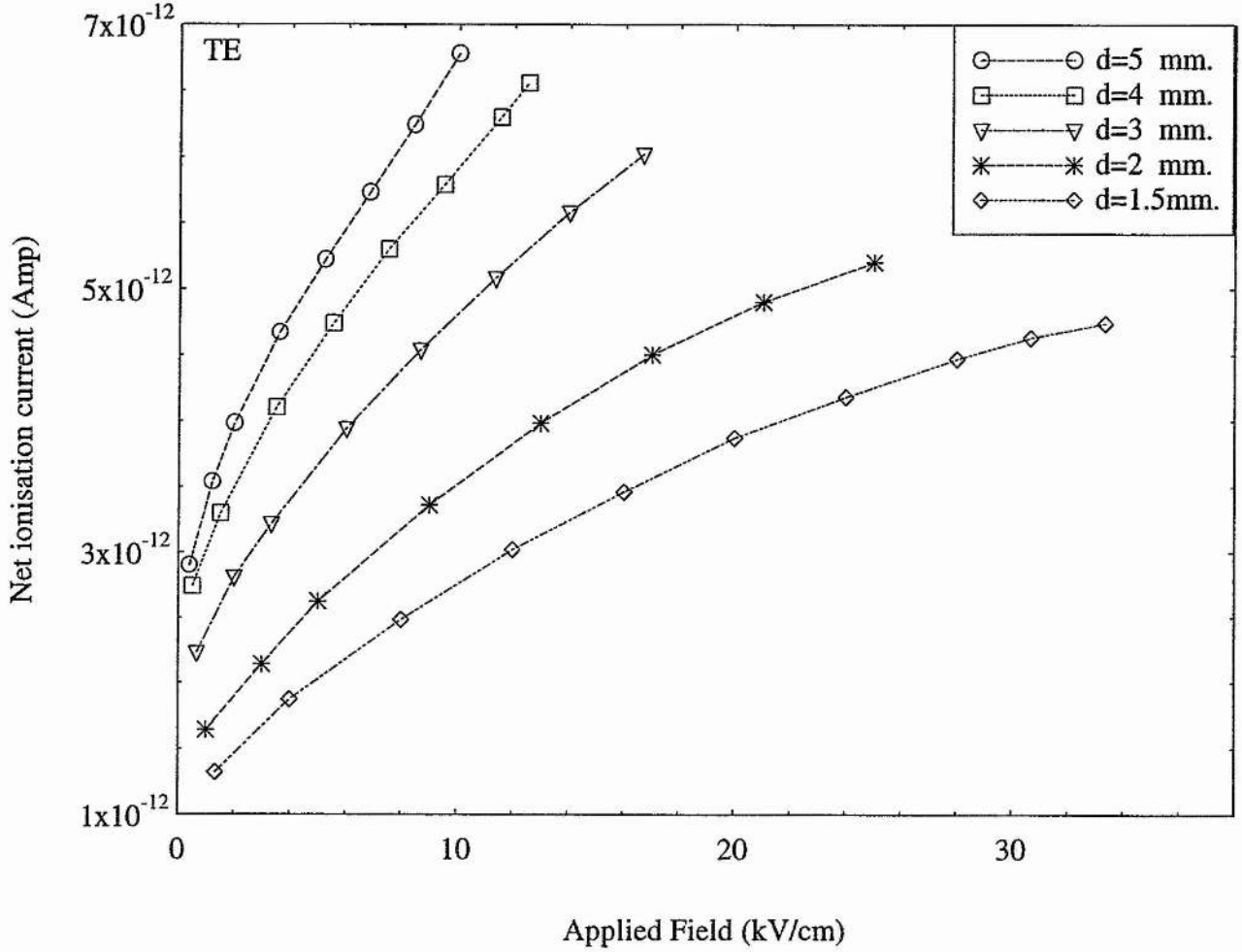

Figure(6-10): Net ionization current versus applied electric field for different electrode spacing, using TE electrodes.

6.1.4.1 Dependence of ionization current on liquid purity

In order to investigate the dependence of ionization current on liquid purity, two liquid samples of different purity were used. The liquid sample regarded as a low purity sample was that used without further purification and exposed to air, whereas that obtained after the purification and introduced to the chamber under vacuum was regarded as a high purity sample. The net ionization current for the two samples was plotted as a function of the applied electric field for different values of electrode spacing, figure (6-11). Due to the short half-life of the gamma source used, ^{57}Co, the intensity of radiation source at the time of performing the measurements with the two liquid samples was different. Hence, to enable a meaningful comparison to be made, the ionization current obtained with each liquid sample was divided by a corresponding factor which represents the amount of energy transmitted, $A_0 \exp(-\mu_{att} x)$. Here, A_0 is the intensity of radiation source (mCi), μ_{att} is the linear-attenuation coefficient (cm^{-1}), and x is the thickness of the window material (cm). Values of the energy transmission factor are listed in table (6-1) for the different electrode materials fitted in the SS chamber, and for various electrode separations, d.

It can be noticed from figure (6-11) that, for electrode spacing d=5 mm the net ionization current for the low purity sample is higher than that of the high purity sample. As the electrode spacing is reduced the current for the low purity sample gradually becomes smaller than that of the high purity sample. The fact that the effect of impurity on ionization current is reduced with decreasing electrode separation can be explained as being due to a higher influence of the electric field which may at a certain value become capable of leading multiplication inside a formed bubble. The

latter effect is believed to predominate as the electrode spacing is gradually reduced. The higher ionization current obtained with the low purity sample at electrode spacing d=5 mm, is thought to be caused by the influence of impurity since the value of the electric field is not enough to start multiplication.

The type of impurities produced in liquid is believed to be of negative nature. They are likely to be oxygen molecules which accumulate in the close proximity of the anode and lowering its work function by tending to extract electrons from its metal surface.

Table (6-1): Energy transmission factor for different electrode materials. x is the thickness of the window and SSP denotes an SS point electrode.

SS	d(cm)	A_0(mCi)	$\mu_{att}(cm^{-1})$	x(cm)	$A_0 e^{-\mu x}$
	0.2	3.592	2.0671	0.02	3.446
	0.3	3.601	2.0671	0.02	3.455
	0.4	3.601	2.0671	0.02	3.455
	0.5	3.610	2.0671	0.02	3.463
SSP	0.1	2.43	2.0671	0.02	2.331
	0.2	2.43	2.0671	0.02	2.331
	0.3	2.43	2.0671	0.02	2.331
	0.4	2.43	2.0671	0.02	2.331
TE	0.15	2.804	0.1803	0.10	2.753
	0.2	2.812	0.1803	0.10	2.761
	0.3	2.769	0.1803	0.10	2.719
	0.4	2.769	0.1803	0.10	2.719
	0.5	2.769	0.1803	0.10	2.719
Al	0.2	3.656	0.4142	0.03	3.61
	0.3	3.666	0.4142	0.03	3.62
	0.4	3.732	0.4142	0.03	3.685
	0.5	3.619	0.4142	0.03	3.547

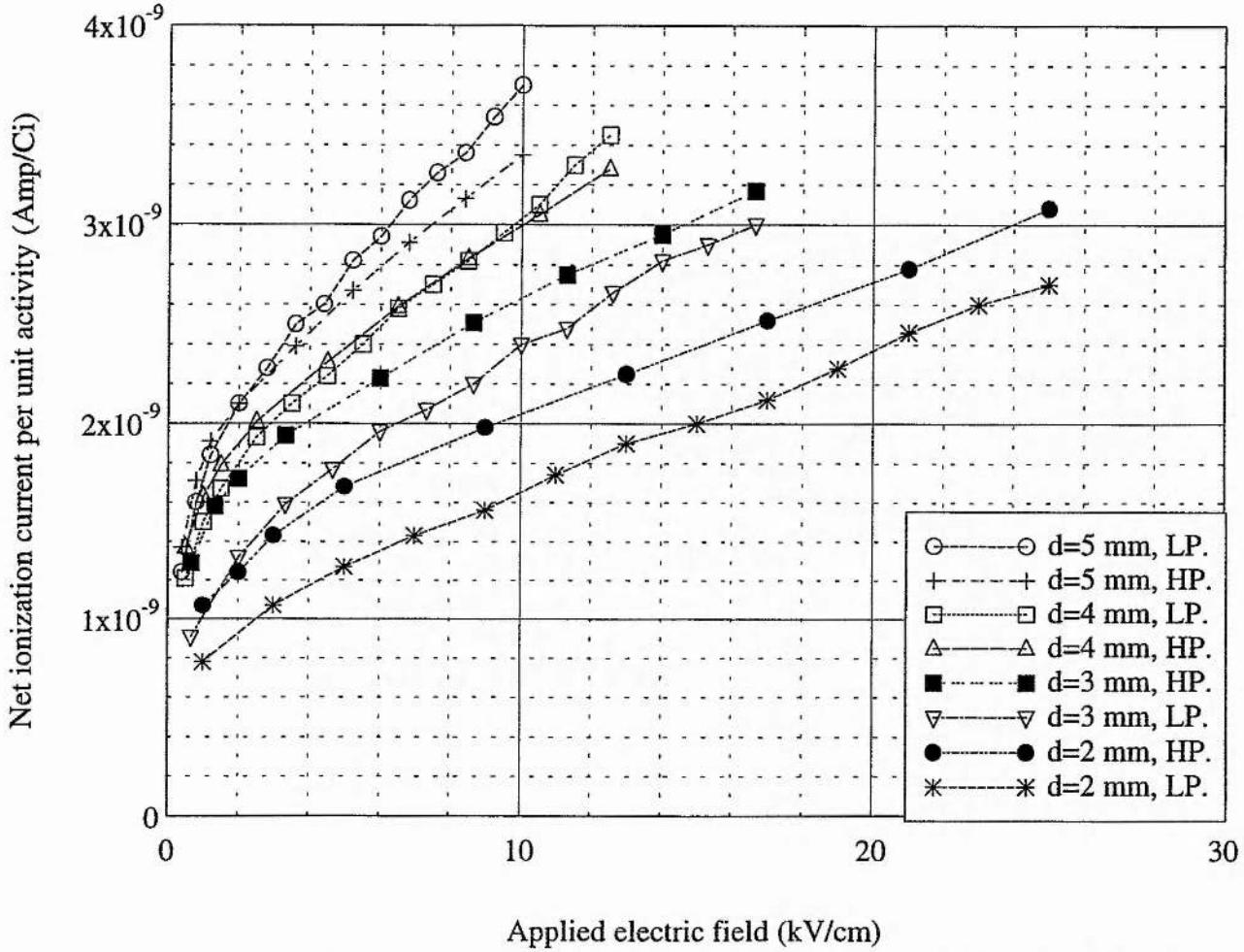

Figure (6-11): Dependence of ionization current-field characteristic on liquid purity for different electrode spacings. LP and HP denote low and high purity.

6.1.4.2 Dependence of ionization current on electrode material

In order to investigate the effect of electrode material on the ionization current in the liquid, electrodes of different materials were fitted. To allow for a direct comparison of the results the energy transmission factors were used, table (6-1). This is because the windows employed were of different thicknesses, and the intensity of the ionization source was also different.

The dependence of the net ionization current on electric field, for three electrode materials and two values of electrode spacings, are shown in figures (6-12) and (6-13). For the chamber fitted with SS electrodes and AL electrodes, there is clearly no dependence of the ionization current on the material of electrodes. This is because the current-field characteristic curves for these materials lie on the same curve. However, for the TE electrodes the current-field characteristic curve is lower than those of the SS and AL electrodes. This indicates that the ionization current is independent of the electrode material and is likely to depend on the smoothness of the cathode surface. The fact that the asperities of the surface of metal electrodes such as SS and AL are sharper than those of the TE surface, explains the lower current observed of the TE materials. In other words, due to the higher asperity of the metal electrodes, bubble formation is more intensive. Inside each bubble, charge multiplication can occur at high electric field. Consequently, the current in the external circuit rises.

A direct comparison between the two figures of different electrode spacing reveals that, the current-field characteristic curve for the TE electrodes is closer to those of the SS and AL curves when the electrode spacing is smaller. This can be explained, according to the model adopted in this work, as being due to a higher pressure

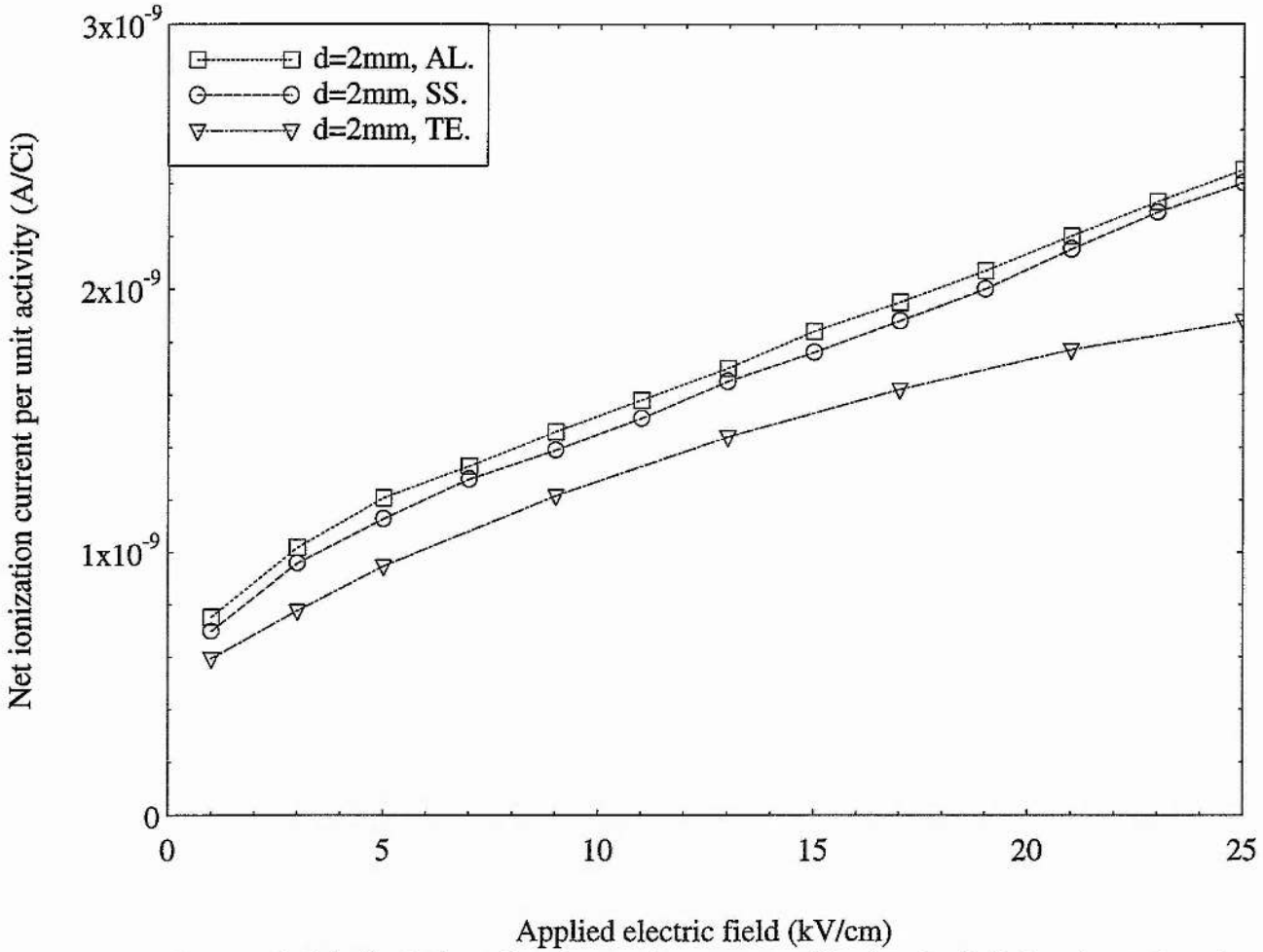

Figure (6-12): Variation of net ionization current with electric field for electrodes of different materials, and electrode spacing of 2 mm.

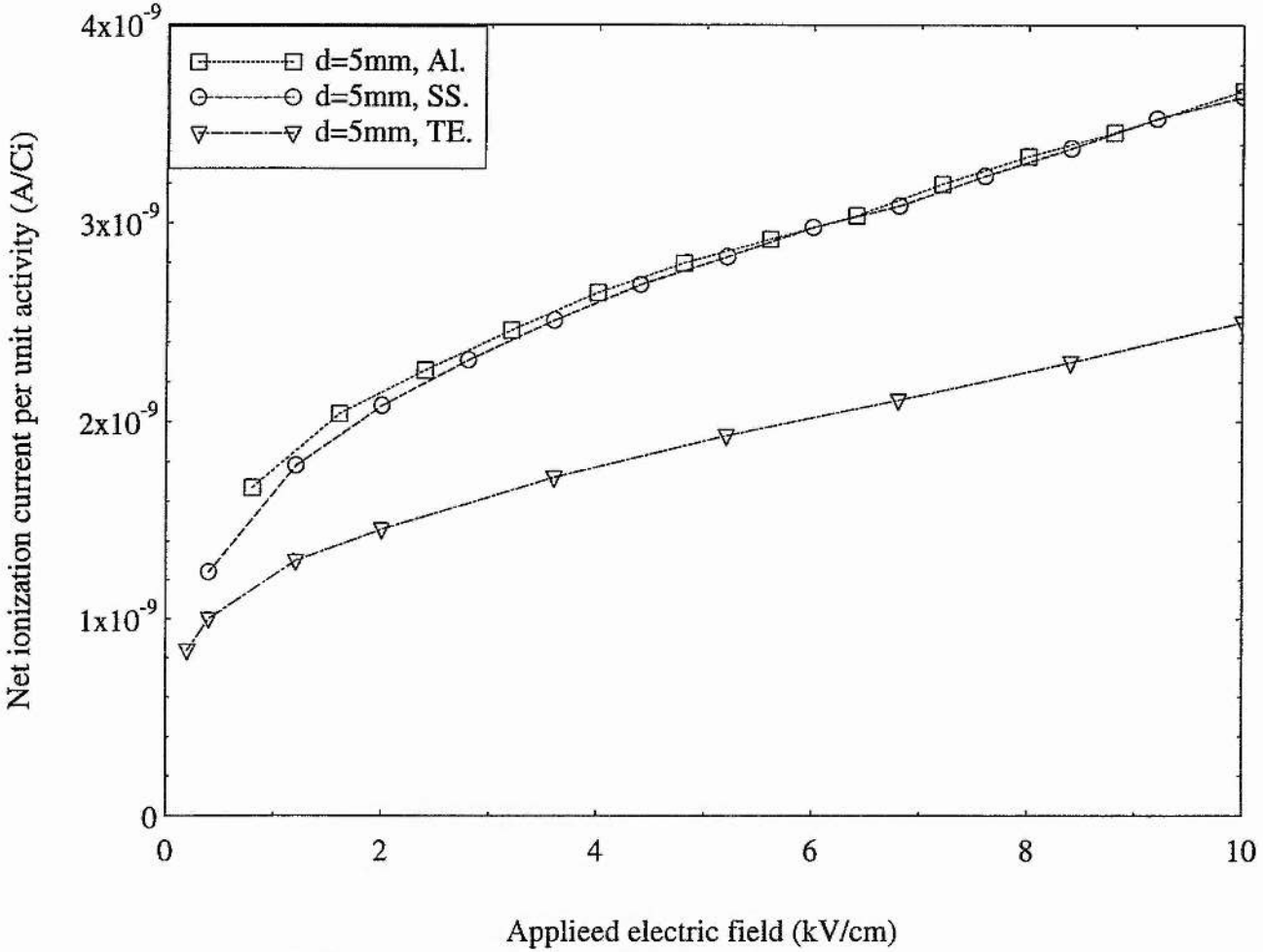

Figure (6-13): Variation of net ionization current with electric field for electrodes of different materials, and electrode spacing of 5 mm.

developed by the local evaporation of the liquid in the immediate vicinity of asperities of the cathode surface, for the smaller electrode separation which has the effect of reducing the size of the formed bubbles. This means that the processes of multiplication occurring inside the bubbles are reduced. Consequently, the difference in the current values for the SS and TE electrodes is less.

6.1.4.3 Dependence of ionization current on radiation intensity.

The intensity of ionizing radiation was varied by placing the source at various distances, D, from the window of the chamber. The dependence of the net ionization current on radiation intensity is shown in figure (6-14) in which the current-field characteristic is plotted for some values of the source-window distance, D, at electrode separation, d=2 mm. This figure indicates that the ionization current is strictly proportional to the intensity of radiation. It decreases with increasing the distance of the source from the window. As the source-window distance is gradually reduced, there is an increased slope of the ionization current as a function of the applied electric field. This is clearly illustrated in figure (6-15) where the dependence of the ionization current on the source-window distance was plotted for some values of the electric field at a constant electrode separation of d=2 mm.

The higher ionization current obtained with the smaller source-window distance, D, is an expected result since for smaller D, the amount of incident radiation is larger. This is despite the fact that for a given value of electric field the rate of ion recombination is higher for a larger amount of energy absorbed. The latter fact can also explain the decreased slope of the ionization current as a function of applied field

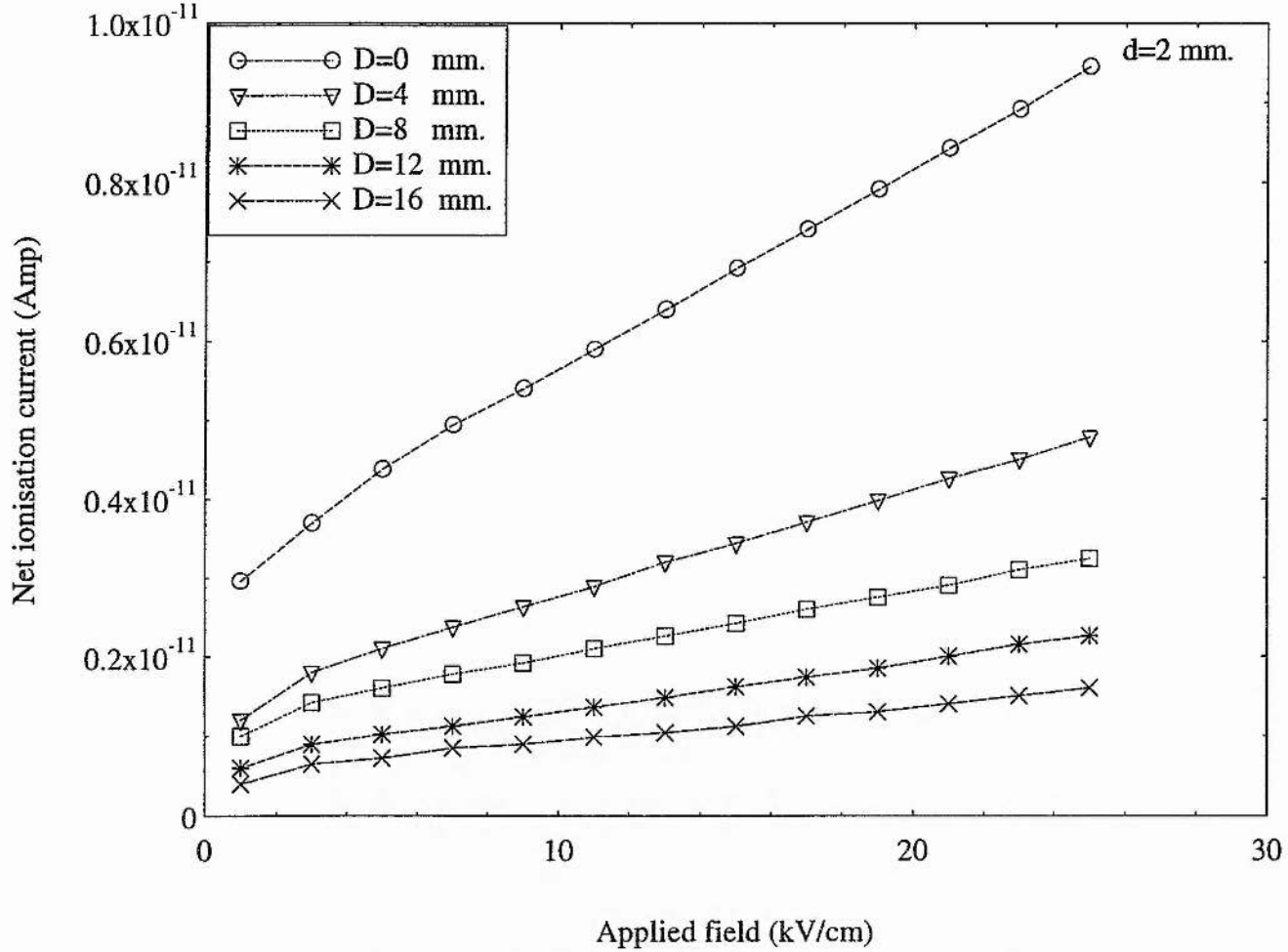

Fig (6-14): Dependence of the ionization current on applied field for different values of radiation intensity, using SS electrodes of 2mm sepation.

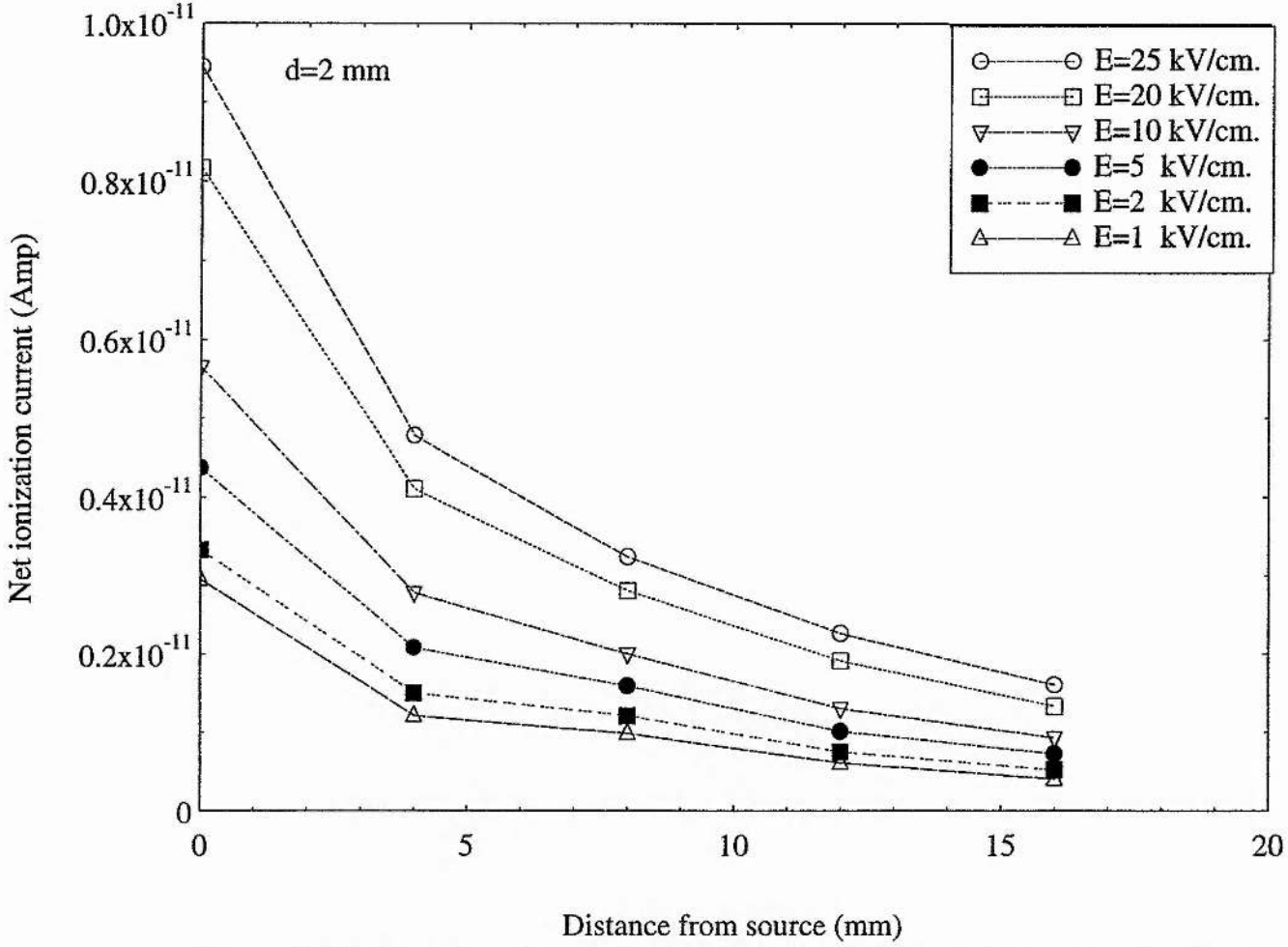

Figuer (6-15): Variation of net ionization current with distance from source for electrode separation, d=2 mm at different values of electric field

when the source-window distance, D, is increased.

It is believed that, if the liquid sample is high in purity and the intensity of radiation is sufficiently strong so that the current-noise ratio is high enough, the accuracy of the measurement is high and the result is more reliable.

6.1.4.4 Dependence of ionization current on electrode area

The dependence of the ionization current on the area of the collector was investigated using a tip anode of radius 0.1 mm. This is shown in figure (6-16) in which the ionization current-field characteristic was plotted for the two sets of electrodes, parallel plate and point-plane electrodes, and various electrode spacings. For the plane-point electrodes the values of the electric field was calculated using equation (6-2) (Denat et al. 1987).

The current field characteristic for both sets of electrodes are different in value and the rise of the current for the parallel-plate electrodes is more accentuated. This is ascribed to a higher amount of charge multiplication since with a low value of the electric field the size of the initiated bubble is bigger. On the other hand the low values of the ionization current for the point-plane electrodes is associated with the smaller sensitive volume.

In comparing the current field characteristic for the dark current, figure (6-8), and that of the ionization current, figure (6-16), we notice that the gap between the initial values of the current for the parallel-plate electrodes and the point-plane electrodes is bigger for the ionization current. This can be attributed to a difference in the amount of charge produced in the sensitive medium and also inside the formed bubbles.

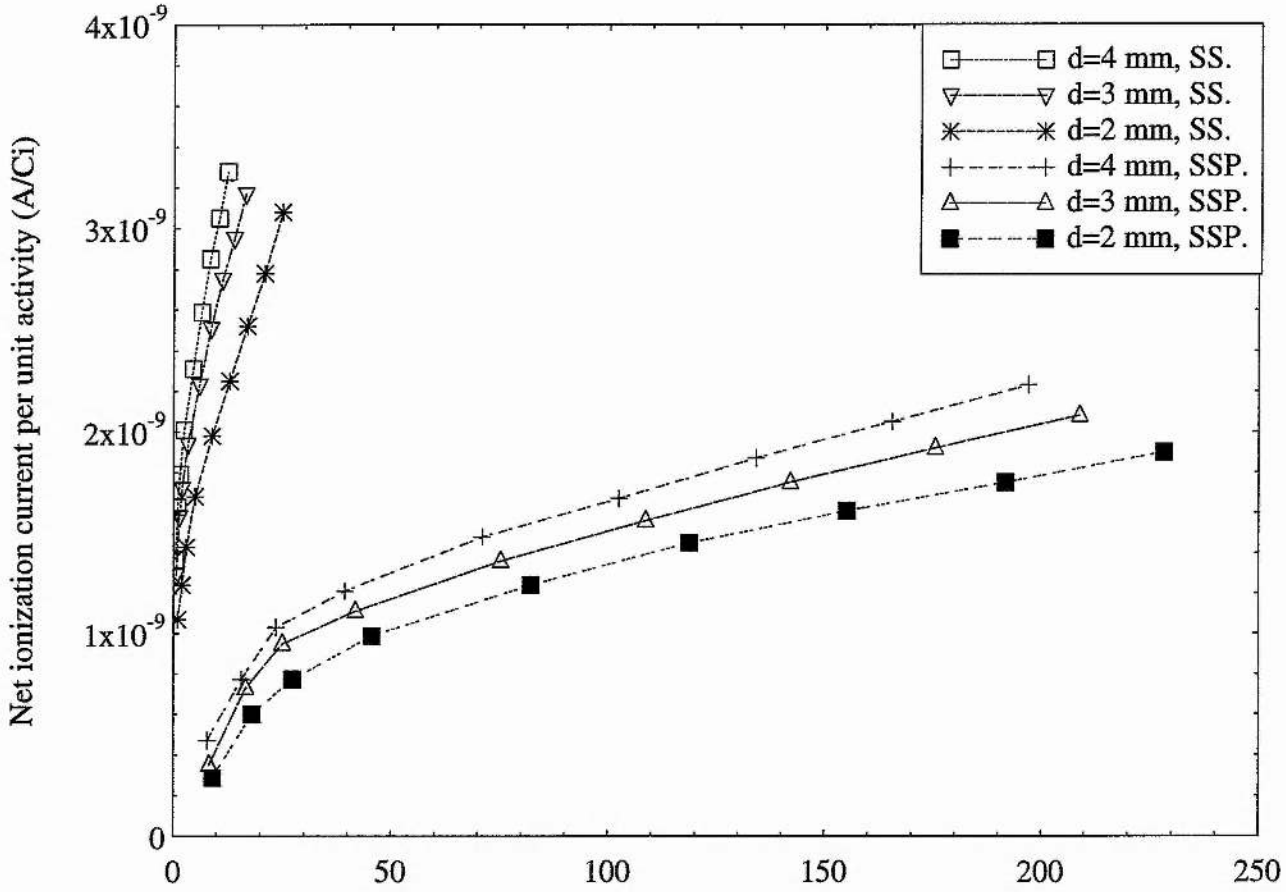

Figure (6-16): Dependence of ionization current-field characteristic on area of anode SSP and SS are for point-plane and parallel electrodes respectively.

6.1.4.5 The current-noise ratio.

As a statistical criterion for the selection of the optimum signal to noise ratio the ratio of I^2_{ion}/I_d can be plotted as a function of the applied electric field, where I_{ion} is the net ionization current and I_d is the dark current. This is shown in figure (6-17) for the two electrode materials, SS and TE, and two values of the electrode separations. The figure shows a relatively constant variation for both types of electrodes indicating that the efficiency of the detector is independent of the size and the value of the electric field. A clear maximum in the ordinate would be expected if an optimum value existed. From the figure (6-17) it can also be inferred that the current-noise ratio for the tissue equivalent electrodes is higher, by 2-3 orders of magnitude, than that of the stainless-steel electrodes. This in fact supports our explanation for the high ionization current obtained with the SS and AL electrodes when compared with that for TE electrodes, see 6.1.4.2. It is also consistent with the behaviour of the dark charge obtained in figure (6-2) for electrodes made of these materials.

6.1.4.6 Dependence of the ionization current on liquid volume.

It is of importance to investigate the dependence of the ionization current density on the sensitive volume of liquid as this would be expected to be independent of any changes that may occur in the liquid in the range of electric field applied. In order to make such an investigation, the variation of the net ionization current per unit volume with the applied electric field was plotted for the SS electrode, figure (6-18). The figure shows a small dependence, with the ionization current being a little higher for

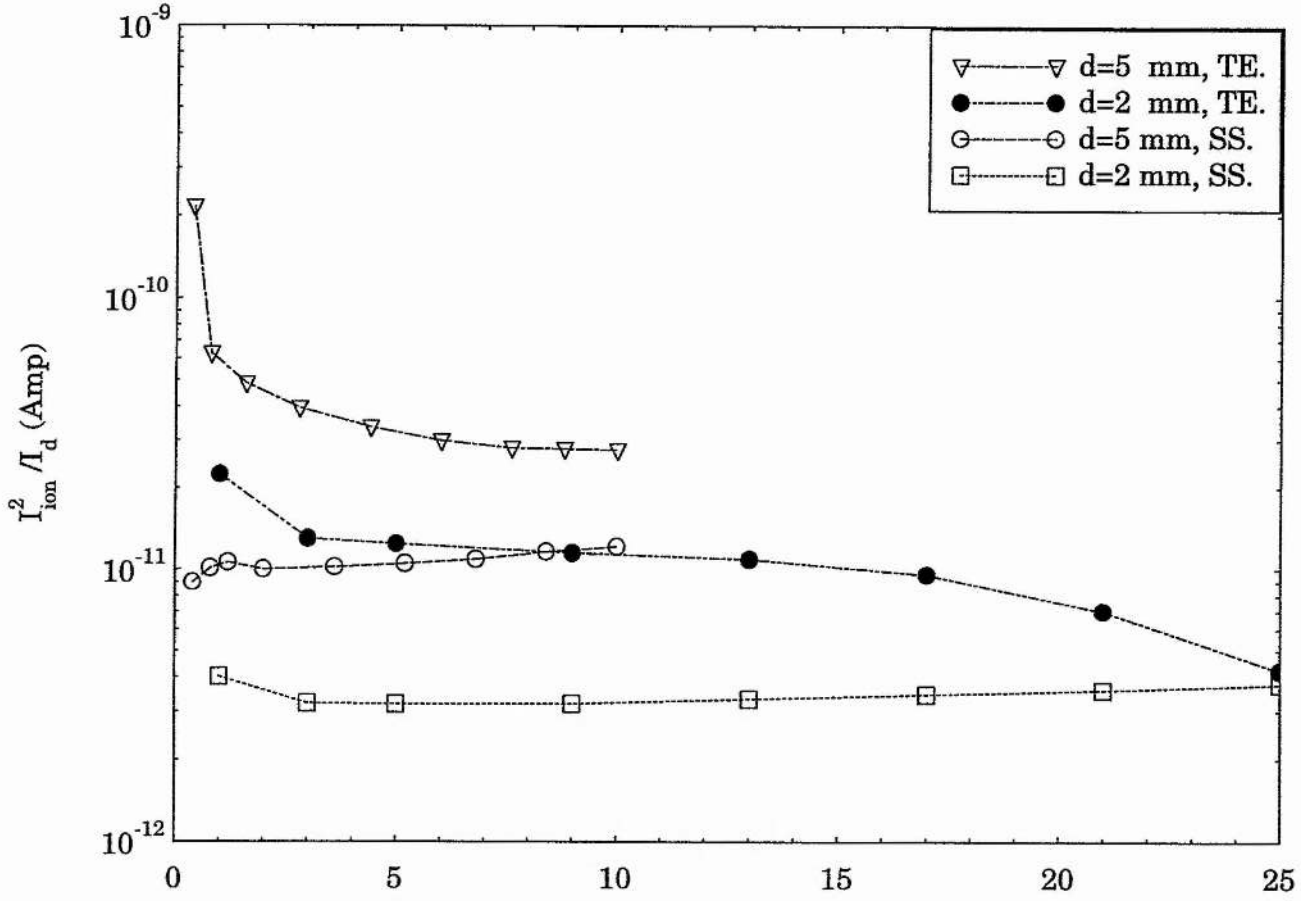

Figure(6-17): Variation of the ratio I^2_{ion}/I_d with applied electric field for two electrode spacings and two electrode materials.

smaller electrode spacing.

In order to ensure that the difference is not due to the effect of the electrode material, the current-field characteristic was plotted for the TE electrodes and a similar result was obtained, figure (6-19). Had the small dependence of the ionization current on liquid volume been due to a change in the liquid structure, such as dissociation, the effect would have been more pronounced for the SS electrodes where the effective electric field is stronger due to the higher asperity. The small dependence of the ionization current on liquid volume is more likely to be due to a small differences in the amount of, inevitable, impurities present in the liquid. However, the similar behaviour obtained with both materials of the electrodes is an expected result since the liquid samples used for the two sets of measurement were taken from the same bottle.

The ionization current per unit volume was also plotted as a function of the sensitive volume for both types of electrode at different values of the electric field, figure (6-20). For a given value of the electric field the current exhibits a small decrease with increasing the sensitive volume of the liquid. This is likely to be due to an increase of the amount of impurities in the liquid. The only difference in results obtained with the two types of electrodes is the magnitude of the current which was discussed earlier. However, for higher value of the electric field the decrease is slightly higher. This is associated with higher influence of the electric field, and therefore higher pressure.

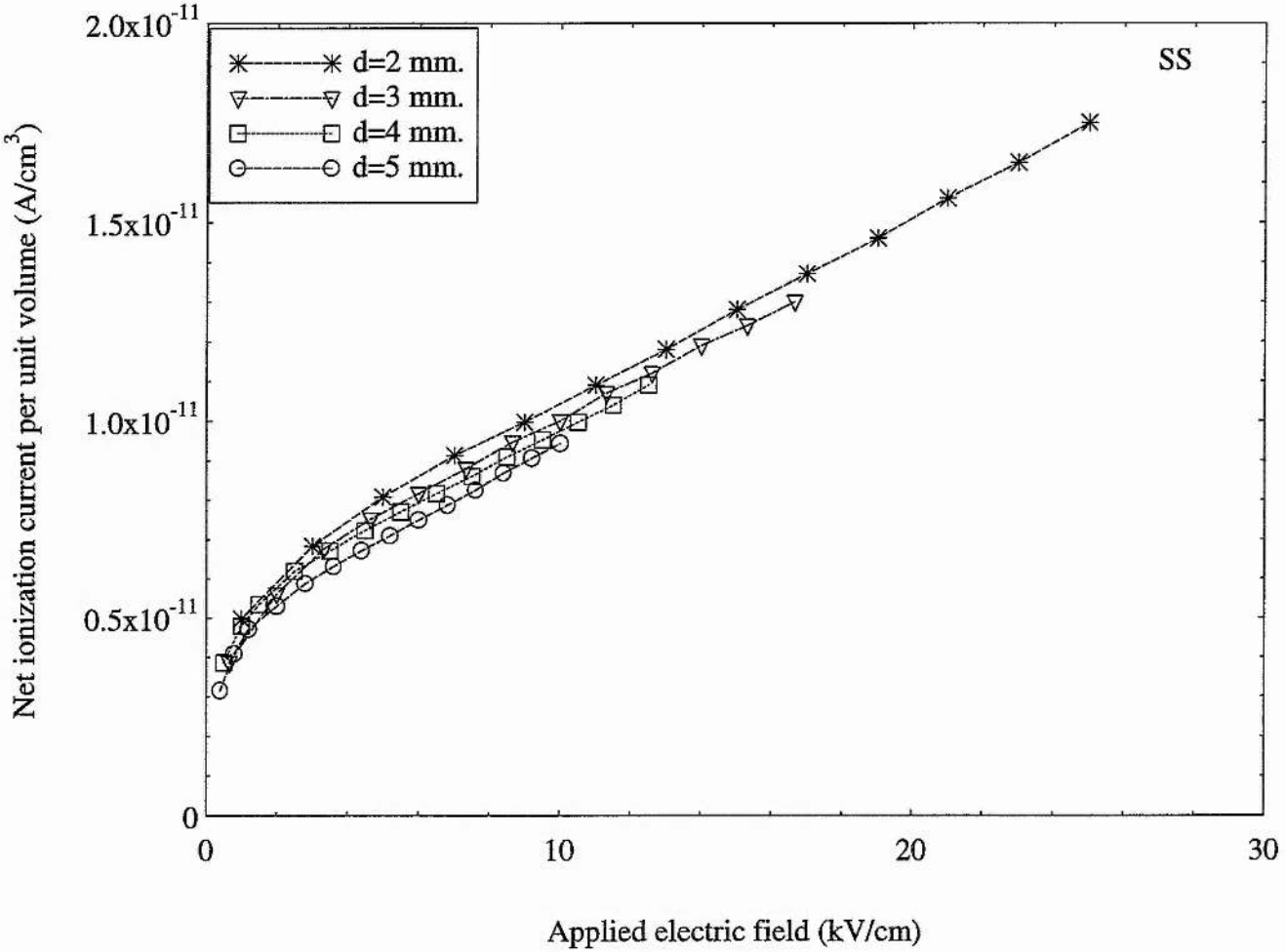

Figure (6-18): Net ionization current versus applied electric field for differen electrode spacings, using SS electrodes.

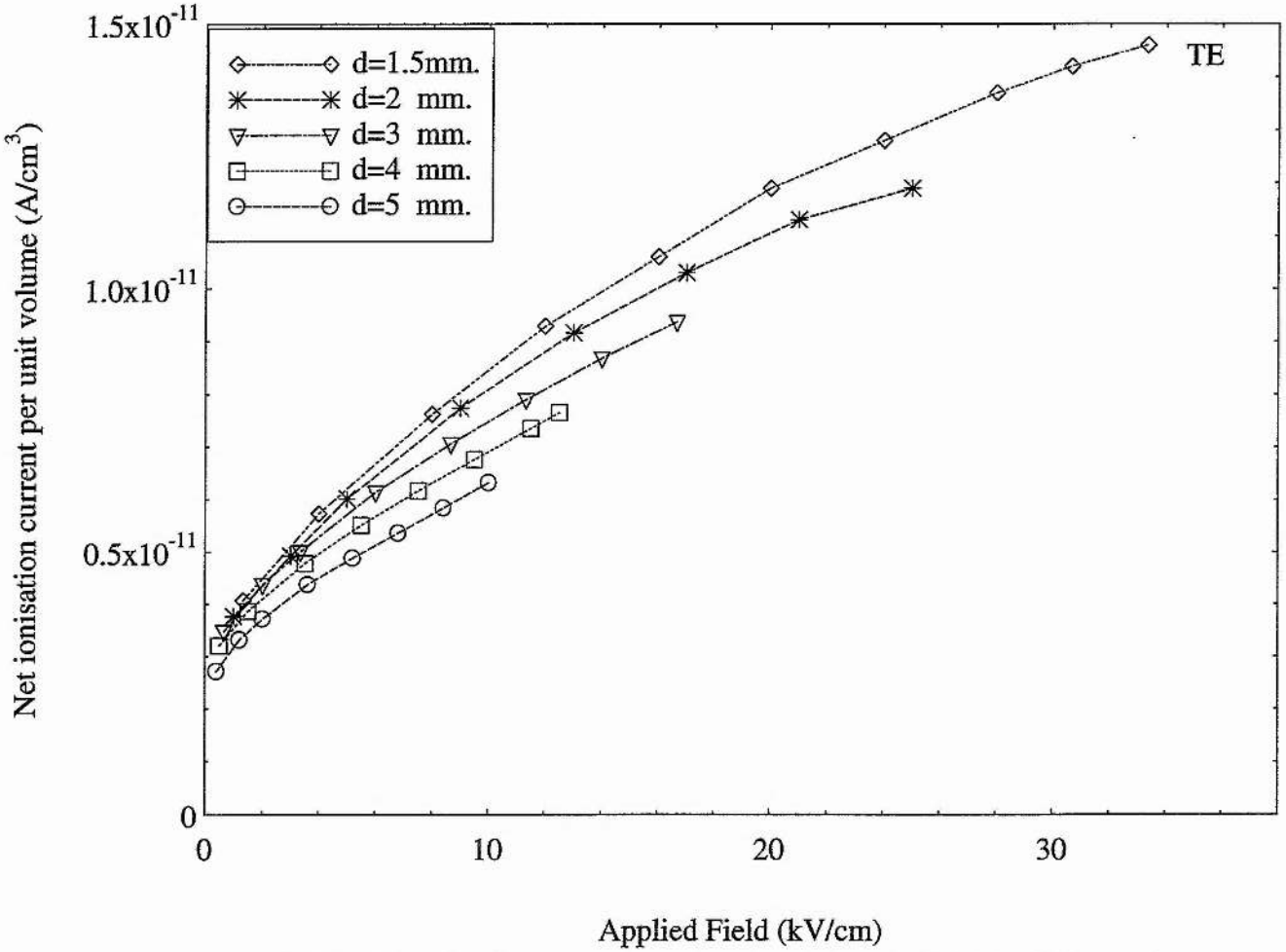

Figure(6-19): Net ionization current versus applied electric field for different electrode spacing, using TE electrodes.

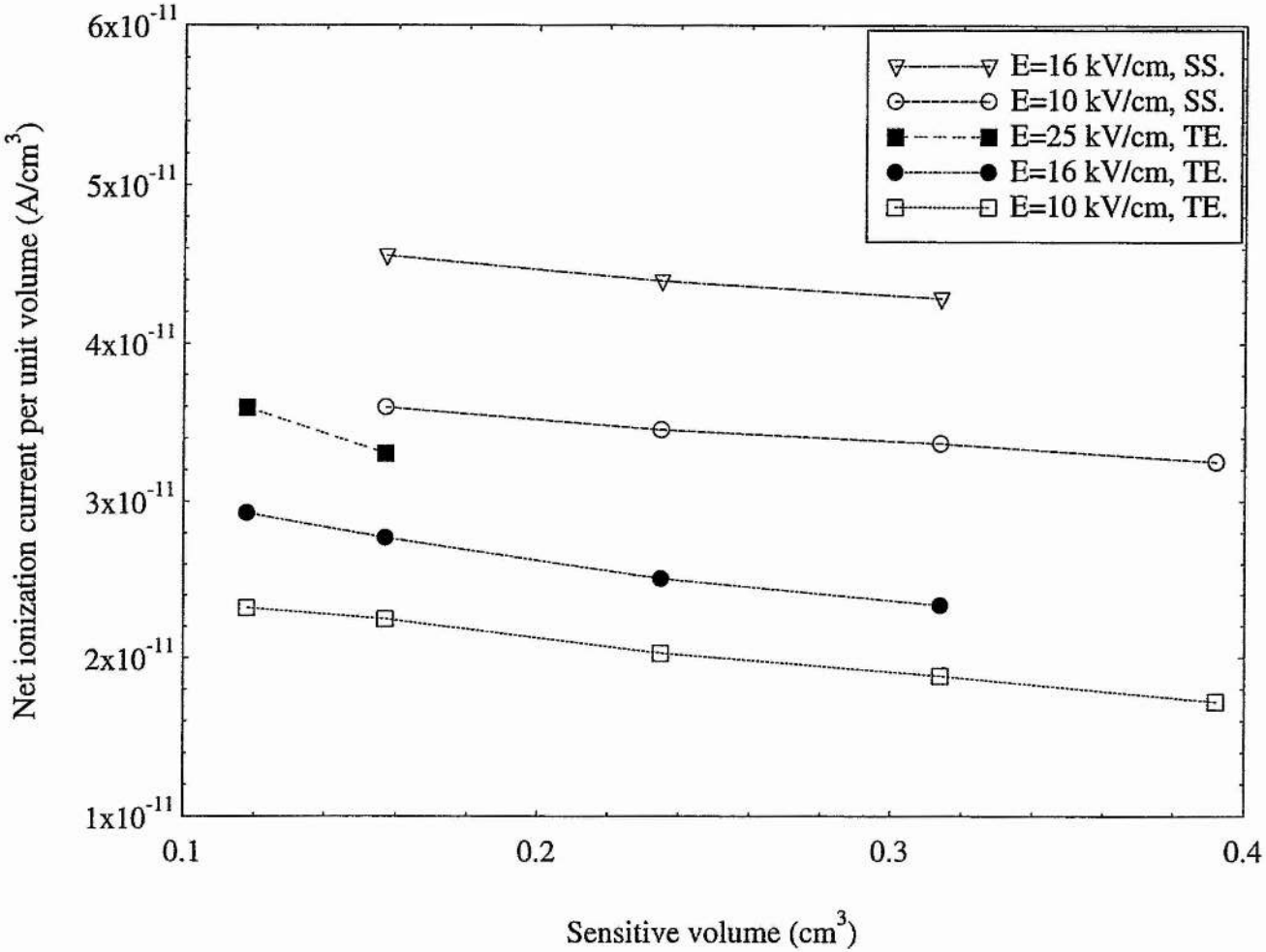

Figure(6-20): Variation of net ionization current with sensitive volume for two electrode materials.

6.1.4.7 The geometrical factor

In order to account for the geometrical configuration of the source-chamber arrangement, which involves the solid angle, W, and the depth of the sensitive volume, and to confirm the result obtained with different electrode materials, the geometrical factor, defined as $G=\Omega/4\pi$, was used. Values of the geometrical factor, G_{s0}, were computed for circular spread sources and detector radius 1 cm in terms of the separation from the source (Bland 1984). Values used in this work, G_s, were those for the chamber configurations, table (6-2). This is because the radius of the detector used in the present experiment, regarded as the radius of the sensitive volume, is different from those for which G_{s0} were obtained. The conversion factor, f, applied to values of G_{s0} represents the ratio of the solid angles for the two different configurations.

Table(6-2): Geometrical factor for two different electrode materials at various electrode spacings. Z is source-detector spacing, Z=x+d/2, where x is the thickness of the window.

SS	d(cm)	x(cm)	Z(cm)	G_{s0} (St.)	G_s= f.G_{s0}	G_s.d(St.cm)
	0.20	0.02	0.12	0.428	0.141	0.028
	0.30	0.02	0.17	0.399	0.132	0.039
	0.40	0.02	0.22	0.372	0.123	0.049
	0.50	0.02	0.27	0.346	0.114	0.057
TE	0.15	0.10	0.175	0.396	0.131	0.019
	0.20	0.10	0.20	0.382	0.126	0.025
	0.30	0.10	0.25	0.356	0.117	0.035
	0.40	0.10	0.30	0.331	0.109	0.043
	0.50	0.10	0.35	0.307	0.101	0.050

f is conversion factor for the actual detector-radius. G_{so} is the geometrical factor for detector radius 1 cm (Bland 1984).

The ionization current for SS and TE electrodes was divided by G_s.d factor and plotted versus the electric field for different electrode spacings. Also, the energy transmition factor was applied to the ionization current to account for the difference in each of the window thicknesses and the intensity of the radiation source. The results are shown in figures (6-21) and (6-22) for SS and TE electrodes respectively. For the fitted TE electrodes, the curves are lying on the same line whereas for the SS electrodes a small difference is observed. The results confirm the adopted model for explaining the behaviour of the ionization current for the SS electrode compared to that of the TE electrode, see 6.1.4.2.

6.1.4.8 'Apparent W-values' in liquid TMS

In order to compare the observed current with respect to the saturation value, the 'apparent W-value', defined as the mean energy expended in a liquid per ion pair collected, was estimated. If the total number of ions produced in the liquid is collected then the W-value should be comparable in value to a gas, being about 30 eV. In other words, this acts as a test for saturation collection of the ion pairs.

The 'apparent W-values' in the TMS were calculated for the two electrodes of different materials, SS and TE, at various values of the electric field. These are listed in tables (6-3) and (6-4) for various and constant values of the electric field respectively. The detailed method of calculation of the W-values is described in the appendix (A).

The dependence of the W-value on the applied electric field for the chamber fitted with each of the two electrode materials, SS and TE, is shown in figure (6-23) at two values of electrode spacings. In general the W-value decreases with increasing electric

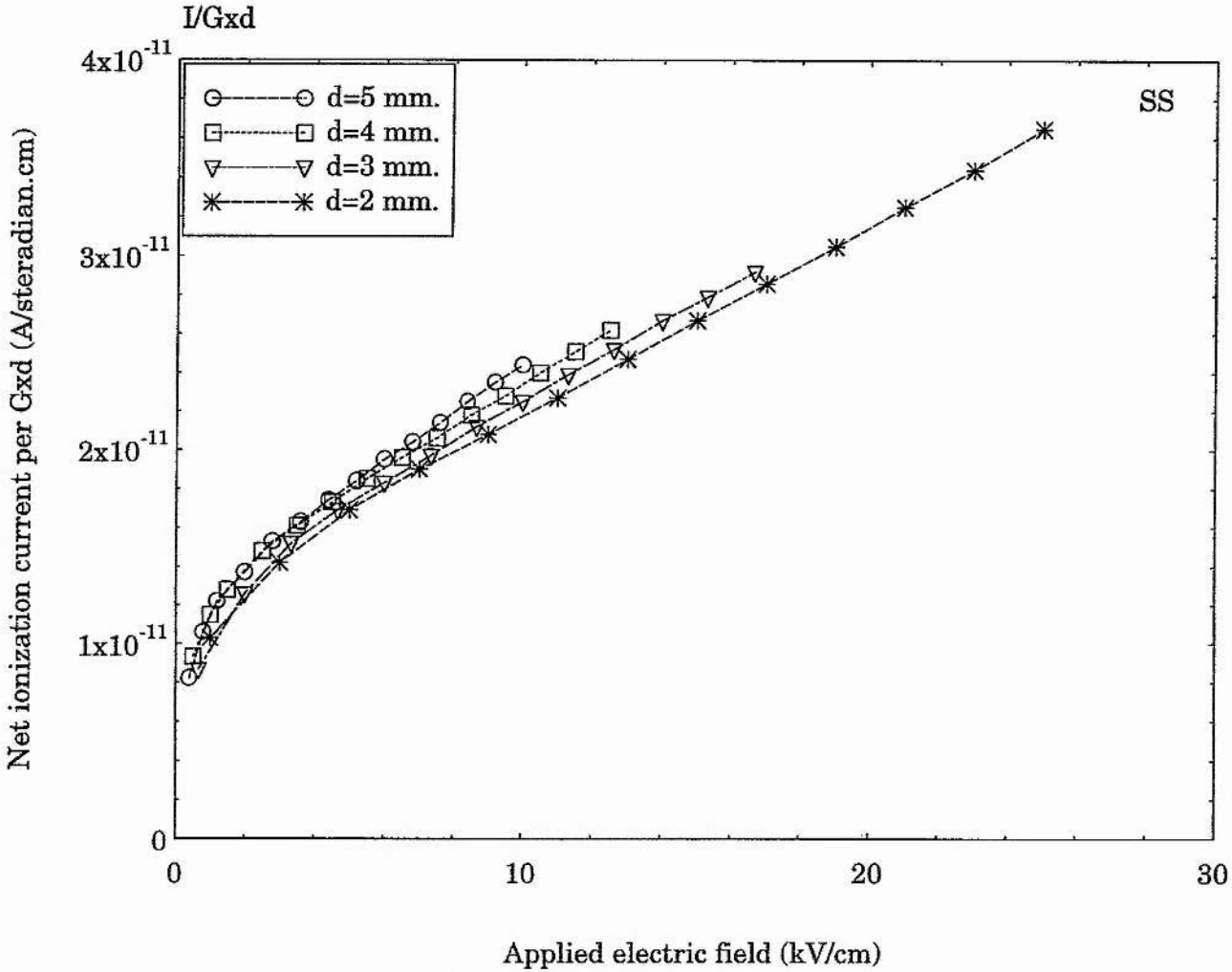

Figure(6-21): Variation of ionization current per Gxd with electric field for SS electrodes and different spacings d. G is a geometrical factor.

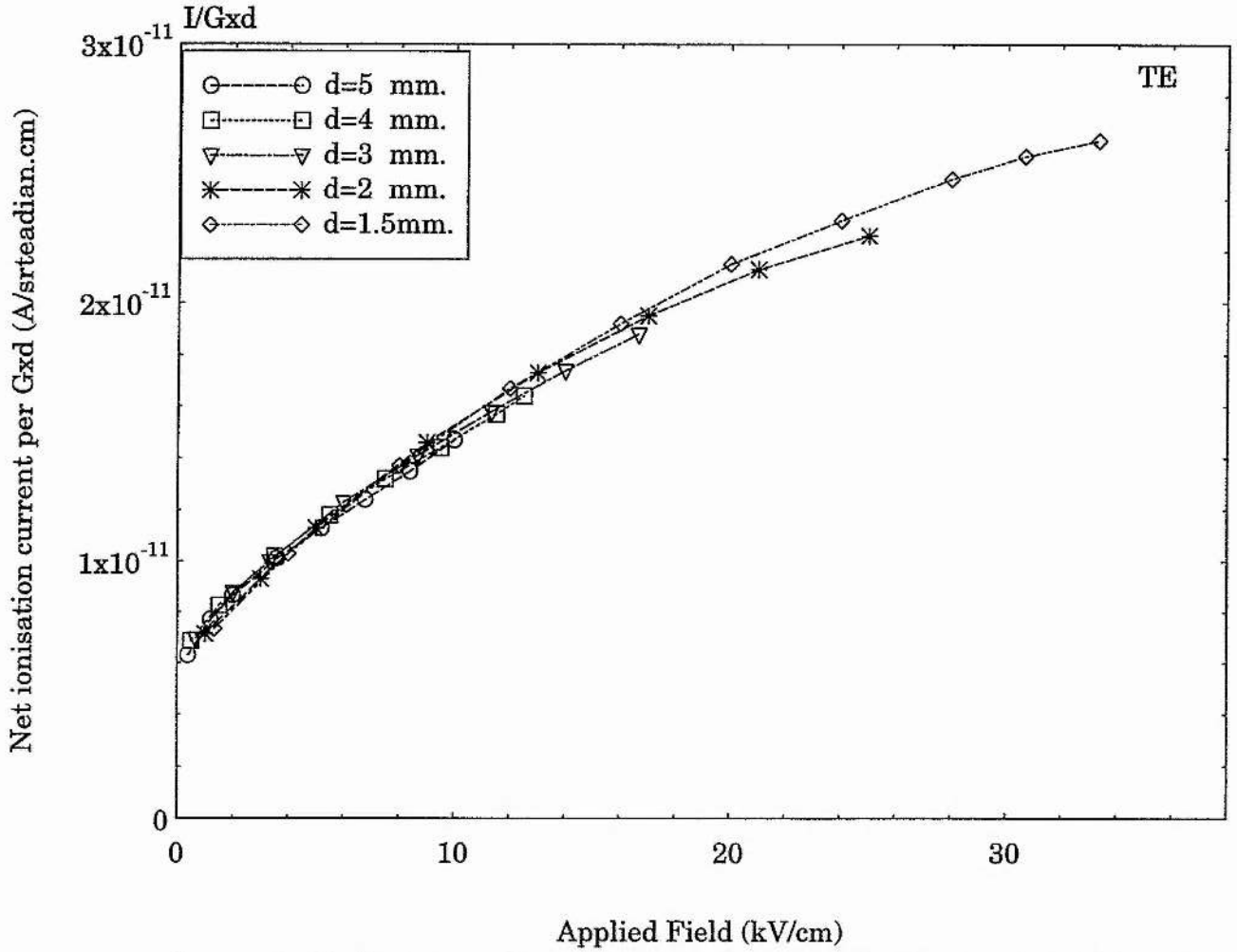

Figure(6-22): Variation of ionization current per Gxd with electric field for TE electrodes and different spacings d. G is geometrical factor.

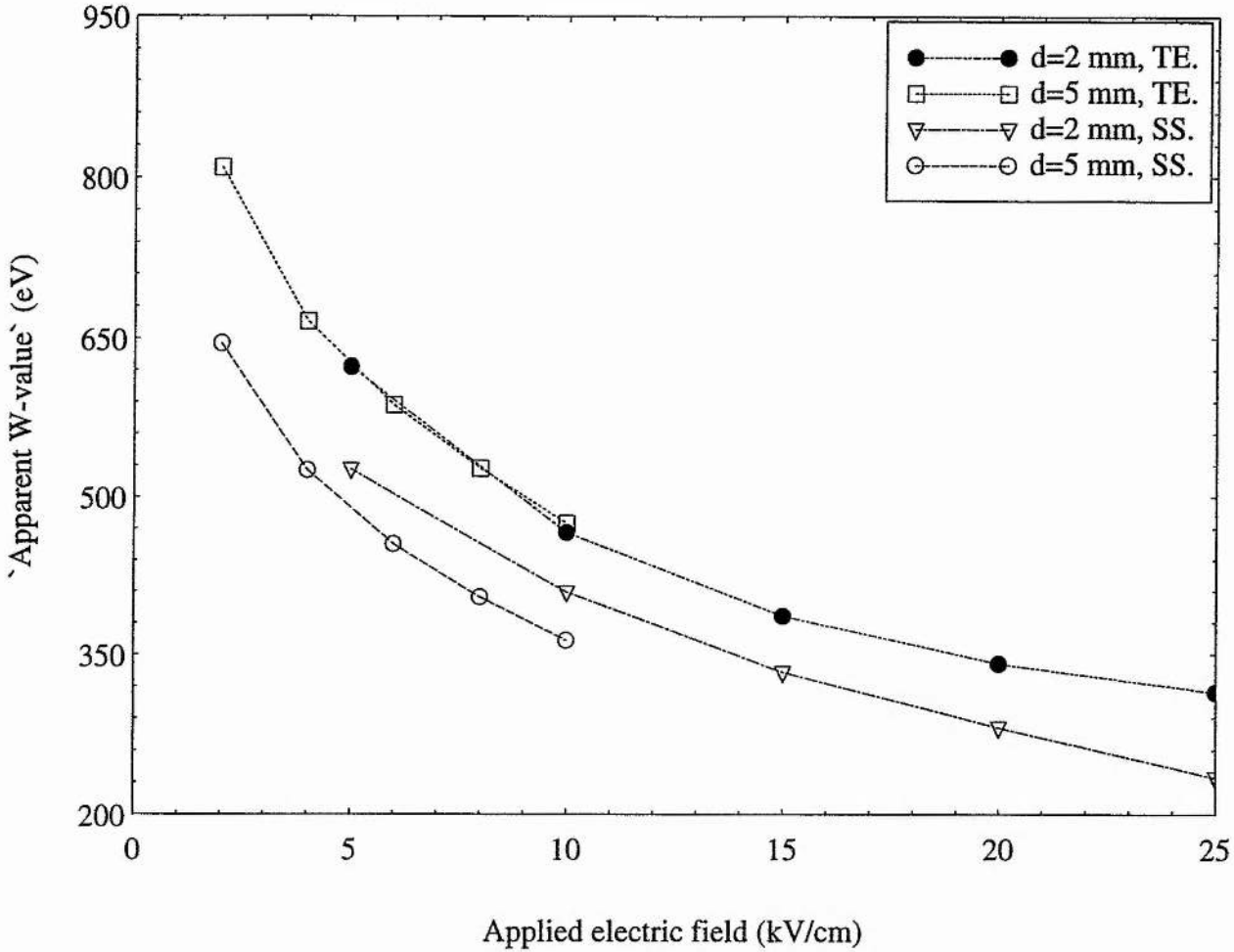

Figure (6-23): Variation of the apparent W-value with applied electric field for two values of electrode spacings and two type of electrode materials.

Table (6-3): Apparent W-values for two values of electrode spacings and different values of the electric field for the chamber fitted with SS and TE electrodes.

	d(cm)	E(kV/cm)	A(mCi)	G_s(St.)	ϕ(cm^{-2}.s)	Ψ(eV/cm^2s)	$\dot{K}$(eV/g.s)	$\dot{E}_{ab}$(eV/s)	I_{exp}(Amp)	W(eV)
SS	0.5	2	3.463	0.114	1.85E+07	2.26E+12	6.91E+10	2.90E+10	7.20E-12	645
	0.5	4	3.463	0.114	1.85E+07	2.26E+12	6.91E+10	2.90E+10	8.84E-12	525
	0.5	6	3.463	0.114	1.85E+07	2.26E+12	6.91E+10	2.90E+10	1.02E-11	455
	0.5	8	3.463	0.114	1.85E+07	2.26E+12	6.91E+10	2.90E+10	1.15E-11	404
	0.5	10	3.463	0.114	1.85E+07	2.26E+12	6.91E+10	2.90E+10	1.28E-11	363
	0.2	5	3.446	0.141	2.29E+07	2.80E+12	8.57E+10	1.44E+10	4.38E-12	526
	0.2	10	3.446	0.141	2.29E+07	2.80E+12	8.57E+10	1.44E+10	5.64E-12	409
	0.2	15	3.446	0.141	2.29E+07	2.80E+12	8.57E+10	1.44E+10	6.92E-12	333
	0.2	20	3.446	0.141	2.29E+07	2.80E+12	8.57E+10	1.44E+10	8.19E-12	281
	0.2	25	3.446	0.141	2.29E+07	2.80E+12	8.57E+10	1.44E+10	9.46E-12	243
TE	0.5	2	2.719	0.101	1.29E+07	1.57E+12	4.80E+10	2.01E+10	3.98E-12	809
	0.5	4	2.719	0.101	1.29E+07	1.57E+12	4.80E+10	2.01E+10	4.83E-12	666
	0.5	6	2.719	0.101	1.29E+07	1.57E+12	4.80E+10	2.01E+10	5.48E-12	587
	0.5	8	2.719	0.101	1.29E+07	1.57E+12	4.80E+10	2.01E+10	6.11E-12	527
	0.5	10	2.719	0.101	1.29E+07	1.57E+12	4.80E+10	2.01E+10	6.78E-12	475
	0.2	5	2.761	0.126	1.64E+07	2.00E+12	6.12E+10	1.02E+10	2.62E-12	623
	0.2	10	2.761	0.126	1.64E+07	2.00E+12	6.12E+10	1.02E+10	3.50E-12	466
	0.2	15	2.761	0.126	1.64E+07	2.00E+12	6.12E+10	1.02E+10	4.23E-12	386
	0.2	20	2.761	0.126	1.64E+07	2.00E+12	6.12E+10	1.02E+10	4.79E-12	341
	0.2	25	2.761	0.126	1.64E+07	2.00E+12	6.12E+10	1.02E+10	5.20E-12	314

Ψ is energy fluence, $\dot{K}$ is kerma rate, $\dot{E}_{ab}$ is energy absorbed rate, and I_{exp} is experimental ionization current.

Table (6-4): Apparent W-values for various values of electrode spacings at ceratain value of the electric field for the chamber fitted with SS and TE electrodes.

	d(cm)	E(kV/cm)	A(mCi)	G_s(St.)	ϕ(cm^{-2}.s)	Ψ(eV/cm^2s)	$\dot{K}$(eV/g.s)	$\dot{E}_{ab}$(eV/s)	I_{exp}(Amp)	W(eV)
SS	0.2	10	3.446	0.141	2.29E+07	2.80E+12	8.56E+10	1.43E+10	9.46E-12	242
	0.3	10	3.455	0.132	2.13E+07	2.60E+12	7.95E+10	2.00E+10	1.06E-11	302
	0.4	10	3.455	0.123	1.99E+07	2.43E+12	7.43E+10	2.49E+10	1.18E-11	338
	0.5	10	3.463	0.114	1.85E+07	2.26E+12	6.91E+10	2.90E+10	1.28E-11	363
TE	0.15	10	2.753	0.131	1.69E+07	2.06E+12	6.30E+10	7.94E+09	4.74E-12	268
	0.2	10	2.761	0.126	1.64E+07	2.00E+12	6.11E+10	1.02E+10	5.20E-12	314
	0.3	10	2.719	0.117	1.49E+07	1.82E+12	5.56E+10	1.40E+10	6.02E-12	372
	0.4	10	2.719	0.109	1.38E+07	1.68E+12	5.13E+10	1.72E+10	6.56E-12	420
	0.5	10	2.719	0.101	1.29E+07	1.57E+12	4.80E+10	2.01E+10	6.78E-12	475

field. This is expected to be due to the higher efficiency of ion collection owing to the higher strength of the electric field.

The fact that values of the W are higher for the TE electrodes than those of the SS electrodes is consistent with the adopted model. In other words, for the SS electrodes the bubble formation is higher and thus multiplication inside bubbles is more enhanced Consequently, the W-values are reduced.

Examination of the difference between the curves for the two different electrode reveals that the two curves of the TE electrodes, for the low and high values of the electric field, are appropriately superimposed to form a single continuous curve whereas for the SS electrodes the components are separated. The difference in the values of the two curves for the SS electrodes is associated with the difference in the size of the bubbles formed owing to the difference in the pressure. For the TE electrodes, the asperities are less and hence the 'bubble' effect becomes negligible.

The difference observed between the low and high field curves for the SS electrode is due to the fact that the experimental measurements of the current were performed at decreasing the electric field starting from the highest values and working downwards. Consequently, in analogy with hysteresis the resulting effects initiated in the high field region influences measurements in the low field region. Conversely, if measurements are made from low to high fields, the curve is of different magnitude.

The dependence of the apparent W-value on the electrode separation was also plotted at a single value of the electric field, 10 kV/cm. This is shown in figure (6-24) for the SS and TE electrodes. The W-value tends to increase with increasing distance between the electrodes. This observation along with that obtained in figure (6-23) indicates that two factors are required for attaining saturation viz. small electrode spacing as well

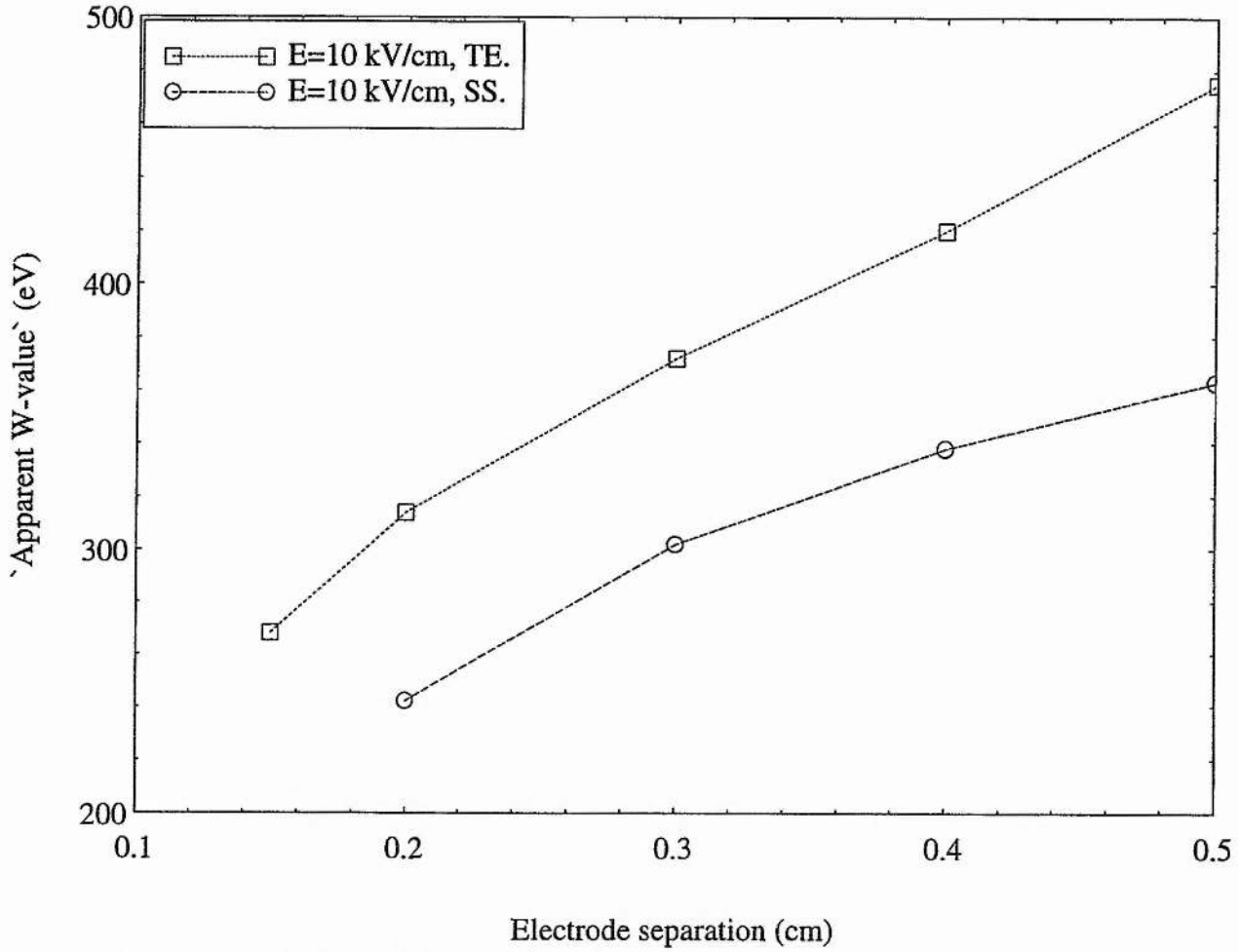

Figure (6-24): Dependence of the apprent W-value on electrode separation at a fixed electric field of 10 kV/cm for two materials of electrode.

as high electric field.

6.2 Glass-ionization chamber

An important requirement for the development of the glass-liquid ionization chamber (GL) was the investigation of each of dark current and ionization current at high values of the electric field since this was precluded by the design of the earlier chamber. As the vessel of the present chamber was made of glass, the cleaning processes were easier and more efficient relative to the SS-chamber. Furthermore, any possible chemical exchanges of the liquid sample with the interior wall of the chamber is reduced to a minimum value.

6.2.1 Liquid prestressing

The liquid sample introduced to the glass chamber under vacuum was subjected to a very high electric field for a long time (~ 40 hours) until a stable current was attained. The gradual increase of the electric field in the high field region was occasionally interrupted by the appearance of sporadic strong pulses which decayed away with time allowing for an additional increase in the electric field.

The time variation of the dark current for the glass-chamber is shown in figure (6-25) for two values of the electric field. In general, the current decreases with time in a way similar to that recorded in the SS-chamber with the following two differences:

i- for the glass ionization chamber the final value of the dark current is one order of magnitude lower than that of the SS-chamber.

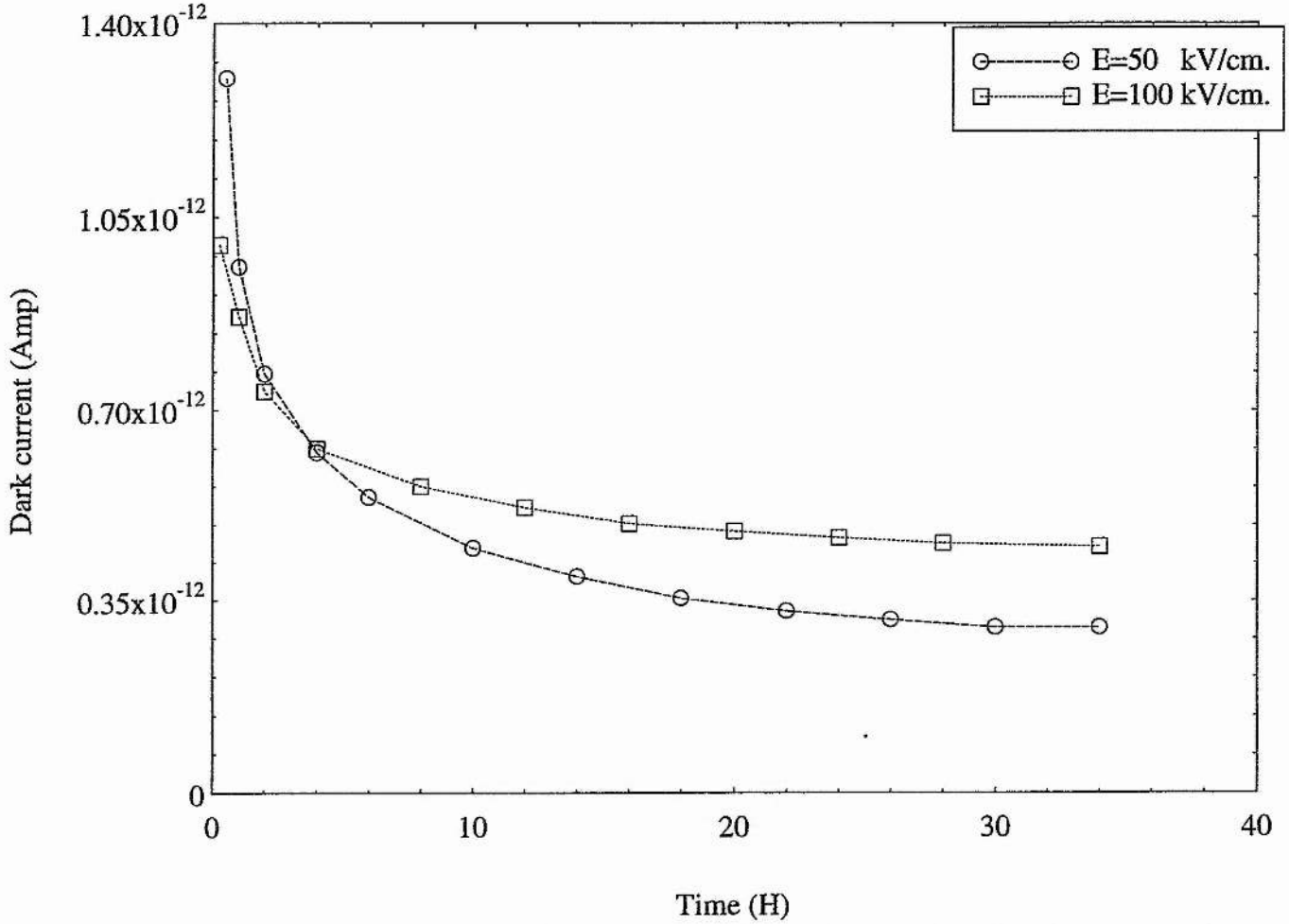

Figure (6-25): Variation of dark current with time for the glass chamber at two values of the electric field.

ii- despite the higher value of the electric field applied in the glass chamber, the systematic decrease of the current was slower and the range of the current was smaller.

The lower value of the dark current obtained with the GL-chamber relative to that of the SS chamber can be explained using the bubble model adopted earlier as being due to lower asperity of the high field electrode. This, in fact, limits the processes of local evaporations and therefore the hydrostatic pressure developed in the chamber is lower. This is also ensured by the fact that the area of the high field electrode in the glass chamber is several times smaller than that of the SS chamber. Furthermore, with regard to the present chamber the liquid does not fill the whole available space inside, as was the case with the SS chamber, and therefore any volume change with temperature is easily compensated.

6.2.2 Dark current-field characteristic.

The dark current measurements in the liquid sample of TMS were conducted in the present chamber at high values of the electric field. The highest value of the electric field applied was 500 kV/cm for 50 mm of electrode separation. No current measurement was attempted beyond this value of the field due to the onset of electrical breakdown.

The dark current-field characteristic curves for high and relatively low values of the electric field are shown in figures (6-26) and (6-27) respectively. For two values of electrode spacings and up to 100 kV/cm of the electric field, the dark current showed two distinct linear regions depending on the field value. In this range of the electric

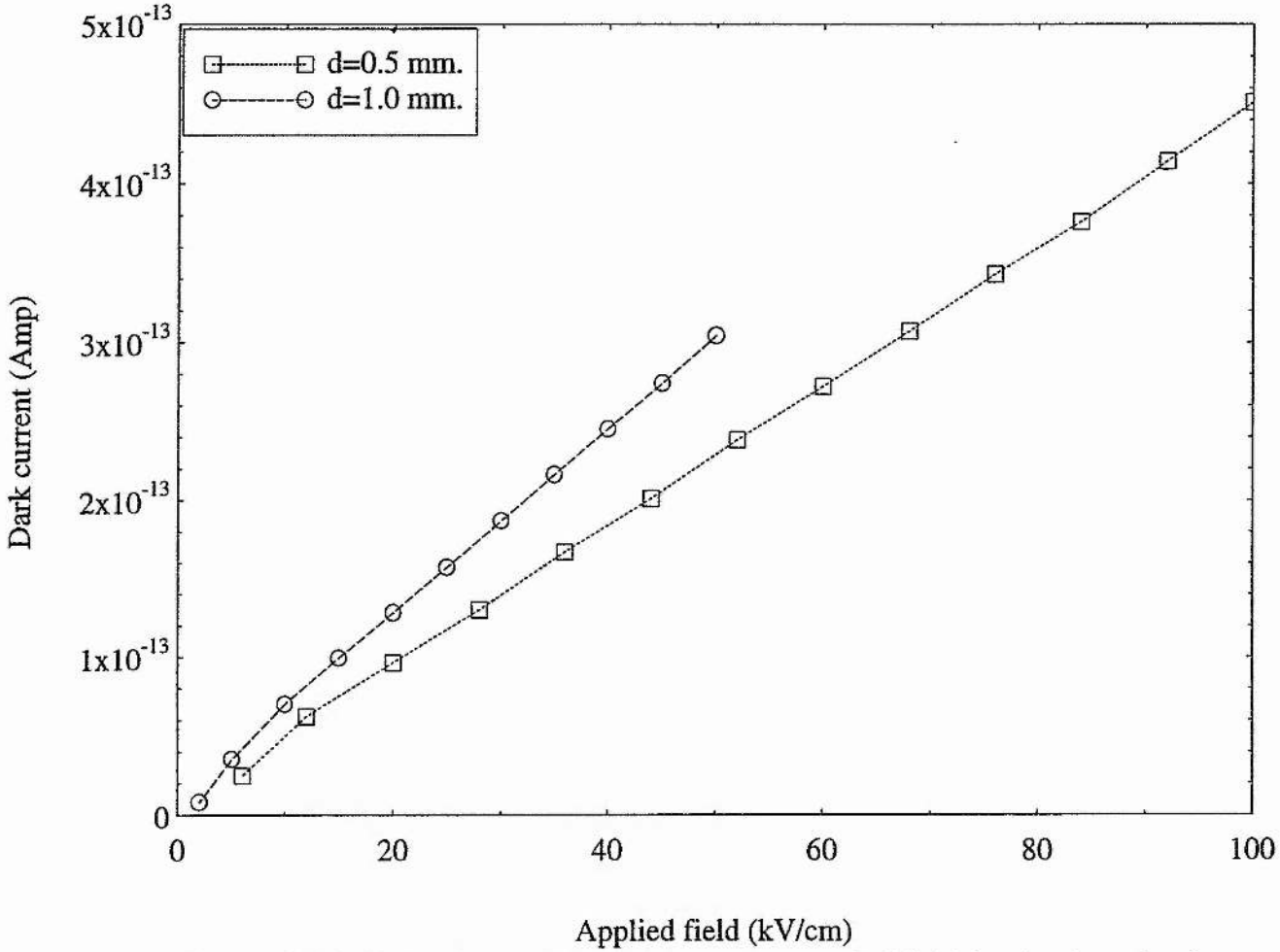

Figure (6-26): Dependence of the dark current on applied field for the glass chamber at two different values of the electrode spacing.

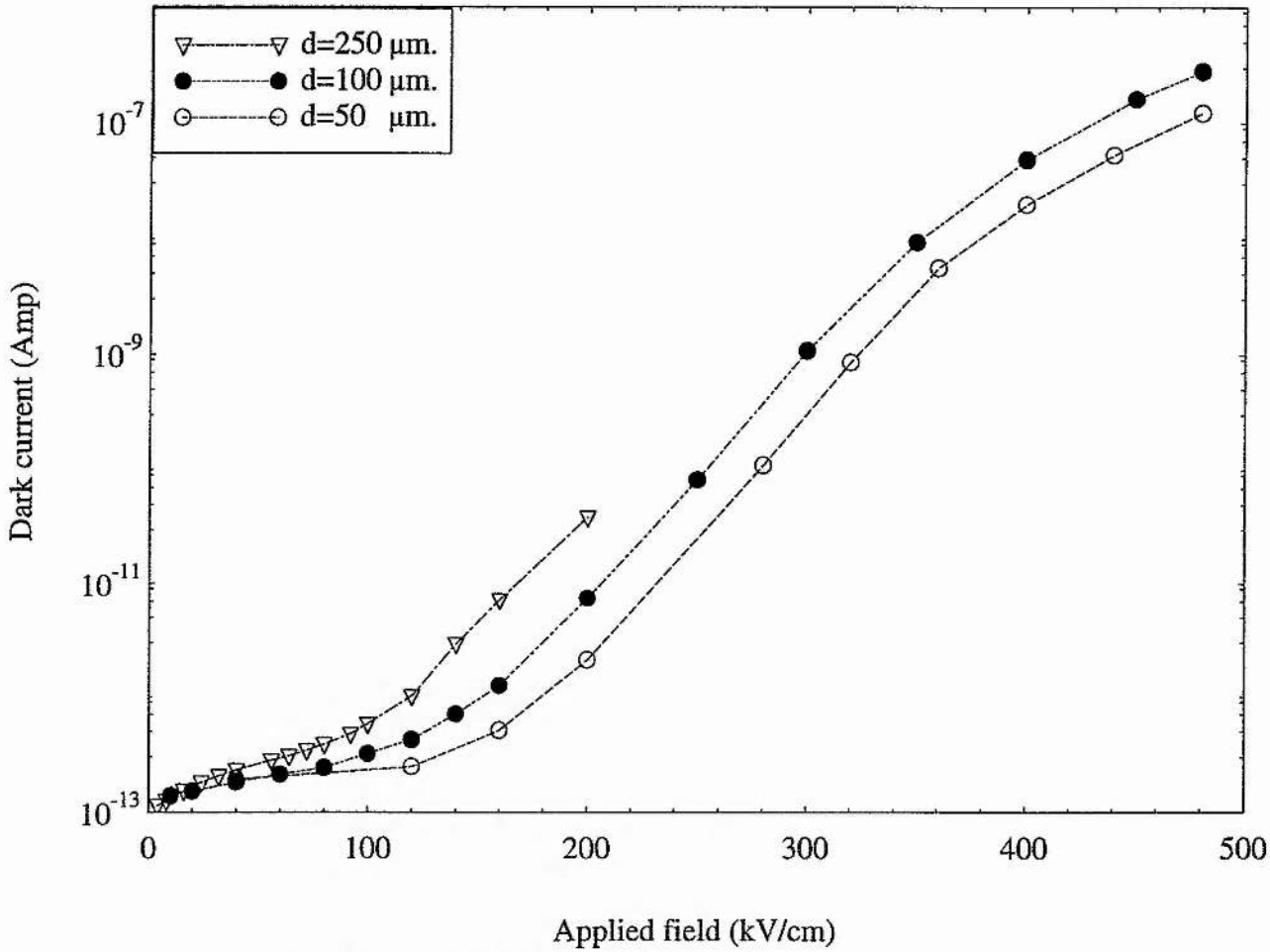

Figure (6-27): Dependence of the dark current on applied field for the glass chamber at some small values of electrode spacing.

field the dark current showed no sharp increase. However, at higher values of the electric field, attained by reducing the space between the two electrodes, a sharp deviation from linearity was obtained. The threshold at which this deviation appeared was a function of the electric field and electrode separation, figure (6-27). The sharp increase of the dark current persisted with increasing the applied field and reached the value 10^{-7} (amp). Approaching that value of the current the curve shows a tendency towards saturation. When the brass electrodes were replaced with the tissue equivalent plastic material electrodes, type A 150, no significant difference in the behaviour and values of the dark current was observed.

With regard to the SS chamber, the sharp increase of the dark current took place at much smaller value of the electric field. This seems to be consistent with the bubble model adopted in this work. This is because with the present chamber the number and size of bubbles formed are likely to be smaller than those in the SS chamber and start at higher value of the electric field. This is due to the boarder asperities..

6.2.3 Hysteresis effect

As mentioned earlier, the application of the electric field was performed by gradually decreasing the steps of the electric field starting from the highest value. The reason for doing this was to maintain the value of the dark current achieved directly after the prestressing stage, and to avoid any extension or sudden changes in the form of the current at some values of the electric field at which certain effects start to take place. By decreasing the steps of the applied electric field always a systematic behaviour of the dark current was obtained. However, when the direction of change of the electric

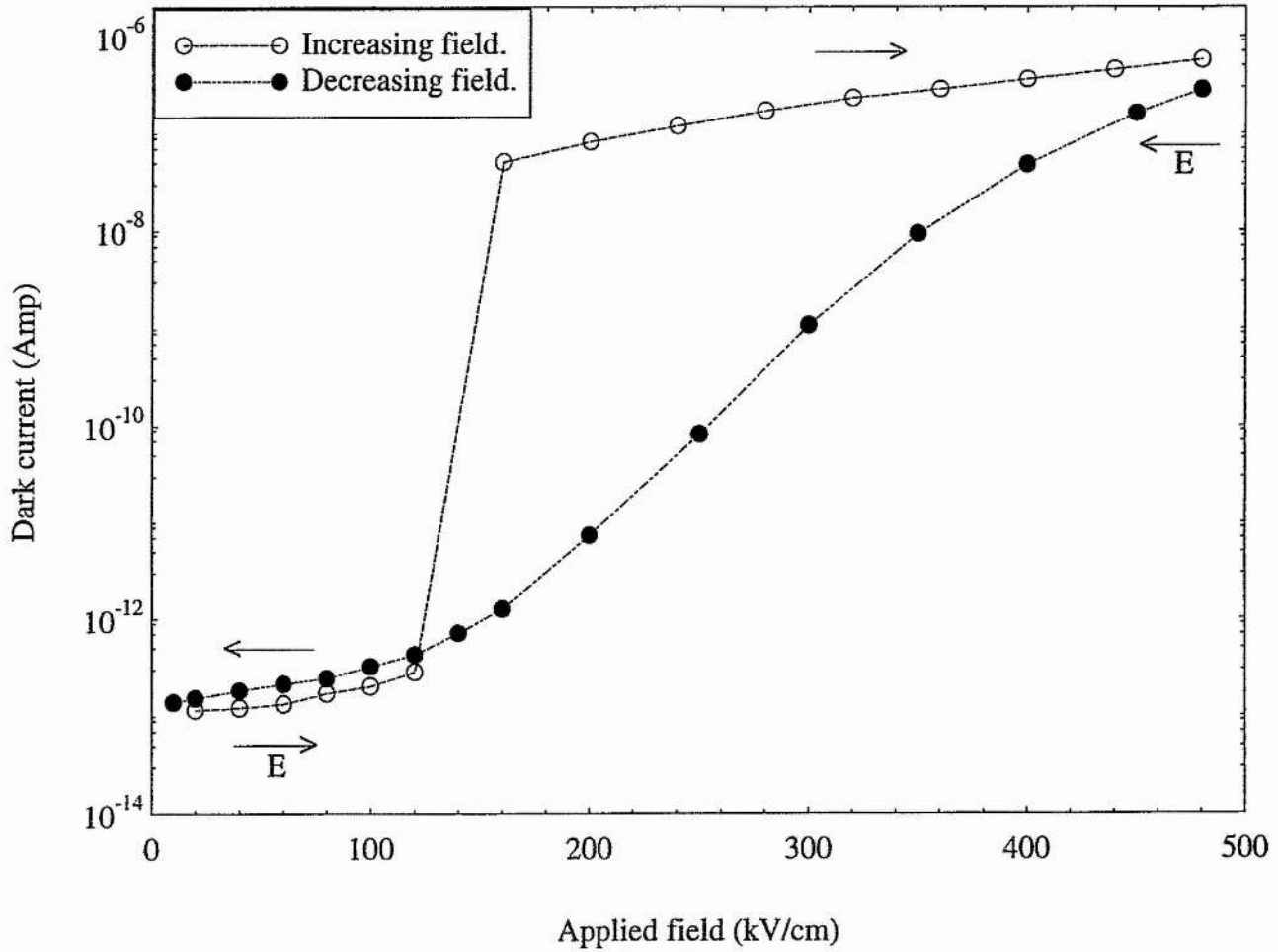

Figure (6-28): Dependence of the dark current on the direction of application of the electric field.

field was reversed the trend in current was different as shown in figure (6-28). In other words, with increasing the steps of the electric field an almost sudden change in the values of dark current was observed. Values of the dark current were divided into two separate regions, low value region of the order of (10^{-12}-10^{-13}) ampere, and high value region (10^{-8}-10^{-7}) ampere. A form of hysteresis occurs at certain value of the electric field and the current graphs are not superimposed.

The value of the electric field at which the sudden change in the dark current occurs is thought to be that at which bubble formation begins. This value of the electric field is expected to be high enough to start multiplication, then a sharp increase in the current is observed.

6.2.4 Ionization current.

With the present chamber the ionization current measurement was extended to 200 kV/cm of the electric field. Beyond this value no further measurements could be attempted since the actual values of the ionization current is masked by a much greater value of the dark current.

Figure (6-29) shows the dependence of the net ionization current in the glass-chamber on applied electric field for different electrode separations down to 50 mm. Despite the high value of the electric field applied the current showed no tendency to saturate. As the electrode spacing was increased the deviation from saturation became more accentuated. However, for the smallest electrode separation, 50 mm, the behaviour of the ionization current was distorted. This uncertainty is thought to be associated with a much higher dark current which influences the ionization current measurement, even

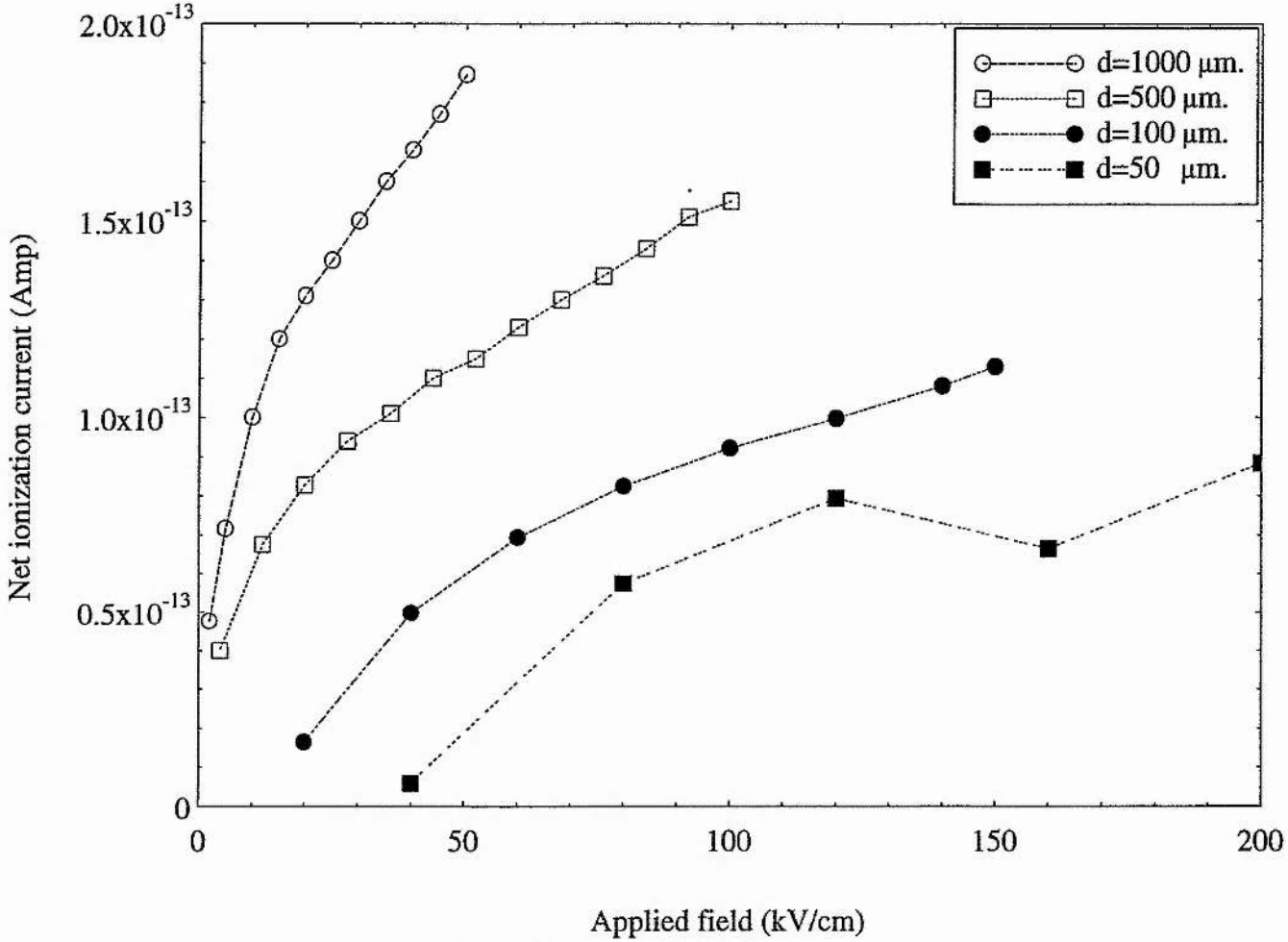

Figure (6-29): Variation of the net ionization current with applied field for some values of electrode spacing.

in the low field region. This is because the bubble phenomenon caused by the high action of the electric field influences the current measurement throughout the whole range of values of the electric fields since the measurement started from the highest value of the electric field.

6.2.5 Estimation of W-value.

An estimation of the W-value in the TMS was attempted for the observed ionization current at various electrode separation and values of the electric field. The method used for this calculation was that explained in appendix B. The geometrical factor used, G_p, was that for a point source which is given by the following equation (Bland 1984).

$$G_p = \frac{1}{2}\left(1 - \frac{z}{D}\right) \qquad (6\text{-}2)$$

where z is the source-detector distance and $D = (z^2+y^2)^{1/2}$, where y represents the radius of the sensitive volume, regarded as the detector. This equation was applied to the present case, where the sensitive volume is very small, as it was considered to be applicable to a point electrode. The calculated W-values are listed in the table (6-5), calculated for some values of the electric field.

Table (6-5): Apparent W-values for the TMS contained in the GL-chamber at some values of the electric field. S is the projected area of the sensitive volume.

For an electrode separation of 1 mm and 50 kV/cm of the applied electric field the W-value was comparable to the saturation value for the gas which means that at this value of the electric field we have total collection of the charge produced. This is not believed to be the case for different reasons:

i- the obtained W-value observed was not repeated for any other value of the electric field and thus no plateau of saturation was observed. Thus this region is likely to be a point region.

ii- when the W-value was plotted as a function of the electric field a strong dependence on the electrode separation was observed even in the same region of the electric field, figure (6-30). One possible reason for this difference is that the electric field was applied by gradually reducing the steps which influenced the measurement in the whole range of the applied field.

The fact that the W-value continued to decrease with increasing applied electric field suggests that the true values of the W-value is much higher than that actually obtained. The reason for such behaviour is believed to be due to charge multiplication inside bubbles formed in close proximity to the cathode asperities. This is because multiplication does increase the number of charged particles produced in the liquid. Consequently, values of W-value are decreased.

In fact, a direct comparison between W-values obtained with the SS-chamber, Tables (6-3) (6-4), and those of the GL-chamber reveals that for the SS chamber the bubble formation starts at a lower value of the electric field. Consequently, the effect of multiplication in bubbles is accentuated.

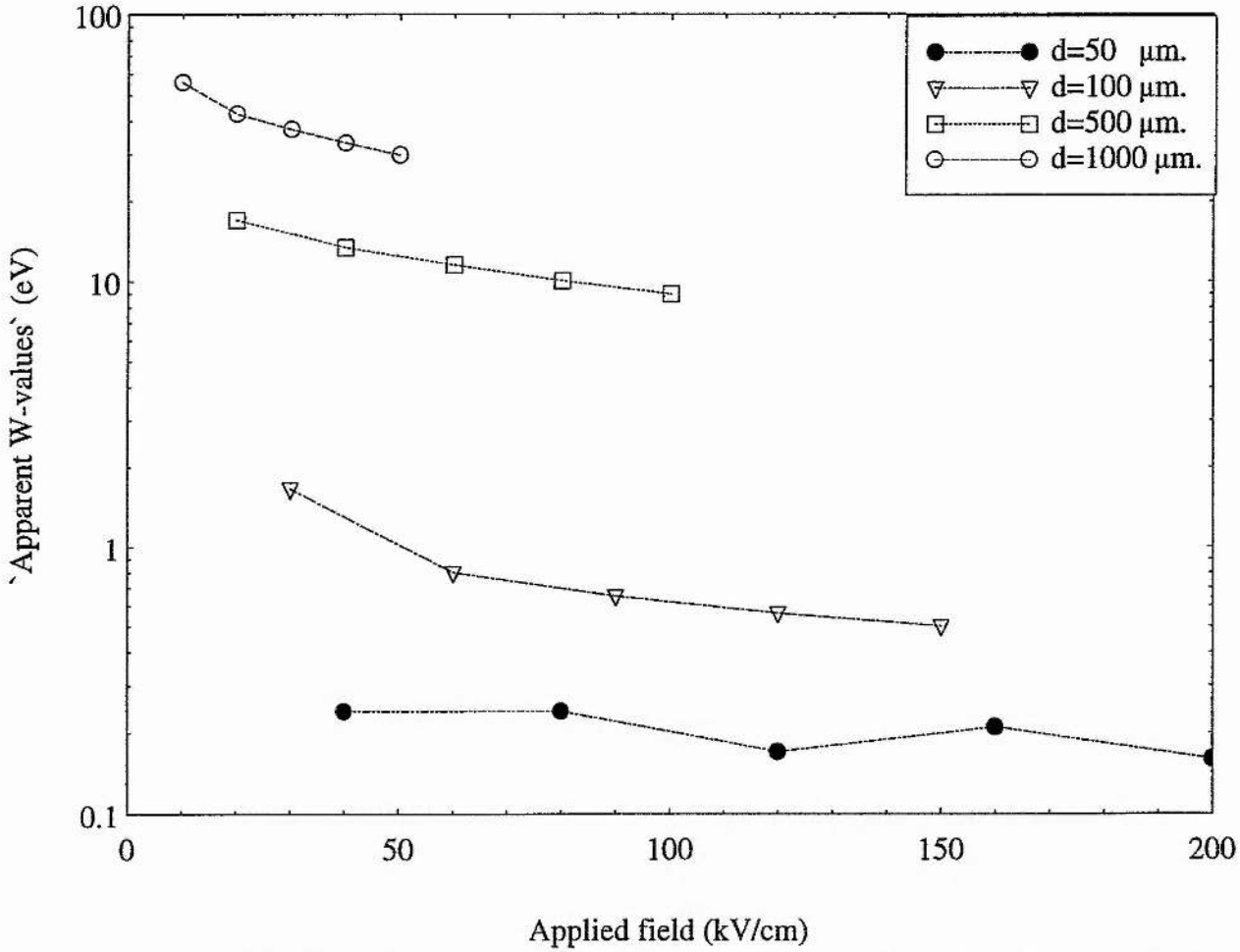

Figure(6-30): Variation of the apparent W-value with electric field for the GL chamber at different values of electrode spacing.

6.2.6 Gas chromatography

Due to the very high values of the electric field applied, it is possible that chemical changes may occur. In order to examine this an analysis test was performed for the liquid sample used, before and after the high field application. The reason for carrying out such a test is to account for any possible dissociation; decomposition; or fragmentation caused by the high strength of the applied electric field. It also allows for the detection of any possible existence of prominent substances devolved in the liquid which limits the processes of charge transport in liquid. For example, the formation of hydrogen may lead to an increase of pressure in the chamber owing to the limited solubility of the liquid (Givernaud et al. 1992). Towards this aim, a gas chromatography (GC) analysis, known as an excellent method for separating and detecting the components of mixtures of organic compounds, was performed. This technique operates in the gas phase and is capable of examining substances at trace levels. At the end of the analysis each component of the mixture can be identified as a separate peak Gaussian distribution.

When the used sample of TME was analyzed, before and after subjecting it to a very high value of the electric field (> 300 kV/cm), no clear indication of any of the phenomena mentioned above was found indicating no effect of the electric field on the chemical structure of the used liquid. Figures (6-31) shows the single peak which appeared before and after prestressing the liquid. This figure is also regarded as a direct evidence that the liquid sample employed in this work is a high purity one.

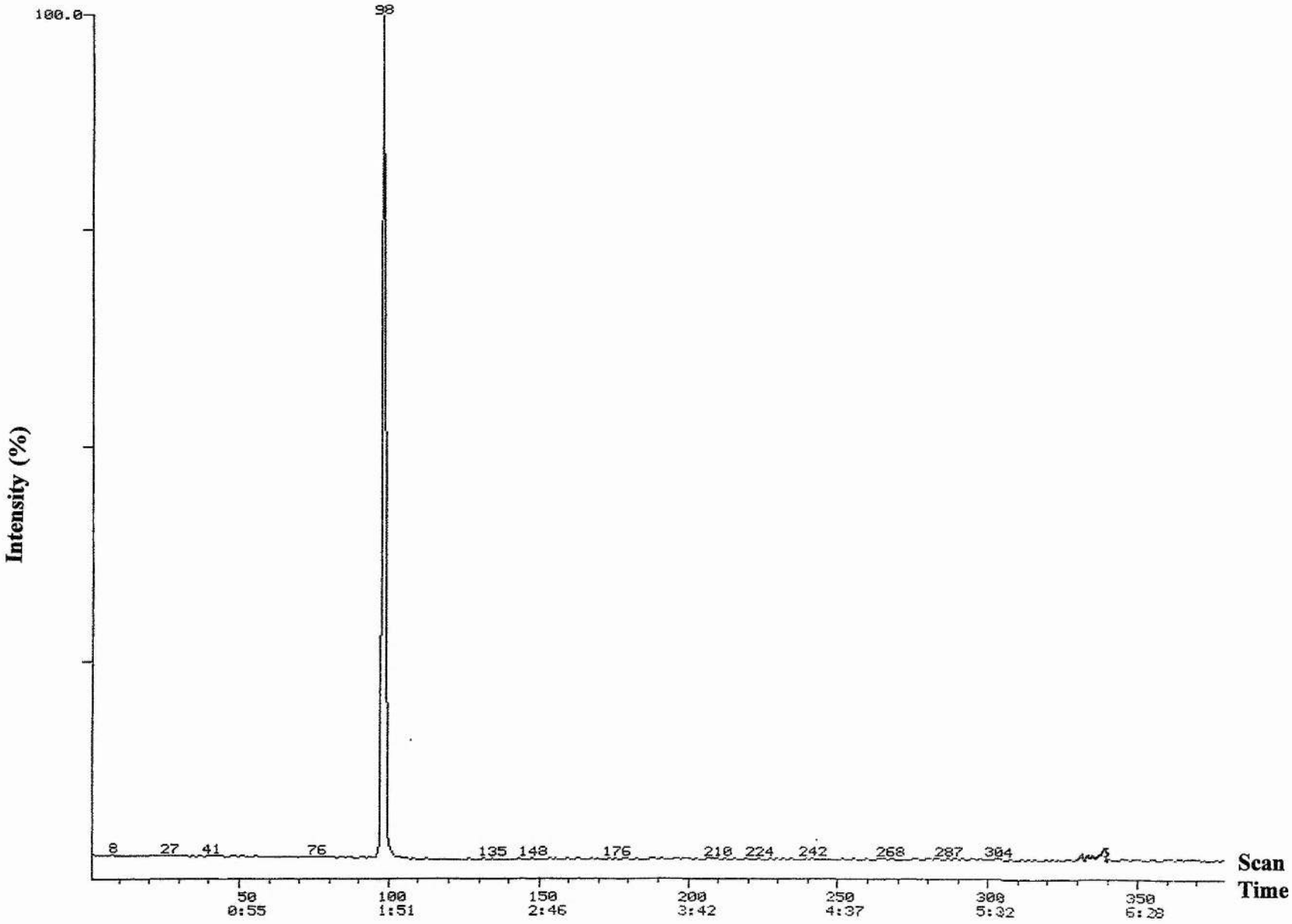

Figure (6-31): Gas chromatography analysis of liquid sample of TMS after the processes of prestressing.

6.3 Conclusion

The collection efficiency is known to be enhanced with increasing electric field. This does not, unfortunately, proceed to the high values of electric field where new sources of charges are likely to be established. A possible source of extra charges is multiplication which may originate inside a bubble formed in the immediate vicinity of the electrode asperity when the intensity of the electric field is sufficiently high. These processes occur only inside bubbles which are created in the high field region close to the high field electrode. In this region of the electric field the electron gains enough energy to produce multiplication in a gas.

In fact multiplication in a gas bubble can take place only for those tracks of charged particle having interaction mean free paths shorter than the size of the bubble containing them. This means that by decreasing the size of these bubbles the multiplication processes is reduced. The pressure is likely to increase by the local evaporation of the liquid in the immediate vicinity of the sharp points covering the surface of the high field electrode. However, if the electrode asperity is reduced bubbles are likely to be formed at higher values of the electric field. Further, there will be less local evaporation and therefore lower hydrostatic pressure. This means any formed bubbles are larger in size and located in a higher field region which is an advantage over that which would have been if the asperities of the surface of the high field electrode is higher. Consequently, the obtained current is much higher as is found to be the case with the GL-chamber as compared with the SS-chamber of higher asperity of electrode.

The aforementioned explanation means that unless the source of extra charge is

eliminated the current will always increase in the external circuit and saturation is not likely to take place.

If the electrode separation is sufficiently small and the density of bubbles is high, channels, consisting of superimposed bubbles, may initiate across the two electrodes. When the intensity of the electric field is sufficiently high multiplication can proceed along these channels resulting eventually in electrical breakdown. Alternatively, if the size of the formed bubbles is large, multiplication may proceed from the bubble on outwards into the liquid region with ultimate consequences of electrical breakdown. The latter phenomenon was observed at lower values of the electric field for the SS and Al electrodes as compared to the TE electrodes in the SS chamber. This is believed to be associated with the higher concentration of bubbles for the former electrodes owing to the higher degree of roughness of the electrode surface. However, for the GL chamber the ionization current was measured at up to 200 kV/cm and no saturation was attained. The distortion and ambiguity of the ionization current is greatly enhanced at high values of the electric field which is very much needed for attaining saturation.

6.4 Future work

To achieve total charge collection in liquids subjected to high electric fields, it is necessary to eliminate the various unwanted effects induced by the field. Bubble formation appears to be one of the most important factors that limits saturation collection of charge in liquid. It can be greatly reduced by minimising the surface roughness of the electrodes. Lapping and polishing of metal electrode surfaces can

reduce roughness to within 5 to 10 nm (e.g. Logitech equipment).

Use of high purity liquid is an essential requirement. In this respect, it is recommended that ion chamber be designed so that it allows for the purification process to be performed internally. This avoids possible contamination that could be introduced during the process of liquid transfer externally.

Having obtained a suitable quality of electrode surface, it is worth attempting saturation collection of charge in frozen liquids as this would have the dual advantage of minimal bubble formation whilst increasing the electron mobility.

The role of field induced dipole moment remains unclear but, if significant, its effects could be reduced by replacing DC-field by a suitably pulsed electric fields. This would avoid the existence of field dependent polarization which could limit the processes of charge collection by creating trapping centers for the drifting electrons. Such an application is also expected to contribute to the reduction of bubble formation in the liquid phase.

There are realistic prospects of producing an ionization chamber which will be capable of saturation charge collection and possible controlled multiplication by operation in proportional counter mode although the applied fields will be very high.

Appendix (A)

Calculation of the apparent W-value

The W-value is given by the folowing equation

$$W = \frac{E_{ab}}{N} \qquad (1)$$

where E_{ab} is the energy absorbed and N is the number of ions of one type produced. E_{ab} is given by

$$E_{ab} = K \times M_{sv} \qquad (2)$$

K is the kerma, and M_{sv} is the mass of the sensitive volume = 1.07x S_v. Kerma is related to the energy fluence, $\Psi = \Phi.E$, by the mass energy-transfer coefficient (μ_{tr}/r) according to the equation

$$K = \Phi_{abs} E . \left(\frac{\mu_{tr}}{\rho}\right) \qquad (3)$$

where

i- Φ_{abs} is the relevent particle fluence, given by

$$\Phi_{rad} = G_s.At/S \qquad (4)$$

where G_s is the geometrical factor, A is the activity of the radiation source (Bq), t is the irradiated time (sec), and S is the projected area (cm^2).

ii- E is the average energy of the ionizing radiation, which here is for γ-rays emitted from ^{57}Co. i.e.

$$E = [88\% \text{ of } 122 + 11\% \text{ of } 136]x10^3 = 122320 \text{ eV}.$$

iii- the mass energy-transfer coefficient for liquid TMS, Si C_4H_{12}, is obtained by summation of the fractional masses i.e.

$$\left(\frac{\mu}{\rho}\right)_{TMS} = F_{Si}\left(\frac{\mu}{\rho}\right)_{Si} + F_C\left(\frac{\mu}{\rho}\right)_C + F_H\left(\frac{\mu}{\rho}\right)_H \qquad (5)$$

where F is the fraction by mass = (At.wt)/(M.wt).

N, the number of charges of one sign created is obtained from the experimental results i.e.

$$N = \frac{I_{exp}}{1.602x10^{-19}} \qquad (6)$$

The procedure used is to calculate apparent W-values from equation (1) and using N determined from equation (6). This gives an 'apparent' W-value for comparison with the more realistic W-value obtained with the saturation current. The methode is used as a test for total charge collection.

Electron and ion mobility in rare-gas liquids ($cm^2/V.sec$)

Compound	El.Mob.	Ion Mob. +	Ion Mob. -	Temp.(K)	Ref.
Ar	1.70E+03			147	80
	1.58E+03			144	125
	3.10E+02			111.5	103
	2.85E+02			111.5	103,123
	4.90E+02			87	80,125
	4.00E+02			87	146
	5.20E+02			85	48
	4.75E+02			85	86,121
	4.50E+02			85	107
	4.40E+02			85	122
		2.61E-03		145	26
		1.22E-03		111.5	26
		6.61E-04		90	26
		1.00E-03		85	121
		8.00E-04		85	53
		7.00E-03		85	50
Kr	3.57E+02			200	62
	1.31E+03			120.4	121
	1.20E+03			120	121,146
	1.80E+03			117	82,86
		1.10E-03		184.3	26
		6.69E-04		141	26
Xe	1.10E+03			167	76
	2.00E+03			165	121,146
	2.20E+03			163	82,86
	1.90E+03			163	86
	2.00E+03			161	107
		3.29E-04		192.1	26
		2.85E-04		184.2	26
		4.00E-03		168	97
4He	1.00E-02			4.2	107
	2.16E-02			4.2	25
		5.30E-02		4.2	97
3He	3.70E-02			3	97
Ne	1.00E-03			27	14
N_2			3.00E-03	77	49
		1.00E-02		77	50
		2.00E-03		77	53
H_2		8.30E-03	8.60E-03	21	147
			3.00E-02	21	49
		4.50E-02		21	50
Deuterium			9.00E-03	21	49
O_2			8.00E-03	77	49
		8.00E-03		77	53

Electron and ion mobility in liquid hydrocarbons ($cm^2/V.sec$)

Compound	El.Mob.	Ion Mob. +	Ion Mob. -	Temp.(K)	Ref.	
Methan(CH_4)	4.20E+02			123	126	
	3.73E+02			120	96	
	3.00E+02			120	33	
	4.00E+02			112	116	
	4.00E+02			111	10,116	
	4.00E+02			110	121	
		2.50E-03		111	116	
		2.00E-03		111	13	
Ethane(C_2H_6)		9.90E-04		216	117	
		8.90E-04		197	117	
		5.30E-04		155	117	
		1.80E-04		110	117	
	3.70E+01			298	37	
	8.50E-01			200	11	
	8.00E-01			200	9	
	1.00E-03			111	11	
Propane(C_3H_8)	2.63E+00			297	36	
	1.00E+00			265	104,129	
n-Butane(C_4H_{10})	3.40E-01			298	38	
	4.00E-01			296	114	
	3.40E-01			296	129	
	2.80E-01			295	38	
n-Pentane(C_5H_{12})	7.00E-02			300	114	
	1.60E-01			296	114	
	1.50E-01			296	29	
	1.40E-02			296	3	
	1.48E-02			295	114	
		8.20E-04	1.50E-03	293	134	
n-Hexane(C_6H_{14})	2.06E-01			343	40	
	1.89E-01			338	40	
	1.22E-01			319	40	
	7.00E-02			300	28,88	
	9.00E-02			296	28,88,112,114,116	
	8.00E-02			296	3	
	7.60E-02			296	87	
	7.40E-02			296	40	
	2.20E-01			296	23	
	9.00E-02			293	13	
			1.40E-03	300	81	
		9.90E-04	1.30E-03	298	102	
		7.10E+00	1.32E-03	297	66	
		6.80E-04	1.30E-03	297	66	
		6.60E+00	1.27E-03	297	66	
		8.50E-04	9.10E-04	296	109	
		5.80E-04	9.20E-04	295	47	
		6.90E-04	1.30E-03	293	66	
		6.40E-04	1.10E-03	293	134	

Compound	El.Mob.	Ion Mob. +	Ion Mob. -	Temp.(K)	Ref.
Continuous Hexane		8.27E-04	4.40E-04	292	1
		4.10E-04	1.30E-03	292	46
	7.60E-02			rt	89
n-Heptane(C_7H_{16})	2.65E-01			372	40
	2.36E-01			366	40
	2.05E-01			359	40
	1.73E-01			350	40
	1.36E-01			338	40
	1.09E-01			329	40
	8.90E-02			319	40
	4.60E-02			296	98
	5.10E-02			295	40
n-Octane(C_8H_{18})	2.07E-01			381	40
	9.80E-02			341	40
	6.30E-02			318	40
	4.00E-02			296	98
	3.80E-02			295	40
	3.05E-01			400	98
n-Nonane(C_9H_{20})	3.48E-01			424	40
	2.50E-01			406	40
	1.45E-01			372	40
	7.70E-02			341	40
	4.40E-02			313	40
	2.80E-02			294	40
n-Decane($C_{10}H_{22}$)	3.69E-01			453	39
	1.02E-01			370	39
	2.50E-02			296	29
	2.50E-02			295	39
n-Undecane($C_{11}H_{24}$)	4.60E-01			472	40
	2.42E-01			431	40
	1.39E-01			391	40
	7.10E-02			352	40
	5.00E-02			332	40
	2.40E-02			296	40
n-Dodecane($C_{12}H_{26}$)	1.72E-01			425	39
	6.00E-02			357	39
	2.00E-02			295	39
n-Tetradecane($C_{13}H_{28}$)	4.00E-01			506	39
	9.40E-02			397	39
	1.60E-01			295	39
2233-TMP	1.10E+01			431	28
	9.00E+00			375	28
	7.50E+00			346	28
	5.90E+00			318	28

Compound	El.Mob.	Ion Mob. +	Ion Mob. -	Temp.(K)	Ref.
Continuous 2233-TMP	5.20E+00			296	28
	5.20E+00			295	28
	29+0.9E+01			rt	30
	2.90E+01			rt	106
	2.80E+01			rt	72
	2.40E+01			rt	28
	23.97+13.73			rt	74
2244-TMP	3.10E+01			556	118
	4.40E+01			385	28
	3.20E+01			324	28
	3.18E+01			297	28
	2.90E+01			296	121
		4.30E-04		296	100
	3.00E+01			296	93
	2.40E+01			295	28
	2.90E+01			293	118
	26+1.9E+01			293	7
		5.10E-05		rt	44
		4.30E-05		rt	44
	23.97+13.73			rt	74
224-TMP(Isooctane)	2.40E+01			544	118
	4.50E+00			293	118
	7+2E+01			300	118
	7+2E+01			rt	28
	6.76+4.34			rt	74
		3.50E-04		rt	142
2255-TMP	1.20E+01			rt	28
TMS	1.11E+02			373(P=50b	95
	7.50E+01			373(P=100	99
	1.04E+02			323(P=50b	95
	7.80E+01			323(P=100	99
	1.02E+02			298(P=1b)	95
	8.50E+01			298(P=250	99
	1.04E+02			298	127
	90+5E+01			298	114,116
	1.19E+02			rt	31
	1.00E+02			rt	118
	9.80E+01			rt	21,93
	99+5E+01			rt	60
	9.70E+01			rt	92
	93+5E+01			rt	112
	93.5+3E+01			rt	30
	9.30E+01			rt	133
	1.00E+02			(180-300)	127
		9.00E-04		rt	44,39
		5.80E-04		rt	142
22-DMP(Neopentane)	5.40E+01			322	28
	5.30E+01			312	28

Compound	El.Mob.	Ion Mob. +	Ion Mob. -	Temp.(K)	Ref.
Continuous 22-DMP	5.10E+01			302	28
	7.00E+01			300	89
	6.50E+01			296	121
	55+5E+01			296	114
	5.00E+01			294	28
	5.50E+01			283	97
	4.80E+01			273	28
	8.00E+01			rt	12
	7.00E+01			rt	89,118
	7.10E+01			rt	31
	66.5+3E+01			rt	12
	60+3E+01			rt	140
	55+5E+01			rt	114
	44.12+23.8			rt	74
		6.20E-01	1.36E+00	293	9
22-Dimethylpentane	1.89+1.35			rt	74
TMG	9.50E+01			296	121
	1.15E+02			rt	121
	9.00E+01			rt	31
TMT	7.00E+01			296	121
	8.55E+01			rt	31
	7.00E+01			rt	118
	69.5+3.5E+01			rt	30
22-DMB(Neohexane)	10+1E+01			300	114
		4.80E-04	9.70E-04	293	118
	1.24E+02			rt	114
	1.20E+02			rt	9,118
	10+1E+01			rt	114
	1.00E+02			rt	88
	6.67+4.29			rt	74
22-DMH	0.77+0.58			rt	74
Cyclohexane	1.70E+00			395	28
	1.40E+00			380	28
	8.90E-01			340	28
	6.20E-01			315	28
	3.50E+00			296	114
	4.50E-01			294	28
	3.50E-01			293	13,114
		2.10E-04	3.80E-04	293	134
2255-TMH	1.90E+01			383	28
	1.60E+01			353	28
	1.40E+01			319	28
	1.20E+01			296	28
	1.20E+01			293	28
	6.76+4.34			rt	74

Compound	El.Mob.	Ion Mob. +	Ion Mob. -	Temp.(K)	Ref.
HMDS	2.13E+01			rt	30
	2.00E+01			rt	133
14-Dioxane		8.00E-01	4.80E-01	297	66
		4.00E-01	3.30E-01	297	66
23-DMB	2.60E+01			500	118
	1.10E+00			296	29
	9.00E-01			293	118
Cyclopentane	1.1+0.1E+01			296	114
3-Methylpentane	1.90E+01			504	118
	2.20E-01			293	118
33-Dimethylpentane	2.60E+01			536	118
	2.30E+00			296	29
	2.00E+00			296	118
	2.00E+00			293	118
	1.89+1.35			rt	74
2-Methylpropane	7.30E+00			296	29
2-Methylbutane	9.40E-01			296	63
	3.60E+00			300	89
	1.46+1.06			rt	74
2-Methylpentane	2.90E-01			296	29
	0.53+0.42			rt	74
3-Methylpentane	2.20E-01			296	118
22-BMB	1.70E+01			373(P=1b)	95
	1.35E+01			373(P=250	99
	1.40E+01			333(P=1b)	95
	1.34E+01			333(P=250	99
	1.10E+01			296(P=1b)	95
	1.40E+01			296(P=250	99
Benzen	6.00E-01			300	89
	0.6+0.1E+01			rt	134
Toluene	0.54+0.1E+01			300	89
Mixtures					
TMS/TMP(1.31/1)	39.1			rt	31
TMS/n-pentane(102/1)	118			rt	31
TMS/n-pentane(17/1)	85			rt	31
TMS/n-pentane(5.6/1)	47.6			rt	31

Some properties of rare-gas liquids.

Compound	W_g(eV)	W_I(eV)	I_{ion}(eV)	T(K)	V_0(eV)	Radiation	Ref.
Ar		25.7+3		87		LE X-rays	137
		22.5+3		87		HE X-rays	77
		26.00		87		^{238}Pu-α	131
		19.5+2		rt		Heavy ion	54
		27.5+2.8		rt		α–Particle	54
		25.1+2.5		rt		1MeV El.	54
		23.60		rt			124
	26.2+0.2			87		HE X-rays	51
	26.3+0.1			87		^{238}Pu-α	51
	26.40			rt			34
				84	-0.20		119
Kr			11.56	121	-0.40		120
				116	-0.40		119
Xe		14.7+1.5				Heavy ion	54
		19.6+2.0				α–Particle	54
		16.3+0.3				α–Particle	90
		23.7+2.4				1MeV El.	54
			9.2	161	-0.67		119,120
He				4	1.05		119
N	36.30						34
Ne				25	0.67		119
O_2	32.10						34
Co_2	34.10						34
Carbon disulfide	26.00			rt		LE X-Rays	136
		24		rt		LE X-Rays	90

Some properties of liquid hydrocarbons.

Compound	W_g(eV)	W_i(eV)	I_{ion}(eV)	T(K)	V_0(eV)	Radiation	Ref.
Methan(CH_4)				100	-0.25		119
n-Pentane(C_5H_{12})				295	0.00		119
			9.15+0.1	294	0.00		120
			8.85+0.05	294			120
				295(P=1b)	0.00		6
				295(P=2500b)	0.29		61
n-Hexane(C_6H_{14})	23.4			rt		^{60}Co-γ	2
		25.5		rt		^{60}Co-γ	141
				295	0.04		119
			8.6+0.05	294	0.04		120
n-Ttidecane			9.25+0.05	294			120
2244-TMP			8.2	295			120
				rt	-0.36		56
224-TMP(Isooctane)		23.5		rt		^{60}Co-γ	141
				295	-0.18		119
			8.3+0.05	294	-0.18		120
				295(P=1b)	-0.24		57
				295(P=2500b)	-0.05		61
TMS				295	-0.57		119
			8.1+0.05	294	-0.62		120
			8.05+0.05	294			120
				rt	-0.55		56
				295(P=1b)	-0.56		94
				295(P=2500b)	-0.43		61
22-DMP(Neopentane)		24.8+2.5		296		HE X-Rays	115
	24			296		HE X-Rays	115
				295	-0.43		119
			8.85+0.05	294	-0.43		120
			8.55+0.05	294			120
				rt	-0.43		56
TMG			7.6+0.05	294			120
TMT			6.9+0.1	294	-0.70		120
				rt	-0.75		56
22-DMB(Neohexane)		27.6+3		295		^{60}Co-γ	84
			8.73+0.05	294	-0.15		120
			8.50+0.05	294			120
				rt	-0.22		56
				295(P=1b)	-0.26		61
				295(P=2500b)	-0.11		61

Compound	W_g(eV)	W_l(eV)	I_{ion}(eV)	T(K)	V_0(eV)	Radiation	Ref.
MB(Isopentane)			9.15+0.05	294			120
Cyclohexane	22.7			tr		^{60}Co-γ	2
		25.4		rt		^{60}Co-γ	141
		23.3		298		^{60}Co-γ	108
		21.7		298		^{60}Co-γ	130
			8.75+0.1	294			120
Cyclopentane		22.7		298		^{60}Co-γ	130
				295	-0.28		119
			8.80+0.05	294			120
3-Methylpentane			8.85+0.1	294			120
Methylcyclopentane		23.8		298		^{60}Co-γ	130
Triethylsilane			8.25+0.1	294			120
Triethylsilane			8.25+0.1	294			120
Hexamethyldisilane			6.75+0.1	294			120
Ethylene			3.77+0.02	295			120
n-Pentene-1			8.33+0.05	294			120
Ethylene			3.77+0.02	295			120
Tetramethylethylene			6.80+0.05	294			120

Free ion-yield for various liquids (eV)

Compound	$^{0}G_{fi}$(/100eV)	$^{E}G_{fi}$(/100eV)	E(V/cm)	T(K)	Radiation	ε (F/m)	Ref.
Methan(CH_4)	0.800			120			104
	0.8+0.1			120	HE X-Rays	1.670	104
	3.7(Tot.)			120			2,86
	0.940			298		1.440	40
Ethane(C_2H_6)	0.009			120			104
	0.013			148			104
	0.017			181			104
	0.060			120			104
	0.080			148			104
	0.130			183			104
	4(Tot.)			120			2,86
	0.13+0.1			183	HE X-Rays	1.800	104
Propane(C_3H_8)		0.026	2000-8000	123		2.050	35
		0.043	2000-8000	148		1.980	35
		0.076	2000-8000	183		1.900	35
		0.120	2000-8000	233		1.790	35
	4.1(Tot)			123		2.050	109
	0.023+0.005			123		2.050	27
	0.040+0.005			148		1.980	27
	0.075+0.005			183		1.900	27
	0.0143+0.005			233		1.790	27
	0.076+0.1			183	HE X-Rays	1.900	104
	0.026			120			104
	0.043			148			104
	0.076			183			104
	0.120			230			104
	4.1(Tot.)			120			2,86
	0.430			297			40
n-Butane(C_4H_{10})		0.120	2000-8000	148		2.070	35
		0.140	2000-8000	183		1.990	35
		0.220	2000-8000	233		1.870	35
		0.310	2000-8000	294		1.750	35
	4.2(Tot.)			148		2.070	109
	0.11+0.02			148		2.070	27
	0.13+0.01			183		1.990	27
	0.21+0.01			233		1.870	27
	0.31+0.01			294		1.750	27
	0.190			296	HE X-Rays	1.760	113
	0.190			295		1.770	40
	0.190			296		1.770	110
	0.190			298		1.760	40
	0.200			299		1.760	71
n-Pentane(C_5H_{12})		1.000	2000-8000	294		1.800	35
	4.3(Tot.)			294		1.800	27
	1.10+0.05			294		1.800	27
	0.120			293		1.840	135
	0.120			293		1.840	32
	0.150			293		1.840	111

Compound	$^{0}G_{fi}$(/100eV)	$^{E}G_{fi}$(/100eV)	E(V/cm)	T(K)	Radiation	ε (F/m)	Ref.
Continuous n-Pentane	0.145			296	HE X-Rays	1.842	113
	0.120			293	HE X-Rays		134
	0.1+25%			296	HE X-Rays		109
	0.145			296		1.842	110
	0.121			271		1.881	110
	0.153			296		1.842	110
	0.158			299		1.838	110
	0.168			306		1.826	110
	0.182			316		1.811	110
	0.202			329		1.791	11
	0.150			295		1.830	40
	0.150			296		1.830	110
n-Hexane(C_6H_{14})							
	0.120			rt	^{60}Co-γ		14
	0.120			296	2MeV-El.		16
	3.92(Tot.)			rt	^{60}Co-γ		141
	0.100			296	HE X-Rays	1.885	67
	0.110			293	HE X-Rays	1.885	134
	0.130			296	HE X-Rays	1.885	113
	0.130			296	HE X-Rays	1.885	69
	0.130			296	^{60}Co-γ		73
	0.130			293	^{60}Co-γ		145
	0.110			293		1.890	134
	0.110			293		1.890	32
	0.130			293		1.890	111
	0.100			296	^{39}Ar-β	1.885	65
	0.009+25%			296	LE X-Rays	1.885	109
	0.050			296	^{37}Ar-β	1.885	65
	0.04+0.01			296	^{3}T-β	1.885	68
	0.040			293	^{3}T-β	1.885	20
	0.008			293	^{239}Pu-α	1.885	19
	0.0058+0.0004			296	^{239}Pu-α	1.885	101
	0.130			296		1.885	113
	0.131			296		1.885	110
	0.138			297		1.884	110
	0.162			314		1.858	110
	0.168			319		1.850	110
	0.183			328		1.835	110
	0.195			333		1.827	110
	0.217			347.5		1.802	110
	0.226			352		1.794	110
	0.239			357		1.785	110
	0.248			363		1.774	110
	0.256			371		1.758	110
	0.140			295		1.890	40
	0.150			296		1.880	18
	0.130			296		1.880	110
	0.120			296+3		1.880	4,138
	0.180			319		1.850	40
	0.220			338		1.820	40
	0.230			343		1.810	40
	0.120			296			5

Compound	$^{0}G_{fi}$(/100eV)	$^{E}G_{fi}$(/100eV)	E(V/cm)	T(K)	Radiation	ε (F/m)	Ref.
Continuous n-Hexane		0.190	10000	296			58
		0.017	10000	296			19
n-Heptane(C_7H_{16})	0.130			295		1.920	40
	0.130			296		1.920	110
	0.170			319		1.890	40
	0.190			329		1.870	40
	0.200			338		1.860	40
	0.220			350		1.840	40
	0.230			359		1.830	40
	0.250			366		1.810	40
	0.260			372		1.800	40
n-Octane(C_8H_{18})	0.120			296	HE X-Rays	1.944	113
	0.124			296	HE X-Rays		110
	0.130			295		1.950	40
	0.130			296		1.950	110
	0.170			318		1.920	40
	0.200			341		1.880	40
	0.270			381		1.820	40
	0.310			400		1.800	40
n-Nonane(C_9H_{20})	0.120			296	HE X-Rays	1.968	113
	0.130			294		1.970	40
	0.120			296		1.970	110
	0.150			313		1.940	40
	0.190			341		1.900	40
	0.240			372		1.860	40
	0.310			406		1.810	40
	0.340			424		1.790	40
n-Decane($C_{10}H_{22}$)	0.120			296	HE X-Rays	1.987	113
	0.140			295		1.990	40
	0.120			296		1.990	110
	0.250			370		1.890	39
	0.400			453		1.770	39
n-Undecane($C_{11}H_{24}$)	0.130			296		2.000	40
	0.180			332		1.960	40
	0.200			352		1.930	40
	0.280			391		1.880	40
	0.350			431		1.830	40
	0.450			472		1.770	40
n-Dodecane($C_{12}H_{26}$)	0.0055+0.0001			296+2	^{210}Po-α		101
	0.120			295		2.010	40
	0.190			357		1.940	39
	0.280			425		1.850	39
n-Tetradecane	0.120			295		2.040	40
	0.120			296		2.040	110
	0.220			397		1.910	39
	0.420			506		1.790	39

Compound	$^{0}G_{fi}$(/100eV)	$^{E}G_{fi}$(/100eV)	E(V/cm)	T(K)	Radiation	ε (F/m)	Ref.
14-Dioxane	0.046			296	HE X-Rays	296.0	110
	0.460			296	HE X-Rays	2.212	113
	0.500			295	^{60}Co-γ	2.212	32
	0.038			296	HE X-Rays	2.212	31
Squalane	2.08(Tot.)			296	HE X-Rays	2.080	113
223-TMB(C_8H_{18})	0.290			296	HE X-Rays	1.926	113
2233-TMB(C_8H_{18})	0.800			379	HE X-Rays	1.840	28
2244-TMB(C_8H_{18})	0.800			379	HE X-Rays	1.840	28
TMP(C_8H_{18})	0.76+0.01			rt			30
	0.730			rt			6
	0.730			rt			106
	0.830			rt			28
	0.700			rt			42
	3.5(Tot.)			rt			30
	2.8(Tot.)			rt			59
2233-TMP(C_8H_{18})		0.440	1000	295			28
		0.480	1000	318			28
		0.540	1000	346			28
		0.620	1000	375			28
		0.830	1000	431			28
	0.380			273	HE X-Rays	2.080	28
	0.420			295	HE X-Rays	2.050	28
	0.460			318	HE X-Rays	2.010	28
	0.520			346	HE X-Rays	1.970	28
	0.600			375	HE X-Rays	1.930	28
	0.700			402	HE X-Rays	1.890	28
	0.810			431	HE X-Rays	1.840	28
2244-TMP(C_8H_{18})		0.860	590	295			28
		0.990	590	324			28
		1.220	590	385			28
		0.7360+0.0018	604	rt	150MeV/c π's		7
		0.7724+0.0016	1209	rt	150MeV/c π's		7
		0.7963+0.0020	1813	rt	150MeV/c π's		7
		0.8105+0.0021	2417	rt	150MeV/c π's		7
		0.8511+0.0031	3625	rt	150MeV/c π's		7
		0.7884+0.0021	604	rt	400MeV/c π's		7
		0.8201+0.0019	1209	rt	400MeV/c π's		7
		0.8495+0.0021	1813	rt	400MeV/c π's		7
		0.8696+0.0026	2417	rt	400MeV/c π's		7
		0.8923+0.0032	3021	rt	400MeV/c π's		7
		0.9135+0.0036	3625	rt	400MeV/c π's		7
		0.4189+0.0003	604	rt	400MeV/c p's		7
		0.4458+0.0004	1209	rt	400MeV/c p's		7
		0.4700+0.0005	1813	rt	400MeV/c p's		7

Compound	$^{0}G_{fi}$(/100eV)	$^{E}G_{fi}$(/100eV)	E(V/cm)	T(K)	Radiation	ε (F/m)	Ref.
Continuous 2244-TMP		0.4930+0.0006	2417	rt	400MeV/c p's		7
		0.5109+0.0007	3021	rt	400MeV/c p's		7
		0.5296+0.0008	3625	rt	400MeV/c p's		7
		1.100	10000	296			106
		0.025	10000	296			92
	0.730			296			5
	0.590			212	HE X-Rays	2.120	28
	0.950			229	HE X-Rays	2.090	28
	0.640			254	HE X-Rays	2.050	28
	0.830			295	HE X-Rays	1.980	28
	0.960			324	HE X-Rays	1.920	28
	1.190			385	HE X-Rays	1.800	28
	0.570			240			106
	0.620			272			106
	0.730			298			106
	0.960			346			106
	1.150			388			106
	1.390			427			106
	1.730			471			106
	2.100			500			106
	2.300			523			106
2-MP(Isobutane)C_4H_{10}	0.310			294	HE X-Rays	1.838	33
Isopentane	0.170			296	HE X-Rays	1.838	113,110
224-TMP(Isooctane)	0.360			rt	^{60}Co-γ		141
	0.210			296	2MeV-El.		15
	0.360			296	2MeV-El.		16
	0.390			296	2MeV-El.		17
	4.26(Tot.)			rt	^{60}Co-γ		141
	0.330			296	HE X-Rays	1.936	113
	0.350			rt	HE X-Rays	1.936	139
	0.11+25%			296	HE X-Rays	1.936	109
	0.0062+0.0001			296+2	^{210}Po-α		101
	0.332			296	HE X-Rays		110
	0.220			240			106
	0.330			299			106,110
	0.470			356			106
	0.670			408			106
	0.880			446			106
	1.080			481			106
	1.240			498			106
	1.410			519			106
	1.570			535			106
	1.700			544			106
	1.710			552			106
	0.330			296			5
	0.520		10000	296			58
	0.018		10000	296			92
234-TMP	0.170			296	HE X-Rays	1.969	113

Compound	$^{0}G_{fi}$(/100eV)	$^{E}G_{fi}$(/100eV)	E(V/cm)	T(K)	Radiation	ε (F/m)	Ref.
2266-TMP	0.470			293	HE X-Rays	1.970	28
2255-TMH$_p$($C_{11}H_{24}$)		0.680	340	293			28
		0.810	340	319			28
		0.980	340	353			28
		1.090	340	383			28
	0.670			293	HE X-Rays	1.970	28
	0.790			319	HE X-Rays	1.930	28
	0.960			353	HE X-Rays	1.890	28
	1.080			383	HE X-Rays	1.850	28
							28
2266-TMH$_p$($C_{11}H_{24}$)	0.470			293	HE X-Rays	1.970	28
	0.590			330	HE X-Rays	1.920	28
	0.700			358	HE X-Rays	1.880	28
	0.780			383	HE X-Rays	1.840	28
	0.920			428	HE X-Rays	1.780	28
	1.120			465	HE X-Rays	1.740	28
TMS($C_4H_{12}Si$)	0.61+0.01			rt			30
	0.740			rt			6
	0.590			rt			75,112
	0.740			rt			113
	0.510			rt			83
	0.600			rt			43
	0.590			rt			42
	0.650			rt			59
	0.740			296	HE X-Rays	1.840	113
	3(Tot.)			rt			30,59
	2.5(Tot)			rt			83
	0.470			294			41,110
	0.650			294			41
	0.740			296			5
		1.190	10000	296			58
		0.029	10000	296			92
22-DMP(Neopentane)C_5H_{12}		1.030	100	273			28
		1.100	100	294			28
		1.140	100	302			28
		1.190	100	312			28
		1.280	100	322			28
		1.800	10000	296			115
		0.036	10000	296			92
	0.810	0.860	100	rt		1.820	134
	1.100			296			5
	0.120			rt		1.820	32
	0.860			rt		1.280	111
	0.860			rt	HE X-Rays	1.777	113
	0.810			rt	HE X-Rays	1.777	134
	0.900			rt	HE X-Rays	1.777	135
	1.100			rt	HE X-Rays	1.777	28
	4.03+0.4(Tot.)			rt	HE X-Rays		115

Compound	$^{0}G_{fi}$(/100eV)	$^{E}G_{fi}$(/100eV)	E(V/cm)	T(K)	Radiation	ε (F/m)	Ref.
Continuous 22-DMP	0.857			296			110
	0.810			293			134
	0.580			293			134
	0.470			293			134
	1.020			273	HE X-Rays	1.840	28
	1.090			294	HE X-Rays	1.800	28
	1.130			302	HE X-Rays	1.780	28
	1.180			312	HE X-Rays	1.760	28
	1.270			322	HE X-Rays	1.740	28
	1.350			333	HE X-Rays	1.710	28
	0.1-0.15			rt			134
33-DMP	0.130			183			106
	0.210			233			106
	0.390			299			106
	0.610			357			106
	0.970			412			106
	1.130			442			106
	1.320			450			106
	1.750			480			106
	2.200			520			106
	2.400			536			106
	2.400			544			106
TMT	0.84+0.01			rt			30
	0.620			rt			113
	0.630			rt			42
	0.620			296	HE X-Rays	2.070	113
	3.9(Tot.)			rt			30
	4(Tot.)			rt			59
22-DMB(Neohexane)	0.400			293		1.870	134
	0.110			293		1.870	32
	0.300			293		1.870	111
	0.300			296	HE X-Rays	1.926	113
	0.400			293	HE X-Rays	1.870	134
	0.0063+0.0001			296+2	^{210}Po-α	1.870	101
	3.62+0.3(Tot.)			295	^{60}Co-γ	1.870	84
	0.304			296			110
	0.400			293			134
	0.200			293			134
	0.540			293			134
	0.300			296			5
		0.470	10000	296			58
		0.021	10000	296			92
23-DMB	0.190			296	HE X-Rays	1.926	113
	0.192			296			110
	0.180			300			106
	0.230			325			106
	0.360			375			106
	0.490			407			106

Compound	$^{0}G_{fi}$(/100eV)	^{E}Gfi(/100eV)	E(V/cm)	T(K)	Radiation	ε (F/m)	Ref.
Continuous 23-DMB	0.610			429			106
	0.720			443			106
	0.910			467			106
	1.030			479			106
	1.230			491			106
	1.420			500			106
	1.400			510			106
22-DMH	0.0061+0.0001			296+2	^{210}Po-α		101
Cyclohexane(C_6H_{12})	0.130			rt	^{60}Co-γ		141
	0.160			296	2MeV-El.		15
	0.130			296	2MeV-El.		16
	0.150			298	2MeV-El.		17
	0.14+0.002			298	^{60}Co-γ		108
	0.080			298	^{60}Co-γ		143
	0.120			293	^{60}Co-γ		79
		0.250	6700	294	^{60}Co-γ		28
		0.290	6700	315	^{60}Co-γ		28
		0.350	6700	340	^{60}Co-γ		28
		0.440	6700	380	^{60}Co-γ		28
		0.480	6700	395	^{60}Co-γ		28
	0.110			293		2.022	134
	0.110			293		2.022	32
	0.150			293		2.022	111
	0.150			296	HE X-Rays	2.022	113
	0.110			293	HE X-Rays	2.022	134
	0.06+25%			296			109
	0.148			296		2.022	110
	0.148			295.5		2.023	110
	0.149			296		2.022	110
	0.169			305		2.009	110
	0.166			307		2.005	110
	0.184			315		1.992	110
	0.195			322		1.981	110
	0.213			333		1.962	110
	0.233			339		1.950	110
	0.245			348		1.933	110
	0.153			354		1.922	110
	0.263			357		1.917	110
	0.279			368		1.896	110
	3.93(Tot.)			rt	^{60}Co-γ		141
	4.3(Tot.)			298	^{60}Co-γ		107
	4.6(Tot.)			298	^{60}Co-γ		129
	0.160			293	HE X-Rays	2.030	28
	0.180			306	HE X-Rays	2.010	28
	0.200			315	HE X-Rays	2.000	28
	0.230			325	HE X-Rays	1.980	28
	0.260			340	HE X-Rays	1.960	28
	0.300			360	HE X-Rays	1.920	28
	0.340			380	HE X-Rays	1.890	28
	0.370			395	HE X-Rays	1.860	28

Compound	$^{0}G_{fi}$(/100eV)	$^{E}G_{fi}$(/100eV)	E(V/cm)	T(K)	Radiation	ε (F/m)	Ref.
Cyclopropane	0.04+0.1			183	HE X-Rays	2.000	104
Cyclopentane	0.155			296	HE X-Rays	1.960	113
	4.400			298			130
Methylpentane	0.150			296	HE X-Rays	1.878	113
	0.0061+0.0001			296+2	^{210}Po-α	1.878	101
3-Methylpentane	0.150			296	HE X-Rays	1.901	113
	0.140			293	^{60}Co-γ	1.901	70
	0.146			296			110
	0.029			184			106
	0.045			217			69
	0.069			252			69
	0.150			299			69
	0.190			326			69
	0.330			382			69
	0.450			416			69
	0.630			444			69
	0.890			470			69
	1.070			488			69
	1.550			504			69
2-Methylheptane	0.0057+0.0001			296+2	^{210}Po-α		101
2-Methylhexane	0.006+0.0001			296+2	^{210}Po-α		101
Methylcyclopentane	4.2(Tot.)			298	^{60}Co-γ		129
HMDS	0.36+0.01			rt			30
	0.330			rt			59
	1.35(Tot.)			rt			30
	2.8(Tot.)			rt			59
2277-TMO	0.340			316	HE X-Rays	2.130	28
	0.500			348	HE X-Rays	2.020	28
	0.580			383	HE X-Rays	1.940	28
	0.750			423	HE X-Rays	1.840	28
n-Tetradecane	0.120			296	HE X-Rays	2.033	113
n-Hexadecane	0.110			rt	HE X-Rays		139
Ethene(C_2H_4)	0.009			120			104
	0.013			148			104
	0.017			181			104
	3.9(Tot.)			120			2,86
Propene(C_3H_6)	0.013			148			104
	0.040			183			104
	0.060			230			104
	4(Tot.)			148			2,86

Compound	$^{0}G_{fi}$(/100eV)	$^{E}G_{fi}$(/100eV)	E(V/cm)	T(K)	Radiation	ε (F/m)	Ref.
Butene-1(C_4H_8-1)	0.009			120			104
	0.019			148			104
	0.027			181			104
	0.054			230			104
	0.105			293			104
	0.027			183	HE X-Rays	2.310	104
	4.1(Tot.)			120			2,86
Hexene-1	0.062			296	HE X-Rays	2.046	113,110
Hexene-2	0.076			296	HE X-Rays	1.950	113
Benzene	0.055			298	2MeV-El.		17
	0.077			293	^{60}Co-γ		78
	0.053			296	HE X-Rays	2.278	113,110
	0.07+25%			296	HE X-Rays	2.278	109
t-Butylbenzene				296	HE X-Rays	2.380	113
Ethylene	0.017			183	HE X-Rays	1.750	104
Propylene	0.040			183	HE X-Rays	2.240	104
Heptene	0.080			rt	HE X-Rays		139
	0.130			296	HE X-Rays	1.926	113
Toluene	0.051			298	^{60}Co-γ		17
	0.068+7%			293	^{60}Co-γ	2.382	145
Cyclohexene	0.150			296	HE X-Rays	2.222	113
Ar	3.9+0.4(Tot.)			87	HE X-Rays		137
	4.4+0.4(Tot.)			87	HE X-Rays		77
	3.85(Tot.)			87	^{239}Pu-α		131
	2.300			296			132
	1.500			296			55
		4.400	10000	296			77
		4.150	10000	296			132
		0.460	10000	296			131
		0.450	10000	296			144
		0.380	10000	296			106
Carbondisulfide	0.260			298	^{60}Co-γ		16
	0.310			296	HE X-Rays	2.633	113
	0.35+8%			293	^{60}Co-γ	2.633	145
	4.16(Tot.)			rt	LE X-Rays		91
	0.150			296	LE X-Rays	2.440	113
	0.314			296	LE X-Rays		110
Carbontetrachloride	0.093			298	^{60}Co-γ		16
	0.096			296	HE X-Rays	2.232	113,110
	0.068			296	HE X-Rays	2.232	65

Compound	$^{0}G_{fi}$(/100eV)	$^{E}G_{fi}$(/100eV)	E(V/cm)	T(K)	Radiation	ε (F/m)	Ref.
Decalin	0.04+25%			293	LE X-Rays		109
33-DMB-1	0.170			296	HE X-Rays	1.950	113
Ethyl ether	0.350			296	HE X-Rays	4.280	113
	0.190			295	^{60}Co-γ	4.280	32
Isopropyl ethyer	0.305			296	HE X-Rays	3.916	113
n-Butylether	0.110			295	^{60}Co-γ	3.100	32
Diethyl ether	0.350			296	HE X-Rays		110
Isobutyl vinyl ether	0.140			298	HE X-Rays	3.400	52
HALIDES							
Perfluoro-n-Pentane	0.035			296	HE X-Rays	1.680	113
Perfluoromethylcyclo H	0.028			296	HE X-Rays	1.850	113
Germanium tetrachloride	0.130			296	HE X-Rays	2.435	113
	0.127			296	HE X-Rays		110
n-Butyle bromide	0.270			295	^{60}Co-γ	6.900	32
n-Butyle chloride	0.390			295	^{60}Co-γ	7.200	32
Triethylamine	0.150			296	HE X-Rays	2.440	113

References of appendix B

1- Adamczewski I., 1937, Ann. Phys. (Paris), **2**, 309.

2- Adler P.A. and Bothe H.K., 1965, Z. Naturforsch, **A20**, 1700.

3- Allen A.O. and Holroyd R.A., 1974, J. Chem. Phys., **78**, 796.

4- Allen A.O., 1976, Natl. Stand. Ref. Data Ser. Natl. Bur. Stand., Circ. **No. 57**, Nat. Bur. Stand. (Washington, D.C., USA).

5- Allen A.O., 1976, Natl. Stand. Ref. Data Ser. Natl. Bur. Stand., Circ. **No. 35**, Nat. Bur. Stand. (Washington, D.C., USA).

6- Allen A.O., 1976, Natl. Stand. Ref. Data Ser. Natl. Bur. Stand., Circ. **No. 58**, Nat. Bur. Stand. (Washington, D.C., USA).

7- Astbury A. et al., 1993, Nucl. Inst., **A324**, 461.

8- Aubert B. et al., 1992, Nucl. Inst., **A316**, 165

9- Bakale G. and Schmidt W.F., 1973, Chem. Phys. Lett., **22**, 164.

10- Bakale G. and Schmidt W.F., 1973, Naturfurch, **28A**, 511.

11- Bakale G. Tauchert W. and Schmidt W.F., 1975, J. Chem. Phys., **63**, 4470.

12- Bakale G. and Schmidt W.F., 1990, Chem. Phys. Lett., **175**, 319.

13- Baxendale J.H. Keen J.P. and Rasbury E.J., 1974, J. Chem. Soc. Faraday Trans I., **70**, 718.

14- Brushi L. Mazzi G. and Santint M., 1972, Phys. Rev. Lett., **28**, 1504.

15- Capellos C. Allen A.O., 1968, J. Phys. Chem., **72**, 4265.

16- Capellos C. Allen A.O., 1969, J. Phys. Chem., **73**, 3264.

17- Capellos C. and Allen A.O., 1970, J. Phys. Chem., **74**, 840.

18- Casanovas J. Grob R. Blanc D. Brunet G. and Mathieu J., 1975, J. Chem.Phys., **63**, 3673.

19- Chybick M., 1966, acta. Phys. Pol., **30**, 927.

20- Chybick M. Gzowski O., 1966, Z Phys.Chem. (Leipzig), **233**, 117.

21- Cipollini N.E. and Allen A.D., 1977, J. Chem. Phys., **67**, 131.

22- Classen N.V. and Schmidt W.F., 1969, Can. J. Chem., **47**, 4286.

23- Conrad E.E. and Allen A.O., 1969, J. Chem. Phys., **51**, 450.

24- Dael W.V. et al., 1966, Physica, **32**, 611.

25- Davis T. Rice S.A. and Meyer L., 1962, Phys. Rev. Lett., **9**, 81.

26- Davis T. Rice S.A. Fuochi P.G. and Freeman G.R., 1971, Can. J. Chem., **49**, 3657.

27- Dodelet J.P. Fuochi P.G. and Freeman G.R., 1972, Can. J. Chem., **50**, 1617.

28- Dodelet J.P. and Freeman G.R., 1972, Can. J. Chem., **50**, 2667.

29- Dodelet J.P. Shoinsaka K. and Freeman G.R., 1976, Can. J. Chem., **54**, 744.

30- Engler J. et al., 1993, Nucl.Inst., **A327**, 102.

31- Faidas H. Christophorou L.G. and McCorkle D.L., 1990, In: 10th international conference on conduction and breakdown in dielectric liquids., 34.

32- Freeman G.R. and Fayadh J.M., 1965, J. Chem. Phys., **43**, 86.

33- Fuchi P.G. and Freeman G.R., 1972, J. Chem. Phys., **56**, 2333.

34- Fulbright H.W., 1958, Hand buch der Physik (Springer, Berlin), **45**.

35- Gallant R.W., 1968, Physical Properties of hydrocarbons., **1** (Gulf Publishing Co., Houston, Texas,

36- Gee N. and Freeman W.F., 1980, Radiat. Phys. Chem., **15**, 267.

37- Gee N. and Freeman G.R., 1980, Phys. Rev., **A22**, 301.

38- Gee N. and Freeman G.R., 1983, J. Chem. Phys., **78**, 1951.

39- Gee N. and Freeman G.R., 1987, J. Chem. Phys., **86**, 5716.

40- Gee N. Senanayake P.C. and Freeman G.R., 1988, J. Chem. Phys., **89**, 3710.

41- Geer K. Holroyd R.A. and Ptohos F., 1991, Nucl. Inst., **A301**, 61.

42- Geer S. holroyd R.A. and ptohos F., 1990, Nucl. Inst., **A287**, 447.

43- Gettert M., 1988, diploma Thesis, Universitat Karlsruke,

44- Givernaud G. et al., 1992, Nucl. Inst., **A321**, 551.

45- Gruhn C.R. Edmiston M.D., 1978, Phys. Rev. Lett., 40, 407.

46- Gzowski O. and Terlecki J., 1959, Acta Phys. Pol., **18,** 191.

47- Gzowski O., 1962, Z. Phys .Chem. (Leipzig), **22**, 288.

48- Halpern B. Lekner J. Rice S.A. and Gomer R., 1967, Phys. Rev., **165**, 351.

49- Halpern B. Gomer R., 1969, J. Chem. Phys., **51**, 1031.

50- Halpern B. Gomer R., 1969, J. Chem. Phys., **51**, 1048.

51- Hand B., 1964, Nat. Bur. Stand., Circ. **No. 85**, (Int. Com. Rad. Units, Rep. 10b. (Washington, D.C., USA).

52 - Hayashi K. Okamura S. Polym J., 1971, Sci, Part A1, **9**, 2305.

53- Henson B.L., 1964, Phys. Rev., **A135**, 1002.

54- Hitachi A., 1993, Liquid Radiation Detectors. (Tokyo, Japan 1992). Nucl.Inst., **A327**, 11.

55- Holroyd R.A. and Allen M., 1971, J. Chem. Phys., **54**, 5014.

56- Holroyd R.A. Tames S. and Kennedy A.J., 1975, Phys. Chem., **79**, 2859.

57- Holroyd R.A. Tames S. and Kennedy A.J., 1975, Phys. Chem., **79**, 2857.

58- Holroyd R.A. and Anderson D.F., 1985, Nucl. Inst., **A236**, 295.

59- Holroyd R.A. Geer S. and Ptohos F., 1991, Phys. Rev., **B43**, 9003.

60- Holroyd R.A. and Schmidt W.F., 1992, Nucl. Inst, **A311**, 631.

61- Holroyd R.A. et al., 1992, Phys. Rev., **B45**, 3215.

62- Honda K. Endou H. Yamada K. Shinsaka K. Uhai M. Kouchi N. and Hatano Y., 1992, J.Chem. Phys., **97**, 2386.

63- Huang S.S.S. and Freeman G.R., 1978, J. Chem. Phys., **56**, 2388.

64- Huang S.S.S. and Freeman G.R., 1979, J. Chem. Phys., **70**, 1538.

65- Hummel A. Allen A.O. and Watson F.H., 1966, J. Chem. Phys., **44**, 3431.

66- Hummel A. and Allen A.O., 1966, J. Chem. Phys., **44**, 3436.

67- Hummel A. and Allen A.O., 1966, J. Chem. Phys., **44**, 3426.

68- Hummel A., 1967, Thesis, Free University of Amesterdam

69- Hummel A. and Allen A.O., 1967, J. Chem. Phys., **46**, 1602.

70- Hummel A., 1974, Rad. Res. Rev., **5**, 199.

71- IEEE, 1988, IEEE Trans. EI-Proc. 9th ICDL,

72- Itoh K. Munoz R.C. and Holroyd R.A., 1989, J. Chem. Phys., **90**, 1128.

73- Jahns A. and Jacobt W., 1966, Z. Naturforsch, **A21**, 1400.

74- Jamal M.A. and watt D.E., 1981, Radiation Effects, **54**, 51.

75- Jungblut H. and Schmidt W.H., 1985, Nucl. Inst., **A241**, 616.

76- Kimura T. and Freeman G.R., 1974, Can. J. Phys., **52**, 2220.

77- Klassen N.V. and Schmidt W.F., 1969, Can. J. Chem., **47**, 4286.

78- Kroh J. and Hankiewicz E., 1969, Int. J. Radiat. Phys. Chem., **1**, 451.

79- Kroh J. Karolczak S. and Zegota H., 1970, Proc. Int. Conger, Radiat.Res., 14th, Evian.

80- Lamp L. et al., 1990, In: 10th international conference on conduction and breakdown in dielectric liquids., 39.

81- Leblanc O.H., 1959, J. Chem. Phys., **30**, 1443.

82- Lin C.C. and Aziz R.A., 1967, Can. J. Phys., **45**, 1275.

83- Lopes M.A. Masuda K. and doke T., 1988, Nucl. Inst, **A271**, 464.

84- Mathieu J., 1968, Etude Physico-Chimique de la Conduction induite par les rayonnem ents nucleaires dans les liquides dielectriques., Thesis Universit de Toulouse.

85- Meisel G.G., 1964, J. Chem. Phys., **41**, 51.

86- Miller L.S. Howe S. and Spear W.F., 1968, Phys. Rev., **166**, 871.

87- Minday R.M. Schmidt L.S. and Davis H.T., 1969, J. Chem. Phys., **50**, 1473.

88- Minday R.M. Schmidt L.S. and Davis H.T., 1971, J. Chem. Phys., **54**, 3112.

89- Minday R.M. Schmidt L.S. and Davis H.T., 1972, J. Phys. Chem., **76**, 442.

90- Miyajima M. Sasaki S. and Shibamura E., 1992, Nucl. Inst., **B63**, 297.

91- Mohler F.L. Taylor L.S., 1943, Nat. Bur. Stand., **13**, 659.

92- Munoz R.C. and Ascarelli G., 1983, Chem. Phys. Lett, **94**, 235.

93- Munoz R.C. Holroyd R.A. and Nishikawa M., 1985, J. Phys. Chem., **89**, 2969.

94- Munoz R.C. and Holroyd R.A., 1986, J. Chem. Phys., **84**, 5810.

95- Munoz R.C. et al., 1987, J. Phy. Chem., **91**, 4639.

96- Nakamura Y. Shinsaka K. and Hatano Y., 1983, J. Chem. Phys., **78**, 5820.

97- Namba H. Shinsaka H. and Hatano Y., 1979, J. Chem. Phys., **70**, 5331.

98- Nyikes L. Zador E. and Schiller R., 1976, 4th. Symosium on Rad. Chem., 179.

99- Plenkiewicz B. Plenkiewicz P. and Jaygerin J.P., 1989, Phys. Rev., **A40**, 4113.

100- Port, 1991, CERN Report PPE/91-224.

101- Ramy J.P., 1971, Thesis University of Tolouse,

102- Reiss K.H., 1937, Ann. Phys. (Leipzing), **28**, 325.

103- Rice S.A., 1968, Accounts Chem. Res., **1**, 81.

104- Robinson M.G. Fuochi P.G. Freeman G.R., 1971, Can. J. Chem., **49**, 3657.

105- Robinson M.G. Freeman G.R., 1974, Can. J. Chem., **52**, 440.

106- Ryan F.G. and Freeman G.R., 1978, J. Chem. Phys., **68**, 5144.

107- Saki Y. Schmidt W.F. and Khrapak A., 1992, Chem. Phys., **164**, 139.

108- Sarget N.H. Reid J.A. and Robinson R.W., 1969, Can. J. Chem., 2655.

109- Schmidt W.F., 1968, Z. Naturforsch, **B23**, 126.

110- Schmidt W.F. Allen A.O., 1968, J. Chem. Phys., **72**, 3730.

111- Schmidt W.F. Allen A.O., 1968, Science, **160**, 301.

112- Schmidt W.F Allen A.O., 1969, Chem. Phys., **50**, 5037.

113- Schmidt W.F. Allen A.O., 1970, J. Chem. Phys., **52**, 2345.

114- Schmidt W.F. and Allen A.O., 1970, Chem. Phys., **52**, 4788.

115- Schmidt W.F., 1970, Radiat. Res., **42**, 73.

116- Schmidt W.F. and Bakale G., 1972, Chem. Phys. Lett., **17**, 617.

117- Schmidt W.F. Bakale G. and Sawada U., 1974, J. Chem. Phys., **61**, 5275.

118- Schmidt W.F., 1977, Can. J. Chem., **55**, 2197.

119- Schmidt W.F., 1979, In: charge storage, charge transport and electrostatic with trheir application., eds., Y.Wada, Perlman, M.M., and Koado, H. (Elsevier, Amsterdam, Oxford-New York).

120- Schmidt W.F., 1984, IEEE Trans. Electr. Insul. (Compilation), **EI-19**, 389.

121- Schmidt W.F., 1993, Nucl. Inst., **A327**, 83.

122- Schnyders H. Rice S.A. and Meyer A., 1965, Phys. Rev. Lett., **15**, 187.

123- Schnyders H. Rice S.A. and Meyer L., 1966, Phys. Rev., **150**, 127.

124- Shibamura E. et al., 1975, Nucl. Inst., **131**, 294.

125- Shinsaka K. Codama M. Srithanratana T. Yamamoto M. and Hatano Y., 1988, J. Chem. Phys., **88**, 7529.

126- Shinsaka K. Codama M. Serizawa K. and Hatano Y., 1989, Radiat. Phys. Chem., **34**, 519.

127- Shinsaka K. et al., 1993, Nucl. Inst., **A327**, 15.

128- Shinsaka K. and Hatano Y., 1988, In proceeding of the third workshop on radiation detector and their uses., 80.

129- Sowada U., 1976, Thesis (Free university of Berlin, Germany),

130- Stover E.D and Freeman G.R., 1968, Can. J. Chem., **46**, 2109.

131- Swan D.W., 1965, Proc. Phys. Soc. London, **85**, 1297.

132- Takahashi T. et al., 1980, Sci. Papers Ins. Phys. Chem. Res., **74**, 65.

133- Takeda S.S. et al., 1971, J. Chem. Phys., **54**, 3195.

134- Tewari P.H. Freeman G.R., 1968, J. Chem. Phys., **49**, 4394.

135- Tewari P.H. Freeman G.R., 1969, J. Chem. Phy., **51**, 1276.

136- Thomson J.J., 1934, (Cited by Mohler and Taylor, NAt. Bur. Stand., **13**, 659).

137- Ullmair H.A., 1966, Phys. Med. **Biol.**, **11**, 95.

138- Van den Ende C.A.M. Warman J.M. and Hummel A., 1984, Radiat. Phys. Chem., **23**, 55.

139- Vannikov A.V. Kovalev J.O. and Zolotarevski, 1971, Khim, Vys. Energy., **5**, 49.

140- Wada T. Shinsaka K. Namba H. and Hatano Y., 1977, Can. J. Chem., **55**, 2144.

141- Warman J.M. and Rzad S.J., 1970, J. Chem. Phys., **52**, 485.

142- Wickman G. Nystrom H., 1992, Phys. Med. Bio., **37**, 1789.

143- Williams F. and Amer J., 1964, Chem. Soc., **86**, 3954.

144- Willis W.J. and Edmiston M.D., 1978, Phys. Rev. Lett., **47**, 407...

145- Wrst H., 1971, Diplomrbeit, Hahn Meitner Institut,

146- Yoshino K. Sowada K. and Schmidt W.F., 1976, Phys. Rev., **A4**, 438.

147- Zessoules N. Brinkerhoff J. and Thomas A., 1963, J. Appl. Phys., **34**, 2010.

References of the thesis

[Ada] Adamczewski I., 1939, Acta Physica Polnica., **8**, 31.

[Ada] Adamczewski I., 1961, Proc. Symp. on selected topics in radiation dosimetry. 191.

[Ada] Adamczewski I., 1964, Sur le mecamisme de ionization et de la conducibilitie electrique dans les liquides dielectriques. PWN Ed. Sci. de Pologne.

[Ada] Adamczewski I., 1965, Induced conduction in dielectric liquids. Brit. J. Appl. Phys. , **16**, 759.

[Ada] Adamczewski I., 1969, Ionization, conductivity and break down in di-electric liquids. Taylor and Francis Ltd. (London). E.C.4.

[Apr] Aprile E., Bolotnikov A., Chen D., and Mukherjee R., 1993, Ionization of liquid krypton by electrons, gamma rays and alpha particles. Nucl. Inst., **A327**, 25.

[Ast] Astbury A., Fincke-Keeler M., Keeler R.K., Poffengerger P.R., Robertson L.P., Rosvick M., and Schenk P., 1993, Saturation of ion yield in 2,2,4,4 tetramethylpentane for non-relativistic particles. Nucl. Inst., **A324**, 461.

[Aub] Aubert B. et al., 1992, A search for materials compatible with warm liquids. Nucl.Inst., **A316**, 165.

[Bak] Bakale G., and Schmidt W.F., 1973, Z. Natureforsch. Teil A, **28**, 511.

[Bak] Bakale G., Tauchert W., and Schmidt W.F., 1975, Electron transport in mixture of liquid methane and ethane. J. Chem. Phys., **63**, 4470.

[Bak] Baker E.B., and Boltz H.A., 1937, Thermionic emission into dielectric liquids.

Phys. Rev., **51**, 275.

[Bar] Bartczak W.M. and Hummel A., 1986, Computer simulation of ion recombination in irradiated nonpolar liquids. J. Radioanal. Nucl. Chem., **101**, 299.

[Bel] Belevtsev A.A., 1990, Theoretical study of electron transport in non-polar liquids. In: 10th international conference on conduction and breakdown in di-electric liquids., 56.

[Ben] Benetti P., et.al., 1993, Detection of energy deposition down to the keV region using liquid xenon scintillation. Nucl. Inst., **A327**, 203.

[Bla] Blance D., Mathieu J., and Boyer J., 1961, Use of an ionization chamber filled with a dielectric liquid at room temperature. Nuovo. Cim., **19**, 929.

[Bla] Blance D., Mathieu. J., and Torres L., 1964, Nucl.Inst., **27**, 353.

[Bla] Bland C.J., 1984, Tables of the geometrical factor for various source-detector configurations. Nucl.Inst., **223**, 602.

[Bor] Borghesani A.F., and Santini M., 1994, Excess electron localization in high-density neon gas. In: linking the gaseous and the condenced phases of matter. Eds. Christophorou L.G. Illenberger E. and Schmidt W.F., **326**, 281, Plenum press, New York.

[Bra] Bragg W.H., and Kleeman R.D., 1906, Recombination of ions. Philos. Mag., **11**, 466.

[Car] Carugno G., Colautti P., and Tornielli G., 1991, Liquid dosimetry in gamma-neutron mixed fields. Proceeding of the 6th conference of italian association of medical biophysics. Topic in biomed. phys., 421.

[Cha] Charalambus S., 1967, The response of a liquids ionization chamber to gamma

radiation and to high energy neutrons and protons. Nucl. Inst., **48**, 181.

[Cha] Charalambus S., 1967, The response of a liquid ionization chamber to gamma radiation and to high-energy neutrons and protons. Nucl. Inst., **48**, 181.

[Cho] Choi H.T., Sehi D.S., and Braun C.L., 1982, Geminate charge recombination in the photo ionization N,N,N,N-tetramethyl-p-pheny-enediamnie (TMPD) in various solvents. J. Chem. Phys., **77**, 6027.

[Chr] Christophorou L.G., 1994, The slow electron and its interactions. In: linking the gaseous and the condenced phases of matter. Eds. Christophorou L.G. Illenberger E. and Schmidt W.F., 326, Plenum press, New York.

[Chu] Chu J. CH., Grant W.H., and Almond P.R., 1980, A liquid ionization chamber for neutron dosimetry. Phys. Med. Biol., **25**, 1133.

[Cip] Cipollini N. E. and Allen A.O., 1977, Electron mobilities in liquid tetramethylsilane at temperature up to the critical point. J. Chem. Phys., **67**, 131.

[Coh] Cohen M.H. Lekner J., 1967, Theory of hot electrons in gases, liquids, and solids. Phys. Rev., 158, 305.

[Con] Conrad E. E. and Silver J., 1969, Short lived transient species in irradiated n-hexane. J. Chem. Phys., **51**, 450L.

[Cur] Curie P., 1902, Conductivity produced in dielectric liquids by the rays from radium. Comptes Rendus. Acad. Sci. Paris., **134**, 420.

[Dar] Darveniza M., and Tropper H., 1961, Electrical properties of organic insulating liquids containing fluorescent solutes. Proc. Phys. Soc., **78**, 854.

[Dav] Davis H.T., Schmidt L.D., and Minday R.M., 1971, Kinetic theory of excess electrons in polyatomic gases, liquids, and solids. Phys. Rev., **A3**, 1027.

[Den] Denat A., Gosse J.P., and Gosse B., 1987, Conduction du cyclohexane tres pur en geometric point-plan. Rev. Phys. Appl., **22**, 1103.

[Dod] Dodelet J.P., and Freeman G.R., 1971, Kinetics of charge scavenging in γ-irradiated liquid cyclohexane:a comparison between different ion electron spacial distribution functions used with two diffusion approximations. Can. J. Chem., **49**, 2643.

[Dod] Dodelet J.P., and Freeman G.R., 1972, Mobilities and ranges of electrons in liquids: effect of molecular structure in C_5-C_{12} alkanes. Can. J. Chem., **50**, 2667.

[Dod] Dodelet J.P., Fuochi P.G., and Freeman G.R., 1972, Effect of electric field strength on the free ion yields in the X-radiolysis of liquids: influence of molecular structure and temperature. Can. J. Chem., **50**, 1617.

[Dod] Dodelet J.P., Shinsaka K., and Freeman G.R., 1975, On electron mobility models for liquid hydrocarbons. J.Chem. Phys., **63**, 2765.

[Dor] Dornte R.W., 1939, The dielectric strength of benzene and heptane. J. Appl. phys., **10**, 514.

[Dor] Dornte R.W., 1940, Ind. Ing. Chem., **32**, 1529.

[Duh] Duhm H.H., Fedder I., and Schiffmann K., 1989, The response of a single gap TMS ionization chamber to 8-23 MeV protons at different angles and to electrons of a ^{207}Bi source. Nucl. Inst., **277A**, 565.

[Eib] Eibl R., Lamp P., and Buschhorn G., 1990, Measurement of electron mobility in liquid and critical argon at low electric field strengths. Phys. Rev., **B42**, 4356.

[Fai] Faidas H., Christophorou L.G., and McCorkle D.L., 1990, Electron transport

in fast di-electric liquid at high applied electric fields. In: 10th international conference on conduction and breakdown in di-electric liquids., 34.

[For] Forster E.O., 1962, Electric conduction in Liquid Hydrocarbons. (I) Benzene. J. Chem. Phys., 37, 1021.

[Fre] Freeman G.R., and Fayadh J.M., 1965, Influence of di-electric constant on the yield of free ions produced during radiolysis of a liquid. J. Chem. Phys., **43**, 86.

[Fuh] Fuhr J., and Schmidt.W.F., 1986, Spar breakdown of liquid hydrocarbons. II. Temperature development of the electric spark resistance in n-pentane, n-hexane, 2,2 dimethylbutane, and n-decane. J. Appl. Phys., **59**, 3702.

[Gee] Gee N., Senanayake. P.C., and Freeman G.R., 1988, Electron mobility, free ion yields, and electron thermalization distances in n-alkane liquids: effect of chain length. J. Chem. Phys., **89**, 3710.

[Gio] Giova A., Ladu M., and pelliccioni M., 1967, Study of the Recombination in hexane ionization chambers irradiated with gamma rays. Nucl. Inst., **57**, 77.

[Giv] Givernaud A., Gonidec A., Maurin G., Placci A., Radermacher E., Schizel D., and Schmidt W.F., 1992, Effect of γ-irradiation on the electron lifetime and positive ion mobility in TMS and TMP. Nucl. Inst., **A321**, 551.

[Gre] Green W.B., 1956, Controlled field emission in hexane. J. App. Phys., **27**, 921.

[Gzo] Gzowski O., Terlecki J., 1959, A method for measuring the mobility of ions in di-electric liquids. Acta Physica Polonica., **XVIII**, 191.

[Hai] Haidara M., and Denat A., 1990, Electron multiplication in liquid cyclohexane and propane: an estimation of the ionization coefficient. In: 10th international conference on conduction and breakdown in di-electric liquids., 397.

[Hol] Holroyd R.A., 1972, Energy of excess electrons in non-polar liquids by photoelectric work function measurements. J. Chem. Phys., **54**, 5014.

[Hol] Holroyd R.A., and Tauchert W., 1974, On the relation of the electron mobility to the conduction state energy in non-polar liquids. J. Chem. Phys., **60**, 3715.

[Hol] Horoyd R.A., Gangwer T.E., and Allen A.O., 1975, Chemical reaction rates 6 quasi-free electrons in non-polar liquids. Chem. Phys. Lett., **31**, 520.

[Hol] Holroyd R.A., and Anderson D.F., 1985, The physics and chemistry of room temperature liquid-field ionization chambers. Nucl. Inst., **A236**, 294.

[Hol] Holroyd R.A., and Sham T.K., 1985, Ion yields in hydrocarbon liquids exposed to X-rays of 5-30 keV energy. J. Phys. Chem., **89**, 2909.

[Hou] House H., 1957, High field conduction currents in hexane. Proc. Phys. Soc. Lond., B70, 913.

[Hua] Huang S.S., and Freeman G.R., 1978, Electron mobilities in gaseous, critical, and liquid xenon: density, electric field, and temperature effects: quasilocalization. J. Chem. Phys., **68**, 1355.

[Hum] Hummel A., and Allen A.O., 1966, Ionization of liquids by radiation. (I) Method for determination of ion mobilities and ion yields at low voltage. J. Chem. Phys., 44, 3426.

[Hum] Hummel A., 1974, Ionization of dielectric liquids by high energy radiation studied by means of electrical conductivity methods. Rad. Res. Rev., **5**, 199.

[Hut] Hutton A.M., 1972, Study of transient conductivity induced in irradiated aqueous solutions using a high voltage pulse. Radiat. phys. Chem., **4**, 479.

[ICR] ICRU, 1989, International commission on radiation units and measurements. Tissue substitutes in radiation dosimetry and measurement, ICRU Report **44**.

[Jaf] Jaffe G., 1908, Ionization of liquid dielectric through radium rays. Ann. d. Physik., **25**, 257.

[Jef] Jaffe G., 1913, Ann.Phys., **42**, 303.

[Jam] Jamal M.A., and Watt D.E., 1981, Novel extension of the trap model for electrons in liquid hydrocarbons. Radiation Effects., **54**, 51.

[Jan] Januszajtis A., 1963, Dependence of ionization in saturated hydrocarbon liquids on radiation energy. Acta physica polonica., **XXIV**, 809.

[Joh] Johansson B., and Wickman G., 1997, General collection efficiency for liquid isooctane isooctane and tetramethylsilane used as sensitive media in a parallel-plate ionisation chamber. Phys. Med. Biol., **42**, 133.

[Kan] Kaneko K., Usami Y., and Kitahara K., 1988, Gas kinetic approach for electron mobility in dense media. J. Chem. Phys., **89**, 6420.

[Kao] Kao K.C., and Calderwood J.H., 1965, Effect of hydrostatic pressure, temperature and impurity on electric conduction in liquid di-electrics. proc. I.E.E., **112**, 597.

[Kes] Kestner N.R. and Jortner J., 1973, Conjecture on electron mobility in liquid hydrocarbons. J. Chem. Phys., **59**, 26.

[Khr] Khrapak A.G., Sakai Y., Bottcher E.H., and Schmidt W.F., 1990, Stability of electron bubbles in liquid neon. In: 10th international conference on conduction and breakdown in di-electric liquids., 61.

[Kno] Knoll, Radiation detection and measurement.

[Kra] Kramer H.A., 1952, On a modification of Jaffe's theory of columnar ionization. Physica, **18**, 665.

[Kra] Krasucki Z., 1963, In: Conference on electronic processes in di-electric liquid.

Brit. J. Appl. Phys., **14**, 469.

[Lad] Ladu M., and Pelliccioni M., 1966, The liquid dielectric ionization chamber as a means to study mixed radiation fields. Nucl. Inst., **39**, 339.

[Lad] Ladu M., and Pelliccioni M., 1967, Use of ionization chambers filled with a dielectric liquid in radiation dosimetry. Nucl. Inst., **53**, 35.

[Lad] Ladu M., Pelliccioni M., and Roccella M., 1967, Determination of the quality factor in a mixed field of gamma-rays and neutrons by an ionization chamber filled with a dielectric liquid, II. Nucl. Inst., **53**, 71.

[Lam] Lamp P., Eibl R., and Buschhorn G., 1990, Measurement of electron mobility in liquid and gaseous argon at low electric field strengths and in the critical region. In: 10th international conference on conduction and breakdown in di-electric liquids., 39.

[Lea] Lea D.E., and Chadwick J., 1934, Attemp to detect a neutral particle of small mass. Proc. Camb. Phil. Soc., **30**, 59.

[Lek] Lekner J., 1967, Motion of electrons in liquid argon. Phys. Rev., **158**, 130.

[Lep] Le Page W.R., and Dubridge L.A., 1940, Electron emission into dielectric liquids. Phys. Rev., **58**, 61.

[Mat] Mathieu J., 1967, J. Chem. Phys., **64**, 1679.

[Mey] Meyer L., and Reif F., 1958, Mobilities of He ions in liquid helium. Phys. Rev., **110**, 279.

[Mey] Meyer L., Davis H.T., Rice S.A., and Donnelly R.J., 1962, Mobility of ions in liquid He I and as a function of pressure and temperature. Phys. Rev., **126**, 1927.

[Mil] Miller L.S., Howe S., and Spear W.E., 1968, Charge transport in solid and

liquid Ar, Kr, and Xe. Phys. Rev., **166**, 871.

[Min] Minday R.M., Schmidt W.F., and Davis H.T., 1969, Free electron in liquid hexane. Chem. Phys., **50**, 1473.

[Min] Minday R.M., Schmidt L.D., and Davis H.T., 1971a, Excess electrons in liquid hydrocarbons. J. Chem. Phys., **54**, 3112.

[Min] Minday R.M., Schmidt L.D., and Davis H.T., Mechanism of excess electron transport in liquid hydrocarbons., 1971b, Phys. Rev. Lett., **26**, 360.

[Min] Minday R.M., Schmidt L.D., and Davis H.T., 1972, Mobility of excess electrons in liquid hydrocarbon mixtures. J. Phys. Chem., **76**, 442.

[Moh] Mohler, F.L., and Taylor L.S., 1934, Ionization of liquid carbon disulphide by X-rays. J. Res. Nat. Bur. Stand., **13**, 659.

[Moz] Mozumder A., 1974a, Effect of an external electric field on the yield of free ions. (I) General results from the Onsager theory. J. Chem. Phys., **60**, 4300.

[Moz] Mozumder A., 1974b, Effect of an external electric field on the yield of free ions. (II) The initial distribution of ion pairs in liquid hydrocarbons. J. Chem. Phys., **60**, 4305.

[Moz] Mozumder A., and Magee J.L., 1967, Theory of radiation chemistry. Ionization of non-polar liquids by radiation in the absence of external electric field. J. Chem. Phys., 47, 939.

[Mun] Munoz R.C., Cumming J.B., and Holroyd R.A., 1986, Ionization of liquid hydrocarbons and tetramethylsilane by ^{241}Am alpha particles. J. Chem. Phys., **85**, 1104.

[Nak] Nakamura Y., Namba H., Shinsaka K., and Hatano Y., 1980, Electron mobility in solid TMS: effect of liquid-solid phase change. Chem. Phys. Lett., **76**, 311.

[Nak] Nakamura Y. et al., 1983, In: Proceeding of 26th symp. on radiation chemistry. Osaka., 48.

[Nak] Nakamura Y., Shinsaka K., and Hatano Y., 1983, Electron mobilities and electron-ion recombination rate constants in solid, liquid, and gaseous methane. J. Chem. Phys., 78, 5820.

[Nam] Namba H., Shinsaka K., and Hatano Y., 1979, Effect of n-butane impurity on electron mobility and electron-ion recombination rate constant in solid neopentane. J. Chem. Phys., **70**, 5331.

[Nik] Nikuradse A., 1932, Phys., **Z33**, 552.

[Nyi] Nyikos L., and Schiller R., 1975, Electron mobility and conduction state energy in hydrocarbon mixtures. Chem. Phys. Lett., **34**, 128.

[Oli] Oliver H., and Leblanc J.R., 1959, Electron drift mobility in liquid n-hexane. J. Chem. Phys., 30, 1443.

[Ons] Onseger L., 1938, Initial recombination of ions. Phys. Rev., **54**, 554.

[Ore] Ore A., and Larsen A., 1964, Radiat. Res., **21**, 331.

[Pao] Pao C.S., 1943, Conduction of electricity in high insulating liquids. Phys. Rev., **64**, 60.

[Pis] Pisarev A.F., Pisarev V.F., Revenko G.S., 1973, Soviet Phys. JETP., **36**, 828.

[Plu] Plumley H.J., 1941, Conduction of electricity by di-electric liquids at high field strengths. Phys. Rev., **59**, 200.

[Pof] Poffenberger P.R., et.al., 1993, Electron mobility and saturation of ion yield in 2,2,4,4 TMP. Nucl. Inst., **A327**, 99.

[Pre] Prewett P., 1997, Making microtips. The newsletter of the central laboratory of the research councils.

[Rao] Rao B.N., Bush R.L., and Funabashi K., 1977, Field dependent electron mobility in methane-ethane liquid mixtures. Can. J. Chem., **55**, 1952.

[Rei] Reif F., and Meyer L., 1960, Study of superfluidity in liquid He by ion motion. Phys. Rev., **119**, 1164.

[Rei] Reiss K., 1937, Ann. Phys., 325.

[Ric] Rice S.A., and Choi C.L., 1962, Phys. Rev., **8**, 410.

[Rob] Robinson M.G., and Fuochi G.R., 1974, Electron mobilities and ranges in the liquid C_1-C_3 hydrocarbons and in Xenon: effect of temperature and field strength. Can J.Chem., **52**, 440.

[Rob] Robinson M.G., Fuochi P.G., and Freeman G.R., 1971, Yields of free ions in the X radiolysis of some simple saturated and unsaturated hydrocarbon liquids: effects of molecular structure and temperature. Can. J. Chem., **49**, 3657.

[Rog] Rogozinski A., 1941, Determination of the residual current of an ionization chamber and the true conductivity of dielectric liquids. Phys. Rev., **60**, 148.

[Rya] Ryan T.G., Freeman G.R., 1978, Electron mobilities and ranges in methyl substituted pentane through the liquid and critical regions. J. Chem. Phys., **68**, 5144.

[Sak] Sakai Y., Schmidt W.F., and Khrapak A., 1992, High and low mobility electrons in liquid neon. J. Chem. Phys., **164**, 139.

[Sak] Sakai Y., Ando T., Kimura K., and Tagashira H., 1993, Excess electrons in N2/Ar liquid mixtures. Nucl. Inst., **A327**, 92.

[Sca] Scalettar R.T., Doe P.J., Mahler H.J., Chen H.H., 1982, Critical test ofgeminate recombination in liquid argon. Phys. Rev., **A25**, 2419.

[Sch] Schiller R., 1972, Localization probability and mobility of electrons in liquid

hydrocarbons. J. Chem. Phys., **57**, 2222.

[Sch] Schiller R., Vertes A., and Nyikos L., 1982, Qussipercolation: charge transport in fluctuating systems. J. Chem. Phys., **76**, 678.

[Sch] Schiller R., 1990, Ion-electron pairs in condenced media treated as H-like atoms. J. Chem. Phys., **92**, 5527.

[Sch] Schiller R., 1992, Energy distribution of low-energy electrons and free-ion yields in irradiated liquid hydrocarbons. J. Chem. Phys., **96**, 6531.

[Sch] Schiller R., 1993, Ion-electron recombination in pairs; critical appraisal of theory. Nucl.Inst., **A327**, 37.

[Sch] Schmidt W.F., and Allen A.O., 1968, Yields of free ions in irradiated liquids; determination by a clearing field. J. Phys. Chem., **72**, 3730.

[Sch] Schmidt W.F., and Allen A.O., 1969, Mobility of free electrons in dielectric liquids. J. Chem. Phys., **50**, 5037.

[Sch] Schmidt W.F., and Allen A.O., 1970a, Mobility of elctrons in dielectric liquids. J. Chem. Phys., **52**, 4788.

[Sch] Schmidt W.F., and Allen A.O., 1970b, Free ion yield in sundry irradiated liquids. J. Chem. Phys., **52**, 2345.

[Sch] Schmidt W.F., 1970, Radiat. Res., **42**, 73.

[Sch] Schmidt W.F., Bakale G., and Sowada U., 1974, Excess electrons and charge carriers in liquid ethane. J. Chem. Phys., **61**, 5275.

[Sch] Schmidt W.F., 1977, Electron mobility in non-polar liquids. The effect of molecular structure, temperature, and electric field. Can. J. Chem., **55**, 2197.

[Sch] Schmidt W.F., 1993, Charge carrier energetics and dynamics in non-polar liquids. Nucl.Inst., **A327**, 83.

[Sch] Schmidt W.F., Sakai Y., and Khrapak A.G., 1993, Self-trapping kinetics of electrons in liquid neon. Nucl.Inst., **A327**, 87.

[Sch] Schnyders H., Rice S.A., and Meyer L., 1966, Electron drift velocities in liquefied argon and krypton at low electric field strengths. Phys. Rev., **150**, 127.

[Shi] Shinsaka K., and Hatano Y., 1988, Free-ion yields, electron mobilities, and electron-ion recombination rate constants in liquid tetramethylsilane and argon. In: Proceeding of the third workshop on radiation detectors and their uses., 80.

[Shi] Shinsaka K., Codama M., Srithanratana T., Yamamoto M., and Hatano Y., 1988, Electron-ion recombination rate constants in gaseous, liquid, and solid argon. J. Chem. Phys., **88**, 7529.

[Shi] Shinsaka K., et.al., 1993, Free-ion yield, electron mobilities, and electron-ion recombination coefficient in liquid tetramethylsilane. Nucl. Inst., **A327**, 15.

[Sut] Sutton L.E., 1946, Applications, including liquid systems, on the application of di-electric measurements to chemistry. Trans. Faraday Soc., **42A.**, 170.

[Tac] Tachiya M., 1988a, Radiat. Phys. Chem., **32**, 37.

[Tac] Tachiya M., 1988b, Breakdown of the Onsager theory of geminate ion recombination. J. Chem. Phys., **89**, 6929.

[Tac] Tachiya M., and Shmidt W.F., 1989, Escape probability of geminate electron-ion recombination in the limit of large electron mean free path. J. Chem. Phys., **90**, 2471.

[Ter] Terleki J., 1966, Measurements of ionisation currents in hexane at high electric fields. Acta Physica Polonica, **XXIX**, 743.

[Tew] Tewari P.H., and Freeman G.R., 1968, Dependence of radiation-induced

conductance of liquid hydrocarbons on molecular structure. J. Chem. Phys., **49**, 4394.

[Tho] Thomson J.J., and Rutherford E., 1896, On the passage of electricity through gases exposed to roentgen rays. Philos. Mag., **42**, 392.

[Tho] Thomson J.J., 1897, Nature, **55**, 606.

[Tho] Thomson J.J., 1899, On the theory of the conduction of electricity through gases by ions. Philos. Mag., **47**, 253.

[Wad] Wada T., Shimsaka K., Namba H., and Hatano Y., 1977, Electron reactivity in liquid hydrocarbon mixtures. Can. J. Chem., **55**, 2144.

[Wat] Watson P.K., and Sharbaugh A.H., 1960, High-field conduction currents in liquid n-hexane under microsecond pules conduction. Electr.chem. Soc., **107**, 516.

[Wat] Watt D.E., 1985, Identification of biophysical mechanisms of damage by ionizing radiation. Radiation protection dosimetry., **13**, 285.

[Watt] Watt D.E., 1997, A unified system of radiation bio-effectiveness and its consequences in practical applications. Radiation protection dosimetry., **70**, 529.

[Wic] Wickman W., and Nystrom H., 1992, The use of liquids in ionization chambers for high precision radiotherapy dosimetry. Phys. Med. Bio., **37**, 1789.

[Yam] Yamashita H., Kawai H., Stricklett K.L., and Kelley E.F., 1990, The effect of high pressure on pre-breakdown phenomena in n-hexane. In: 10th international conference on conduction and breakdown in di-electric liquids., 404.

[Yos] Yoshino K., Sowada U., and Schmidt W.F., 1976, Effect of molecular solutes on electron drift velocity in liquid Ar, Kr, and Xe. Phys, Rev., **A14**, 438.